

**THE PROCESS OF DIMETHYL CARBONATE TO  
DIPHENYL CARBONATE:  
THERMODYNAMICS, REACTION KINETICS AND  
CONCEPTUAL PROCESS DESIGN**

Samenstelling promotiecommissie:

Prof. dr. ir. H. van den Berg, voorzitter	Universiteit Twente
Prof. dr. ir. J.A.M. Kuipers, promotor	Universiteit Twente
Prof. dr. ir. G.F. Versteeg, promotor	Universiteit Twente
Dr. ir. J.A. Hogendoorn, assistent-promotor	Universiteit Twente
Dr. ir. M. Van Sint Annaland, assistent-promotor	Universiteit Twente
Prof. dr. ing. M. Wessling	Universiteit Twente
Prof. dr. ir. A.B. de Haan	Universiteit Eindhoven
Prof. dr. ir. H.A. Kooijman	Clarkson University, USA
Prof. dr. R. Taylor	Clarkson University, USA
Prof. dr. D.W. Agar	University of Dortmund, Duitsland

This work was financially supported by Shell Global Solutions International BV.

No part of this work may be reproduced by print, photocopy or any other means without permission in writing from the author.

©J. Haubrock, Enschede, The Netherlands, 2007

---

Haubrock, J.

The Process of Dimethyl Carbonate to Diphenyl Carbonate:

Thermodynamics, Reaction Kinetics and Conceptual Process Design

PhD thesis, University of Twente, The Netherlands

ISBN: 90-365-2609-8

---

**THE PROCESS OF DIMETHYL CARBONATE TO  
DIPHENYL CARBONATE:  
THERMODYNAMICS, REACTION KINETICS AND  
CONCEPTUAL PROCESS DESIGN**

PROEFSCHRIFT

ter verkrijging van  
de graad van doctor aan de Universiteit Twente,  
op gezag van de rector magnificus,  
prof. dr. W.H.M. Zijm,  
volgens besluit van het College van Promoties  
in het openbaar te verdedigen  
op vrijdag 14 december 2007 om 16.45 uur

door

Jens Haubrock

geboren op 13 april 1977

te Herford

Dit proefschrift is goedgekeurd door de promotoren

**Prof. dr. ir. G.F. Versteeg**

**Prof. dr. ir. J.A.M. Kuipers**

en de assistent-promotoren

**Dr. ir. J.A. Hogendoorn**

**Dr. ir. M. van Sint Annaland**

*To my parents  
and Ruth*



## Summary

Polycarbonate (PC) is widely employed as an engineering plastic important to the modern lifestyle and used in, for example, the manufacture of electronic appliances, office equipment and automobiles. In 2003 more than 93% of the industrially produced PC was manufactured via interfacial polycondensation of Bisphenol A and phosgene (Fukuoka et al., 2003).

In the near future it is expected that the share of the phosgene based process contributing to the world production of PC will go below 75%, mainly due to the introduction of the phosgene free transesterification process which is licensed by Asahi Kasei (Fukuoka et al., 2007). In the traditional phosgene based process, Bisphenol A reacts with phosgene at 20 - 40 °C in a two-phase mixture consisting of an aqueous, alkaline phase and an immiscible organic phase (Serini, 2000).

The phosgene process entails a number of drawbacks. Firstly, 4 tons of phosgene is needed to produce 10 tons of PC. Phosgene is very toxic and when it is used in the production of PC the formation of undesired hazardous salts as by-products cannot be avoided. Secondly, the phosgene-based process uses 10 times as much solvent (on a weight basis) as PC is produced. The solvent, dichloromethane, is a suspected carcinogen and is soluble in water. This means that a large quantity of waste water has to be treated prior to discharge (Ono, 1997).

Many attempts have been made to overcome the disadvantages of the phosgene based process (Kim et al., 2004). The main point of focus has been a route through dimethyl carbonate (DMC) to diphenyl carbonate (DPC), which then reacts further with Bisphenol-A to produce polycarbonate by melt transesterification (Serini, 2000). In this process high purity diphenyl carbonate, which is required for the production of high quality PC, can be synthesized via the transesterification of DMC and phenol. Since the transesterification reactions involved in this conversion are severely equilibrium limited, it is impossible to obtain a high conversion without taking special measures (Buysch, 2000). The most critical step in the synthesis of DPC from DMC is the transesterification step from DMC and phenol to methyl phenyl carbonate (MPC) and methanol having a mole fraction based equilibrium value  $K_x$  of around  $1 \times 10^{-3}$  at 180 °C (Buysch, 2000).

The equilibrium conversions of the reactions to MPC and DPC are highly unfavorable: in a batch reactor with an equimolar feed of DMC and phenol at 180 °C, an equilibrium conversion of phenol of only 3% can be expected with a MPC yield of  $0.98 \times 3\%$  and a DPC yield of  $0.02 \times 3\%$ . As one of the reaction products, methanol in this case, is the most volatile component in the mixture, it might be attractive to use reactive distillation to remove excess methanol directly from the reaction zone to enhance the conversion of DMC towards MPC and therewith also increase the conversion towards DPC.

Potential process configurations for reactive distillation can only be developed reliably using not only information on kinetics and chemical equilibria but also information on the vapour-liquid equilibria (VLE) of the different species involved in the reactions.

However, the information available in literature on the chemical equilibria and kinetics for the transesterification of DMC and phenol and the two consecutive reaction of the intermediate MPC to DPC is still rather limited and -if available- mostly of a semi-quantitative nature. On top of this, also comprehensive information on the VLE of the system in this study is not available in literature. This information can also not be obtained using a predictive Gibbs excess energy ( $G^E$ ) model like UNIFAC because an important group needed for the description of the carbonate molecules DMC, MPC and DPC is missing from the UNIFAC database.

Before paying attention to the process yielding DPC from DMC, in Chapter 2 the applicability of activities instead of concentrations in kinetic expression has been investigated using the reaction of  $\text{CO}_2$  in sodium hydroxide solutions also containing different non-reacting salts (LiCl, KCl and NaCl) as model system. For hydroxide systems it is known that when the reaction rate constant is based on the use of concentrations in the kinetic expression, this "constant" depends both on the counter-ion in the solution and the ionic strength which is probably caused by the strong non-ideal behavior of various components in the solution. Absorption rate experiments have been carried out at 298 K in the so-called pseudo first order absorption rate regime and the experiments have been interpreted using a new activity based kinetic rate expression instead of the traditional concentration based



rate expression.

The absorption liquids were various NaOH (1, 1.5, 2.0 mol/l)-salt (LiCl, NaCl or KCl)-water mixtures, using salt concentrations of 0.5 and 1.5 mol/l. Interpretation of the data additionally required the use of an appropriate equilibrium model (needed for the calculation of the activity coefficients), for which the Pitzer model was applied. The addition of the salts proved to have a major effect on the observed absorption rate. The experiments were evaluated with the traditional concentration based approach and the "new" approach utilizing activity coefficients. With the traditional approach, there is a significant influence of the counter-ion and the hydroxide concentration on the reaction rate constant. The evaluation of the experiments with the 'new' approach - i.e. incorporating activity coefficients in the reaction rate expressions- reduced the influence of the counter-ion and the hydroxide concentration on the reaction rate constant considerably. The absolute value of the activity based reaction rate constant  $k_{OH^-}^m(\gamma)$  for sodium hydroxide solutions containing LiCl, KCl or NaCl is in the range between 10000 and 15000  $\text{kg kmol}^{-1}\text{s}^{-1}$  compared to the traditional approach where the value of the lumped reaction rate constant  $k_{OH^-}$  is between 7000 and 34000  $\text{m}^3 \text{ kmol}^{-1}\text{s}^{-1}$ .

For deriving activity based chemical equilibrium values and activity based reaction kinetics from experimental data, information of the VLE of the carbonate system investigated in this study is required. Therefore, in Chapter 3 VLE data available in literature comprising the following binaries: phenol-DMC, toluene-DMC, alcohol-DMC/DEC, and alkanes-DMC/DEC, ketones-DEC and chloro-alkanes-DMC have been fitted to a simplified "gamma-phi" model assuming the values of the Poynting correction, the fugacity coefficient of the gas and the liquid phase being equal to unity. Two  $G^E$ -models -viz. UNIFAC and NRTL- have been applied and the adjustable parameters in these two models have been fitted to the experimental VLE data. The two  $G^E$ -models could reproduce the experimental activity coefficients and therewith the experimental VLE data well (<10% deviation with NRTL) to fairly (<15% deviation with UNIFAC). The activity coefficients of the industrial important multi component system methanol, dimethyl carbonate, phenol, methyl phenol carbonate and diphenyl carbonate have been predicted with the derived UNIFAC

parameters to investigate the non-idealities of the system and to assess the need for the application of activity coefficients.

It has been shown that the activity coefficients of DMC and methanol deviate substantially from unity whereas the activity coefficients of the other three components deviate only slightly (<15%) from unity. It seems therefore necessary to employ activity coefficients for the description of the VLE in this system and probably also for the sound and uniform description of the chemical equilibria and reaction kinetics in this system.

As information regarding the chemical equilibria of the three reactions taking place in the carbonate system is rather limited in literature, in Chapter 4 a dedicated experimental study has been conducted to determine the chemical equilibrium data for various experimental conditions. In this Chapter 4, the activity based equilibrium constants of the reaction of dimethyl carbonate (DMC) and phenol to methyl phenyl carbonate (MPC) and the subsequent disproportion and transesterification reaction of MPC to diphenyl carbonate (DPC) are presented. Experiments have been carried out in the temperature range between 160 °C and 200 °C and for initial reactant ratios of DMC/phenol from 0.25 to 3. By employing activities instead of 'only' mole fractions in the calculation of the reaction equilibrium coefficients, the influence on the reactant ratio DMC/phenol on the derived equilibrium values for the reaction of DMC to MPC could be reduced, especially for temperatures of 160 °C. The activity based equilibrium coefficient for the transesterification reaction from MPC with phenol to DPC and methanol is constant within experimental uncertainty and, therefore, largely independent of the initial reactant ratio DMC/phenol at temperatures of 160 °C and 180 °C.

The temperature dependence of the equilibrium coefficients  $K_{a,1}$  and  $K_{a,2}$  has been fitted by applying the well known Van't Hoff equation, resulting in the expressions  $\ln K_{a,1} = -2702/T[\text{K}] + 0.175$  and  $\ln K_{a,2} = -2331/T[\text{K}] - 2.59$ .

In literature no quantitative description of the reaction kinetics in the investigated carbonate system is available. Accordingly a comprehensive kinetic study has been performed to determine the reaction kinetics of the three different reactions in the carbonate system. In this study, which is described in Chapter 5, the initial

reactant ratio DMC/phenol, catalyst amount and temperature were varied. Experiments were carried out in a batch reactor in the temperature range from 160 °C to 200 °C for initial reactant ratios of DMC/phenol from 0.25 to 3 and varying catalyst (Titanium-(n-butoxide)) concentrations. The concept of a closed ideally stirred, isothermal batch reactor incorporating an activity based reaction rate model, has been used to fit kinetic parameters to the experimental data.

For exploring the industrial production process using reactive distillation, a tray column model originating from the software package ChemSep (Taylor and Kooijman, 2000) was used. This study and the results thereof are described in Chapter 6. The influence of various parameters - feed location(s), number of stages, temperature and pressure - which are of relevance for a reactive distillation process, was studied and the results are evaluated. The chemical/physical data as obtained in the previous chapters was used as input to the model. First a process comprising of one reactive distillation column and then a process employing two reactive distillation columns has been investigated. The results show that a two-column configuration is required to achieve industrially feasible yields of DPC. While there are sufficient opportunities for the optimization of the first column, the design and operation of the second column seems to be less critical.

It is expected that the thermodynamics, the reaction kinetics and thermodynamic UNIFAC data as presented in this thesis will be very helpful in the design and optimization of the production process of DPC from DMC.



## Samenvatting

Polycarbonaat (PC) vindt op uitgebreide schaal toepassing als engineering plastic bij onder andere de productie van huishoudelijke apparaten, kantoorartikelen en auto's. In 2003 werd meer dan 93% van alle wereldwijd geproduceerde PC bereid via zogenaamde grensvlak polymerisatie van bisfenol A met fosgeen (Fukuoka et al., 2003).

Er wordt verwacht dat in de nabije toekomst het productieaandeel van het traditionele, op fosgeen gebaseerde, PC productieproces tot minder dan 75% zal dalen, met name als gevolg van de introductie van het fosgeenvrije omesteringsproces gelicenseerd door Asahi Kasei (Fukuoka et al., 2007). In het op fosgeen gebaseerde proces reageert Bisfenol A tot PC bij een temperatuur van 20-40 °C in een 2-fase systeem bestaande uit een alkalische waterige fase en een niet mengbare organische fase (Serini, 2000).

Dit proces kent echter een belangrijk aantal nadelen. Ten eerste is 4 ton fosgeen nodig om 10 ton PC te produceren. Fosgeen is een extreem toxische stof en bij de productie van PC kan de vorming van ongewenste, gevaarlijke zouten niet worden voorkomen. Ten tweede wordt bij het traditionele op fosgeen gebaseerde proces 10 keer zoveel oplosmiddel (op gewichtsbasis) gebruikt als aan PC geproduceerd wordt. Het gebruikte solvent is DiChloorMethaan waarvan vermoed wordt dat het carcinogeen is. Aangezien dit oplosmiddel tevens oplosbaar is in de waterige fase zoals in het proces aanwezig, moeten grote waterstromen worden gereinigd voordat deze gespuid kunnen worden (Ono, 1997).

Er zijn in het verleden vele procesalternatieven onderzocht om de nadelen van het op fosgeen gebaseerde proces te vermijden (Kim et al., 2004). Het meestbelovende productiealternatief is een proces dat van DiMethylCarbonaat (DMC), via MethylPhenylCarbonaat (MPC) naar DiPhenylCarbonaat (DPC) loopt, dat vervolgens met bisfenol A kan worden omgezet tot PC in een smelt omesteringsproces (Serini, 2000). In dit proces kan de benodigde hoge zuiverheid van DPC verkregen worden door de reactie van fenol met DMC. Aangezien de omesteringsreacties in dit proces sterk evenwichtsgelimiteerd zijn, kan een hoge conversiegraad alleen gerealiseerd worden door het in acht nemen van speciale maatregelen (Buysch, 2000).

De meest kristische stap in de synthese van DPC uit DMC is de omesteringsreactie van DMC met fenol tot respectievelijk MPC en methanol, met een op molfracties gebaseerde evenwichtsconstante van  $K_x = 1 \times 10^{-3}$  [-] bij 180 °C (Buysch, 2000).

De evenwichtsconversies van de reacties naar MPC en DPC zijn zeer laag: in een batch-reactor worden bij een equimolaire voeding van DMC en fenol evenwichtsconversies van fenol van slechts 3% behaald, met daarbij een yield van  $0.98 \times 3\%$  aan MPC en  $0.02 \times 3\%$  aan DPC. Aangezien methanol, een van de reactieproducten, vluchtig is, kan het aantrekkelijk zijn dit product aan het reactiemengsel te onttrekken om daarmee hogere conversies te realiseren. Bij toepassing van reactieve destillatie voor dit systeem is het in principe mogelijk methanol in-situ uit het reactiemengsel te verwijderen en daarmee de conversie naar MPC en daarmee tevens ook DPC te verhogen.

Mogelijk geschikte proces configuraties voor reactieve destillatie kunnen alleen ontwikkeld en beoordeeld worden indien informatie over de kinetiek, thermodynamica en gas-vloeistof evenwichten (VLE) bekend is.

In de literatuur is echter slecht op zeer beperkte schaal informatie te vinden over de kinetiek en thermodynamica van de reacties van DMC naar MPC en vervolgens DPC. Bovendien is de informatie die beschikbaar is over het algemeen slechts semi-quantitatief en vormt daarmee geen betrouwbare basis voor het ontwerp en de optimalisatie van een productieproces. Voor het ontwerp van een reactieve destillatiekolom zijn betrouwbare gegevens over gas-vloeistof evenwichten in dit systeem tevens onontbeerlijk, maar ook deze informatie is niet beschikbaar in de literatuur. Deze informatie kan ook niet verkregen worden met behulp van Gibbs vrije energie ( $G^E$ ) modellen, zoals bijvoorbeeld UNIFAC, aangezien de carbonaatgroep, een belangrijk onderdeel van DMC, DPC en MPC, geen onderdeel uitmaakt van de UNIFAC database.

Voordat aandacht is geschonken aan het proces van DMC naar MPC en DPC, is in dit proefschrift eerst een algemeen fundamenteel vraagstuk bestudeerd aan de hand van een modelsysteem. Het is op dit moment nog steeds gebruikelijk om in kinetiekuitdrukkingen gebruik te maken van concentraties, terwijl het voor de beschrijving van chemische evenwichten en VLE data gebruikelijk (noodzakelijk) is

om activiteiten te gebruiken. Voor een consistent ontwerp van een reactieve destillatiekolom, waar alle drie deze zaken een rol spelen, zou het goed zijn indien zowel kinetiek, thermodynamica als VLE op eenzelfde wijze, namelijk met behulp van activiteiten, worden uitgedrukt.

In Hoofdstuk 2 is voor een modelsysteem, de reactie van  $\text{CO}_2$  met alkalische oplossingen, bestudeerd of het mogelijk is de kinetiek van deze reactie uit te drukken met behulp van activiteiten in plaats van concentraties. Voor dit systeem is bekend dat bij toevoeging van verschillende inerte zouten aan het systeem, de op basis van concentraties gevonden reactiesnelheidsconstante aanzienlijk varieert en afhankelijk is van het inerte counter-ion ( $\text{Li}^+$ ,  $\text{Na}^+$  en  $\text{K}^+$ ) en de ion-sterkte van de oplossing. Dit wordt hoogstwaarschijnlijk veroorzaakt door het sterk niet-ideale gedrag van verschillende componenten in de oplossing. Wanneer nu activiteiten in de kinetiekuitdrukking zouden worden gebruikt, zou dit verschijnsel ondervangen kunnen worden.

In Hoofdstuk 2 staat dit onderzoek en de resultaten daarvan beschreven. Experimenten zijn uitgevoerd bij 298 K in het zogenaamde pseudo-eerste orde regime en genterpreteerd met behulp van een op activiteiten gebaseerde kinetiekuitdrukking in plaats van de tot nu toe gebruikelijke op concentraties gebaseerde kinetiekuitdrukking. Als absorptieoplossingen zijn verschillende NaOH (1, 1.5 en 2 mol/l)-zout ( $\text{LiCl}$ ,  $\text{NaCl}$  of  $\text{KCl}$ )-water mengsels gebruikt, met zoutconcentraties van 0.5 en 1.5 mol/l. Voor de interpretatie van de experimentele data was additioneel tevens een geschikt evenwichtsmodel nodig, om daarmee de activiteiten van de componenten in oplossing te kunnen bepalen. Hiertoe is het Pitzer model gebruikt. De toevoeging van de zouten aan de NaOH oplossing bleek een sterk effect op de waargenomen absorptiesnelheid te hebben. De kinetiekexperimenten zijn niet alleen genterpreteerd op basis van de nieuwe -op activiteiten- gebaseerde kinetiekexpressie, maar tevens op de op concentraties gebaseerde kinetiekuitdrukking. Bij de traditionele -op concentraties- gebaseerde kinetiekuitdrukking bleek er een sterke invloed van het counter-ion ( $\text{Li}^+$ ,  $\text{Na}^+$  en  $\text{K}^+$ ) en de hydroxide concentratie op de gevonden waarde van de reactiesnelheidsconstante. De reactiesnelheidsconstante die op basis van de op activiteiten gebaseerde kinetiekuitdrukking kon worden bepaald bleek veel minder gevoelig voor zowel het counter-ion als de hydroxide concentratie van de oplossing.

De waarde van de op activiteiten gebaseerde kinetiekconstante  $k_{OH^-}^m(\gamma)$  voor de gebruikte oplossingen bleek in de range tussen 10000-15000  $\text{kg kmol}^{-1}\text{s}^{-1}$  te liggen, en daarmee was de variatie veel kleiner dan voor de op concentraties gebaseerde kinetiekconstante  $k_{OH^-}$ , die in de range tussen 7000 en 34000  $\text{m}^3 \text{ kmol}^{-1}\text{s}^{-1}$  lag.

Voor de bepaling van de op activiteiten gebaseerde evenwichtsconstanten en reactiesnelheidsconstanten voor het DMC/MPC/DPC systeem zoals beschreven in dit proefschrift, is het noodzakelijk de activiteiten te kennen. Dit kan mits de activiteitscoëfficiënten bepaald kunnen worden, maar deze zijn voor het carbonaatsysteem zoals van belang in deze studie niet bekend. Aan de hand van VLE-data is het in principe mogelijk de activiteitscoëfficiënten te bepalen, echter, voor het onderhavige systeem zijn geen VLE data beschikbaar. Daarom was het voor de bepaling van activiteitscoëfficiënten nodig een voorspellende methode zoals UNIFAC te gebruiken. Daartoe zijn voor soortgelijke binaire systemen -fenol-DMC, toluen-DMC, alcohol-DMC/DEC en alkanen-DMC/DEC, ketonen-DEC en chlooralkanen-DMC- de VLE data uit de literatuur achterhaald en deze zijn gefit op een vereenvoudigd "gamma-phi" model. In dit model zijn de waarden van de Poynting correctiefactor, en de fugaciteitscoëfficiënten van zowel het gas als de vloeistof gelijkgesteld aan 1. Niet alleen het UNIFAC model, maar ook het NRTL model- een ander  $G^E$ -model- is gebruikt om de VLE data te beschrijven waarbij voor beide modellen de interactieparameters bepaald zijn. Beide  $G^E$ -modellen bleken in staat de experimentele data redelijk (<15% afwijking voor UNIFAC) tot goed (<10% afwijking voor NRTL) te kunnen beschrijven. Aan de hand van de gevonden interactieparameters was het met UNIFAC nu mogelijk de activiteitscoëfficiënten voor het industrieel van belang zijnde systeem methanol, DMC, fenol, MPC en DPC te voorspellen. Met behulp van de waarde van de activiteitscoëfficiënten kon nu de noodzaak van het gebruik van activiteiten in plaats van concentraties in zowel de kinetiekuitdrukkingen als evenwichtsuitdrukkingen worden bepaald.

Voor met name DMC en methanol bleek de waarde van de activiteitscoëfficiënt substantieel van 1 (ideaal gedrag) af te wijken, terwijl de activiteitscoëfficiënten van de andere 3 componenten slechts beperkt (<15%) van 1 afweken. Gebaseerd op de resultaten van Hoofdstuk 3 lijkt het nodig om zowel het chemische evenwicht als de



kinetiekuitdrukking uit te drukken op basis van activiteiten.

Aangezien er in de literatuur nauwelijks informatie over het chemische evenwicht van DMC naar MPC en vervolgens DPC te vinden is, is er een uitgebreide studie naar het chemisch evenwicht van dit systeem uitgevoerd waarvan de resultaten in Hoofdstuk 4 beschreven staan. In dit hoofdstuk worden de evenwichten van de reactie van DMC met fenol en de daaropvolgende disproportioneerings- en omesteringsreactie van MPC tot DPC beschreven op basis van activiteiten. Experimenten zijn uitgevoerd in het temperatuurtraject van 160-200 °C met initiale reactantverhoudingen van DMC/fenol van 0.25-3. Het bleek dat bij gebruik van activiteiten in de evenwichtsrelaties de waarde van de evenwichtsconstante van DMC naar MPC veel minder gevoelig was voor de reactant-ratio van DMC/fenol dan bij gebruik van concentraties in de evenwichtsrelaties. De op activiteiten gebaseerde waarde van de evenwichtsconstante voor de reactie van MPC tot DPC bleek voor temperaturen van zowel 160 als 180 °C binnen de experimentele onzekerheid constant en daarmee onafhankelijk van de initiale reactant ratio. De temperatuurafhankelijkheid van de evenwichtsconstante is uitgedrukt met behulp van de Van 't Hoff relatie waarbij voor de reactie van DMC naar MPC gevonden werd dat  $\ln K_{a,1} = -2702/T[\text{K}] + 0.175$  en voor de reactie van MPC naar DPC dat  $\ln K_{a,2} = -2331/T[\text{K}] - 2.59$ .

In de literatuur is geen kwantitatieve beschrijving van de reactiekinetiek van het DMC/MPC/DPC systeem te vinden. Daarom is een uitgebreide kinetiekstudie uitgevoerd waarvan de resultaten in Hoofdstuk 5 beschreven staan. In deze studie zijn de initiale reactant-ratio DMC/fenol, de katalysatorconcentratie en de temperatuur gevarieerd. Experimenten zijn uitgevoerd in een batch-reactor in het temperatuurgebied van 160-200 °C, initiale reactant-ratios van DMC/fenol van 0.25-3 en verschillende katalysatorconcentraties. De omzetting bleek relatief snel (evenwicht binnen 15-60 minuten, afhankelijk van condities) te verlopen, terwijl op basis van de literatuur een langzame reactie verwacht werd (reactietijden tot 20 uur). De kinetiekconstanten voor de reactie van DMC naar MPC en vervolgens MPC naar DPC -via zowel de omesteringsreactie als de disproportioneeringsreactie van MPC- zijn gefit met behulp van een op activiteiten gebaseerd kinetisch model. De gevonden kinetiekconstante voor de reactie van DMC naar MPC bleek van dezelfde orde

grootte te zijn als de reactie van MPC naar DPC via de omesteringsreactie. De omzettingssnelheid via de disproportioneeringsreactie van MPC naar DPC bleek voor de uitgevoerde experimenten van dezelfde orde grootte als via de omesteringsreactie van MPC naar DPC. Onder industriële condities wordt echter verwacht dat de disproportioneeringsreactie de belangrijkste bijdrage zal leveren aan de omzetting van MPC naar DPC.

Om een potentieel productieproces van DPC met gebruik van reactieve destillatie te verkennen, is een model van een schotelkolom ontwikkeld dat vervolgens gecomplementeerd is in het softwarepakket ChemSep (Taylor and Kooijman, 2000). De details van deze simulaties en resultaten daarvan staan beschreven in Hoofdstuk 6. De invloed van verschillende parameters -voedingsschotel, aantal schotels temperatuur en druk - zijn daarbij gevarieerd. Als input van het simulatiemodel zijn de fysisch/chemische data gebruikt zoals in de voorafgaande hoofdstukken gevonden. Eerst is de performance van een proces met gebruik van 1 destillatiekolom beschreven, waarbij bleek dat 1 destillatiekolom onvoldoende is om een hoge yield aan DPC te krijgen. Daarom zijn er simulaties uitgevoerd waarbij een serieel gekoppelde tweede reactieve destillatiekolom is gebruikt. Hieruit bleek dat deze tweede kolom de DPC yield sterk verhoogde. In de eerste kolom zijn er meerdere mogelijkheden om de performance van deze eerste kolom te optimaliseren, terwijl het ontwerp van de tweede kolom veel minder kritisch lijkt te zijn.

Er wordt verwacht dat de in dit proefschrift gevonden gegevens over de chemische evenwichten, de kinetiek en de thermodynamische UNIFAC data een bijdrage zullen leveren aan het ontwerp en optimaliseren van het productieproces van DPC vanuit DMC.

# Contents

<b>Summary</b>	<b>i</b>
<b>Samenvatting</b>	<b>vii</b>
<b>1 General Introduction</b>	<b>1</b>
1.1 The process from dimethyl carbonate to diphenyl carbonate . . . . .	1
1.2 This thesis . . . . .	4
<b>2 The applicability of activities in kinetic expressions: a more fun-     damental approach to represent the kinetics of the system CO<sub>2</sub> -     OH<sup>-</sup> - salt in terms of activities</b>	<b>9</b>
2.1 Introduction . . . . .	10
2.2 Experimental section . . . . .	12
2.2.1 Experimental setup and procedure . . . . .	12
2.3 Chemicals . . . . .	14
2.4 Determination of the reaction rate constant from experimental data .	14
2.5 Physical properties employed in the interpretation of the flux data . .	16
2.6 Experimental Results and their interpretation using the traditional approach . . . . .	22
2.7 Equilibrium model . . . . .	28

2.7.1	Thermodynamic model . . . . .	28
2.8	Experimental Results and their interpretation using the activity based approach . . . . .	31
2.9	Conclusion . . . . .	40
2.A	Brief outline of the Pitzer model . . . . .	43
2.B	Parameters used in the equilibrium model incorporating the Pitzer model . . . . .	46
2.C	Derivation of equations used in the activity based kinetic approach . . . . .	51
2.C.1	Conversion between molalities and concentrations of mixed salt solutions . . . . .	51
2.C.2	Relation between the activity based rate constant and the concentration based rate constant . . . . .	52
2.D	Experimental data . . . . .	53
2.D.1	Experimental data for the kinetics of CO <sub>2</sub> in 'pure' aqueous sodium hydroxide solutions . . . . .	53
2.D.2	Applied activity coefficients to derive the activity based kinetics for the reaction of CO <sub>2</sub> in 'pure' aqueous sodium hydroxide solutions . . . . .	54
2.D.3	Raw data: Absorption experiments of CO <sub>2</sub> in salt-doped NaOH solutions . . . . .	55
<b>3</b>	<b>A new UNIFAC-group: the OCOO-group of carbonates</b>	<b>57</b>
3.1	Introduction . . . . .	58
3.2	Description of the vapour liquid equilibrium model (VLE) . . . . .	60
3.3	The UNIFAC Method . . . . .	61
3.4	The NRTL Method . . . . .	63
3.5	Segmentation of carbonate-molecules in UNIFAC . . . . .	64
3.6	Modelling VLE data with UNIFAC and NRTL . . . . .	65

<i>Contents</i>	xv
3.7 Correlation and Prediction . . . . .	71
3.8 Activity coefficients of the multicomponent system methanol-DMC-phenol-MPC-DPC . . . . .	80
3.9 Conclusion . . . . .	83
3.10 Appendix . . . . .	86
<b>4 Experimental determination of the chemical equilibria involved in the reaction from Dimethyl carbonate to Diphenyl carbonate</b>	<b>87</b>
4.1 Introduction . . . . .	88
4.2 Reactions . . . . .	89
4.3 Thermodynamics . . . . .	91
4.4 Catalysts . . . . .	95
4.5 Chemicals . . . . .	97
4.6 Experimental setup and procedure . . . . .	97
4.7 Experimental results . . . . .	99
4.7.1 General remarks . . . . .	99
4.8 Equilibrium coefficient $K_{x,1}$ . . . . .	101
4.9 Equilibrium coefficient $K_{x,2}$ . . . . .	105
4.10 Equilibrium coefficient $K_{a,1}$ . . . . .	107
4.11 Equilibrium coefficient $K_{a,2}$ . . . . .	113
4.12 Temperature dependence of the equilibrium coefficients $K_{a,1}$ and $K_{a,2}$	115
4.13 Comparison between $K_{a,i}$ values derived from own experiments and literature . . . . .	116
4.14 Conclusion . . . . .	119
4.A Raw data . . . . .	121

<b>5</b>	<b>The conversion of Dimethyl carbonate (DMC) to Diphenyl carbonate (DPC): Experimental measurements and reaction rate modelling</b>	<b>125</b>
5.1	Introduction . . . . .	126
5.2	Reactions . . . . .	127
5.3	Catalysts . . . . .	129
5.4	Experimental work . . . . .	131
5.5	Effect of catalyst concentration . . . . .	134
5.6	Does the disproportionation reaction occur? . . . . .	136
5.7	Reaction kinetics and modelling . . . . .	137
5.8	Estimation of rate constants . . . . .	141
5.9	Effect of the reactant ratio DMC/phenol . . . . .	142
5.10	Effect of temperature . . . . .	150
5.11	Conclusion . . . . .	152
<b>6</b>	<b>Preliminary process design for the production of Diphenyl carbonate from Dimethyl carbonate: Parameter studies and process configuration</b>	<b>155</b>
6.1	Introduction . . . . .	157
6.2	The Equilibrium Stage model . . . . .	158
6.3	Phase equilibrium, thermodynamics and reaction kinetics . . . . .	160
6.4	Reactions . . . . .	161
6.5	Thermodynamics . . . . .	162
6.6	Reaction rate equations . . . . .	163
6.7	Process description and assumptions . . . . .	164
6.8	Comparison between the simulation results of Tung and Yu (2007) and this work . . . . .	181
6.9	Conclusion . . . . .	186

<i>Contents</i>	xvii
<b>Bibliography</b>	<b>190</b>
<b>List of Publications</b>	<b>201</b>
<b>Curriculum Vitae</b>	<b>203</b>
<b>Acknowledgements</b>	<b>205</b>





# Chapter 1

## General Introduction

### 1.1 The process from dimethyl carbonate to diphenyl carbonate

Polycarbonate (PC) is widely employed as an engineering plastic important to the modern lifestyle and used in, for example, the manufacture of electronic appliances, office equipment and automobiles. About 3.4 million tons of PC was produced worldwide in 2006. Production is expected to increase by around 6% per year at least until 2010 with the fastest regional growth expected in East Asia, averaging 8.7% per year through 2009 (Westervelt, 2006).

In 2003 more than 93% of the industrially produced PC was manufactured via interfacial polycondensation of Bisphenol A and phosgene (Fukuoka et al., 2003). In the near future it is expected that the share of the phosgene based process contributing to the world production of PC will go below 75%, mainly due to the introduction of the phosgene free melt transesterification process which is licensed by Asahi Kasei (Fukuoka et al., 2007). In the traditional phosgene based process, Bisphenol A reacts with phosgene at 20 - 40° C in a two-phase mixture consisting of an aqueous, alkaline phase and an immiscible organic phase (Serini, 2000).

The phosgene process entails a number of drawbacks. Firstly, 4 tons of phosgene is needed to produce 10 tons of PC. Phosgene is very toxic and when it is used in the

production of PC the formation of undesired hazardous salts as by-products cannot be avoided. Secondly, the phosgene-based process uses 10 times as much solvent (on a weight basis) as PC is produced. The solvent, dichloromethane, is a suspected carcinogen and is soluble in water. This means that a large quantity of waste water has to be treated prior to discharge (Ono, 1997).

Many attempts have been made to overcome the disadvantages of the phosgene based process (Kim et al., 2004). The main point of focus has been a route through dimethyl carbonate (DMC) to diphenyl carbonate (DPC), which then reacts further with Bisphenol-A to produce polycarbonate by melt transesterification (Serini, 2000). This route seems increasingly attractive compared to the at present industrially used interfacial polycondensation process for several reasons. Firstly, the process starting with DMC is environmentally more favorable as:

1. No poisonous phosgene is employed anymore in the process.
2. It prevents the use of copious amounts of the organic solvent Dichloromethane
3. Large amounts of waste water contaminated with the organic solvent are avoided.

Furthermore, the melt transesterification process has gained renewed interest because of the justifiable optimism that secondary reactions with deleterious effects on quality (e.g., discoloration) can be suppressed by using high-purity starting materials (Diphenyl carbonate and Bisphenol A) (Serini, 2000). The phosgene based polycondensation process suffers from chlorine impurities in the produced PC which can cause the deterioration of the PC properties such as heat resistance and color.

High purity Diphenyl carbonate can be synthesized via the transesterification of DMC and phenol. Since these transesterification reactions involved in this conversion are severely equilibrium limited, it is impossible to obtain a high conversion without additional measures (Buysch, 2000).

The most critical step in the synthesis of DPC from DMC is the transesterification step from DMC and phenol to methyl phenyl carbonate (MPC) (Reaction 1.1) having a mole fraction based equilibrium value  $K_{x,1}$  of about  $1 \times 10^{-3}$  (Buysch, 2000).

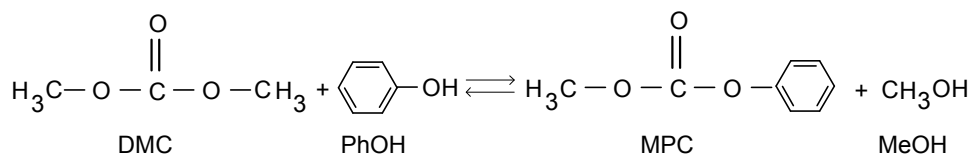


Figure 1.1: Transesterification 1

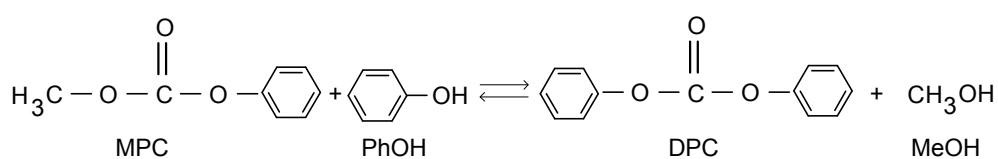


Figure 1.2: Transesterification 2

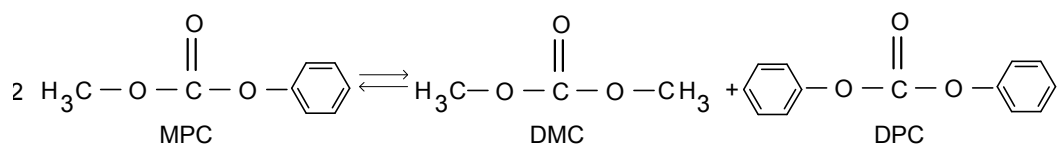


Figure 1.3: Disproportionation

The equilibrium conversions of the reactions to MPC and DPC (Reactions 1.1 and 1.2) are very low: in a batch reactor with an equimolar feed of DMC and phenol at 180° C, an equilibrium conversion of phenol of only ~3% can be expected with a MPC yield of 0.98×3% and a DPC yield of 0.02×3%. As one of the reaction products, methanol in this case, is the most volatile component in the mixture, it might be attractive to use reactive distillation to remove methanol directly from the reaction zone to enhance the conversion of DMC towards MPC and therewith also increase the conversion towards DPC.

A reactive distillation process to produce DPC preferably would be operated as close to chemical equilibrium as possible in order to achieve the highest possible conversion of the reactants towards DPC. This, in turn, requires the rates of the

involved reactions to proceed sufficiently fast. To assess whether reactive distillation is an attractive process alternative to improve on the conversion of DMC towards MPC, it is essential not only to describe and understand the chemical equilibrium but also to know the reaction rates to achieve equilibrium, i.e. the kinetics, as this determines the required residence time in the reaction zone and hence also the dimensions of the equipment.

Potential process configurations for reactive distillation can only be developed reliably using not only information on kinetics and chemical equilibrium but also information on the vapour-liquid equilibria (VLE) of the different species involved in the reactions 1.1-1.3.

However, the information available in literature on the chemical equilibria and kinetics for the transesterification of DMC and phenol and the two consecutive reaction of the intermediate MPC to DPC is still rather limited and -if available- mostly of a semi-quantitative nature. On top of this, also information on the VLE of the same system -as of relevance for the design of reactive distillation columns- is not available in literature. This information can also not be obtained using a predictive Gibbs excess energy ( $G^E$ ) model like UNIFAC because an important group -the carbonate group- needed for the description of the carbonate molecules DMC, MPC and DPC is missing from the UNIFAC database.

## 1.2 This thesis

As indicated in the previous section knowledge on chemical equilibria, VLE and reaction kinetics of the reactions from DMC to MPC and DPC, respectively is rather limited. Therefore, it is the incentive of this thesis to provide more insights into the process step from dimethyl carbonate to diphenyl carbonate via methyl phenyl carbonate, both from the experimental and theoretical point of view. It is intended to describe the whole process on a more fundamental and consistent basis especially with respect to the design of a reactive distillation column. In such a column all aforementioned phenomena (kinetics, chemical; equilibria and physical equilibrium) play a role simultaneously. It is known that for a proper description of VLE

data as of importance in distillation columns, the use of activity coefficients is indispensable. To make the description of chemical equilibrium consistent with the description of physical phase equilibrium, chemical equilibrium should preferably also be expressed using an activity based approach. This should prevent the frequently seen phenomenon that the equilibrium constant changes with composition of the mixture. To make the process description completely consistent the kinetics should therefore also be expressed using activities. Otherwise the description of the reactive distillation process cannot be realized with a uniform methodology. Moreover, at equilibrium the rate of the forward and backward reaction is assumed to be equal for elementary reactions and therefore:

$$K_{eq} = \frac{k_{forward}}{k_{backward}}. \quad (1.1)$$

If equilibrium is expressed using activities, this also means implicitly that the reaction rates need to be expressed using activities if consistency in the process design is demanded. To study the use of activities in kinetic expressions the well-known system  $\text{CO}_2\text{-OH}^-$  was studied using different salts as inert additions in Chapter 2. This system was chosen to investigate whether it is possible to account for the observed non-idealities of the system in a more generic and fundamental way by applying an activity based reaction rate equation. It is expected that the use of activities in the reaction rate will yield a much better description of the experimental data as compared to the traditional concentration based approach in the sense that the activity based rate constant is hardly influenced by the ionic strength of the solutions and the different cations being present in the solution. Moreover, the activity based reaction rate expression will be consistent with the description of the chemical equilibrium where likewise activities are employed.

This fundamental work indicates whether activities instead of concentrations should preferably be used for describing reaction kinetics, especially when dealing with highly non-ideal systems. Owing to the intrinsic consistency, the activity-based approach is also applied for the reaction system DMC/MPC/DPC. However,

to apply this approach it should be possible to predict activity coefficients and as already indicated these are not available for the carbonate system. There is a way to get around this, by using a predictive method like UNIFAC. Nevertheless a new problem arises when using this UNIFAC approach as the carbonate group, as present in the key components DMC, MPC and DPC, is absent from the UNIFAC databank.

Therefore, in Chapter 3 the interaction parameters of a carbonate group and various other functional groups are determined using available VLE data from literature for analogous systems. In this chapter UNIFAC parameters are fitted to binary vapour-liquid equilibrium data of systems containing carbonates and different other relevant substances. The derived UNIFAC parameters are used for the calculation of activity coefficients which are the basis for a sound description of the chemical equilibria and reaction kinetics. Furthermore, activity coefficients are needed to assess the separation characteristics (VLE data) of the different species involved in the here studied carbonate system.

Chapter 4 reports about the investigation of the influence of temperature, as well as the influence of the initial reactant ratio of DMC/phenol on the chemical equilibria in the present reaction system as described by reaction 1.1-1.3. The equilibrium experiments, carried out in thermostatted batch reactor at different temperatures, are interpreted in two ways: a simple manner using only mole fractions and in a more fundamental way by using activities, respectively. Moreover, the temperature dependence of the three chemical equilibria is described.

Chapter 5 deals with the influence of temperature, catalyst concentration, as well as the influence of the initial reactant ratio of DMC/phenol on the reaction kinetics of the DMC/MPC/DPC system. The experiments are carried out in a thermostatted batch reactor at different temperatures and are interpreted using an activity based approach. The concept of a closed ideally stirred, isothermal batch reactor incorporating an activity based reaction rate model is used to derive an activity based reaction rate model for the three reactions in the carbonate system. Moreover, the temperature dependence of the reaction rate constants is determined.

In Chapter 6 the process from dimethyl carbonate (DMC) to diphenyl carbonate (DPC) via the intermediate methyl phenyl carbonate (MPC) carried out in a

reactive distillation column has been modelled with the commercial software package ChemSep. The influence of various parameters on the yields of MPC and DPC has been studied to find suitable optimization parameters.

Based on the modelling results of the "first" column - with DMC, phenol and catalyst as feed- it seems necessary to use a "second" column in which MPC is converted to DPC and moreover excess phenol is separated from the product DPC. The influence of the reflux ratio, bottom flow rate and the number of stages on the DPC yield in the bottom of the "second" column has been studied. The chapter concludes with a comparison of the calculated composition profiles taken from Tung and Yu (2007) and those calculated in this work for a column producing DPC from phenol and DMC.





## Chapter 2

# The applicability of activities in kinetic expressions: a more fundamental approach to represent the kinetics of the system $\text{CO}_2$ - $\text{OH}^-$ - salt in terms of activities

### Abstract

The applicability of utilizing activities instead of concentrations in kinetic expressions has been investigated using the reaction of  $\text{CO}_2$  in sodium hydroxide solutions also containing different neutral salts (LiCl, KCl and NaCl) as model system. For hydroxide systems it is known that when the reaction rate constant is based on the use of concentrations in the kinetic expression, this "constant" depends both on the counter-ion in the solution and the ionic strength which is probably caused by the strong non-ideal behavior of various components in the solution. In this study absorption rate experiments have been carried out in the pseudo first order absorption rate regime. The experiments have been interpreted using a new activity based kinetic rate expression instead of the traditional concentration based rate expression.

A series of CO<sub>2</sub> absorption experiments in different NaOH (1, 1.5, 2.0 mol/l)-salt (LiCl, NaCl or KCl)-water mixtures has been carried out, using salt concentrations of 0.5 and 1.5 mol/l all at a temperature of 298 K. Interpretation of the data additionally required the use of an appropriate equilibrium model (needed for the calculation of the activity coefficients), for which, in this case, the Pitzer model was used. The additions of the salts proved to have a major effect on the observed absorption rate. The experiments were evaluated with the traditional concentration based approach and the 'new' approach utilizing activity coefficients. With the traditional approach, there is a significant influence of the counter-ion and the hydroxide concentration on the reaction rate. The evaluation of the experiments with the 'new' approach - i.e. incorporating activity coefficients in the reaction rate expressions- reduced the influence of the counter-ion and the hydroxide concentration on the reaction rate constant considerably. The absolute value of the activity based reaction rate constant  $k_{OH^-}^m(\gamma)$  for sodium hydroxide solutions containing either LiCl, KCl or NaCl is in the range between 10000 and 15000 kg kmol<sup>-1</sup> s<sup>-1</sup>) compared to the traditional approach where the value of the lumped reaction rate constant  $k_{OH^-}$  is between 7000 and 34000 m<sup>3</sup>/(kmole s).

Therefore it can be concluded that the application of the new methodology is thought to be very beneficial especially in processes where "the thermodynamics meet the kinetics". Based on this it is anticipated that the new kinetic approach will first find its major application in the modelling of integrated processes like Reactive Distillation, Reactive Absorption and Reactive Extraction processes where both, thermodynamics and kinetics, are of essential importance and, additionally, activity coefficients deviate substantially from unity.

## 2.1 Introduction

The kinetics of CO<sub>2</sub> in caustic solutions, especially in sodium hydroxide solutions, have been extensively studied within the last decades by doing absorption rate experiments. In these studies it has been found that the reaction rate constant is not only dependent on the concentrations of the reacting species, but also affected by

the ionic strength of the caustic solution and the nature of the cations present in the hydroxide solution (Nijsing et al. (1959), Pohorecki and Moniuk (1988), Kucka et al. (2002)). The following two reactions are generally accepted to take place:



The rate of reaction 2 is significantly higher than that of reaction 1 as it involves only a proton transfer (Hikita and Asai, 1976) and therefore the first reaction is rate determining for the overall observed reaction rate. In literature, the kinetics of reaction 1 are typically described using an irreversible-second-order reaction rate expression ( $r = k_{OH^-} c_{CO_2} c_{OH^-}$ ), where all possible effects of non-idealities are lumped in the reaction rate constant  $k_{OH^-}$  (Pohorecki and Moniuk (1988), Kucka et al. (2002)). This approach is generally sufficient to represent the experimental data of a single specific study but lacks the fundamental character of the reaction rate constant only being a function of temperature.

In the present study it is attempted to derive a generally applicable rate expression for the reaction of  $CO_2$  with  $OH^-$  in mixed electrolyte solutions based on the activities of the species, and not on the commonly used concentrations. It is studied whether the new approach will yield a reaction rate constant that is (nearly) independent on the ionic strength and on the counter-cation in the solution, respectively.

New data obtained from  $CO_2$  absorption experiments in sodium hydroxide solutions containing variable amounts of various dissociating salts (LiCl, NaCl or KCl) are presented and will be used to study the activity based kinetic concept over a wide range of liquid compositions. For the activity based approach it is of course necessary to use activity coefficients, and in this study the Pitzer model (Pitzer, 1973) has been used for this purpose. The newly developed kinetic expression is compared to the traditional approach where 'only' concentrations are used.

## 2.2 Experimental section

### 2.2.1 Experimental setup and procedure

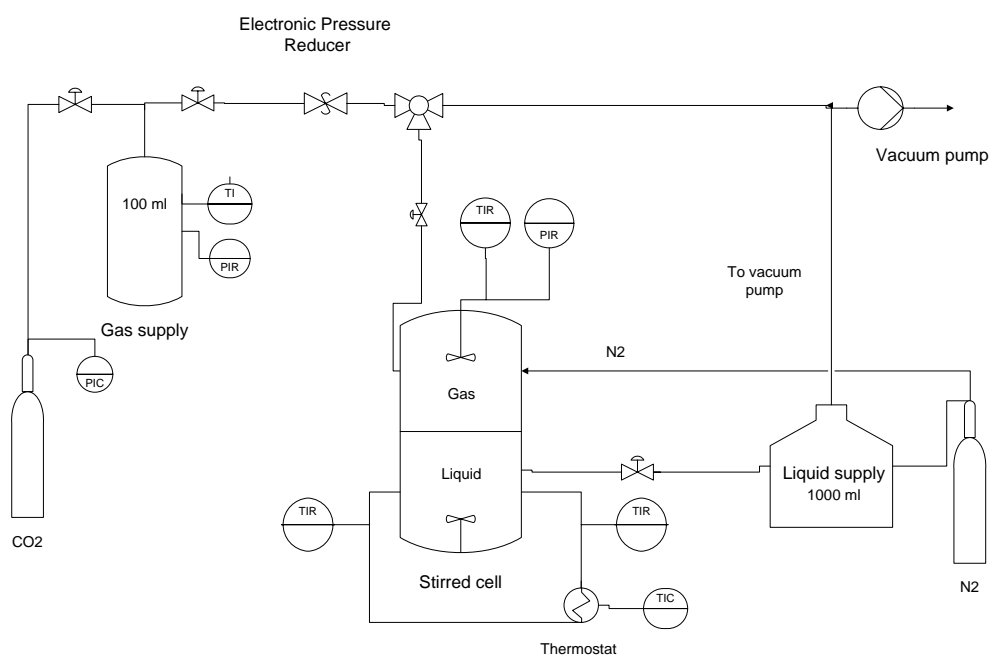


**Figure 2.1: Setup**

The absorption rate experiments needed to derive the kinetics of the reaction of CO<sub>2</sub> with OH<sup>-</sup> were carried out in a stirred vessel with a smooth gas-liquid interface. The reactor was operated batchwise with respect to the gas and liquid phases (see Figure 2.1). A similar setup was used by Derks et al. (2006) for measuring fast reaction kinetics hence the setup is only shortly described here. The reactor was completely made of glass, thermostatted and consisted of an upper and lower part, sealed gas tight using an O-ring and screwed flanges. The reactor was equipped with magnetic stirrers in the gas (upper) and in the liquid phase (lower). The stirring speed could be controlled independently of one another. The dynamic

pressure in the gas supply vessel was measured using a digital pressure transducer (Druck) while a constant pressure in the reactor was maintained by using a pressure controller (Brooks 5866). The pressure in the reactor was monitored by a pressure transducer (Dresser), with a maximum absolute deviation of 0.15 mbar under the experimental conditions applied. Furthermore the temperatures in the reactor and the gas supply vessel were measured by means of PT 100 elements. Pressures and temperatures were digitally recorded every second. The typical temperatures in the reactor and the CO<sub>2</sub> gas supply vessel were around 298 K and measured exactly during each experiment.

The partial CO<sub>2</sub> pressure in the reactor was set at a pressure between 6 and 16 mbar. The total volume of the reactor was 1070 ml whereof around 600 ml was filled with hydroxide solution. The horizontal gas-liquid contact area in the reactor was determined to be 71.5 cm<sup>2</sup>. The gas supply vessel had a volume of 100 ml and the pressure in that vessel at the start of an experiment was close to 5 bar. The experimental procedure for a batch experiment was as follows: a freshly prepared alkaline-salt solution was charged into an evacuated reactor from the liquid supply vessel where it was shortly degassed under vacuum to remove possibly dissolved ambient gas. After that, the vapor-liquid equilibrium was allowed to establish in the reactor and the vapour phase pressure ( $p_{vap}$ ) was noted. Pure CO<sub>2</sub> from the gas supply vessel was introduced into the reactor at a desired set-pressure which was maintained by the pressure controller. The CO<sub>2</sub> pressure was chosen to meet the conditions for absorption in the so-called pseudo first reaction regime (Danckwerts, 1970) under the respective experimental conditions. The stirrer in both phases was turned on and the pressure in the gas supply vessel was monitored for around 300 s. The pressure decrease in time is due to the absorption of CO<sub>2</sub> in the liquid and can be related to the kinetics if the experiments are carried out in the pseudo first order absorption regime.

Some experiments have been carried out to measure the physical solubility of N<sub>2</sub>O. The physical solubility of N<sub>2</sub>O is related to the physical CO<sub>2</sub> solubility via the well-known N<sub>2</sub>O/CO<sub>2</sub> analogy (Laddha et al., 1981). For these measurements the procedure was slightly different than described above (see also Versteeg and Vanswaaij

(1988)). In this case, after admittance of  $N_2O$  to the reactor, the valve between the supply vessel and the reactor was directly closed and thereafter equilibrium was awaited. The difference between the initial and end pressure of  $N_2O$  in the reactor can be used to determine the physical solubility of  $N_2O$  in the solution, and, therewith, the physical solubility of  $CO_2$  in the same solution can be estimated. The experimental procedure was validated with solubility experiments of  $N_2O$  in water, for which extensive and reliable literature data are available (Versteeg and Vanswaaij (1988), Xu et al. (1991)). The physical solubility of  $N_2O$  as obtained for these validation experiments was within 5% of literature data.

## 2.3 Chemicals

Carbon dioxide (> 99.99 Vol.%; Hoekloos) was used without further purification. Sodium hydroxide (> 99% mass), Sodium chloride (> 99.5% mass), Lithium chloride (> 99% mass) and Potassium chloride (> 99.5% mass) were purchased from Merck and used as received. The solutions were prepared using deionized water and the actual hydroxide concentration was determined by potentiometric titration.

## 2.4 Determination of the reaction rate constant from experimental data

For fast gas-liquid reactions, a reliable determination of the forward reaction rate constant using an analytical evaluation method is only possible for irreversible pseudo-first-order reaction conditions as only in that regime an accurate analytical expression for the enhancement factor can be found (van Swaaij and Versteeg, 1992). Moreover, in the pseudo first order regime the mass transfer coefficient is not required for the evaluation of the experiments. Hence a possible error introduced by the application of the mass transfer coefficient can be avoided. For irreversible reactions, reactions in the pseudo-first-order regime have to fulfill the subsequent

two conditions:

$$Ha > 3 \quad (2.3)$$

$$\frac{E^\infty}{Ha} > 5 \quad (2.4)$$

The Hatta-number for a pseudo-first-order reaction is defined by Hikita and Asai (1976):

$$Ha = \frac{\sqrt{k_1 \cdot D_{CO_2-solution}}}{k_L} \quad (2.5)$$

with  $k_L$  being the mass transfer coefficient and  $k_1$  being the pseudo-first-order reaction rate constant which traditionally reads as follows:

$$k_1 = k_{OH^-} \cdot c_{OH^-} \quad (2.6)$$

The enhancement factor for instantaneous, irreversible reactions in terms of the film theory is expressed as follows (Baerns et al., 1992):

$$E_\infty = 1 + \frac{D_{OH^-solution} c_{OH^-}}{D_{CO_2solution} c_{CO_2}^{interface}} \quad (2.7)$$

If the experimental conditions are chosen to obey the two relations 2.3 and 2.4, an approximate -but very accurate- analytical solution can be applied to interpret the experiments. The two above noted criteria (Eq. 2.3 and 2.4) have been checked after every experiment to ascertain the condition of a pseudo first order reaction: in all experiments referred to in this section the conditions of an irreversible pseudo-first order reaction have been met. If the conditions for a pseudo first order reaction are fulfilled, the generic  $CO_2$  absorption rate ( $J_{CO_2} A$ ) is given by e.g. Kumar et al. (2003):

$$J_{CO_2} A = \sqrt{k_1 D_{CO_2-solution}} m_{CO_2,solution} p_{CO_2,t} \left( \frac{A}{RT} \right) \quad (2.8)$$

In this expression the implicit assumption of the CO<sub>2</sub> concentration in the liquid bulk being zero is included. During the experiments the total pressure in the reactor was kept constant by the pressure controller. Hence the total pressure was in fact not depending on time. The partial pressure of CO<sub>2</sub> in the reactor was calculated from the experimentally observed pressure according to the following relation:

$$p_{CO_2, t=const.} = p_{tot, t=const.} - p_{vap} \quad (2.9)$$

The absorption rate can then be calculated from the dynamic pressure in the gas supply vessel:

$$J_{CO_2} A = \frac{dp_{Reservoir, t}}{dt} \cdot \frac{V_{Reservoir, t}}{RT_{Reservoir, t}} \quad (2.10)$$

## 2.5 Physical properties employed in the interpretation of the flux data

For the evaluation of the experimental data reliable physical data are needed. Both the diffusion coefficient of CO<sub>2</sub> in the hydroxide/salt solutions as well as the physical solubility of CO<sub>2</sub> in these solutions are physical properties required for the evaluation of the experimental data. The dimensionless physical solubility of CO<sub>2</sub> in the hydroxide-salt solution has been estimated with the model suggested by Schumpe (1993). In this model the dimensionless solubility of CO<sub>2</sub> in mixed electrolyte solutions is given as:

$$m_{CO_2, solution} = m_{CO_2, water} \left( \frac{c_{g,0}}{c_g} \right)^{-1} \quad (2.11)$$

where the ratio  $c_{g,0}/c_g$  is defined as:

$$\log \left( \frac{c_{g,0}}{c_g} \right) = \sum_i (h_i + h_g) c_i \quad (2.12)$$



The parameters  $h_i$  and  $h_g$  for the species of interest are given in Table 2.1 (Schumpe, 1993). To validate Schumpe's method for the estimation of the physical solubility of  $\text{CO}_2$  in reactive solutions (as described by Eq. 2.11 and 2.12), a limited number of experimental determinations of the physical solubility of  $\text{N}_2\text{O}$  in hydroxide-salt solutions containing  $1.5 \text{ kmol/m}^3$  of the particular salt has been carried out according to the method as described in section 2.2.

The experimental  $\text{N}_2\text{O}$  solubility was converted to the  $\text{CO}_2$  solubility by using the well known  $\text{CO}_2/\text{N}_2\text{O}$  analogy (Laddha et al., 1981) to be able to compare the experimentally determined solubility to the  $\text{CO}_2$  solubility predicted by Schumpe's method.

**Table 2.1:** Parameters needed for the determination of the dimensionless  $\text{CO}_2$  solubility (Schumpe, 1993)

Cation	$h_i \text{ m}^3 \text{ [kmol}^{-1}\text{]}$	Anion	$h_i \text{ m}^3 \text{ [kmol}^{-1}\text{]}$	Gas	$h_i \text{ m}^3 \text{ [kmol}^{-1}\text{]}$
Li	0.0691	$\text{OH}^-$	0.0756	$\text{CO}_2$	- 0.0183
Na	0.1171	$\text{Cl}^-$	0.0334		
K	0.0959				

The values reported in Table 2.2 are dimensionless physical solubilities ( $m_{\text{CO}_2\text{-Solution}}$ ) but can also be converted to the frequently encountered Henry coefficient using Equation 2.13.

$$m_{i,j} = \frac{H_i}{RT} = \frac{(p^{\text{Initial}} - p^{\text{EQ}})}{p^{\text{EQ}}} \frac{V_{\text{gas}}}{V_{\text{liquid}}} \quad (2.13)$$

The experimentally derived dimensionless physical solubilities reported in Table 2.2 are approximately 20% lower compared to those estimated with Schumpe's method (Schumpe, 1993). Assuming the  $\text{CO}_2/\text{N}_2\text{O}$  analogy also holds for these

**Table 2.2:** Dimensionless physical solubility  $m_{CO_2-Solution}$  of  $CO_2$  in caustic salt solutions derived from 1) Schumpe's method and 2)  $N_2O$  solubility experiments

$c_{NaOH}$ [kmole m <sup>-3</sup> ]	Salt	$c_{Salt}$ [kmole m <sup>-3</sup> ]	$m_{CO_2-Solution}$ [-] Schumpe	$m_{CO_2-Solution}$ [-] Own measurements
1.7558	LiCl	1.47	0.31	0.26
0.986	LiCl	1.5	0.42	0.36
1.9181	NaCl	1.5	0.24	0.21
0.9876	NaCl	1.5	0.35	0.32
1.9382	KCl	1.5	0.26	0.22
0.979	KCl	1.5	0.38	0.32

solutions, this indicates that the physical solubility of  $CO_2$  in caustic salt solutions seems to be overpredicted with Schumpe's method with about 20% for all experiments. Nevertheless the estimation method exhibits the same trend as the (indirectly) measured  $CO_2$  solubility and also predicts a substantially higher  $CO_2$  solubility of solutions containing LiCl.

As experimental  $N_2O$  data were not determined for all combinations/concentrations of salts mixtures, no attempt has been made to adapt Schumpe's parameters and it was decided to utilize the physical solubilities estimated by Schumpe's method to evaluate the experimental absorption rate experiments to maintain consistency throughout this study.

The diffusivity of  $CO_2$  in aqueous electrolyte solutions as needed in Eq. 2.8 was calculated from the application of the Stokes-Einstein relationship (Eq. 2.14) and the diffusivity of carbon dioxide in water as given by Danckwerts (1970). The use of the Stokes-Einstein relationship is generally accepted in this form to calculate the diffusion coefficient of carbon dioxide in hydroxide solutions (Nijsing et al. (1959), Kucka et al. (2002)).

$$D_{\text{Solution}} \mu_{\text{Solution}} = D_{\text{water}} \mu_{\text{water}} = \text{const.} \quad (2.14)$$

$$\log D_{\text{CO}_2\text{-water}} = -8.176 + \frac{712.5}{T[\text{K}]} - \frac{2.591 \cdot 10^5}{T[\text{K}]^2} \quad (2.15)$$

The viscosities of hydroxide-salt solutions containing 1.5 kmol/m<sup>3</sup> and 0.5 kmol/m<sup>3</sup> of the particular salt have been experimentally determined. The kinematic viscosities have been measured with a Lauda Processor - Viscosity - System 2.49e. This semi-automated system comprises of an oil thermostat bath -in which the standardized capillary is immersed- and a control unit. The temperature of the oil bath could be controlled within +/- 0.1°C. The control unit is linked to a computer to program the control unit and to read out and store the residence times of the fluids in the capillary. The viscosity of every solution listed below has been measured five times. The deviation of the residence time was in all cases less than 3 seconds. This corresponds to an error of around 2-3% in the derived value of the diffusion coefficient. The measured kinematic viscosities are listed in Table 2.3.

For deriving the dynamic viscosities from the experimentally determined kinematic viscosities the following basic equation was applied (Bird et al., 1960):

$$\nu \cdot \rho = \mu \quad (2.16)$$

As there are no data available on the density for the mixtures used in the experiments presented here, an estimation method had to be used. According to Sipos et al. (2001) the density of a pure NaOH/water mixture at 25°C can be calculated with the following relation:

$$\rho = \rho_{\text{H}_2\text{O}} + 46.92210 m_{\text{OH}^-} - 4.46892 m_{\text{OH}^-}^{1.5} \quad [\text{g}/\text{cm}^3] \quad (2.17)$$

**Table 2.3:** Viscosities of salt solutions at 25C

$c_{NaOH}$ [kmole m <sup>-3</sup> ]	Salt	$c_{Salt}$ [kmole m <sup>-3</sup> ]	$\nu$ [mm <sup>2</sup> s <sup>-1</sup> ]
0	LiCl	0.5	0.9811
1.006	LiCl	0.5	1.1415
1.983	LiCl	0.5	1.3810
0	LiCl	1.5	1.0981
0.986	LiCl	1.5	1.3149
1.7558	LiCl	1.5	1.5465
0	NaCl	0.5	0.9498
0.9010	NaCl	0.5	1.1041
1.9468	NaCl	0.5	1.3434
0	NaCl	1.5	0.9948
0.9876	NaCl	1.5	1.2297
1.9181	NaCl	1.5	1.5255
0	KCl	0.5	0.9045
1.0014	KCl	0.5	1.0610
1.9592	KCl	0.5	1.2792
0	KCl	1.5	0.8531
0.9790	KCl	1.5	1.0497
1.9382	KCl	1.5	1.2934

In this work it has been assumed that by replacing the molality  $m_{OH^-}$  in Equation 2.17 by the total anion molality of the solution, the density of a mixed NaOH/salt/water mixture can be estimated. Although this seems like a rough approach, the following will show that it yields very acceptable results for the solutions of importance in this study.

First experimental liquid density data of the pure salt/water solutions (NaCl, KCl,

LiCl and NaOH) (Lide, 2004) at 20°C were compared at a concentration of 3.5 mol/l (highest total concentration used in this study), as the difference in density is expected to increase with concentration. The experimental liquid density data from Lide (2004) have been used for interpolation to compare the liquid densities at exactly 3.5 mol/l. The LiCl solution has a density of 1.079 g cm<sup>-3</sup>, the KCl solution a density of 1.153 g cm<sup>-3</sup> and the NaCl solution a density of 1.133 g cm<sup>-3</sup> whereas a 3.5 mol/l NaOH solution has a liquid density of 1.135 g cm<sup>-3</sup>.

From the values given in the previous paragraph it can be concluded that all density values are within 6.5% of each other. Secondly, considering now that a 3.5 mol/l salt solution as used in this study always contains 2 mol/l NaOH and 1.5 mol/l of LiCl, NaCl or KCl respectively, the density difference among these three 3.5 mol/l solutions is most likely lower than 6.5%. The density difference of a pure salt/water solution (LiCl, NaCl and KCl, respectively) at 2 mol/l and 3.5 mol/l has been calculated based on the experimental data of Lide (2004) and simply added to the liquid density of a 2 mol/l NaOH solution to obtain an estimated density (assuming ideal mixing) for the mixture.

When comparing these "estimated" NaOH/salt/water densities with the liquid density of a single 3.5 mol/l NaOH solution as predicted by Equation 2.17, the relative differences were as follows: LiCl containing solution difference <2.0%, NaCl containing solution difference <0.2% and KCl containing solution difference <0.9%.

These differences are so small, that it seems justified to estimate the densities of the solutions using the total anion molality in Equation 2.17. The deviation of the  $k_{OH^-}$  values for LiCl-doped solutions due to uncertainty in the density (which affects the estimate of the viscosity and therewith the estimated diffusion coefficient) is estimated to be less than 2%. For NaCl-doped solutions this deviation is less than 0.5% and for KCl-doped solutions less than 1%.

It must be noted that some input parameters, like the physical solubility of CO<sub>2</sub> in the corresponding salt solution and the viscosity of the salt solution (which affects the value of the estimated corresponding diffusion coefficient, see Eq. 2.14), have a strong influence on the derived reaction rate constant as determined using Eq. 2.8.

In this study, the required physical properties needed in the interpretation of the experiments (e.g. physical solubility of CO<sub>2</sub>, diffusion coefficient of CO<sub>2</sub> in the solution) have always been evaluated at the actual composition of the solvent used and the actual reaction temperature of 25°C. Considering the uncertainty in the aforementioned physical parameters and the experimental error in the current experiments, the overall uncertainty in the reaction rate constant is estimated to be 10%.

## 2.6 Experimental Results and their interpretation using the traditional approach

For validation purposes absorption rate experiments of CO<sub>2</sub> in "pure" sodium hydroxide/water solutions have been carried out in the setup as described in section 2.2, as for this solution many literature data on the kinetics are available. The experimental results of these validation experiments have been evaluated according to the method described in Section 2.4 of this study. The kinetic constants, as derived from the validation experiments carried out at different OH<sup>-</sup>-concentrations have been fitted to an OH<sup>-</sup> concentration dependent equation having the form:

$$k_{OH^-}(T, I) = k_{OH^-}^{inf}(T = 25^\circ C) \cdot 10^{P_1 \cdot c_{OH^-}^2 + P_2 \cdot c_{OH^-}} \quad (2.18)$$

This equation has also been used by Pohorecki and Moniuk (1988). The applied fit criterion was the minimization of the squared errors between the measured  $k_{OH^-}$ -values and the corresponding fitted values which yielded  $k_{OH^-}^{inf} = 9904 \text{ m}^3 \text{ kmol}^{-1} \text{ s}^{-1}$ ,  $P_1 = -4.51 \cdot 10^{-3} \text{ kmol}^2 \text{ m}^{-6}$  and  $P_2 = 0.155 \text{ kmole m}^{-3}$ . The resulting fit and the experimental data points are depicted in Figure 2.2.

The maximum relative deviation between the rate constant derived from the present measurements and those of Pohorecki and Moniuk (1988) amounts to 14%, obtained for a hydroxide concentration of 0.8 kmol/m<sup>3</sup>. For all other concentrations the difference between the prediction based on the experiments from this work and the

prediction by the relation of Pohorecki was less than 10%. It can be concluded that the presently used experimental setup and procedure yields results that agree well with the results obtained with the correlation proposed by Pohorecki.

Moreover, the results also again clearly demonstrate that no real "constant" rate constant is encountered. To elucidate the influence of different cations on the reaction rate, experiments were carried out with NaOH-solutions to which LiCl, NaCl and KCl were added, respectively.

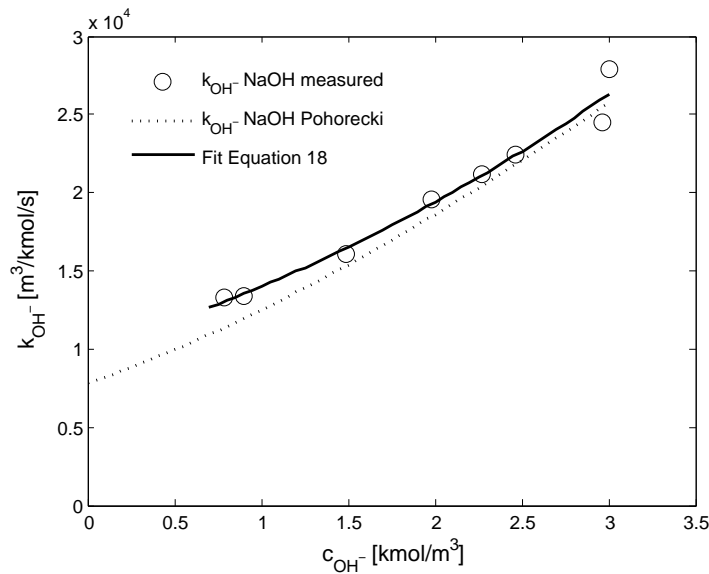


**Figure 2.2: Comparison between own measurements and results as predicted by Pohorecki for aqueous NaOH solutions.**

To study the influence of the type of cation on the reaction rate of CO<sub>2</sub> in a caustic solution, various solutions have been prepared and used. Table 2.4 below gives the matrix of all solutions employed in this study.

The results for the absorption of CO<sub>2</sub> in a sodium hydroxide solution with a varying amount of LiCl are presented in Figure 2.3. Note that in Figure 2.3 the kinetic constant is still expressed using the traditional approach, i.e. the reaction rate constant is based on the use of concentrations in the kinetic expression. The continuous line in Figure 2.3 is the curve for the kinetic rate constant in pure NaOH

**Table 2.4:** Matrix of solutions employed in the experimental study

$c_{NaOH}$ [kmole m <sup>-3</sup> ]	Salt	$c_{Salt}$ [kmole m <sup>-3</sup> ]
1.0	LiCl/NaCl/KCl	0.5
1.0	LiCl/KCl	1.0
1.0	LiCl/NaCl/KCl	1.5
1.5	LiCl/NaCl/KCl	0.5
1.5	LiCl/NaCl/KCl	1.0
1.5	LiCl/NaCl/KCl	1.5
2.0	LiCl/NaCl/KCl	0.5
2.0	LiCl/NaCl	1.0
2.0	LiCl/NaCl/KCl	1.5

solutions as obtained using Equation 2.18.

As can be seen from Figure 2.3 the addition of LiCl generally diminishes the reaction rate constant as compared to a single "pure" NaOH solution, although the diminishing effect of the addition of LiCl is decreasing with a rising hydroxide concentration. This has also been reported in literature where it was stated that the effect of the lithium cation on the reaction rate constant is substantially smaller as compared to the effect of sodium or potassium cations (Nijsing et al. (1959), Pohorecki and Moniuk (1988)).

As can be seen in Figure 2.4, the sodium cation indeed has a more distinct effect on the reaction rate constant  $k_{OH^-}$  than the lithium ion, and that effect increases with the concentration of sodium ions. At the highest concentration of NaCl added (1.5M), the reaction rate constant is almost 1.5 times larger compared to the pure NaOH solution.

The effect of adding potassium chloride to a sodium hydroxide solution is even



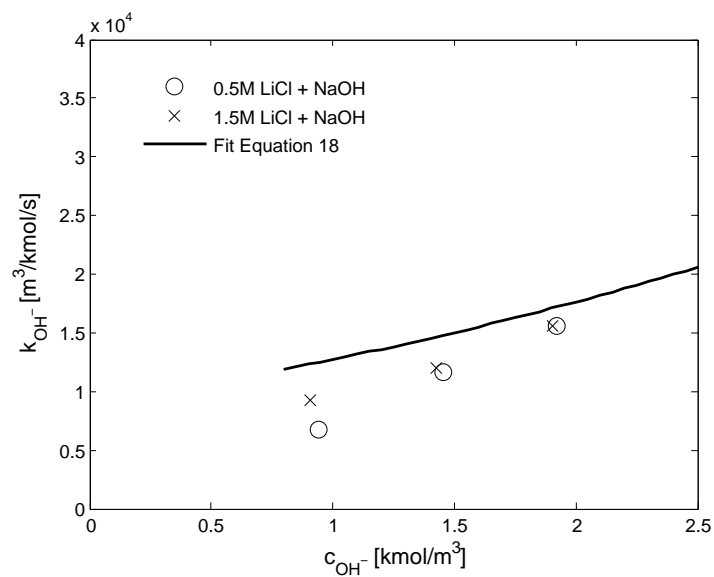


Figure 2.3: Dependence of the reaction rate constant on the amount of dissolved  $\text{LiCl}$ . Kinetic rate constant based on the use of concentrations.

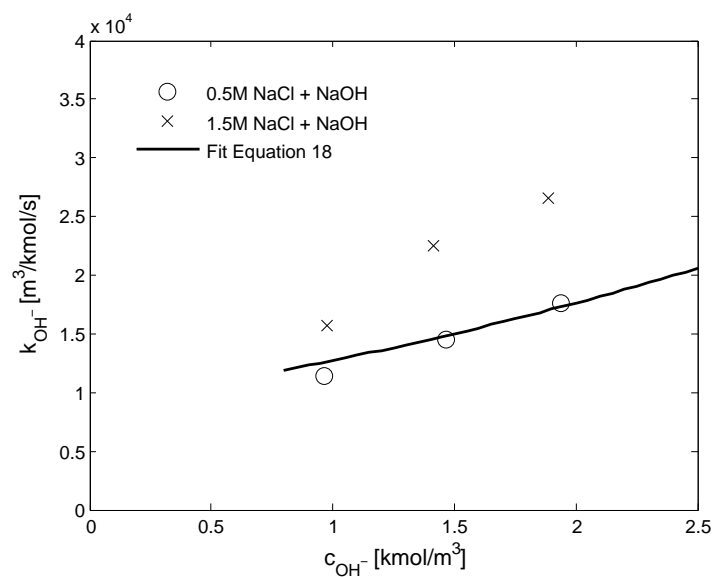
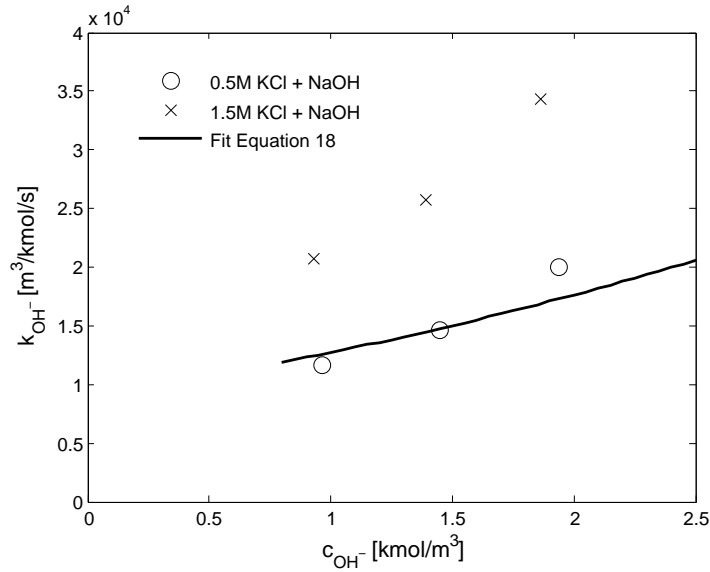


Figure 2.4: Dependence of the reaction rate on the amount of dissolved  $\text{NaCl}$ . Kinetic rate constant based on the use of concentrations.



**Figure 2.5: Dependence of the reaction rate on the amount of dissolved KCl. Kinetic rate constant based on the use of concentrations in the kinetic expression.**

more pronounced than the effect of the addition of sodium chloride (see Figure 2.5). In this case the reaction rate constant for a 1.5M KCl solution is almost doubled as compared to a pure NaOH solution. This phenomenon is completely in line with the previous findings of Nijsing et al. (1959) and Pohorecki and Moniuk (1988) who reported that the reaction rate constant for the reaction of CO<sub>2</sub> in potassium hydroxide solutions is larger than in sodium hydroxide solutions.

From Figures 2.3, 2.4, 2.5 and Table 2.5 it can be concluded that it is not possible to arrive at a 'constant' rate constant in case only concentrations are used for the description of the reaction rate expression. Moreover, for solutions with identical ionic strength but different added salt, large differences are encountered for the rate constants ( see Table 2.5).

As already proposed by Haubrock et al. (2005) the experiments will be reevaluated with the aid of activity coefficients. Before it is possible to reinterpret the current results using an activity based approach, first a link between the concentra-

tion and the activity must be established. This will be done using the equilibrium model as described in the next section.

**Table 2.5:** Dependence of the reaction rate constant  $k_{\text{traditional}}$  on the Ionic strength (I)

$c_{\text{NaOH}}$ [kmole m <sup>-3</sup> ]	Salt	$c_{\text{Salt}}$ [kmole m <sup>-3</sup> ]	I [kmole m <sup>-3</sup> ]	$k_{\text{traditional}} (= k_{\text{OH}^-})$ [m <sup>3</sup> kmol <sup>-1</sup> s <sup>-1</sup> ]
0.9402	LiCl	0.5	1.4402	6769
0.9650	NaCl	0.5	1.4650	11377
0.9638	KCl	0.5	1.4638	11648
1.4528	LiCl	0.5	1.9528	11621
1.4650	NaCl	0.5	1.9650	14542
1.4503	KCl	0.5	1.9503	14570
1.9202	LiCl	0.5	2.4202	15612
0.9098	LiCl	1.5	2.4098	9297
1.9370	NaCl	0.5	2.4370	17660
0.9739	NaCl	1.5	2.4739	15736
1.9363	KCl	0.5	2.4363	20053
0.9302	KCl	1.5	2.4302	20869
1.4267	LiCl	1.5	2.9267	11957
1.4125	NaCl	1.5	2.9125	22503
1.3937	KCl	1.5	2.8937	25780
1.9028	LiCl	1.5	3.4028	15613
1.8850	NaCl	1.5	3.3850	26593
1.8652	KCl	1.5	3.3652	34272

## 2.7 Equilibrium model

### 2.7.1 Thermodynamic model

In this section the thermodynamic model used in the re-interpretation of the experiments will be described. For the vapor-liquid equilibrium of the system  $\text{CO}_2$ - $\text{NaOH}$ -Salt- $\text{H}_2\text{O}$  it has been assumed that the only species present in the gas phase, are  $\text{CO}_2$  and  $\text{H}_2\text{O}$ , respectively. Furthermore it will be assumed that all salts added are completely dissolved. The model presented here has been implemented in the simulation environment gProms.

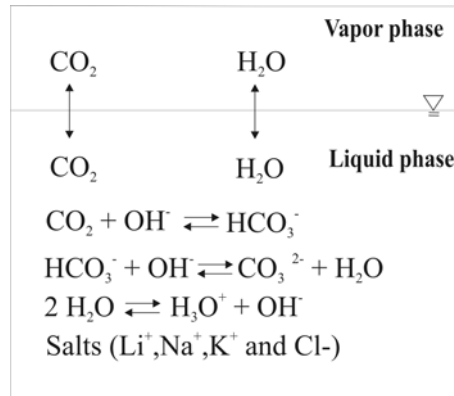
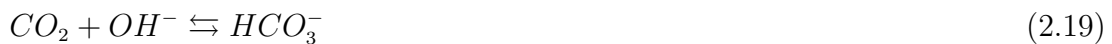


**Figure 2.6:** VLE and chemical reactions in the system  $\text{CO}_2 - \text{NaOH} - \text{H}_2\text{O} - \text{salt}$

In Figure 2.6 the system is schematically represented. In the liquid phase  $\text{CO}_2$ ,  $\text{H}_2\text{O}$ ,  $\text{OH}^-$  and the products of the chemical reactions as depicted in Figure 2.6 are present. The cations stemming from the different salts are not directly taking part in the reaction but influence the reaction rate considerably as shown in the previous section (see Table 2.5). For the description of the chemical reactions the temperature dependent equilibrium constants of the following reactions are taken into account:





In the liquid phase the condition for equilibrium as defined according to Rumpf and Maurer (1993) is used:

$$K_i^{EQ} = \prod_{i=1}^3 (a_i^{\nu_i, EQ}) = \prod_{i=1}^3 (\gamma_i \cdot m_i)^{\nu_i, EQ} \quad (2.22)$$

The equilibrium constants for the reactions 2.19-2.21 together with the material balances for carbon and hydrogen as well as an electro-neutrality balance allow for the unique calculation of the composition of the liquid phase. Activity coefficients in the equilibrium equations are introduced to take the non-ideality of the liquid phase into account. The material balances applied in this model are as follows:

$$\text{Carbon-balance:} \quad n_{\text{CO}_2}^0 = n_{\text{CO}_2} + n_{\text{HCO}_3^-} + n_{\text{CO}_3^{2-}} \quad (2.23)$$

$$\begin{aligned} \text{Hydrogen-balance:} \quad 2 \cdot n_{\text{H}_2\text{O}}^0 + n_{\text{OH}^-}^0 &= 2 \cdot n_{\text{H}_2\text{O}} + n_{\text{OH}^-} + n_{\text{HCO}_3^-} \\ &+ 3 \cdot n_{\text{H}_3\text{O}^+} \end{aligned} \quad (2.24)$$

The electro-neutrality balance gives:

$$n_{\text{OH}^-} + n_{\text{HCO}_3^-} + 2 \cdot n_{\text{CO}_3^{2-}} + n_{\text{Cl}^-} - n_{\text{H}_3\text{O}^+} - n_{\text{Na}^+} - n_{\text{Salt, cation}^+} = 0 \quad (2.25)$$

The phase equilibrium for water and carbon dioxide is described with the subsequent equations:

$$p \cdot y_w \cdot \phi_w'' = p_w^s \cdot \phi_w^s \cdot a_w \cdot \exp\left(\frac{v_w \cdot (p - p_w^s)}{R \cdot T}\right) \quad (2.26)$$

$$p \cdot y_{CO_2} \cdot \phi_{CO_2}'' = H_{CO_2,w}^m(T, p_w^s) \cdot m_{CO_2} \cdot \gamma_{CO_2}^* \exp\left(\frac{v_{CO_2,w}^\infty \cdot (p - p_w^s)}{R \cdot T}\right) \quad (2.27)$$

As it can be seen from the above listed equations the model requires the knowledge of a number of parameters like the equilibrium constants  $K_1^{EQ}$  to  $K_3^{EQ}$ , the activities  $\gamma_i^*$  of all species in the liquid phase, Henry's constant for carbon dioxide dissolved in pure water ( $H_{CO_2,w}^m$ ), the vapor pressure ( $p_w^s$ ), the molar volume ( $v_w$ ) of pure water and the partial molar volume ( $v_{CO_2,w}^\infty$ ) of carbon dioxide, as well as information on the fugacity coefficients  $\phi_w''$  and  $\phi_{CO_2}''$  in the gas phase. These parameters and their values are discussed in the Appendix.

It should be noted that the developed VLE model has not been experimentally validated as there is a lack of experimental VLE data. Nevertheless, the VLE model where only sodium hydroxide and  $CO_2$  are present has been validated with data taken from Rumpf et al. (1998). The current thermodynamic model predicts the experimentally determined overall pressures within an error of 6% if low pressure values ( $< 1$  bar) are excluded (Figure 2.7).

However, the deviation in terms of the predicted pressure at low loadings (low pressures) can be significant (up to 45%). Nevertheless, in the low loading region the activity coefficients as predicted by the model -being the actual parameters needed in the interpretation of the absorption rate experiments- are not showing a significant different behaviour than in the high loading regime (see Haubrock et al. (2005) for a comparison).

This means that the current prediction of the activity coefficients for  $CO_2$  and  $OH^-$  is considered to be sufficiently accurate to be used in the kinetic expression for at least "pure" NaOH solutions.

It might be expected that the error in terms of VLE data is larger for mixed electrolyte systems than for the 'simple' sodium hydroxide- $CO_2$  system. One reason

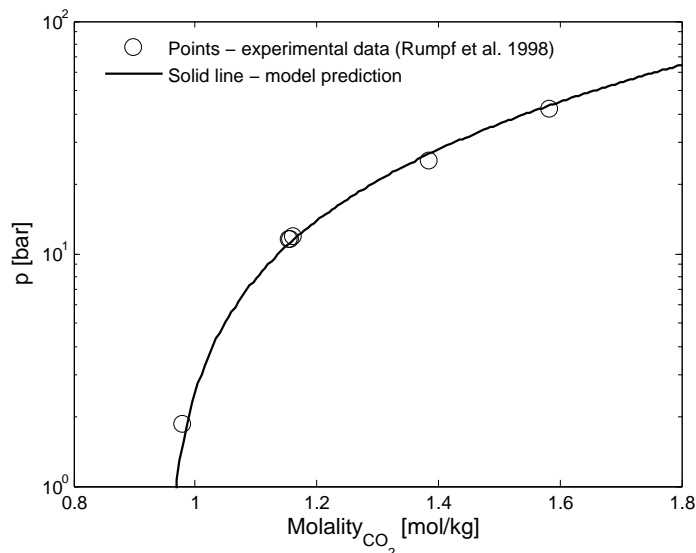


**Figure 2.7:** Comparison of experimental data with the VLE model of CO<sub>2</sub>-NaOH-H<sub>2</sub>O

leading to this assumption is that for NaOH/salt solutions more interaction parameters are needed than for a NaOH solution alone, and, moreover, not all required interaction parameters are stemming from the same literature source (especially for solutions containing LiCl). This might introduce errors in the predicted values of the activity coefficients of CO<sub>2</sub> and OH<sup>-</sup> which are difficult to quantify at this stage.

## 2.8 Experimental Results and their interpretation using the activity based approach

In section 2.6 the experimental absorption rate data have been interpreted using the conventional approach i.e. using "only" concentrations in the reaction rate expression. That section showed that there is a substantial influence of the kind of cations being present in the solution and the concentration of the cations on the reaction rate constant, respectively.

In this section the experimental results will be reinterpreted using the activity coefficients of the reacting species in the reaction rate expression.

From a fundamental thermodynamic point of view the kinetics of reaction 1 should be written in terms of activities to be consistent with the activity based equilibrium constant (see Eq. 2.22). The suggested reaction rate equation for the forward reaction of  $\text{CO}_2$  and  $\text{OH}^-$  to  $\text{HCO}_3^-$  is thus written as follows:

$$r^m = k_{\text{OH}^-}^m(\gamma) \cdot a_{\text{CO}_2} \cdot a_{\text{OH}^-} \quad (2.28)$$

where the activity  $a_{\text{CO}_2}$  is equal to the product  $m_{\text{CO}_2} \gamma_{\text{CO}_2}$  and the activity  $a_{\text{OH}^-}$  is equal to  $m_{\text{OH}^-} \gamma_{\text{OH}^-}$ , respectively. To obtain the activity based reaction rate constants the values as derived for the concentration based rate expression can be used. The relation between the two of them can be shown to be (see Appendix for derivation):

$$k^m(\gamma)_{\text{OH}^-} = \frac{k_{\text{OH}^-}}{\gamma_{\text{OH}^-} \gamma_{\text{CO}_2}} \frac{\rho^2}{\left(\rho - \sum_{\text{all ions } i} c_i M_i\right) \left(1 + \sum_{\text{all ions } i} m_i M_i\right)^2} \quad (2.29)$$

Applying Equation 2.28 is supposed to have two advantages compared to the traditional concentration based rate expression. Firstly, the change of the solution density (especially at a higher ionic strength) is accounted for by using molalities instead of density dependent concentrations. Secondly it is expected that the introduction of activity coefficients in the reaction rate equation will diminish the influence of the different ions on the reaction rate constant and moreover the dependence of the reaction rate constant on the ionic strength.

The results of applying the activity based approach and the traditional approach to the system  $\text{NaOH-CO}_2\text{-water}$  is shown in Figure 2.8 (see also Haubrock et al. (2005)).

For the  $\text{NaOH-CO}_2\text{-water}$  system the difference between molalities and concentrations in the applied range of concentrations was always less than 1% therefore in



Figure 2.8 it has been decided to use concentrations as the x-coordinate for the sake of simplicity. The black solid line is representing the kinetic rate constant for the pure NaOH system according to the activity based approach and will be used in the following Figures as a reference to assess the results for the NaOH-CO<sub>2</sub>-salt-water system. The activity based reaction rate constant has a value of approximately 16500 kg kmol<sup>-1</sup> s<sup>-1</sup> and is nearly constant for sodium hydroxide concentrations between 1 and 3 kmol/m<sup>3</sup> (see Figure 2.8).

From Figure 2.8 it can be concluded that the use of activity based kinetics indeed results in a near constant rate constant! However, it must be noted that at lower values of the ionic strength the value of the rate constant is somewhat lower (< 10%). This deviation can probably be attributed on the one hand to uncertainties in the physical parameters used in the interpretation of the experiments and on the other hand on the use of the presently developed equilibrium model which is used to estimate the required activity coefficients.

The values of the activity coefficients of CO<sub>2</sub> and the OH<sup>-</sup> anion according to the Pitzer equilibrium model (Section 2.7) are shown in Figures 2.9 and 2.10. The activity coefficients are plotted for the systems NaOH-LiCl, NaOH-NaCl and NaOH-KCl. For a comparison the activity coefficients of a pure NaOH solution are also shown.

In case of a pure NaOH solution the activity coefficient of OH<sup>-</sup> steeply decreases from unity until a hydroxide concentration of 0.5 M and then increases slightly again. This behavior cannot be observed for the other solutions. This is due to the fact that the ionic strength is equal to zero for a pure sodium hydroxide solution at an hydroxide molality of zero (i.e. water) whereas the doped solutions already contain 1.5 mol kg<sup>-1</sup> salt at a hydroxide concentration of zero. Hence the ionic strength of the doped solutions is well above zero and therefore the course of the OH<sup>-</sup> activity coefficient of pure NaOH is different from the others.

It can be clearly seen that the activity coefficients of OH<sup>-</sup> are well below unity for mixtures containing LiCl and NaCl whereas the activity coefficient of the KCl containing mixture is slightly above unity. The activity coefficients of CO<sub>2</sub> for all

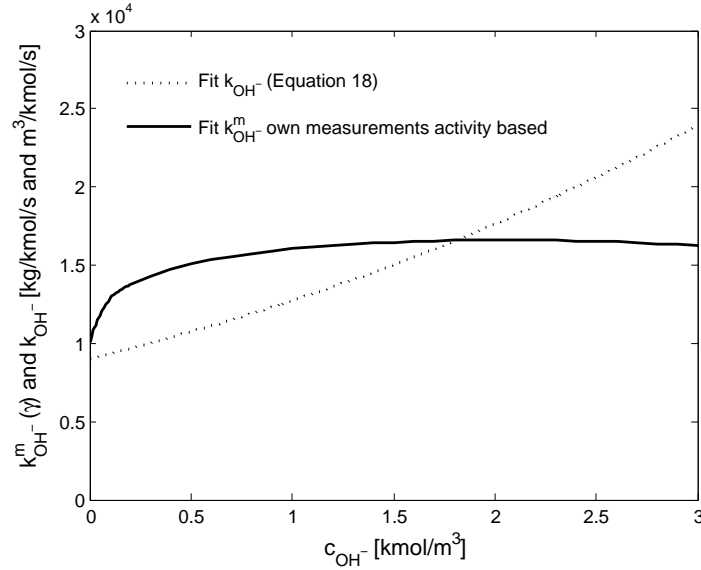


**Figure 2.8: Comparison between the kinetic constant derived with the traditional approach and the activity based approach for the system NaOH-CO<sub>2</sub>-water**

three salt mixtures are starting at values above unity and do substantially increase with rising hydroxide concentration.

The activity coefficient of CO<sub>2</sub> in the three doped solutions has a larger value at a hydroxide molality of zero. This fact can be attributed to the higher ionic strength of the doped solutions. Nevertheless the shape of the curves is not altered by the unequal ionic strength. Looking at the structure of the equations used in the Pitzer approach (see Rumpf et al. (1998)) and keeping in mind that 'only' the interaction parameter  $\beta_0$  (see Table 2.11) is employed to calculate the activity coefficients of CO<sub>2</sub>, it could be expected that the shape of the curve would barely change.

The CO<sub>2</sub> and OH<sup>-</sup> activity coefficients of the mixture containing LiCl are clearly below the values for the mixtures containing NaCl and KCl salts, respectively. Nevertheless, the dependency of the activity coefficients of CO<sub>2</sub> and OH<sup>-</sup> on the hydroxide concentration seems to be the same for all three salts.

As it can be seen in section 2.6 the influence of the addition of LiCl to the

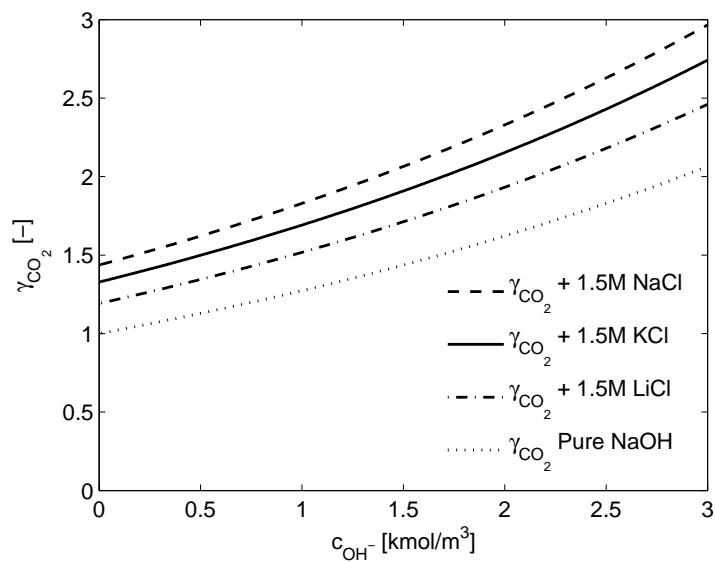


**Figure 2.9: Activity coefficients of CO<sub>2</sub> as a function of the hydroxide concentration**

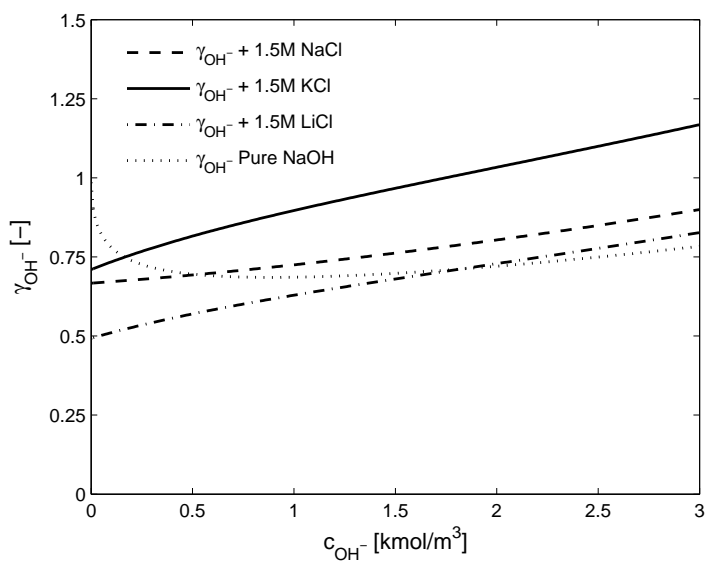


**Figure 2.10: Activity coefficients of OH<sup>-</sup> as a function of the hydroxide concentration**

caustic solution on the reaction rate constant is least pronounced if compared to the two other salts, i.e. NaCl and KCl. This was also expected as in pure lithium hydroxide solutions only a limited effect of the LiOH concentration on the reaction rate constant was observed (Pohorecki and Moniuk, 1988). In the following the impact of using activity coefficients in the reaction rate equation will be presented. First the effect of using activities for the most non-ideal system containing potassium chloride will be shown; subsequently the three hydroxide-salt solutions will be compared among each other.

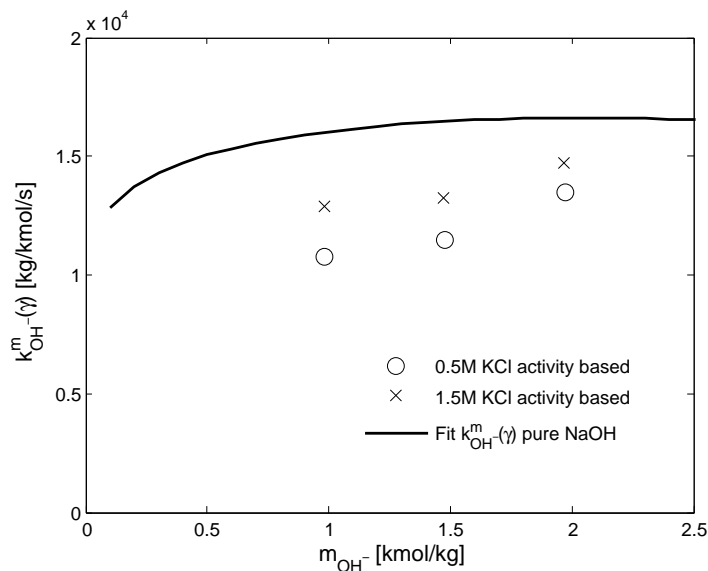


**Figure 2.11:** Comparison of the reaction rate constant using the new approach for NaOH solutions with added KCl in a molarity of 0.5 and 1.5 KCl (see also Figure 2.5)

In Figure 2.11 the values of the activity based reaction rate constant for two different potassium chloride concentrations are depicted. When compared to Figure 2.5 (showing the concentration based kinetic rate constant) it can be clearly seen that the influence of the potassium chloride concentration is dramatically decreased and the absolute values of the reaction rate constants for both potassium chloride concentrations are relatively close to each other and also close to the "new" reinter-

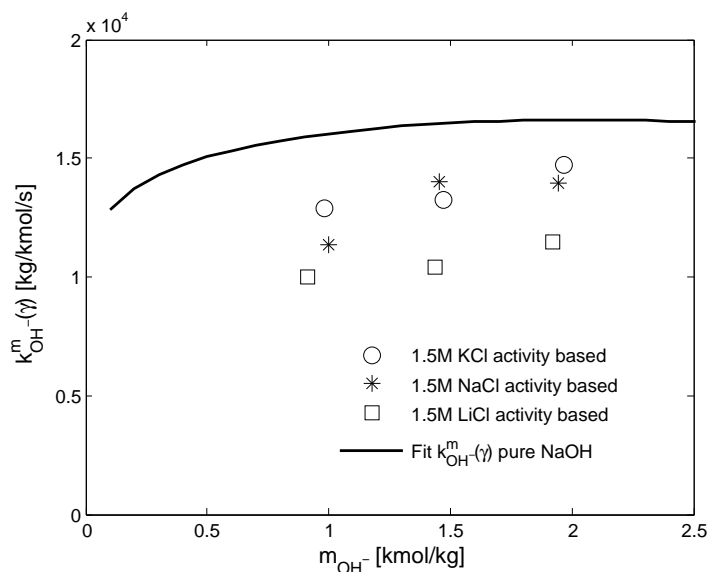


**Figure 2.12: Comparison of the reaction rate constant using the traditional and new approach for NaOH solutions with various salts added to it in a concentration of 1.5M.**

puted reaction rate constant for pure NaOH solutions. Furthermore, the absolute value of  $k_{OH^-}^m(\gamma)$  is only slightly ( $< 20\%$ ) increasing with the hydroxide concentration for both KCl concentrations and also for a "pure" NaOH solution.

As previously shown in Figure 2.4 and Figure 2.5 the values of the "traditional" reaction rate constant with added sodium chloride and potassium chloride are increasing with rising hydroxide concentration and the absolute values are all substantially higher than those for the pure sodium hydroxide solution. Furthermore the values of the reaction rate constant for the caustic sodium and potassium chloride solutions are diverging from each other with rising hydroxide concentration.

Applying activity coefficients in the reaction rate expression considerably reduces the dependence of the reaction rate constant on the ionic strength as shown in Figure 2.12. The activity based values of the reaction rate constant  $k_{OH^-}^m(\gamma)$  differ -in the investigated sodium hydroxide concentration range and for 1.5 M KCl or NaCl- less than 15% and 20% among each other, respectively.

The activity based reaction rate constant has a value of approximately  $16500 \text{ kg kmol}^{-1} \text{ s}^{-1}$  and is nearly constant for sodium hydroxide concentrations between 1 and 3  $\text{kmol kg}^{-1}$  (see Figure 2.8). With the exception of the activity based reaction rate constant  $k_{OH^-}^m(\gamma)$  of LiCl doped solutions, the  $k_{OH^-}^m(\gamma)$  values of KCl and NaCl doped solutions deviate only 20% and 30% from the average  $k_{OH^-}^m(\gamma)$  value of a the pure sodium hydroxide solution, respectively.

Moreover, by applying activity coefficients in the calculation of the reaction rate constant it is possible to compensate almost completely for the increase of the reaction rate constant with an increasing sodium hydroxide concentration. As can be seen from Figure 2.12 this holds for all three doped sodium hydroxide solutions as the value of the activity based reaction rate constant of one particular solution is nearly unchanged over the investigated sodium hydroxide concentration range.

As can be seen from Figure 2.12, the absolute values of the "new" reaction rate constant for the sodium and sodium-potassium salt solutions are merging to the same line - slightly below the pure NaOH line- if activity coefficients are applied in the reaction rate expression. Hence the application of activity coefficients in the reaction rate expression seems to reduce both the dependence of the reaction rate constant on the hydroxide concentration and on the type and concentration of cations being present in the solution.

In Figure 2.13 the activity based approach of hydroxide-salt solutions is compared to the 'base case' where  $\text{CO}_2$  is only absorbed in a sodium hydroxide solution.

This parity plot again clearly shows that the effect of adding the salts NaCl and KCl to NaOH can be well accounted for by introducing activity coefficients in the reaction rate constant. In case of LiCl doped NaOH solutions the result is still fair (within 40%) whereas it should be mentioned that the offset between the results for a LiCl doped solution and KCl/NaCl doped solutions seems to be systematic and near constant. Taking into account the fact that the kinetic constant for solutions where either sodium or potassium ions are present have substantially higher reaction rates -a factor 2 (NaCl) and a factor 2.5 (KCl) at 2 mol/l NaOH and 1.5 mol/l salt, respectively- the application of activity coefficients in the reaction rate

equation reduces the influence on the cations and the ionic strength considerably (see Figure 2.13).

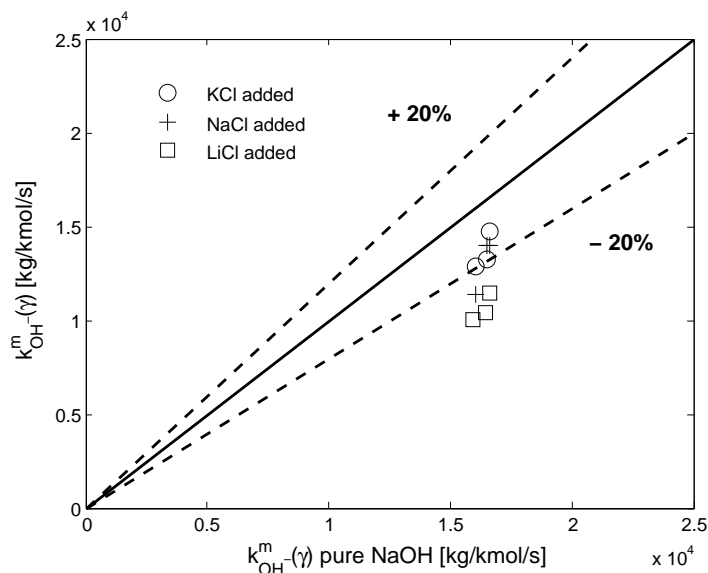


**Figure 2.13: Parity plot: Comparison of the activity based rate constants of pure NaOH and NaOH solutions containing the specified salts.**

The remaining difference (see Figure 2.12 and Figure 2.13) in the absolute values of the reaction rate constant might be explained with the accuracy of some input data:

- The activity coefficients needed for the calculation of the activities may be inaccurate. As an example of this, the interaction parameters for lithium have been taken from several different sources and it is likely that this will introduce errors.
- Furthermore the diffusion coefficients have been assumed to be reciprocally proportional to the viscosities of the salt (see Equation 2.14). Hence the diffusion coefficient does strongly depend on the viscosities whereas if e.g. a modified Stokes-Einstein relation would have been used (using an exponent of 0.8 (van Swaaij and Versteeg, 1992)) this influence would have been lower.

Using the modified Stokes-Einstein relationship would have resulted in lower values of the kinetic rate constant.

- The physical solubility of CO<sub>2</sub> has been determined using Schumpe's method. A preliminary comparison with experimentally derived CO<sub>2</sub> solubilities (based on the use of the N<sub>2</sub>O analogy) shows that this method might introduce errors in this parameter of approximately 20%.

A further reduction or elimination of these uncertainties will probably yield even better results for the new kinetic approach (i.e. further reduce the influence of the NaOH concentration on the kinetic rate constant for "pure" NaOH solutions and further close the gap between the kinetic rate constants as observed for NaOH solutions with different added salts).

However, a further elimination or reduction of the remaining uncertainties of the input data requires various complete new and extensive studies and is therefore beyond the scope of this thesis. The input data as used in the evaluation of the experimental absorption rate experiments have shown to be sufficiently accurate to be able to show the potential of the new kinetic approach.

## 2.9 Conclusion

In this study it has been shown that the kinetics of CO<sub>2</sub> and OH<sup>-</sup> in aqueous salt-solutions can be reasonably described with a single kinetic rate constant, if this constant has been determined using an activity based kinetic rate expression. Both, the influence of the hydroxide concentration and the concentration of the additionally added salt on the kinetic rate constant, were reduced significantly as compared to the kinetic rate constants using the traditional, concentration based, approach. The reaction rate constant  $k_{OH^-}^m(\gamma)$  derived using an activity based approach was calculated to be  $12500 \pm 2000 \text{ kg kmol}^{-1} \text{ s}^{-1}$ . This relatively small range in the kinetic rate constant is remarkable compared to the traditional concentration based approach where a huge (up to a factor of  $\sim 4$ ) difference between the reaction rate constants can be observed.



This means that in the activity based approach, the reaction rate constant is much more a real constant compared to the traditional approach. The scatter of the "new" reaction constant which can still be observed might be attributed to errors in the required chemical/physical input data used in the evaluation of the experimental data as e.g. the diffusion coefficients, physical solubility data and the interaction parameters needed for the determination of the activity coefficients.

Still, overall it seems that the new approach incorporating activities in the reaction rate expression is well suited to represent the kinetics of a non-ideal system as currently studied, and may also be suited to describe other non-ideal systems. Besides giving a uniform reaction rate constant, there is another profound reason to apply this method, especially so for reactive systems operated close to equilibrium. This is because, in the new approach non-idealities are not lumped in the reaction rate constant which makes the formulation of the kinetics, over the entire conversion range, consistent with the thermodynamically sound formulation of the chemical equilibrium, where also activities are employed.

Therefore the application of the new methodology is thought to be very beneficial especially in processes where "the thermodynamics meet the kinetics". Hence it is anticipated that the new kinetic approach will firstly find its major application in the modelling of integrated processes like Reactive Distillation, Reactive Absorption and Reactive Extraction where both, thermodynamics and kinetics, are of essential importance and activity coefficients deviate substantially from ideal behavior.

## **Acknowledgement**

The author gratefully acknowledges the financial support of Shell Global Solutions International B.V. Also, H. F. G. Moed is acknowledged for the construction of the experimental setup and S.F.P. ten Donkelaar for his part in the experimental work.

## **Notation**

$A_\phi$	Debye-Hueckel parameter
$A$	area, $m^2$
$a$	liquid phase activity, $\text{kmol kg}^{-1}$
$B_{CO_2,w}$	mixed virial coefficient $\text{CO}_2$ -water, $\text{cm}^{-3} \text{ mol}$
$c$	concentration, $\text{kmol m}^{-3}$
$C^\phi$	third virial coefficient in Pitzer's model, Pa or bar
$D$	relative dielectric constant of water
$e$	proton charge, C
$H_{CO_2}$	Henry's constant in the thermodynamic model, $\text{MPa kg mol}^{-1}$
$He$	Henry's constant, $\text{Pa m}^3 \text{ mol}^{-1}$
$I$	ionic strength, $\text{kmol m}^{-3}$
$J_{CO_2}$	Flux, $\text{mol s}^{-1} \text{ m}^{-2}$
$k$	Boltzmann's constant, $\text{J K}^{-1}$
$k_1$	Pseudo first order reaction rate constant, $\text{s}^{-1}$
$k_{OH^-}$	Second order reaction rate constant, $\text{m}^3 \text{ kmol}^{-1} \text{ s}^{-1}$
$k_{OH^-}^{inf}$	Second order reaction rate constant at infinite dilution, $\text{m}^3 \text{ kmol}^{-1} \text{ s}^{-1}$
$k_{OH^-}^m(\gamma)$	Second order reaction rate constant activity based, $\text{kg kmol}^{-1} \text{ s}^{-1}$
$k_L$	mass transfer coefficient, $\text{m s}^{-1}$
$K_i^{EQ}$	chemical equilibrium constant, [-] or $\text{kg mol}^{-1}$
$m_i$	molality of species $i$ , $\text{mol kg}^{-1}$
$m_{i,j}$	dimensionless solubility of a gas $i$ in a solution (solvent) $j$
$mass_i$	mass of component $i$ , kg
$M_i$	molar mass, $\text{kg mol}^{-1}$
$n$	mol of substance, mol
$N_A$	Avogadro's number
$p$	pressure, MPa
$P_1$	Fit parameter 1 in Equation 2.18, $\text{kmol}^2 \text{ m}^{-6}$
$P_2$	Fit parameter 2 in Equation 2.18, $\text{kmol m}^{-3}$
$r$	second order reaction rate, $\text{kmol m}^{-3} \text{ s}^{-1}$
$r^m$	second order reaction rate molality based, $\text{kmol kg}^{-1} \text{ s}^{-1}$
$R$	universal gas constant, $\text{J mol}^{-1} \text{ K}^{-1}$
$T$	temperature, K
$v$	partial molar volume, $\text{cm}^3 \text{ mol}^{-1}$
$V$	volume, $\text{m}^3$
$y$	mol fraction in the gas phase
$z$	number of charges
Greek symbols	
$\beta_{i,j}$	second virial coefficient, $\text{cm}^3 \text{ mol}^{-1}$
$\epsilon_0$	vacuum permittivity, $\text{C}^2 \text{ N}^{-1} \text{ m}^{-2}$
$\phi$	fugacity
$\gamma$	activity coefficient
$\nu$	stoichiometric coefficient

$\nu$	kinematic viscosity, $\text{m}^2 \text{s}^{-1}$
$\mu$	dynamic viscosity, $\text{Pa s}^{-1}$
$\rho$	density, $\text{kg m}^{-3}$
$\tau_{i,j,k}$	ternary interaction parameter
Others	
EQ	equilibrium
i	component i or index
interface	Phase interface liquid-gas
j	component j or index
k	component k or index
m	molality scale
s	saturated
$\infty$	at infinite dilution or infinite
0	initial value
"	gas phase
*	normalized to infinite dilution
w	water

## 2.A Brief outline of the Pitzer model

In the Pitzer model for the excess Gibbs energy of an aqueous, salt containing system the osmotic coefficient and the mean activity coefficients are represented by a virial expansion in terms of molalities (Pitzer, 1973). The Pitzer model has been applied successfully to numerous electrolyte systems. Beutier and Renon (1978) used a simplified form of Pitzer's model for the calculation of vapor-liquid equilibria in aqueous solutions of volatile weak electrolytes such as  $\text{NH}_3$ ,  $\text{CO}_2$  and  $\text{H}_2\text{S}$ . Engel (1994) applied the multicomponent, extended Pitzer model to allow for the liquid phase non-idealities in aqueous solutions of 1:1 bicarbonate and formate salts with a common ion. For this system the equilibrium conversion and the solubility of the electrolyte mixture were predicted within 5 % error on the basis of the thermodynamic model used. Rumpf et al. (1998) applied the Pitzer model to correlate new data for the solubility of carbon dioxide in aqueous solutions of acetic acid. According to the authors the developed model for the description of simultaneous chemical and phase equilibria correlates the experimental data in the range of the experimental uncertainty.

For a summary of the Pitzer model and its modifications the reader is referred to Pitzer (1991) and Zemaitis et al. (1986). The latter monograph gives a very good overview of models used for calculating activity coefficients in electrolyte solutions.

Pitzer's equation for the excess Gibbs energy reads as follows (Pitzer, 1973) :

$$\frac{G^E}{R \cdot T \cdot n_w \cdot M_w} = f_1(I) + \sum_{i \neq w} \sum_{j \neq w} m_i m_j \cdot \left( \beta_{i,j}^{(0)} + \beta_{i,j}^{(1)} f_2(x) \right) + \sum_{i \neq w} \sum_{j \neq w} \sum_{k \neq w} m_i \cdot m_j \cdot m_k \cdot \tau_{i,j,k} \quad (2.30)$$

whereas  $\beta_{i,j}^{(0)}$  and  $\beta_{i,j}^{(1)}$  are binary and  $\tau_{i,j,k}$  are ternary interaction parameters, respectively. The function  $f_1(I)$  is a modified Debye-Hueckel term

$$f_1(I) = -A_\phi \frac{4I}{b} \ln \left( 1 + \sqrt{I} \right) \quad (2.31)$$

wherein the ionic strength  $I$  is defined as:

$$I = 0.5 \cdot \sum_i m_i z_i^2 \quad (2.32)$$

and  $b = 1.2(kg/mol)^{0.5}$  is a fixed parameter. In equation 2.31  $A_\phi$  is the Debye-Hueckel parameter for the osmotic coefficient which is defined as

$$A_\phi = \frac{1}{3} \left( 2\pi N_A \frac{\rho_w}{1000} \right)^{0.5} \left( \frac{e^2}{4\pi \epsilon_0 D k T} \right)^{1.5} \quad (2.33)$$

The function  $f_2(x)$  is defined as

$$f_2(x) = \frac{2}{x^2} (1 - (1 + x) e^{-x}) \quad (2.34)$$

with  $x = \alpha \sqrt{I}$ . For the salts considered in this study,  $\alpha$  equals  $1.2(kg/mol)^{0.5}$ .

The activity coefficients of the dissolved species  $i$  can be obtained by differentiation

of equation 2.30:

$$\begin{aligned} \ln \gamma_i^* = & -A_\phi z_i^2 \left( \frac{\sqrt{I}}{1 + b\sqrt{I}} + \frac{2}{b} \ln(1 + b\sqrt{I}) \right) + \\ & 2 \sum_{j \neq w} m_j \left( \beta_{i,j}^{(0)} + \beta_{i,j}^{(1)} f_2(x) \right) - z_i^2 \sum_{j \neq w} \sum_{k \neq w} m_j m_k \beta_{j,k}^{(1)} f_3(x) \\ & + 3 \sum_{j \neq w} \sum_{k \neq w} m_j m_k \tau_{i,j,k} \end{aligned} \quad (2.35)$$

where  $f_3$  is defined as

$$f_3 = \frac{1}{I x^2} (1 - (1 + x + 0.5 x^2) e^{-x}) \quad (2.36)$$

The activity of water follows from the Gibbs-Duhem equation

$$\begin{aligned} \ln a_w = & M_w \left( 2 A_\phi \frac{I^{1.5}}{I + b\sqrt{I}} - \sum_{i \neq w} \sum_{j \neq w} m_i m_j \left( \beta_{i,j}^{(0)} + \beta_{i,j}^{(1)} e^{-x} \right) \right) \\ & - M_w \left( 2 \sum_{i \neq w} \sum_{j \neq w} \sum_{k \neq w} m_i m_j m_k \tau_{i,j,k} + \sum_{i \neq w} m_i \right) \end{aligned} \quad (2.37)$$

For systems containing a single salt of the form  $M_{\nu^+} X_{\nu^-}$ , the binary and ternary parameters involving two or more species of the same sign of charge are typically neglected. The ternary parameters  $\tau_{M,X,X}$  and  $\tau_{M,M,X}$  are usually reported as third virial coefficients  $C^\phi$  for the osmotic coefficient.

To circumvent the rewriting of equations 2.35 and 2.37 in terms of  $C^\phi$ , the ternary parameter  $\tau_{M,X,X}$  has been set to zero and the parameters  $\tau_{M,M,X}$  have been calculated from numbers reported for  $C^\phi$ :

$$\begin{aligned} 1:1 \quad \text{salt} & \quad \tau_{M,M,X} = \frac{1}{3} C^\phi \\ 2:1 \quad \text{salt} & \quad \tau_{M,M,X} = \frac{\sqrt{2}}{6} C^\phi \end{aligned}$$

## 2.B Parameters used in the equilibrium model incorporating the Pitzer model

The temperature dependent equilibrium constant for water was taken from Edwards et al. (1978) whereas the equilibrium constants for the other two reactions have been taken from Kawazuishi and Prausnitz (1987) (see Table 2.7).

**Table 2.7:** Equilibrium constants for chemical reactions (based on activities )

$$\ln K_i^{EQ} = A_i / (T[\text{K}]) + B_i \ln(T[\text{K}]) + C_i(T[\text{K}]) + D_i$$

Equ. constant	A	B	C	D
$K_1^{EQ}{}^a$ (reaction 2.19)	5719.89	7.97117	-0.0279842	-38.6565
$K_2^{EQ}{}^a$ (reaction 2.20)	4308.64	4.36538	-0.0224562	-24.1949
$K_3^{EQ}{}^b$ (reaction 2.21)	-13445.9	-22.4773	0	140.932

<sup>a</sup>Kawazuishi and Prausnitz (1987)

<sup>b</sup>Edwards et al. (1978)

Henry's constant for the solubility of  $\text{CO}_2$  in water was taken from Rumpf and Maurer (1993) (see Table 2.8). The value of the Henry constant at 298 K was compared to the one measured by Versteeg and Vanswaaij (1988) which showed that the deviation between the two constants was less than 3%.

Saul and Wagner (1987) was used to provide the equations for the vapor pressure and the molar volume of pure water. The fugacity coefficients were calculated with the virial equation of state truncated after the second virial coefficient. The second virial coefficients of water and carbon dioxide were calculated from correlations based on data from Dymond and Smith (1980) (see Table 2.9). The mixed virial coefficient  $B_{\text{CO}_2,w}$  was taken from Hayden and O'Connell (1975) (see Table 2.10). The partial molar volume of carbon dioxide dissolved in water at infinite dilution  $v_{\text{CO}_2,w}^\infty$  was calculated according to the method of Brelvi and O'Connell (1972) (see Table 2.10).

**Table 2.8:** Henry's constant for the solubility of carbon dioxide in pure water  
 $\ln H_{CO_2,w} [MPa \cdot kg \cdot mol^{-1}] = A_{CO_2,w} + B_{CO_2,w}/T[K] + C_{CO_2,w}(T[K])$   
 $+ D_{CO_2,w} \ln(T[K])$

	$A_{CO_2,w}$	$B_{CO_2,w}$	$C_{CO_2,w}$	$D_{CO_2,w}$	Reference
$H_{CO_2,w}$	192.876	-9624.4	0.01441	-28.749	Rumpf and Maurer (1993)

The activity coefficients in the liquid phase were calculated with Pitzer's equation for the Gibbs energy of an electrolyte solution (Pitzer, 1973). The semi-empirical Pitzer model has been successfully applied by a number of authors (Engel (1994), Rumpf et al. (1998), van der Stegen et al. (1999)) for the description of different electrolyte systems.

Interactions between ions and neutral molecules can also be considered in the extended Pitzer model which is important for systems where neutral molecules are dissolved in electrolyte solutions as e.g.  $CO_2$  in caustic solutions. A general shortcoming of the Pitzer model is that its application is restricted to the aqueous solutions (Pitzer, 1991), however, in the present study this is not a limitation as attention is focused on the  $CO_2$ -NaOH- $H_2O$ -salt system.

An outstanding property of Pitzer's model is the ability to predict the activity coefficients in complex electrolyte solutions from data available for simple subsystems. This avoids the use of triple or quadruple interaction parameters which are very scarcely reported in the open literature whereas for the most common single electrolytes binary interaction parameters are readily available.

In the extended Pitzer equation, which is described in more detail by Rumpf et al. (1998), the ion-ion binary interaction parameters  $\beta_{i,j}^0$  and  $\beta_{i,j}^1$  as well as the ternary interaction parameter  $\tau_{i,j,k}$  are characteristic for each aqueous single electrolyte solution. These parameters are solely determined by the properties of the pure electrolytes.

**Table 2.9:** Pure component second virial coefficients ( $273 \leq T[\text{K}] \leq 473$ )

$$B_{i,i} [\text{cm}^3 \cdot \text{mol}^{-1}] = a_{i,i} + b_{i,i} \cdot (c_{i,i}/T[\text{K}])^{(d_{i,i})}$$

<b>i</b>	<b>a<sub>i,i</sub></b>	<b>b<sub>i,i</sub></b>	<b>c<sub>i,i</sub></b>	<b>d<sub>i,i</sub></b>	<b>Ref.</b>
CO <sub>2</sub>	65.703	-184.854	304.16	1.4	<sup>a</sup>
H <sub>2</sub> O	-53.53	-39.29	647.3	4.3	<sup>a</sup>

<sup>a</sup>Dymond and Smith (1980)

**Table 2.10:** Mixed second virial coefficients and partial molar volumes

<b>T[K]</b>	<b>B<sub>CO<sub>2</sub>,w</sub></b>	<b>Ref.</b>	<b>v<sub>CO<sub>2</sub>,w</sub><sup>∞</sup></b>	<b>Ref.</b>
	[cm <sup>3</sup> mol <sup>-1</sup> ]		[cm <sup>3</sup> mol <sup>-1</sup> ]	
313.15	-163.1	a	33.4	b
333.15	-144.6	a	34.7	b
353.15	-115.7	a	38.3	b
373.15	-104.3	a	40.8	b
393.15	-94.3	a	43.8	b
413.15	-85.5	a	47.5	b

<sup>a</sup>Hayden and O'Connell (1975)

<sup>b</sup>Brelvi and O'Connell (1972)

In the liquid phase the reactions 2.19-2.21 take place. For the computation of the equilibrium constants  $K_i^{EQ}$  the activity coefficients of the following species were evaluated with the Pitzer model: CO<sub>2</sub>, OH<sup>-</sup>, HCO<sub>3</sub><sup>-</sup>, CO<sub>3</sub><sup>2-</sup> and H<sub>3</sub>O<sup>+</sup>.

For the sodium hydroxide-CO<sub>2</sub>-salt the Pitzer interaction parameters applied in the Pitzer model as used in this study will be discussed.

In the Pitzer model, as well as in other electrolyte models (i.e. electrolyte NRTL) (Zemaitis et al., 1986), interactions between neutral molecules as well as interactions



between neutral molecules and anions ( i.e.  $\text{Cl}^-$ ,  $\text{OH}^-$  in this study) are neglected. Therefore interactions between neutral molecules ( $\text{CO}_2$ , water) as well as interactions between the anions in the present system and the neutral molecules have not been taken into account in the form of interaction parameters.

Parameters describing interactions between charged species in the system  $\text{CO}_2$ -sodium hydroxide-water-salt have been taken from Pitzer and Peiper (1982). On the basis of expected relative concentrations of the various components in the solution, the ion-ion interactions listed in Table 2.11 are foreseen to be significant. These interaction parameters have been incorporated as the ions or molecules will be present in high concentrations in the solution. It is anticipated that the interactions between these species account for a large extent for the non-idealities in the solution.

Parameters describing interactions between the molecule carbon dioxide and charged species have been considered as follows: for the interaction between carbon dioxide and salt cations (Li,Na,K) the parameters as given in Table 2.11 were used. Interactions between carbon dioxide and dissolved bicarbonate or carbonate have been omitted as those interactions are reported to be negligible ( Edwards et al. (1978) and Pawlikowski et al. (1982)). Due to the low concentration of  $\text{H}_3\text{O}^+$  ions in the caustic solutions, all interaction parameters between this component and  $\text{CO}_2$  have been set to zero.

The addition of different salts to the system  $\text{CO}_2$ - $\text{NaOH}$ - $\text{H}_2\text{O}$  influences the activity coefficients of all the components in the system. The Pitzer interaction parameters that have been considered in the different  $\text{CO}_2$ - $\text{NaOH}$ - $\text{H}_2\text{O}$ -salt systems and those which are needed for the calculation of the activities are summarized in Table 2.11.

As can be seen in Table 2.11 all required interaction parameters for the systems of interest in the present study are available in literature. The possible effect of temperature on the interaction parameters has been assumed to be negligible. This basically corresponds to the assumption that the temperature effect on the activity coefficient is the same for each component (Engel, 1994). The dielectric constant of pure water as used in the Pitzer model was taken from Horvath (1985).

**Table 2.11:** Ion-ion interaction parameters incorporated in the model (at 25° C)

Interaction	$10^2 \cdot (\beta^0, \lambda)$ (kg/mol)	$10 \cdot \beta^1$ (kg/mol)	$10^3 \cdot C^\phi$ (kg <sup>2</sup> /mol <sup>2</sup> )	Ref.
Na <sup>+</sup> - OH <sup>-</sup>	+ 8.64	+ 2.53	+ 4.40	Pitzer and Peiper (1982)
Na <sup>+</sup> - HCO <sub>3</sub> <sup>-</sup>	+ 2.80	+ 0.44	0	Pitzer and Peiper (1982)
Na <sup>+</sup> - CO <sub>3</sub> <sup>2-</sup>	+ 3.62	+ 15.1	+ 5.2	Pitzer and Peiper (1982)
Na <sup>+</sup> - Cl <sup>-</sup>	+ 7.65	+ 2.664	+ 1.27	Zemaitis et al. (1986)
CO <sub>2</sub> - Na <sup>+</sup>	+ 12.8	-	-	Pitzer and Peiper (1982)
K <sup>+</sup> - OH <sup>-</sup>	+ 12.98	+ 3.20	+ 4.1	Roy et al. (1984)
K <sup>+</sup> - HCO <sub>3</sub> <sup>-</sup>	- 1.07	+ 0.48	0	Roy et al. (1984)
K <sup>+</sup> - CO <sub>3</sub> <sup>2-</sup>	+ 12.88	+ 14.33	+ 0.5	Roy et al. (1987)
K <sup>+</sup> - Cl <sup>-</sup>	+ 4.835	+ 2.122	+ 0.84	Zemaitis et al. (1986)
CO <sub>2</sub> - K <sup>+</sup>	+ 9.46			Engel (1994)
Li <sup>+</sup> - OH <sup>-</sup>	+ 1.5	1.4	-	Zemaitis et al. (1986)
Li <sup>+</sup> - HCO <sub>3</sub> <sup>-</sup>	no	data	available	
Li <sup>+</sup> - CO <sub>3</sub> <sup>2-</sup>	- 38.934	- 22.737	- 162.859	Deng et al. (2002)
Li <sup>+</sup> - Cl <sup>-</sup>	+ 14.94	+ 3.074	+ 3.59	Zemaitis et al. (1986)
CO <sub>2</sub> - Li <sup>+</sup>	+ 5.8	-	-	Schumpe (1993)

In the Pitzer model only binary interaction parameters have been taken into account as ternary interaction parameters are only scarcely reported in literature, especially for the mixed electrolyte systems as used in this study. Therefore ternary interaction parameters have been disregarded to prevent the possible introduction of more inconsistencies in the model.

Already at this point it can be stated that to further improve the accuracy of the Pitzer model for the predictions of activity coefficients of CO<sub>2</sub> and OH<sup>-</sup> in solutions as investigated in this study, it seems necessary to carry out additional VLE-experiments, especially at low partial pressures of CO<sub>2</sub> and low CO<sub>2</sub> loadings. This would yield more reliable interaction parameters for the systems of interest in

this study and hence more precise values of the required activity coefficients. As this was not the scope of the present study these experiments have not been carried out at this stage.

## 2.C Derivation of equations used in the activity based kinetic approach

### 2.C.1 Conversion between molalities and concentrations of mixed salt solutions

The concentration and the molality of hydroxide ions can be expressed as follows:

$$c_{OH^-} = \frac{mass_{OH^-}}{M_{OH^-} V} \quad (2.38)$$

$$m_{OH^-} = \frac{mass_{OH^-}}{M_{OH^-} mass_{solvent}} \quad \rightarrow \quad mass_{OH^-} = m_{OH^-} M_{OH^-} mass_{solvent} \quad (2.39)$$

Combining Equations 2.38 and 2.39 gives:

$$c_{OH^-} = \frac{mass_{OH^-}}{M_{OH^-} V} = \frac{m_{OH^-} M_{OH^-} mass_{solvent}}{M_{OH^-} V} = \frac{mass_{solvent} m_{OH^-}}{V} \quad (2.40)$$

The volume of a mixed salt solution can be expressed as:

$$\begin{aligned} V &= \frac{mass}{\rho} = \frac{mass_{solvent} + \sum_{all\ ions\ i} mass_i}{\rho} \\ &= \frac{mass_{solvent} + mass_{solvent} \sum_{all\ ions\ i} m_i M_i}{\rho} \\ &= \frac{mass_{solvent} (1 + \sum_{all\ ions\ i} m_i M_i)}{\rho} \end{aligned} \quad (2.41)$$

This yields:

$$c_{OH^-} = \frac{\rho m_{OH^-}}{1 + \sum_{\text{all ions } i} m_i M_i} \quad (2.42)$$

Rearranging the last formula yields the conversion from concentration to molality:

$$m_{OH^-} = \frac{c_{OH^-} (1 + \sum_{\text{all ions } i, i \neq OH^-} m_i M_i)}{\rho - c_{OH^-} M_{OH^-}} \quad (2.43)$$

## 2.C.2 Relation between the activity based rate constant and the concentration based rate constant

The activity based reaction rate reads as follows:

$$r^m = k_{OH^-}^m(\gamma) a_{CO_2} a_{OH^-} = k_{OH^-}^m(\gamma) \gamma_{CO_2} \gamma_{OH^-} m_{CO_2} m_{OH^-} \quad [mol \, kg_{solvent}^{-1} s^{-1}] \quad (2.44)$$

The concentration based reaction rate can be written as:

$$r = k_{OH^-} c_{CO_2} c_{OH^-} \quad [kmol \, m^{-3} s^{-1}] \quad (2.45)$$

Replacing concentrations by molalities in Equation 2.45 by using Equation 2.42 yields:

$$r = k_{OH^-} \frac{\rho^2 m_{OH^-} m_{CO_2}}{\left(1 + \sum_{\text{all ions } i} m_i M_i\right)^2} \quad (2.46)$$

From Equation 2.44 it can be derived that:

$$m_{OH^-} m_{CO_2} = \frac{r^m}{k^m(\gamma) \gamma_{OH^-} \gamma_{CO_2}} \quad [mol^2 \, kg_{solvent}^{-2}] \quad (2.47)$$

Using Equation 2.47 in Equation 2.46 gives:

$$r = \frac{k_{OH^-}}{k^m(\gamma) \gamma_{OH^-} \gamma_{CO_2}} \frac{\rho^2 \cdot r^m}{\left(1 + \sum_{\text{all ions } i} m_i \cdot M_i\right)^2} \quad (2.48)$$

Rearranging yields:

$$k^m(\gamma) = \frac{k_{OH^-}}{\gamma_{OH^-} \gamma_{CO_2}} \frac{\rho^2 \frac{r^m}{r}}{\left(1 + \sum_{\text{all ions } i} m_i M_i\right)^2} \quad (2.49)$$

Now a final link between between the ratio of r (see Equation 2.45) and  $r^m$  (see Equation 2.44) will eliminate these parameters from the equation:

$$\frac{r}{r^m} = \rho - \sum_{\text{all ions } i} c_i M_i \quad \rightarrow \quad \frac{r^m}{r} = \frac{1}{\rho - \sum_{\text{all ions } i} c_i M_i} \left[ \frac{kg_{\text{solvent}} * 1000}{m_{\text{solution}}^3} \right] \quad (2.50)$$

Using the last two equations gives the relation to calculate  $k_{OH^-}^m(\gamma)$  from  $k_{OH^-}$ :

$$k^m(\gamma) = \frac{k_{OH^-}}{\gamma_{OH^-} \gamma_{CO_2}} \frac{\rho^2}{\left(1 + \sum_{\text{all ions } i} m_i M_i\right)^2 \left(\rho - \sum_{\text{all ions } i} c_i M_i\right)} \quad (2.51)$$

## 2.D Experimental data

### 2.D.1 Experimental data for the kinetics of CO<sub>2</sub> in 'pure' aqueous sodium hydroxide solutions

**Table 2.12:** Kinetic constants derived from own measurements (as shown in Figure 2.2)

$c_{NaOH}$ [kmol m <sup>-3</sup> ]	$k_1$ [s <sup>-1</sup> ]	$k_{OH^-}$ [m <sup>3</sup> kmol <sup>-1</sup> s <sup>-1</sup> ]
0.7848	10404	13257
0.8981	12022	13386
1.4852	23862	16067
1.9797	38747	19572
2.2679	48117	21217
2.464	55342	22460
2.9599	72594	24526
3.0076	83849	27879

## 2.D.2 Applied activity coefficients to derive the activity based kinetics for the reaction of CO<sub>2</sub> in 'pure' aqueous sodium hydroxide solutions

**Table 2.13:** Activity coefficients of CO<sub>2</sub> and OH<sup>-</sup> for the system NaOH-CO<sub>2</sub>-water

$c_{NaOH}$	$\gamma_{CO_2}$	$\gamma_{OH^-}$
0	1.0000	0.9857
0.1	1.0245	0.7796
0.2	1.0495	0.7382
0.3	1.0752	0.7167
0.4	1.1015	0.7037
0.5	1.1284	0.6955
0.6	1.1560	0.6903
0.7	1.1843	0.6872
0.8	1.2132	0.6856
0.9	1.2429	0.6852

1	1.2733	0.6858
1.1	1.3044	0.6871
1.2	1.3363	0.6891
1.3	1.3690	0.6916
1.4	1.4025	0.6946
1.5	1.4368	0.6981
1.6	1.4719	0.7019
1.7	1.5079	0.7061
1.8	1.5448	0.7106
1.9	1.5826	0.7154
2	1.6213	0.7204
2.1	1.6609	0.7258
2.2	1.7015	0.7313
2.3	1.7431	0.7371
2.4	1.7858	0.7432
2.5	1.8294	0.7494
2.6	1.8742	0.7559
2.7	1.9200	0.7625
2.8	1.9669	0.7694
2.9	2.0150	0.7764
3	2.0643	0.7837

---

### 2.D.3 Raw data: Absorption experiments of CO<sub>2</sub> in salt-doped NaOH solutions

**Table 2.14:** Raw data: Absorption experiments of CO<sub>2</sub> in salt-doped NaOH solutions

$c_{NaOH}$	Salt	$c_{Salt}$	$p_{CO_2}$	Flux	$D_{CO_2-salt}$	$m_{CO_2-salt}$	$k_{OH^-}$
$\frac{kmol}{m^3}$		$\frac{kmol}{m^3}$	mbar	$\frac{mmol}{m^2s}$	$10^{-9} \frac{m^2}{s}$		$\frac{m^3}{kmols}$
0.940	LiCl	0.5	10.4	0.673	1.51	0.519	6769
0.965	NaCl	0.5	10.3	0.826	1.50	0.486	11377
0.964	KCl	0.5	12.5	0.857	1.50	0.498	11648
1.453	LiCl	0.5	12.7	0.846	1.35	0.422	11621
1.465	NaCl	0.5	11.8	0.894	1.35	0.397	14542
1.450	KCl	0.5	15.6	0.919	1.35	0.410	14570
1.920	LiCl	0.5	11.3	0.891	1.23	0.350	15612
0.910	LiCl	1.5	13.9	0.638	1.46	0.432	9297
1.937	NaCl	0.5	12.6	0.893	1.23	0.329	17660
0.974	NaCl	1.5	14.6	0.705	1.44	0.357	15736
1.936	KCl	0.5	11.5	0.975	1.23	0.337	20053
0.930	KCl	1.5	11.8	0.872	1.46	0.391	20869
1.427	LiCl	1.5	15.6	0.698	1.32	0.351	11957
1.413	NaCl	1.5	12.3	0.813	1.32	0.299	22503
1.394	KCl	1.5	13.9	0.939	1.33	0.325	25780
1.903	LiCl	1.5	14.2	0.725	1.20	0.290	15613
1.885	NaCl	1.5	15.8	0.805	1.20	0.248	26593
1.865	KCl	1.5	12.9	0.988	1.20	0.269	34272



# Chapter 3

## A new UNIFAC-group: the OCOO-group of carbonates

### Abstract

VLE data available in literature comprising the following binary systems: phenol-dimethyl carbonate (DMC), alcohol-DMC/diethyl carbonate (DEC), and alkanes-DMC/DEC, ketones-DEC and chloro-alkanes-DMC have been fitted to a simplified "gamma-phi"-model assuming the values of the Poynting correction, the fugacity coefficient of the gas and the liquid phase being equal to unity. Two  $G^E$ -models - viz. UNIFAC and NRTL- have been applied and the adjustable parameters in these two models have been fitted to the experimental VLE data. The two  $G^E$ -models could reproduce the experimental activity coefficients and therewith the experimental VLE data well (<10% deviation with NRTL) to fairly (<15% deviation with UNIFAC). This seems to justify the application of the UNIFAC parameters derived in this work to predict the VLE data and thus the activity coefficients of experimentally unknown multicomponent systems containing different organic carbonates. The activity coefficients of the industrial important multicomponent system methanol, dimethyl carbonate, phenol, methyl phenol carbonate and diphenyl carbonate have been estimated with the UNIFAC parameters as derived in this work to investigate the extent of non-ideal behavior of the system and to assess the need for

the application of activity coefficients in this particular system. It has been shown clearly that the activity coefficients of DMC and methanol deviate substantially from unity whereas the activity coefficients of the other three components deviate only moderately (<15%) from unity. It seems therefore necessary to employ activity coefficients for the description of the VLE in this system and probably also for the sound description of the chemical equilibria and reaction kinetics in this particular multicomponent system. It is expected that the UNIFAC parameters derived in this work will be of further benefit to e.g. develop activity coefficient based chemical equilibrium expressions and activity based reaction rates. Moreover, the UNIFAC interaction parameters can be used to describe the VLE of other systems containing organic carbonates and e.g. alcohols, alkanes, aromatics.

### 3.1 Introduction

The production of the polycarbonate precursor diphenyl carbonate (DPC) is today still to about 90% carried out via the route in which hazardous chemicals as phosgene are involved and huge amounts of the extremely environmentally unfriendly substance methyl chloride are used. The remaining 10% of the world production of DPC is produced with an alternative process starting from dimethyl carbonate (DMC) and phenol yielding the intermediate Methyl Phenyl carbonate (MPC) which then reacts to diphenyl carbonate (DPC) by a subsequent esterification with phenol and a disproportionation, respectively. This latter process can be considered to be substantially more sustainable as it excludes the use phosgene and methyl chloride. Despite the fact that the process via DMC and phenol has been already known for years it must be concluded that there is still a considerable lack of fundamental thermodynamic data in the open literature. This deficiency concerns especially vapour-liquid-equilibrium (VLE) data required for determining interaction parameters to a  $G^E$ -model like e.g. NRTL or UNIFAC to calculate the corresponding activity coefficients. Only some binary VLE data containing carbonates are available in literature and thus it is not possible to fit all required interaction parameters for the process from DMC to DPC to experimental data with e.g. NRTL. Neverthe-

less activity coefficients are indispensable to describe correctly chemical equilibria that occur for the reactive system of DMC to MPC and of MPC to DPC, respectively. Moreover, this information is also needed in the design of distillation steps in separating these components. A predictive method like UNIFAC is developed to enable the calculation of activity coefficients and construction of VLE curves for systems that lack experimental data, as for e.g. a mixture of DMC/MPC/DPC and methanol. The one and only restriction in the use of this method is that the characteristics of all functional groups are present in the databank of UNIFAC. Unfortunately the carbonate group- attached to an aliphatic or aromatic group as for DMC/MPC or DPC- is not yet present in the UNIFAC databank. Although interaction parameters for binary systems involving carbonates have been published these parameters are however not sufficient to constitute the desired molecules of the system in this study (i.e. DMC, MPC, DPC). Lohmann and Gmehling (2001) used Modified Dortmund UNIFAC and introduced a new carbonate group into UNIFAC derived to model aliphatic carbonates. The segmentation of this carbonate group containing molecule is not applicable to estimate the activity coefficients of molecules which comprise an aromatic carbonate and/or an asymmetrical aliphatic/aromatic carbonate, respectively. Therefore it must be concluded that the carbonate group -attached to an aliphatic or aromatic group- has to be introduced into the UNIFAC databank before it is possible to use this technique to estimate activity coefficients of the system methanol, DMC, phenol, MPC and DPC. As UNIFAC is a group contribution method data of VLE systems with a carbonate group in one of the molecules can be used to derive interaction parameters between the carbonate group and the various other functional groups. The main goal of this study is to develop a consistent set of UNIFAC interaction parameters which can be used to predict the activity coefficients of a multicomponent mixture consisting of at least the following species: methanol, DMC, phenol, MPC and DPC. Therefore, in this work the available experimental VLE data from literature for various sets of components have been used to determine UNIFAC interaction parameters between a carbonate group (-O-CO-O-) and various other functional groups. The predictions of UNIFAC using the derived interaction parameters have been compared to the well established NRTL

model for the same systems taken from literature. By comparison of the UNIFAC predictions to the corresponding NRTL fits and the actual experimental VLE data, it is possible to quantify the accuracy of UNIFAC for systems for which experimental data are available. Ultimately this yields an indirect indication of the precision of the UNIFAC predicted data for the DMC/MPC/DPC/methanol system for which no experimental VLE data are available. Although the NRTL model is generally considered to be more reliable (Reid et al., 1988) it does not have, as mentioned before, UNIFACs predictive capabilities for new systems. The NRTL model uses a distinct set of three interaction parameters for each binary system whereas UNIFAC deploys two interaction parameters to account for each interaction between two functional groups. As these functional groups are used for a multitude of molecules, the UNIFAC method generally requires less fit parameters. Hence, to compare the potentially less accurate UNIFAC fits to another VLE model the NRTL model has been chosen as it is considered to yield more accurate estimations. Of course also the Wilson or Uniquac model could have been applied but in this study NRTL has been used as the accuracy of all these models is reported to be very similar (Reid et al., 1988) (Hu et al., 2004).

## 3.2 Description of the vapour liquid equilibrium model (VLE)

Experimental VLE data present in the open literature (see Table 3.1) for various systems containing a carbonate group will serve as basis for the derivation of the interaction parameters. A first step in this process is the conversion of VLE data into activity coefficients, as this is the actual parameter predicted by UNIFAC or NRTL, respectively. The experimental binary vapour-liquid equilibria investigated in this study are described with a simplified version of the so called "gamma-phi" model (Sandler, 1999) which is also used for fitting VLE data in the DECHEMA series (Gmehling et al., 1991). For the conditions (moderate T, low p) and the species used in this study the following simplifications apply to the gamma-phi model (Sandler, 1999): the vapour and liquid phase fugacity coefficient as well as

the Poynting correction factor can be set equal to unity. The resulting model is often referred to as the DECHEMA-K-model (Taylor and Kooijman, 2000) and reads as follows:

$$y_i p = x_i \gamma_i p_i^{vap} \quad (3.1)$$

In Equation 3.1  $y_i$  denotes the vapour phase mole fraction of species  $i$ ,  $p$  the overall pressure in the gas phase,  $x_i$  the mole fraction of species  $i$  in the liquid phase,  $\gamma_i$  the liquid phase activity coefficient of species  $i$  and  $p_i^{vap}$  the saturated vapour pressure of species  $i$ , respectively.

For calculating the activity coefficient from experimental VLE data of a particular binary system also the vapour pressures of the pure substances have to be known (see Eq. 3.2). For calculating the pure vapour pressures of component  $i$  the Antoine equation is used:

$$\ln p_i^{vap} [Pa] = A_i - \frac{B_i}{T + C_i} \quad (3.2)$$

$A_i$ ,  $B_i$  and  $C_i$  - being the Antoine parameters- have been tabulated in the Appendix (Table 3.12) for the different components in the binaries used for the determination of the interaction parameters. By fitting the experimental VLE data to the model (Eq. 3.1) it is possible to derive the interaction parameters in the corresponding Gibbs excess energy ( $G^E$ ) model, i.e. UNIFAC or NRTL. Next, the derived interaction parameters can then be implemented in the  $G^E$  model in the model (Eq. 3.1) to calculate the activity coefficients of the species of interest.

### 3.3 The UNIFAC Method

In this section the UNIFAC method, as developed by Fredenslund et al. (1975), has been used. This method is described in many textbooks e.g. (Sandler, 1999)

therefore only the key features will be shortly summarized. The fundamental idea of a solution-of-groups model is to utilize existing phase equilibrium data for predicting phase equilibria of systems for which no experimental data is available. Basically, the UNIFAC method derives the activity coefficients of components in mixtures from the interactions between the functional groups of the molecules in the mixture. The essential features are:

1. Reduction of experimentally obtained activity-coefficient data to yield parameters characterizing interactions between pairs of structural groups in non-electrolyte systems
2. Use of those parameters to predict activity coefficients for other non-electrolyte systems that have not been studied experimentally but that contain the same functional groups.

The molecular activity coefficient is separated into two parts (Sandler, 1999): one part provides the contribution due to molecular size and shape (combinatorial effects,  $\gamma_c$ ), and the other provides the contribution due to molecular interaction (residual effects,  $\gamma_r$ ).

$$\ln \gamma_i = \ln \gamma_i^c + \ln \gamma_i^r \quad (3.3)$$

The combinatorial part is given by:

$$\ln \gamma_i^c = \ln \frac{\phi_i}{x_i} + \frac{z}{2} q_i \ln \frac{\theta_i}{\phi_i} + \frac{(r_i - q_i)z}{2} - (r_i - 1) - \frac{\phi_i}{x_i} \sum_j x_j \left( \frac{(r_i - q_i)z}{2} - (r_i - 1) \right) \quad (3.4)$$

And the residual part by:

$$\ln \gamma_i^r = \sum_k v_k^{(i)} \left[ \ln \Gamma_k - \ln \Gamma_k^{(i)} \right] \quad (3.5)$$

$$\ln \Gamma_k = Q_k \left[ 1 - \ln \left( \sum_m \Theta_m \Psi_{mk} \right) - \sum_m \frac{\Theta_m \Psi_{km}}{\sum_n \Theta_n \Psi_{nm}} \right] \quad (3.6)$$

with

$$\Theta_m = \frac{X_m Q_m}{\sum_n X_n Q_n}, \quad r_i = \sum_k v_k^{(i)} R_k, \quad q_i = \sum_k v_k^{(i)} Q_k$$

and

$$\Psi_{mn} = \exp \left[ \frac{-A_{mn}}{T} \right]$$

For the calculation of the combinatorial part only pure component data are required while for the residual part interaction parameters are needed. The interaction parameters between the functional groups have to be derived from sets of experimentally available VLE data. The actual fit parameters in the UNIFAC equation are the values of  $A_{mn}$  and  $A_{nm}$  for the interaction between groups  $m$  and  $n$ .

### 3.4 The NRTL Method

For comparing the accuracy of the UNIFAC predictions to another  $G^E$ -model, the NRTL model (Renon and Prausnitz, 1968) will be used in this study. Three adjustable parameters, namely  $\tau_{12}$ ,  $\tau_{21}$  and  $\alpha$ , are used in the NRTL model to fit the experimental VLE data. In a binary mixture the activity coefficients of component 1 according to the NRTL model is given by (Sandler, 1999):

$$\ln \gamma_1 = x_2^2 \left[ \tau_{21} \left( \frac{G_{21}}{x_1 + x_2 G_{21}} \right)^2 + \frac{\tau_{12} G_{12}}{(x_2 + x_1 G_{12})^2} \right] \quad (3.7)$$

with

$$\ln G_{12} = -\alpha \tau_{12} \quad \text{and} \quad \ln G_{21} = -\alpha \tau_{21}$$

being the adjustable parameters.

The expression for  $\ln\gamma_2$  can be obtained from Eq.3.7 by interchanging the subscripts 1 and 2. The three parameters  $\tau_{12}$ ,  $\tau_{21}$  and  $\alpha$  of the NRTL model will be fitted to the same experimental binary VLE data as the UNIFAC model and the NRTL model predictions will be compared to the experimental data. Moreover, the NRTL predictions will be compared to those made with the UNIFAC model. This comparison serves to assess the model accuracy of the UNIFAC approach and will indicate whether UNIFAC can be used to predict the activity coefficients for the carbonate system as of interest in this study.

### 3.5 Segmentation of carbonate-molecules in UNIFAC

In this work the application of UNIFAC will be restricted to binaries containing organic carbonates with aliphatic and/or aromatic groups and another molecule. There exist also inorganic carbonates or carbonates with other groups containing e.g. nitrogen or sulfur atoms (Shaikh and Sivaram, 1996), but these carbonates will not be considered in the present work.

Organic carbonate molecules like DMC, MPC and DPC (Figure 3.1) consist of a carbonate group (-OCOO-) and two - different or equal- alkyl (e.g. CH<sub>3</sub>- or C<sub>2</sub>H<sub>5</sub>-) and/or aromatic fragments (e.g. C<sub>6</sub>H<sub>5</sub>-). For predicting experimental VLE data with the UNIFAC model, the corresponding functional groups have to be taken from the UNIFAC library (see e.g. Reid et al. (1988)) to "build" the molecules occurring in the mixture. If not all constitutional groups are available for describing the molecule of interest, as in case of organic carbonates like DMC, MPC and DPC, a new constitutional group has to be defined. This is the case for the carbonate group in the aforementioned molecules therefore the OCOO-group has been added to the UNIFAC database in this study.

The carbonate containing molecules like DMC, MPC and DPC were segmented into a carbonate group (-OCOO-), as a new UNIFAC group, and the already existing well



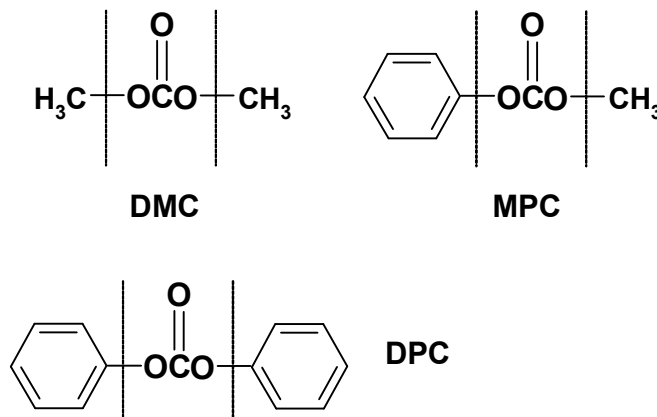


**Figure 3.1: Segmentation of the carbonate molecules DMC, MPC and DPC**

known aliphatic (-CH<sub>3</sub>) and aromatic (ACH) UNIFAC groups (see Figure 3.1). A similar segmentation has been applied by Rodriguez et al. (2002b) to derive UNIFAC interaction parameters for carbonate-alcohol systems. The  $R_k$  and  $Q_k$  values of the new carbonate group (-OCO-), necessary to compute the parameters  $r_i$  and  $q_i$  (Eq. 3.4), have been calculated to be  $R_{OCO}=1.5821$  and  $Q_{OCO}=1.3937$ . The van der Waals group volume and external surface areas required for the calculation of  $R_{OCO}$  and  $Q_{OCO}$  have been estimated by using the group contribution data given by Bondi (1964).

### 3.6 Modelling VLE data with UNIFAC and NRTL

In this section the experimental Txy-data and in part pxy-data for systems involving carbonate groups are fitted to the DECHEMA-K model (see Eq. 3.1), thereby adjusting the parameters of the  $G^E$ -models, either UNIFAC or NRTL.

For the derivation of the relevant UNIFAC interaction parameters between the OCOO-group and other UNIFAC groups which are required to calculate the activity coefficients in a multicomponent mixture consisting of at least methanol, DMC, phenol, MPC and DPC, experimental data have been taken from different literature sources (Table 3.1) and had to fulfill the following conditions:

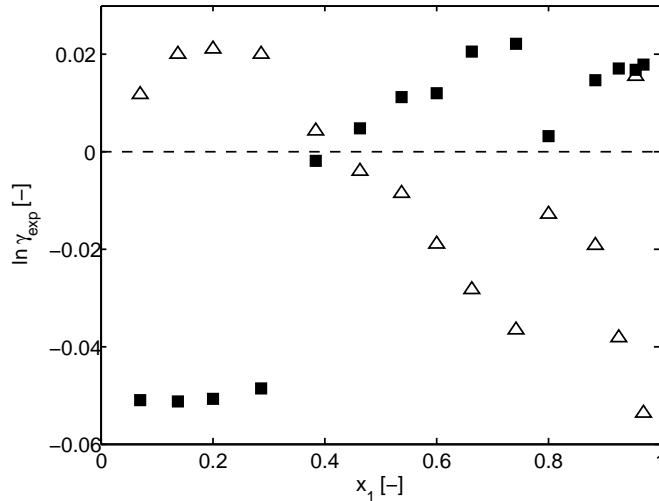
1. carbonate group in the presence of one of the following groups: aliphatic, aromatic or hydroxyl
2. VLE data has to be consistent
3. "Enough" data points (>15) for a reliable use of the VLE data should be available.

**Table 3.1:** Literature sources of the experimental VLE data used for fitting interaction parameters.

System	Group interaction	Source of experimental VLE data
methanol-carbonate	CH <sub>3</sub> OH-OCOO	Rodriguez et al. (2002b), Rodriguez et al. (2003)
alcohol-carbonate	OH-OCOO	Rodriguez et al. (2002b), Rodriguez et al. (2003)
alkane-carbonate	CH <sub>2</sub> -OCOO	Rodriguez et al. (2002a), Rodriguez et al. (2002c)
aromatic-carbonate	ACH-OCOO	Hu et al. (2004), Oh et al. (2006)
aromatic-carbonate	ACOH-OCOO	Hu et al. (2004)
toluene-carbonate	CH <sub>2</sub> CO-OCOO	Pereiro et al. (2005)
chloroalkanes- carbonate	CCl-OCOO	Comelli and Francesconi (1994)
chloroalkanes- carbonate	CCl <sub>3</sub> -OCOO	Comelli and Francesconi (1994)

The following VLE data, either Txy- or pxy-data, have been taken from literature and will be used to fit the corresponding UNIFAC group interaction parameters given in Table 3.1: phenol-DMC, alcohol-DMC/DEC, and alkanes-DMC/DEC. Additionally, VLE data sets comprising ketones-DEC and chloro-alkanes-DMC will be used to derive the corresponding interaction parameters. These parameters might

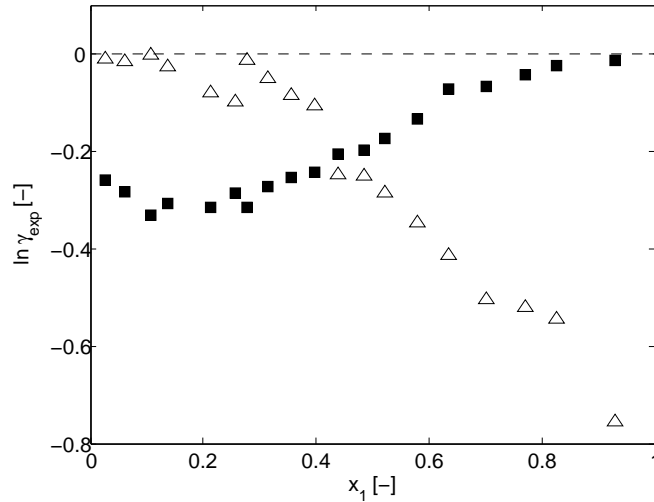
be useful later on to assess e.g. if extractive distillation with a suitable solvent is a feasible method to separate the components in the above mentioned reaction mixture.



**Figure 3.2: Experimental  $\ln \gamma$  vs.  $x_1$  (DMC (1) - squares, Dichloro-ethane (2) - triangles). The dashed line represents ideal behaviour ( $\gamma = 1$ ). Data source: Comelli and Francesconi (1994).**

Before starting to fit the experimental VLE data to the  $G^E$ -models UNIFAC and NRTL, the degree of non-ideality of the different VLE taken from literature will be investigated by plotting the natural logarithm of the activity coefficients - derived for each experimental data point by using Eq. 3.1 with the earlier mentioned simplifications - as function of the liquid phase mole fraction  $x$  (see Figure 3.2 to Figure 3.5 for examples). These examples elucidate how much the different binaries deviate from ideal behavior, according to Raoult's law. Furthermore, these plots indicate how consistent, and therefore accurate, the experimental data are and if it can be expected that fitting will yield sound interaction parameters.

The pure component activity coefficients of species 1 and 2 as derived from each set of binary VLE data as well as the minimum or maximum value of the activity coefficient, if occurring, are listed in Table 3.2. It can be seen from this



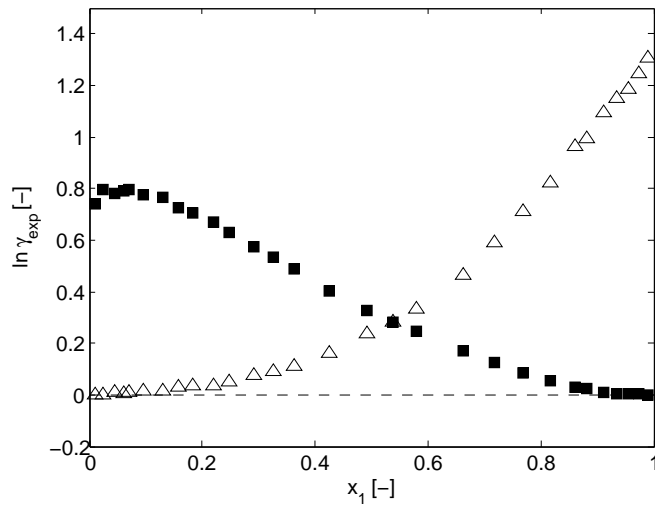
**Figure 3.3:** Experimental  $\ln \gamma$  vs.  $x_1$  (DMC (1) - squares, Phenol (2) - triangles). The dashed line represents ideal behaviour ( $\gamma = 1$ ). Data source: Hu et al. (2004).

table that generally all experimental activity coefficients differ substantially from 1,  $\ln \gamma$  being larger or smaller than zero, which means that Raoult's law cannot be used to correlate the experimental VLE data necessitating the use of a  $G^E$  model to account for the non-idealities in the liquid phase. As already indicated, in this study the UNIFAC and the NRTL model will be employed to correlate the experimental data.

The  $\ln \gamma$ -plots (see Figure 3.2 to Figure 3.5) have revealed that all experimental activity coefficients show a consistent course over the entire range of compositions except for the binary systems 1,2-Dichloroalkane-DMC and the ketone-DEC, respectively. For these two experimental activity coefficients are slightly flawed as the non-ideality of these binary mixtures is not very pronounced. Therefore small errors in the VLE measurements will yield errors in the derived activity coefficients which are of the same order of magnitude as the actual trend (see e.g. Figure 3.2). Nevertheless, these inconsistencies are small and it therefore seems justified to use these data to fit the corresponding interaction parameters.

**Table 3.2:** Values of experimental Activity coefficients derived from binary VLE data

System		At $x_1 = 0$	At $x_2=0$	$\gamma_{max/min}$		$x_1^{max/min}$
Comp (1)	Comp (2)	$\gamma_1$	$\gamma_2$	$\gamma_1$	$\gamma_2$	
DMC	Phenol	0.772	0.469	-	0.998	0.107
MeOH	DMC	2.1	3.68	2.21	-	0.0252
EtOH	DMC	1.81	3.24	1.87	-	0.113
DMC	1-PropOH	2.28	2.35	-	-	-
DMC	1-ButOH	2.96	2.23	-	-	-
MeOH	DEC	1.87	3.26	2.11	-	0.117
EtOH	DEC	1.52	2.95	1.73	-	0.162
1-PropOH	DEC	1.41	2.52	1.49	-	0.13
1-ButOH	DEC	1.34	2.03	1.39	-	0.0912
n-hexane	DMC	4.12	2.16	-	-	-
cyc-hexane	DMC	3.15	4.64	-	-	-
DMC	n-heptane	3.2	4.77	-	-	-
DMC	n-octane	2.66	3.06	2.7	-	0.436
n-hexane	DEC	1.36	3.13	1.46	-	0.244
cyc-hexane	DEC	2.21	2.62	-	-	-
n-heptane	DEC	2.24	2.29	-	-	-
n-octane	DEC	2.18	2.48	-	-	-
Acetone	DEC	0.91	0.64	-	-	-
2-butanone	DEC	1.01	0.9	-	-	-
2-pentanone	DEC	1.1	0.83	-	-	-
DMC		0.95	0.95	-	-	-
1,2-Dichloroethane						
DMC		1.41	1.42	-	-	-
1,1,1-Trichloroethane						



**Figure 3.4:** Experimental  $\ln \gamma$  vs.  $x_1$  (Methanol (1) - squares, DMC (2) - triangles). The dashed line represents ideal behavior ( $\gamma = 1$ ). Data source: Rodriguez et al. (2002b).

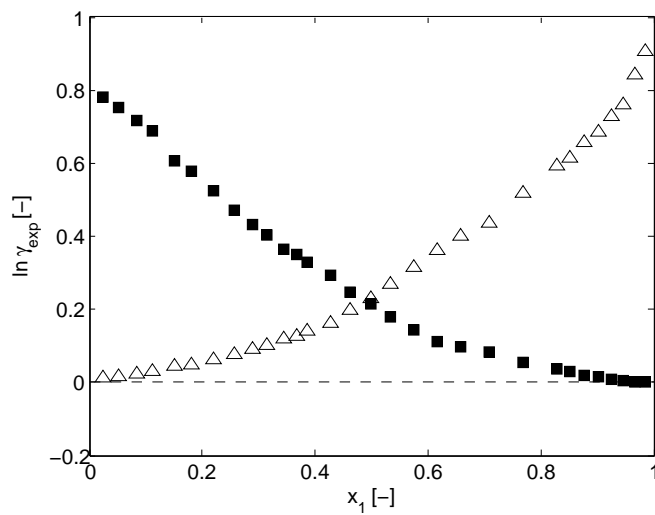


**Figure 3.5:** Experimental  $\ln \gamma$  vs.  $x_1$  (n-octane (1) - squares, DEC (2) - triangles). The dashed line represents ideal behavior ( $\gamma = 1$ ). Data source: Rodriguez et al. (2002c).

### 3.7 Correlation and Prediction

The specific UNIFAC interaction parameters,  $A_{mn}$  and  $A_{nm}$  respectively, have been determined by using the "objective function" (OF) defined in Eq. 3.8. An objective function incorporating relative deviations for the temperature (or pressure, dependent on the type of data) and vapour phase mole fractions instead of the absolute deviations (Eq. 3.8) has also been tested but did not yield a better representation of the experimental results and has therefore not been applied.

$$OF = \min \sum_{i=1}^n (T_i^{\text{exp}} - T_i^{\text{calc}})^2 + (y_i^{\text{exp}} - y_i^{\text{calc}})^2 \quad (3.8)$$

For the optimization of a specific UNIFAC interaction parameter set ( $A_{mn}$  and  $A_{nm}$ ) all available VLE binaries containing molecules which at least consist of the functional groups m and n have been used. As a starting point the  $A_{mn}$  and  $A_{nm}$  UNIFAC parameters for a certain group interaction e.g. OCOO-CH have been set both equal to zero. Then one parameter - either  $A_{mn}$  or  $A_{nm}$  - has been modified while keeping the other parameter -  $A_{mn}$  or  $A_{nm}$  - constant. This procedure was repeated until the optimization routine yielded the optimized UNIFAC interaction parameters. The deviation between experimental x-y (VLE-) data and the UNIFAC predicted x-y (VLE-) data is thereby minimized.

The three parameters  $\tau_{12}$ ,  $\tau_{21}$  and  $\alpha$  of the NRTL equations have been optimized simultaneously by using the objective function given in Eq. 3.8. The parameter  $\alpha$  has been ultimately set to a value of 0.3 as setting  $\alpha$  to an adjustable parameter  $>0.1$  did not improve or affect the accuracy of the fits (Renon and Prausnitz, 1968). The objective function has been applied to each single set of experimental VLE data (e.g. MeOH-DMC) yielding the three corresponding NRTL model parameters for the particular binary.

It is expected that applying the NRTL method will yield a more accurate representation of the experimental data as each binary is fitted to a distinct set of three interaction parameters whereas in UNIFAC a series of binaries is fitted to the same

**Table 3.4:** Mean absolute Deviations of T and vapour mole fraction y; Mean relative deviation of pressure p.

System ( T <sub>xy</sub> or p <sub>xy</sub> data)	$\Delta T$ [K]		$\Delta y$	
	$\Delta p$ [-]			
	UNIFAC	NRTL	UNIFAC	NRTL
DMC-Phenol (T <sub>xy</sub> )	4.42	0.84	0.05	0.02
MeOH-DMC (T <sub>xy</sub> )	1.45	0.22	0.03	0.01
EtOH-DMC (T <sub>xy</sub> )	0.82	0.42	0.02	0.01
DMC- 1-PropOH (T <sub>xy</sub> )	0.41	0.12	0.01	0.01
DMC -1-ButOH (T <sub>xy</sub> )	1.14	1.21	0.02	0.03
MeOH-DEC (T <sub>xy</sub> )	3.13	0.70	0.04	0.01
EtOH-DEC (T <sub>xy</sub> )	1.11	0.87	0.03	0.01
1-PropOH-DEC (T <sub>xy</sub> )	0.98	0.46	0.03	0.01
1-ButOH-DEC (T <sub>xy</sub> )	0.99	0.41	0.02	0.01
n-hexane-DMC (T <sub>xy</sub> )	0.59	0.35	0.01	0.01
cyc-hexane-DMC (T <sub>xy</sub> )	0.53	0.56	0.01	0.01
DMC - n-heptane (T <sub>xy</sub> )	0.44	0.36	0.01	0.01
DMC - n-octane (T <sub>xy</sub> )	0.57	0.35	0.02	0.01
n-hexane-DEC (T <sub>xy</sub> )	2.31	0.05	0.04	0.01
cyc-hexane-DEC (T <sub>xy</sub> )	1.27	0.68	0.02	0.01
n-heptane-DEC (T <sub>xy</sub> )	0.89	0.36	0.03	0.12
n-octane-DEC (T <sub>xy</sub> )	0.68	0.18	0.01	0.01
Acetone-DEC (p <sub>xy</sub> )	1.79	0.66	0.02	0.01
2-butanone-DEC (T <sub>xy</sub> )	0.42	0.57	0.00	0.00
2-pentanone-DEC (T <sub>xy</sub> )	0.53	0.41	0.01	0.01
DMC-1,2- Dichloroethane (p <sub>xy</sub> )	0.02	0.01	0.00	0.00
DMC-1,1,1- Trichloroethane (p <sub>xy</sub> )	0.01	0.01	0.01	0.00



set of  $A_{mn}$  and  $A_{nm}$  values. Hence, the UNIFAC interaction parameters can be thought of as a kind of averaged interaction parameter value as the same set of parameters is employed to represent usually more than one binary.

The graphical comparison between the two model predictions (UNIFAC & NRTL) and the experimental data is presented in Figure 3.6 to Figure 3.8 which show the quality of the individual fits as well as the difference between the two models in predicting the experimental VLE data. The averaged deviation in temperature and pressure, respectively as well as the averaged deviation in  $x_1$  direction is given for all investigated binaries in Table 3.4. The averaged deviation between experimental and predicted values of  $z_n$  is calculated as follows:

$$\Delta Z = \frac{1}{n} \sum_{n=1}^n |z_n^{pred} - z_n^{exp}|$$

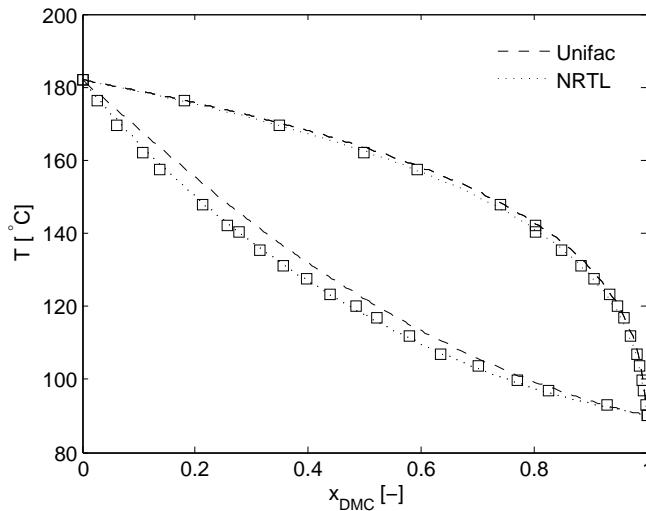


**Figure 3.6:** Experimental results of boiling temperatures versus  $x_{DMC}$  and the corresponding fitted curves using NRTL and UNIFAC for the binary system DMC-phenol (Hu et al., 2004).

Generally, it can be seen that the NRTL model reproduces the experimental data slightly better than the UNIFAC based model (compare also Table 3.4). This was also expected as for NRTL three parameters- namely  $\tau_{12}$ ,  $\tau_{21}$  and  $\alpha$  are

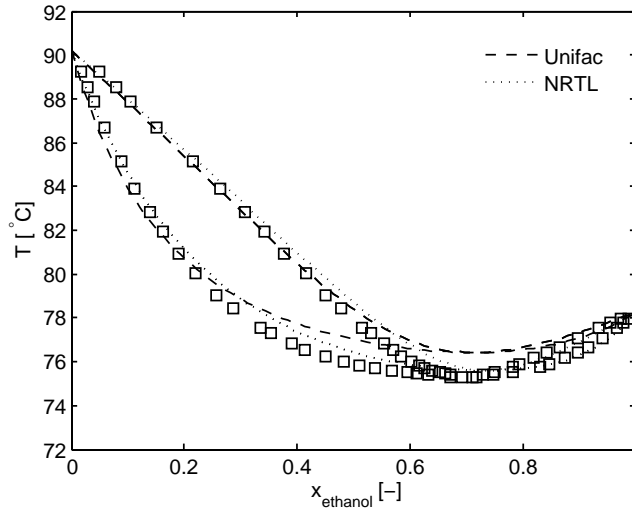


**Figure 3.7:** Experimental results of boiling temperatures versus  $x_{DMC}$  and the corresponding fitted curves using NRTL and UNIFAC for the binary system ethanol-DMC (Rodriguez et al., 2002b).

employed in each binary to match the experimental data whereas for UNIFAC only two functional group interaction parameters ( $A_{nm}$  and  $A_{mn}$ ) are used for every group interaction.

In case of e.g. alkanes-DMC/DEC binaries only two interaction parameters for the binary interaction  $\text{CH}_2\text{-OCOO}$  are deployed to fit the experimental data thereby reproducing the experimental data of eight binaries whereas in case of NRTL overall 24 fit parameters are used. The NRTL fit parameters are given in Table 3.6 and the UNIFAC group interaction parameters in Table 3.7, respectively.

From Figure 3.6 to Figure 3.8 as well as the deviations listed in Table 3.4 it can be concluded that both  $G^E$  models, NRTL and UNIFAC, can be used to properly describe the experimental data of the different investigated binaries in this study. In some cases (e.g. Figure 3.8) UNIFAC predicts the experimental data only fair where in the same situation the NRTL model still yields a good fit. Nevertheless, the UNIFAC based fits are in all cases fair and the predictive power of UNIFAC outweighs the, in some cases observed, slightly less accurate predictions

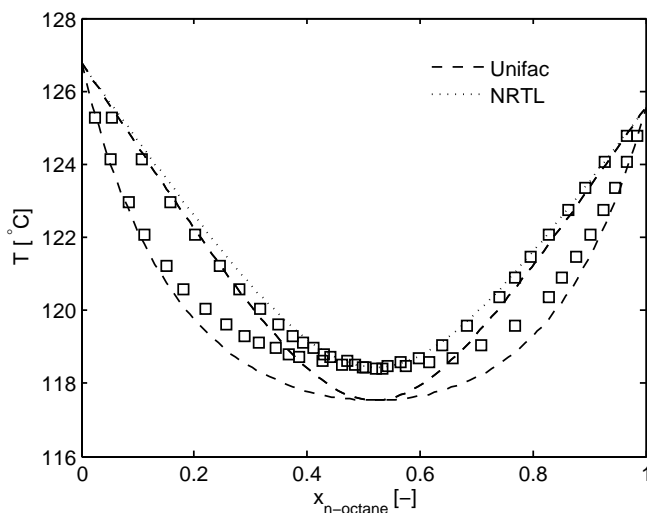


**Figure 3.8:** Experimental results of boiling temperatures versus  $x_{DMC}$  and the corresponding fitted curves using NRTL and UNIFAC for the binary system n-octane-DEC (Rodriguez et al., 2002c).

of the experimental data. Therefore it seems justified to use the derived UNIFAC parameters to "predict" activity coefficients and therewith also VLE data in systems where no experimental data are available.

As the main goal of this study is to fit UNIFAC interaction parameters which can be used to predict activity coefficients for unknown carbonate systems, it is worthwhile to compare the UNIFAC and NRTL predicted activity coefficients with the experimentally derived activity coefficients. The parity plots between experimental and predicted activity coefficients, using both UNIFAC and NRTL, for the prediction of the activity coefficients for different binary systems are shown in Figure 3.9 to Figure 3.11. The following systems have been considered in the parity plots: alcohols-carbonates, alkanes-carbonates and aromatics-carbonates.

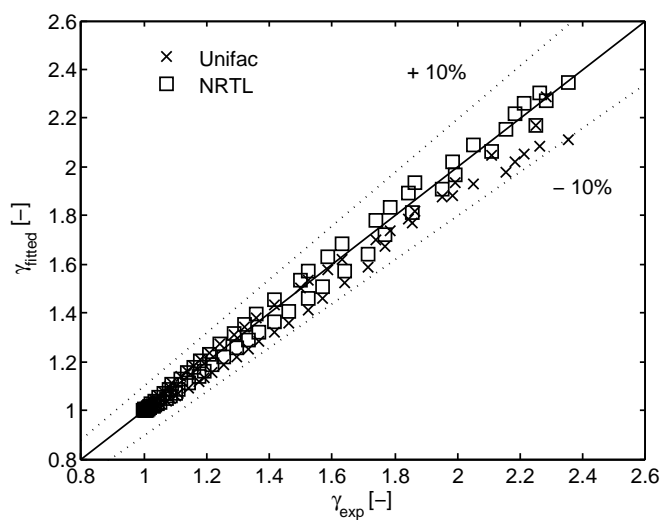
It can be seen that the activity coefficients predicted with NRTL deviate on average <10% from the experimental activity coefficients and those predicted with UNIFAC <15%. It can therefore be concluded that the deviations observed in the Txy- and pxy-diagrams (see Table 3.4) are proportional to those observed in the parity plots.

**Table 3.6:** NRTL Parameters  $\tau_{i,j}$ ,  $\tau_{j,i}$  and  $\alpha = 0.3$  derived from the literature data listed in Table 3.1.

Binary	$\tau_{i,j}$ [J mole <sup>-1</sup> ]	$\tau_{j,i}$ [J mole <sup>-1</sup> ]
Comp <sub>i</sub> - Comp <sub>j</sub>		
DMC-Phenol	9346	-6107
MeOH-DMC	3902	1
EtOH-DMC	4172	-548
DMC-1-PropOH	1614	1212
DMC-1-ButOH	-51	3709
MeOH-DEC	2753	618
EtOH-DEC	4818	-1243
1-PropOH-DEC	4212	-1308
1-ButOH-DEC	4318	-1664
n-hexane-DMC	1990	2820
cyc-hexane-DMC	3419	1233
DMC - n-heptane	3763	1152
DMC - n-octane	5227	368
n-hexane-DEC	5679	-1837
cyc-hexane-DEC	1670	1049
n-heptane-DEC	1419	1344
n-octane-DEC	1506	1592
Acetone-DEC	2417	-2404
2-butanone-DEC	1385	-1310
2-pentanone-DEC	-124	384
DMC-1,2-Dichloroethane	-803	767
DMC-1,1,1-Trichloroethane	385	861

**Table 3.7:** UNIFAC interaction parameters derived from VLE data taken from literature (Table 3.1).

Interaction Group <sub>m</sub> -Group <sub>n</sub>	$A_{m,n}$	$A_{n,m}$
CH <sub>3</sub> OH-OCOO	180	300
OH-OCOO	80	250
CH <sub>2</sub> -OCOO	450	500
ACH-OCOO	-220	250
ACOH-OCOO	189	187
CH <sub>2</sub> CO-OCOO	35	40
CCl-OCOO	135	57
CCl <sub>3</sub> -OCOO	215	160

**Figure 3.9:** Parity plot: comparison between experimental and predicted gamma (NRTL & UNIFAC) for the binary DMC-1-propanol as an example for carbonate-alcohol systems.

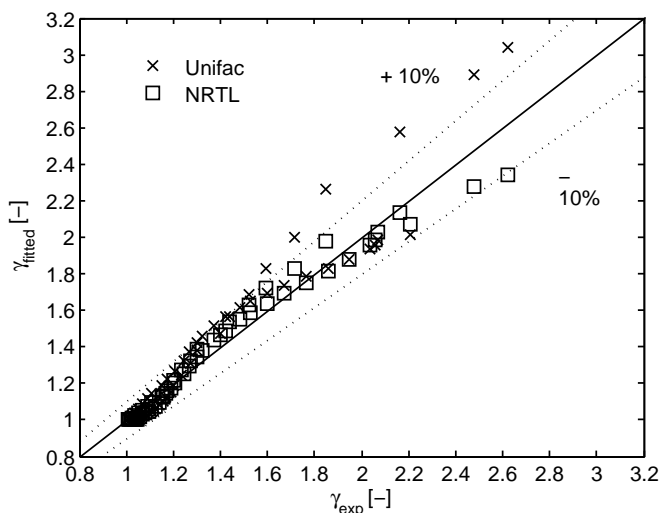


**Figure 3.10: Parity plot: comparison between experimental and predicted gamma (NRTL & UNIFAC) for the binary cyclo-hexane-DEC as an example for carbonate-alkane systems.**

Extending the database with new available VLE data might necessitate the refitting of already fitted groups as the following example will show. The binary system DMC-toluene has been used here as an example to see if the UNIFAC interaction parameter set for ACH-OCOO derived from fitting the binary system DMC-phenol can be used without modification to represent the experimental VLE data of the system DMC-toluene by only fitting the new required interaction parameter set for ACCH<sub>2</sub>-OCOO.

From these results it can be concluded that it is necessary to "refit" the ACH-OCOO interaction parameter set to get a proper fit for both binaries (DMC-phenol and DMC-toluene). Furthermore, also an alteration of the AOH-OCOO group was necessary for an accurate representation of the binary system DMC-phenol. The new interaction parameters are listed in Table 3.8. Therefore it has to be concluded that an extension of the interaction parameter data base will usually require a refitting of all binary systems with molecules involving the same functional groups as the newly introduced molecule (toluene in the example).

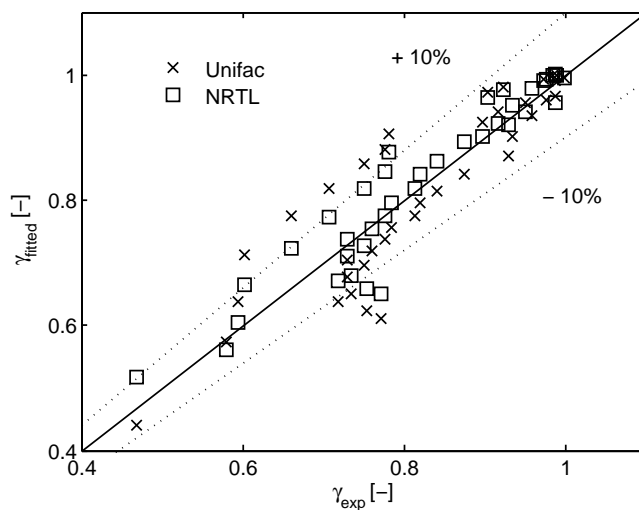


**Figure 3.11:** Parity plot: comparison between experimental and predicted  $\gamma$  (NRTL & UNIFAC) for the binary DMC-phenol as an example for carbonate-aromatic systems.

**Table 3.8:** Revised UNIFAC interaction parameters when adding the ACCH<sub>2</sub>-OCOO interactions for fitting the binary system DMC-toluene.

Interaction Group <sub>m</sub> -Group <sub>n</sub>	$A_{m,n}$	$A_{n,m}$
ACH-OCOO	85	60
ACOH-OCOO	235	20
ACCH <sub>2</sub> -OCOO	1800	1800

### 3.8 Activity coefficients of the multicomponent system methanol-DMC-phenol-MPC-DPC

It has been shown that the experimental activity coefficients derived from VLE data considered in this study generally differ substantially from unity (see Table 3.2). Therefore it seems inevitable to use activity coefficients not only for the description of the VLE but also for a correct and consistent description of the chemical equilibria and reaction kinetics of carbonate containing systems.

In this section the derived UNIFAC interaction parameters will therefore be used to predict the activity coefficients of the system methanol-DMC-phenol-MPC-DPC, for which no experimental VLE data are available. The hypothetic liquid phase compositions (Table 3.9) which might typically be encountered at the bottom, the feed tray -located in the middle of the column- and the top tray of a reactive distillation column, respectively (equimolar feed of DMC & phenol,  $T=180^{\circ}\text{C}$ ,  $p=1\text{atm}$ ) will be used to calculate the corresponding activity coefficients of the 5 different species. This will show to what extent the activity coefficients in a (reactive) distillation column differ from unity (= ideal behaviour) and therefore show if the application of activity coefficients (in chemical equilibrium, VLE data and reaction kinetics) is required for the proper design of a reactor/distillation column involving these components.

The activity coefficients have been calculated with the DECHEMA-K model (Eq. 3.1 with simplifications mentioned earlier). For this purpose the different UNIFAC interaction parameters (Table 3.7) and the Antoine coefficients of the involved species have been used (Table 3.10 & Table 3.12).

For the calculation of the activity coefficients at the compositions specified in Table 3.9, also the vapour pressures and the  $R_k$  and  $Q_k$  values of the components MPC and DPC are required. As there is no information in literature available regarding the vapour pressures and the  $R_k$  and  $Q_k$  values of MPC and DPC, it is necessary to estimate these properties with suitable estimation methods. The Antoine coefficients will be estimated with the well known Riedel equation (Reid et al., 1988) which requires as input the boiling point of the pure component  $T_b$



**Table 3.9:** Hypothetical liquid phase compositions of the multicomponent system MeOH-DMC-PhOH-MPC-DPC in a distillation column.

Mole fraction [-]	Bottom (T=183°C)	Feed (T=173°C)	Top (T=145°C)
MeOH	$3.10 \times 10^{-5}$	$2.30 \times 10^{-3}$	$8.90 \times 10^{-3}$
DMC	$1.50 \times 10^{-2}$	$6.30 \times 10^{-2}$	$2.40 \times 10^{-1}$
PhOH	$8.50 \times 10^{-1}$	$9.30 \times 10^{-1}$	$7.50 \times 10^{-1}$
MPC	$9.20 \times 10^{-2}$	$8.10 \times 10^{-3}$	$5.00 \times 10^{-4}$
DPC	$3.80 \times 10^{-2}$	$5.60 \times 10^{-4}$	$8.40 \times 10^{-8}$

**Table 3.10:** Estimated pure component data and UNIFAC volume (R) and surface area (Q) parameters of MPC and DPC.

	MPC	DPC	Method/Source
Anointe coeff.	A = 21.722	A=23.412	Reid et al. (1988)
	B = 3253.55	B=6810.36	
	C= -44.25	C=0	
$T_c$ [K]	711.76	799.32	Constantinou and Gani (1994)
$P_c$ [Pa]	3441136	2796493	Constantinou and Gani (1994)
$T_b$ [K]	491.76	572.99	Constantinou and Gani (1994)
R UNIFAC	5.505	7.626	Fredenslund et al. (1975)
Q UNIFAC	4.362	5.634	Fredenslund et al. (1975)

as well as its critical temperature  $T_c$  and the critical pressure  $p_c$ , respectively. As data on the critical properties ( $T_{c,p_c}$ ) and the boiling point are not available, these

properties have been estimated with the method of Constantinou and Gani (1994). The numerical values of these properties, the estimated Antoine coefficients of MPC and DPC and the corresponding R and Q values as used in the combinatorial part of the UNIFAC equation are given in Table 3.10. With data provided in Table 3.7, Table 3.10 and Table 3.12 the activity coefficients for the compositions given in Table 3.9 can be calculated. The results are shown in Figure 3.12.

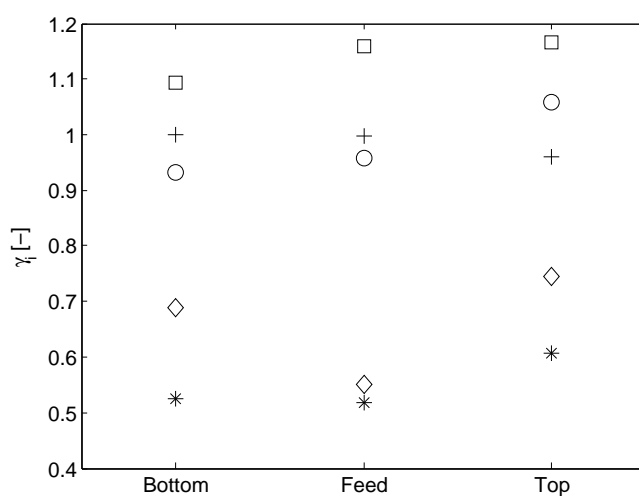


**Figure 3.12: Activity coefficients at three different locations in a distillation column. (◇) MeOH, (\*) DMC, (+) PhOH, (○) MPC, (□) DPC.**

Figure 3.12 shows the calculated activity coefficients at three different locations in a distillation column. The activity coefficients of phenol and MPC deviate only slightly (<10%) from unity whereas the other activity coefficients, especially those of methanol and DMC, deviate substantially from unity. These results indicate clearly the need to use activity coefficients for the description of the VLE, the reaction rates and the chemical equilibria for the considered system.

As can be seen from Figure 3.12 the activity coefficient of phenol remains virtually constant while other activity coefficients as those of DPC (~7%) and MPC (~10%) change moderately over the whole column length. The activity coefficients which vary more pronounced over the column length are those of methanol (~25%) and

DMC ( $\sim 15\%$ ). The binary methanol-DMC exhibits a far from ideal behavior - see  $\ln \gamma$ -plot (Figure 3.4)- and therefore it could be expected that also the calculated activity coefficients of methanol and DMC would 1) deviate substantially from unity and 2) vary considerably over the column height.

It is expected that these non-idealities will be even more pronounced at higher conversions of phenol and DMC, respectively compared to the conversion of  $\sim 11\%$  (w.r.t. PhOH) which has been assumed in this example.

### 3.9 Conclusion

The DECHEMA-K model incorporating either the UNIFAC or the NRTL  $G^E$ -model to describe the activity coefficients has been applied to fit the experimental VLE data of the following systems: phenol-DMC, toluene-DMC, alcohol-DMC/DEC, and alkanes-DMC/DEC, ketones-DEC and chloro-alkanes-DMC. The model predictions have been compared to the experimental data showing a good ( $<10\%$  dev. NRTL) to fair ( $<15\%$  dev. UNIFAC) agreement between model and experimental data which seems to justify the use of the deduced UNIFAC parameters for the prediction of unknown activity coefficients of organic carbonate containing systems.

The newly derived UNIFAC parameters have been applied to predict the activity coefficients of the experimentally unknown multicomponent system methanol, dimethyl carbonate, phenol, methyl phenyl carbonate and diphenyl carbonate at three different compositions which are likely to be encountered in a reactive distillation column. It can be concluded from these estimations that the activity coefficients 1) deviate substantially from unity and 2) vary considerably over the "hypothetical" column height. Hence, it is recommended to use activity coefficients for the description of the VLE when studying the separation characteristics at considerably changing system compositions.

Moreover, it seems also necessary to use activity coefficients for the description of chemical equilibria and reaction kinetics of the herein investigated carbonate system. This is recommended as the concentrations seem to change considerably over the height of a distillation column and concentration based chemical equilibrium values

tend to be concentration dependent and therefore are not constant. This concentration dependence can be avoided or at least alleviated by introducing activity coefficients thereby using the thermodynamically sound formulation for a chemical equilibrium value (Sandler, 1999). Furthermore, it seems advisable to employ activity based reaction rates as this kind of description is consistent with the thermodynamically sound formulation of the chemical equilibrium. Since a reactive distillation column is preferably operated close to chemical equilibrium, activity based reaction rates are preferred for reasons of consistency compared to simple concentration based kinetics which usually suffice for the description of nearly ideal systems where the chemical equilibrium constant changes only marginally.

## Acknowledgement

The author gratefully acknowledges the financial support of Shell Global Solutions International B.V. Furthermore Harry Kooijman is acknowledged for extending the thermodynamic-interface of ChemSep which has been used in this work.

## Notation

$A_i$	Antoine coefficient	[Pa]
$A_{m,n}$	Interaction parameter between groups m and n	[K]
$B_i$	Antoine coefficient	[Pa K]
$C_i$	Antoine coefficient	[K]
$p$	Pressure	[Pa]
$p_i^{vap}$	Saturated vapour pressure of molecule i	[Pa]
$p_c$	Critical pressure	[Pa]
$q_i$	Surface area parameter for species i	[-]
$Q_k$	Surface area parameter of group k	[-]
$r_i$	Volume parameter for species i	[-]
$R_k$	Volume of group k	[-]
$T_b$	Normal boiling point	[K]
$T_c$	Critical temperature	[K]
$x_i$	Liquid phase mole fraction of molecule i	[-]
$X_m$	Mole fraction of group m in mixture	[-]

$y_i$	Vapour phase mole fraction of molecule i	[-]
Greek symbols		
$\nu_k^i$	Number of functional groups k in species i	[-]
$\alpha_{i,j}$	Nonrandomness constant for binary i-j interactions	[-]
$\tau_{i,j}$	Interaction parameter between molecules i and j in the NRTL model	[J mol <sup>-1</sup> ]
$\phi_i$	Volume fraction of species i	[-]
$\theta_i$	Area fraction of species i	[-]
$\Theta_m$	Surface area fraction of group m	[-]
$\psi_{m,n}$	Temperature dependent interaction parameter between groups m and n	[-]
Subscripts and Superscripts		
c	combinatorial part	[-]
r	residual part	[-]
i,j	Molecule i,j	[-]
k,m,n	Groups k,m,n	[-]

### 3.10 Appendix

**Table 3.12:** Antoine parameters used to calculate the vapour pressures ( $\ln p^{vap} [\text{Pa}] = A - B/(T[\text{K}] + C)$ ) in the DECHEMA-model.

	A	B	C	Source
DMC	21.72	3253.60	-44.25	Luo et al. (2000)
DEC	20.45	2817.80	-84.30	Rodriguez et al. (2002b)
methanol	23.35	3555.30	-37.16	Kooijman and Taylor (2007)
ethanol	22.99	3337.30	-60.41	Kooijman and Taylor (2007)
1-propanol	22.11	2968.40	-89.94	Kooijman and Taylor (2007)
1-butanol	21.47	2804.00	-108.82	Kooijman and Taylor (2007)
phenol	21.47	3610.50	-91.90	Kooijman and Taylor (2007)
n-hexane	20.75	2711.80	-47.91	Kooijman and Taylor (2007)
cyclo-hexane	21.08	3073.10	-32.25	Kooijman and Taylor (2007)
n-heptane	21.00	3044.20	-50.15	Kooijman and Taylor (2007)
n-octane	20.91	3157.80	-62.16	Kooijman and Taylor (2007)
Toluene	20.86	3019.20	-60.13	Kooijman and Taylor (2007)
Acetone	21.43	2850.70	-41.68	Kooijman and Taylor (2007)
2-butanone	21.45	3070.50	-43.31	Kooijman and Taylor (2007)
2-pentanone	22.09	3681.20	-26.75	Kooijman and Taylor (2007)
1,2-Dichloroethane	21.38	3088.60	-43.10	Kooijman and Taylor (2007)
1,1,1-Trichloroethane	20.67	2724.10	-49.44	Lide (2004)

## Chapter 4

# Experimental determination of the chemical equilibria involved in the reaction from Dimethyl carbonate to Diphenyl carbonate

### Abstract

New experimental equilibrium data of the reaction of Dimethyl Carbonate (DMC) and Phenol to Methyl Phenyl Carbonate (MPC) and the subsequent disproportion and transesterification reaction of MPC to Diphenyl Carbonate (DPC) are presented and interpreted in terms of the reaction equilibrium coefficients. Experiments have been carried out in the temperature range between 160°C and 200°C and for initial reactant ratios of DMC/phenol from 0.25 to 3. By employing activities instead of 'only' mole fractions in the calculation of the reaction equilibrium coefficients, the influence on the reactant ratio DMC/phenol on the derived equilibrium values for the reaction of DMC to MPC could be reduced, especially for temperatures of 160°C. The activity based equilibrium coefficient for the transesterification reaction from MPC with phenol to DPC and methanol is constant within experimental uncertainty

and, therefore, largely independent of the initial reactant ratio DMC/phenol at temperatures of 160°C and 180°C.

The temperature dependence of the equilibrium coefficients  $K_{a,1}$  and  $K_{a,2}$  has been fitted by applying the well known Van't Hoff equation, resulting in the expressions  $\ln K_{a,1} = -2702/T[K] + 0.175$  and  $\ln K_{a,2} = -2331/T[K] - 2.59$ . It has been demonstrated that these equations have fair, in case of  $\ln K_{a,1}$ , and excellent, in the case of  $\ln K_{a,2}$ , predictive capabilities, even for experimental conditions that deviate significantly from those used in this study. Hence, it is expected that the derived temperature dependent correlations for  $K_{a,1}$  and  $K_{a,2}$  based on activities can be used in reactive distillation models to assess different process configuration in the manufacture of DPC starting from DMC and phenol.

## 4.1 Introduction

Diphenyl Carbonate is a precursor in the production of Polycarbonate (PC). Polycarbonate is widely employed as an engineering plastic important to the modern lifestyle; used in, for example, the manufacture of electronic appliances, office equipment and automobiles. About 3.4 million tons of PC was produced worldwide in 2006. Production is expected to increase by around 6% per year until 2010 with the fastest regional growth is expected in East Asia, averaging 8.7% per year through 2009 (Westervelt, 2006).

Traditionally, PC is produced using phosgene as an intermediate. The phosgene process entails a number of drawbacks. First, 4 tons of phosgene are needed to produce 10 tons of PC. Phosgene is very toxic and when it is used in the production of PC the formation of undesired hazardous salts as by-products cannot be avoided. Furthermore, the phosgene-based process uses 10 times as much solvent (on a weight basis) as PC is produced. The solvent, methylene chloride, is a suspected carcinogen and is soluble in water. This means that a large quantity of waste water has to be treated prior to discharge (Ono, 1997).

Many attempts have been made to overcome the disadvantages of the phosgene based process (Kim et al., 2004). The main point of focus has been a route



through Dimethyl carbonate (DMC) to diphenyl carbonate (DPC), which then reacts further with Bisphenol-A to produce PC. The most critical step in this route is the synthesis of DPC from DMC via transesterification to methyl phenyl carbonate (MPC), usually followed by a disproportionation and/or transesterification step to DPC. The equilibrium conversions of the reactions to MPC and DPC are highly unfavorable: in a batch reactor with an equimolar feed, an equilibrium conversion to DMC of only 3% can be expected. Therefore, good process engineering is required in the design of a process to successfully carry out the reaction of DMC to DPC on a commercial scale. The reaction appears to be a candidate for being carried out in a reactive distillation column to help realize high conversions (Rivetti, 2000). Reactive distillation appears to be a viable production technology as methanol, an intermediate product, can be separated from the other components by simple distillation and hence the conversion of DMC and phenol in the transesterification step can be increased. Regardless of the type of reactor chosen, it is important to know the chemical equilibria and kinetics involved in this system. In this section chemical equilibrium data determined from batch reactor experiments are presented.

## 4.2 Reactions

The synthesis of diphenyl carbonate (DPC) from dimethyl carbonate (DMC) and phenol takes place through the formation of methyl phenyl carbonate (MPC) and can be catalyzed either by homogeneous or heterogeneous catalysts. The reaction of DMC to DPC is a two-step reaction. The first step is the transesterification of DMC with phenol to the intermediate MPC and methanol (Ono, 1997; Fu and Ono, 1997):

For the second step two possible routes exist: The transesterification of MPC with phenol the disproportionation of two molecules of MPC yielding DPC and DMC (Reaction 4.3).

Ono (1997) suggests that DMC and phenol may also react to produce anisole.

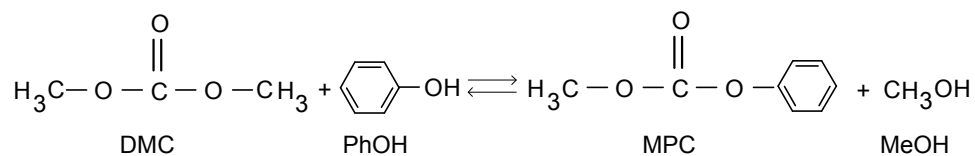


Figure 4.1: Transesterification 1

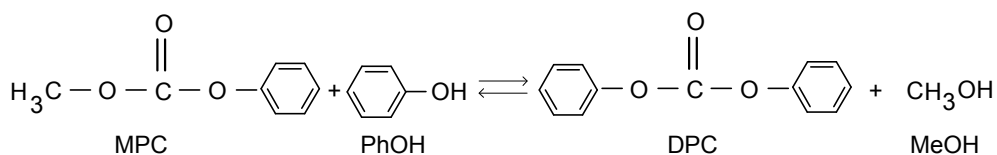


Figure 4.2: Transesterification 2

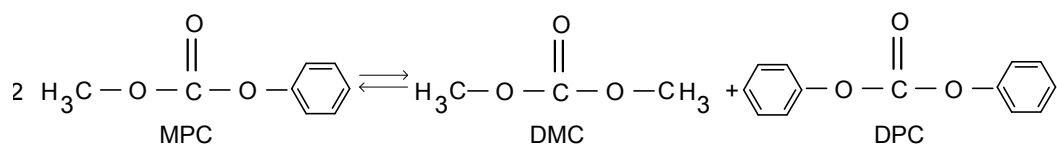


Figure 4.3: Disproportionation

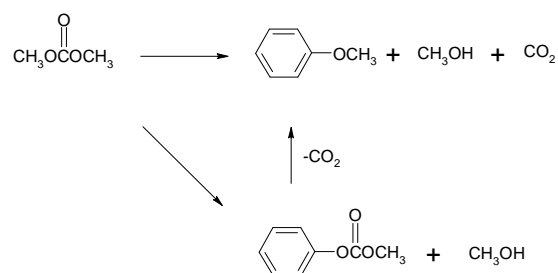


Figure 4.4: Side reaction forming anisole, methanol and carbon dioxide

### 4.3 Thermodynamics

The reaction of DMC to DPC can either proceed through the transesterification-disproportionation step (see Reactions 4.1 and 4.3) or the transesterification- transesterification step (see Reactions 4.1 and 4.2). From a thermodynamic point of view the second step from MPC to DPC -via either the transesterification reaction (4.2) or the disproportionation reaction (4.3)- is interchangeable, and one of the reaction equilibria involved can be left out of the thermodynamic description.

First, the special case of the equilibrium coefficients with all activity coefficients set to one will be considered to compare the equilibrium values derived from the experiments in this study to those in literature. At the end of this section the general formulation of the equilibrium coefficients incorporating activity coefficients will be presented. The mathematical formulation of the different simplified equilibrium coefficients is given in Equations 4.1 to 4.4, with the overall equilibrium coefficient as defined by Eq. 4.4.

$$K_{x,1} = x_{MPC} x_{MeOH} x_{DMC}^{-1} x_{PhOH}^{-1} \quad (4.1)$$

$$K_{x,2} = x_{DPC} x_{MeOH} x_{MPC}^{-1} x_{PhOH}^{-1} \quad (4.2)$$

$$K_{x,3} = x_{DPC} x_{DMC} x_{MPC}^{-2} = \frac{K_{x,2}}{K_{x,1}} \quad (4.3)$$

$$K_{x,ov} = x_{DPC} x_{MeOH}^2 x_{DMC} x_{PhOH}^2 = K_{x,1} K_{x,2} = (K_{x,1})^2 K_{x,3} \quad (4.4)$$

The reaction equilibrium coefficients for the reactions 4.1 to 4.3 have been determined by several authors as summarized in Table 4.1 (note: in this table the equilibrium coefficients have been calculated on a mole fraction basis). The equilibrium coefficients for both transesterification reactions are quite low (Rivetti, 2000; Harrison et al., 1995) and it must be concluded that these values do not allow for high conversions if the reaction is carried out in a batch reactor. In Table 4.1 equilibrium data taken from the literature are reported at 298K and at 491K for the

equilibrium coefficients of all three reactions. Unfortunately, only one value for one reaction is provided in the relevant temperature window between 433K and 473K. Therefore a systematic experimental study has been carried out to determine the equilibrium values of the three different reactions at varying experimental conditions as e.g. different initial reactant ratios and temperatures.

Since both reactions have a very low equilibrium coefficient at 298K it is plausible that low conversions are obtained even when no specific measures would be taken. If the values of the equilibrium coefficients of reaction 4.1 and 4.3 as given in Table 4.1 are correct, it can be concluded from the values of the Gibbs free energy that both the reactions are slightly endothermic (assuming of course, that the entropy change of reaction is small compared to the enthalpy change of reaction). The value of the Gibbs free energy of the disproportionation reaction is close to zero and thus it is expected that also the heat of reaction is close to zero. Hence, it is likely that the disproportionation reaction is not very sensitive to temperature variations.

The values of the equilibrium coefficients given in Table 4.1 taken from different sources should be interpreted with some care. It is unclear if the values of the equilibrium coefficient reported by Rivetti (2000) were determined experimentally or were calculated from standard Gibbs enthalpies at 298K. Furthermore, the equilibrium coefficient given by Tundo et al. (1988) must be interpreted carefully as only the reaction temperature of 453K is given in the source; no information is provided concerning reactant ratio and reaction time. Harrison et al. (1995) do give all of the liquid phase concentrations needed to calculate the  $K_{x,i}$  values and also most of the experimental conditions. From the experimental data given in the patent of Harrison et al. (1995), equilibrium coefficients of reaction 4.1 and 4.3 can be estimated. For the calculation of the equilibrium values the concentrations of the involved species, given in example 1 and 3 of the patent, were used and averaged. The two experiments (examples 1 and 3 in the patent) were carried out at a molar DMC/phenol ratio of 1:1 at 491.15K with durations of 30 minutes and 60 minutes, respectively. The catalyst used in example 1 was a tetraphenyl titanate catalyst prepared by the investigators, whereas in example 3 a commercially available mixture of titanium tetraisopropylate and tetra-n-butylate was used as catalyst. The

amount of catalyst used in the experiments corresponds to a mole fraction of around  $2.3 \cdot 10^{-2}$ , which is roughly 30 times higher than the amount of catalyst typically used in one of the equilibrium experiments presented in this study. Thus, it seems likely that chemical equilibrium was achieved under the conditions reported in the patent.

**Table 4.1:** Literature values of the equilibrium coefficients for the DPC synthesis

Equilibrium constant	$K_{T=298K}$ Rivetti (2000)	$K_{T=453K}$ Tundo et al. (1988)	$K_{T=491K}$ Harrison et al. (1995)	$\Delta G_{298K}$ Rivetti (2000) kJ/mole
$K_{x,1}$	$6.3 \cdot 10^{-5}$	$3.0 \cdot 10^{-4}$	$2.72 \cdot 10^{-3}$	+ 23.9
$K_{x,2}$	$1.2 \cdot 10^{-5}$		$5.73 \cdot 10^{-4}$	+ 28.1
$K_{x,3}$	$1.9 \cdot 10^{-1}$		$2.11 \cdot 10^{-1}$	+ 4.2
$K_{x,ov}$ Reaction 1+2	$7.6 \cdot 10^{-10}$		$1.56 \cdot 10^{-6}$	+ 50.7
$K_{x,ov}$ Reaction 1+3	$1.2 \cdot 10^{-5}$		$5.74 \cdot 10^{-4}$	+ 28.1

The thermodynamically sounder formulation of the chemical equilibrium would involve the additional use of activity coefficients of the species and the following equations for the reaction equilibrium coefficients (Sandler, 1999):

$$K_{a,i} = K_{x,i} \cdot K_{\gamma,i} \quad (4.5)$$

$$K_{a,i} = \underbrace{\frac{\prod_{j=1}^n x_{\text{Products}}^j}{\prod_{k=1}^n x_{\text{Reactants}}^k}}_{K_{x,i}} \cdot \underbrace{\frac{\prod_{j=1}^n \gamma_{\text{Products}}^j}{\prod_{k=1}^n \gamma_{\text{Reactants}}^k}}_{K_{\gamma,i}} \quad (4.6)$$

The activity coefficients needed for the evaluation of the activity based chemical equilibrium coefficients can, in principal, be calculated with any applicable activity coefficient model e.g. NRTL, Wilson, UNIQUAC or UNIFAC (Prausnitz and

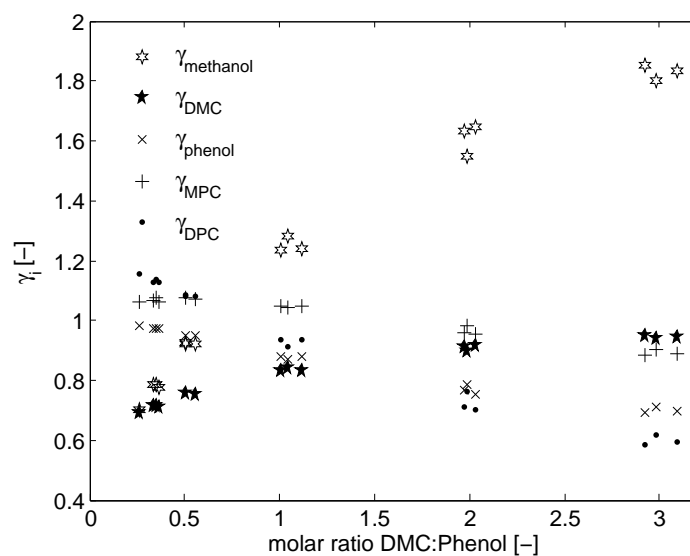
Tavares, 2004). In this study, it has been decided to use the UNIFAC model as this then provides a predictive character not shared by any of the other activity coefficient models mentioned above. Hence, it is not necessary to have experimental VLE data for every component involved as the UNIFAC method is based on group contributions. However, using the UNIFAC method to predict the activity coefficients might yield larger deviations from available experimental data than those that would have been obtained with other VLE models where every molecule-molecule interaction is fitted separately. For standard systems, i.e. acetone- n-pentane, the deviation between UNIFAC predicted and experimentally determined infinite dilution activity coefficients can amount up to around 15%, whereas for the other VLE models mentioned the difference is typically in the range of 1-10%, depending on the non-ideality of the binary solution. The deviation of 15% is representative for the accuracy of the predictive UNIFAC VLE method (Reid et al., 1988). Experimental VLE data of the components essential to this study are very scarce in the open literature and so the benefits of using the UNIFAC method seem to outweigh the possible lack of accuracy in this particular case.

In order to apply the UNIFAC method in this study, a new UNIFAC group had to be introduced, namely the carbonate group O-CO-O, which was until now not present in the published UNIFAC database. The interaction parameters of this new OCOO-group with other UNIFAC groups, which are of importance for the system presented here, have been fitted to VLE data taken from the open literature. For the exact determination of the interaction parameters between the OCOO- group and the other functional groups involved in the present system, the reader is referred to Haubrock et al. (2007a).

The activity coefficients calculated by means of UNIFAC for various ratios of DMC/Phenol at 180°C are shown in Figure 4.5. From this figure it can be clearly seen that the activity coefficients deviate substantially from unity and the mixtures cannot be regarded as ideal. The activity coefficient of methanol spans the range from 0.7 to 1.9 over the initial reactant ratio DMC/phenol whereas the other species vary only between 0.6 and 1.3. This suggests that methanol seems to interact strongly with either DMC and/or phenol.

As the activity coefficients suggest that the mixture is far from ideal, it is likely that the use of activity coefficients in the formulation of the equilibrium coefficient will differ from the mole-fraction-based chemical equilibrium coefficients in Table 4.1.

As already stated, if the value of  $K_{x,2}$  (or  $K_{a,2}$ ) is known, the value of  $K_{x,3}$  (or  $K_{a,3}$ ) can be derived, and therefore, in the remainder of this section only  $K_{x,2}/K_{a,2}$  and not  $K_{x,3}/K_{a,3}$  will be determined and discussed.



UNIFAC predicted

**Figure 4.5:**  $\gamma_i$  for different initial DMC-Phenol ratios at 180°C (at chemical equilibrium); Conversions w.r.t. phenol are between 0.5 and 3%.

## 4.4 Catalysts

Numerous catalysts are known to promote common transesterification reactions. Nevertheless, many of these catalysts are not suited for the transesterification of DMC to DPC as they also catalyze the decarboxylation to anisole (Ono, 1997).

Heterogeneous catalysts usually are more desirable than homogeneous catalysts because it is easier to separate the former from the other liquid species in the mixture (Kim and Lee, 1999). Most such catalysts are supported metal oxides, such as  $\text{MoO}_3$  on silica. Ono (1997) investigated different types of heterogeneous catalysts and showed that the selectivity of these catalysts for the reaction towards anisole is much higher than that of homogeneous catalysts where only traces of anisole can be detected. As anisole formation should be minimized, it is preferable to use a homogeneous catalyst.

For the system in this study homogenous catalysts often are commercially available and hence no tailor-made manufacture of a supported heterogeneous catalyst is necessary. Moreover, the reproducibility of the kinetic experiments is improved when using a homogenous, commercially available catalyst as the grade of this kind of catalyst will change only marginally compared to tailor-made heterogeneous catalysts. Hence, a consistent quality of the catalyst is more likely when using a commercially available homogeneous catalyst.

For this study the homogenous catalyst Titanium(n-butoxide) will be used. A tin-based catalyst ( $\text{n-Bu}_2\text{SnO}$ ) has been disregarded as the DPC made with this type of catalyst exhibits an undesirable grayish color (Fuming et al., 2002).  $\text{AlCl}_3$  and  $\text{ZnCl}_2$  have been rejected as these catalysts are both susceptible towards water and do therefore hydrolyze to  $\text{TiO}_2$  in aqueous media thereby losing their catalytic activity (Fuming et al., 2002).

Samarium-trifluoromethanesulfonate (STFMS) has been rejected as a possible catalyst to avoid the lab synthesis of this commercially unavailable catalyst and to eliminate the formation of anisole.

The conversion rate of DMC as well as the selectivity towards MPC and DPC with a Titanium(n-butoxide) catalyst is close to that of the STFMS catalyst and the tin-based catalyst, and no noticeable anisole is formed (Shaikh and Sivaram, 1992). Therefore Titanium(n-butoxide) seems to be the most suitable homogeneous catalyst to promote the reactions from DMC to DPC (see Eq. 4.1 to 4.3). The sensitivity of the Titanium (n-butoxide) catalyst towards water is not a concern here since all chemicals used were either water free or contained only traces of water



(as e.g. phenol), which did not seem to reduce the catalyst activity during the experiments.

## 4.5 Chemicals

All chemicals were used as received from the supplier. Dimethyl carbonate (purity: 99+%) was purchased from Alldrich, Phenol (99+%) and Tetra-(n-butyl orthotitanate) (98+%) were acquired from Merck. The catalyst was stored over molecular sieves (Type 4a) to prevent degradation due to moisture from air.

## 4.6 Experimental setup and procedure

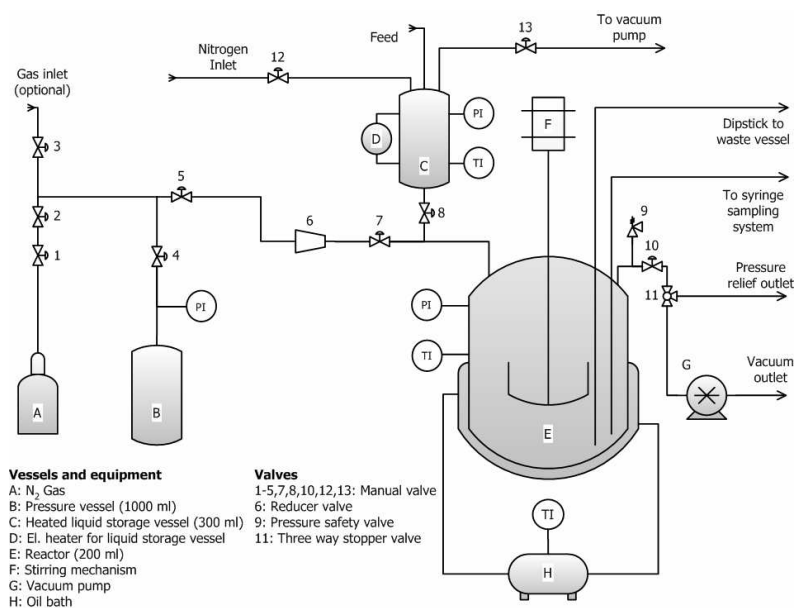


**Figure 4.6: Experimental Setup - Closed batch reactor with supply vessel containing DMC.**

The setup used for the experiments is shown schematically in Figure 4.6 and consisted of a stainless steel reactor of 200 ml and a storage vessel of 300 ml. The

reactor could be heated with an oil-bath and the storage vessel with an electrical heater. The pipes of the apparatus were traced to maintain the desired reaction temperature and to prevent cold spots and possible condensation of phenol. Valve 8 separates the two vessels (see Figure 4.6) and was opened to start the reaction; this is also the moment when the recording of data was started. The two reactants were heated separately to prevent reaction prior to their introduction into the reactor. The catalyst was located in the reactor with the reactant phenol. Both vessels were connected to a nitrogen source, which allowed the reaction to proceed under a complete nitrogen atmosphere to suppress possible oxidation reactions. The temperature of both vessels was monitored. The reactor itself was also provided with a pressure transducer for recording the pressure during the experiment. During the reaction, samples of 1 ml could be taken from the liquid phase in the reactor by means of a syringe sampling system.

After the sampling procedure, the filled vials were cooled down in an ice-bath to stop the reaction. The time from the start of the experiment ( $t=0$ ) to the moment the vials were put in the ice-bath was taken as the reaction time. All vials were analyzed with a GC within 24 hours after the experiment concluded. The gas chromatograph used in this study was a Varian 3900 equipped with a FID detector. The column in the GC was a 50-meter long fused silica column (Varian CP 7685). The gas chromatograph applied a temperature ramp for the analysis: the column temperature was kept at 50°C for 2 minutes, then the temperature was raised 20°C per minute until a temperature of 300°C was reached. This temperature was maintained for three minutes before the column oven was cooled down to 50°C for the next analysis run.

For the quantification of the components present in the samples, two internal standards were used in the GC analysis, namely toluene and n-tetradecane. These internal standards were chosen because their retention times are close to those of the components to be measured and moreover, the peaks of the two internal standards do not overlap with other peaks. Roughly 4 weight percent of each internal standard was added to each sample. Toluene was used as internal standard for methanol and DMC, whereas n-tetradecane was used as the internal standard for phenol, MPC

and DPC. The relative error in the GC analysis was typically <5% for species such as DMC and phenol, <10% MPC, <15% methanol and up to 20% for DPC as this species was only present in very small amounts. The GC error for DPC was generally smaller (<10%) for experiments where an initial excess of DPC was added to the reactants.

To verify that the reaction was effectively stopped after the sample has been taken from the reactor, a sample from the reactor was divided in several identical sub-samples. The time between sampling and analysis of these sub-samples was varied between 0 and 48 hours. The sample analysis showed no sign of change with increasing time, demonstrating that no reaction (including degradation/side reactions) occurred during the first 48 hours between the sampling and the analysis.

## 4.7 Experimental results

### 4.7.1 General remarks

The equilibrium conversion of the reactants phenol and DMC at 180°C was typically around 4%. The time to achieve chemical equilibrium depended on two factors, namely the amount of catalyst and the ratio of DMC/phenol, but was typically in the range of 15 minutes to 1 hour. As expected, a larger amount of catalyst results in a higher reaction rate and chemical equilibrium is achieved faster. Experiments have been performed with around 130g overall reactant mixture and with different catalyst mole fractions ( $\sim 1.0 \cdot 10^{-4}$  and  $2.5 \cdot 10^{-4}$ ) while maintaining otherwise the same experimental conditions. No indication has been found that the amount of catalyst changes the numerical value of the inferred reaction equilibrium coefficient (see Figure 4.7).

A material balance calculation for the experiments showed a mismatch in the amounts of the reaction products: methanol on one side and (MPC + 2 DPC) on the other side. Looking at reaction 4.1 it can be expected that both methanol and MPC would be produced in equal amounts. However, as MPC can react further to DPC according to reaction 4.2 or 4.3, again under the formation of methanol, the mole

fraction of MPC would be expected to be lower than the mole fraction of methanol. However, the sum of the mole fractions of MPC and 2 DPC should be equal or higher (in which case a good deal of methanol would be present in the gas phase) to the mole fraction of methanol and this typically was not seen. Based on VLE calculations it has been estimated, that the amount of methanol in the liquid phase is more than 95% of the overall amount of methanol. The molar amount of methanol in the liquid phase should, therefore, be around 5% less than the cumulated molar amount of MPC+ 2DPC.

The experimentally determined mole fractions of (MPC + 2 DPC) and methanol were deviating by around 20 to 35% whereupon the latter one was always larger. This deviation cannot be attributed to an analysis fault caused by the gas-chromatograph (GC) as the GC error is estimated to be no more than 5%.

A GC analysis of the starting reactants Phenol and DMC showed that there was an initial amount of methanol present in DMC, typically around 0.5 weight% of the amount of DMC. This also explains why the methanol mole fraction was never zero at the start of an experiment. The amount of methanol in the reactant DMC was always less than 0.50 weight% but considering the low conversion of the reactants and hence low yields of the products, this initial amount can easily explain the previously mentioned mismatch in the mass balance. As the initial mole fraction of methanol in the reactor depends on the ratio of Phenol/DMC (with Phenol having no methanol in it), the mismatch in the mass balance also increased with decreasing ratio of Phenol to DMC.

Anisole was not detected by GC analysis in any of the experiments within the detection limit of the GC (mole fraction anisole < 0.001%). It can be concluded that the side reaction to make anisole either does not occur or if it occurs it is to a very small extent. In addition, no peaks, other than those expected, appeared in the GC plots, suggesting that no other byproducts were formed.

An extra series of measurements at 180°C was carried out in which a small amount of DPC was added to the reaction mixture at the start of the experiment. The initial concentration of DPC of around 1 mol% is between 10 and 50 times larger than the actual equilibrium concentration of DPC. It was hoped that these

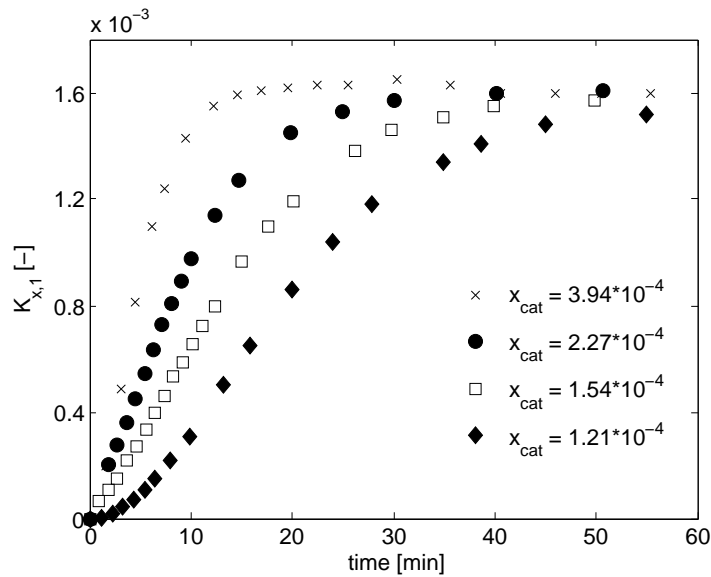


**Figure 4.7: Course of the equilibrium coefficient  $K_{x,1}$  over time at varying catalyst amounts.**

experiments would demonstrate that the same equilibrium state is approached even if the initial DPC concentration was not zero.

Experiments show that chemical equilibrium is achieved in a relatively short time (<60min) and that the catalyst amount does not influence the results in terms of the equilibrium coefficients (up to a catalyst mole fraction of at least  $2.5 \cdot 10^{-4}$ ). Our own reference experiments with no additional catalyst show that even after 24 hours the composition was still far from chemical equilibrium (<5% of the equilibrium concentration of MPC was detected after 24h). It can be concluded that even if a partial deactivation/decomposition of the catalyst takes place, the influence on the chemical equilibrium measurements is negligible.

## 4.8 Equilibrium coefficient $K_{x,1}$

Figure 4.8 shows typical mole fraction profiles for the reaction products MPC and DPC. The mole fraction profiles in Figure 4.8 are typical for all of the experiments

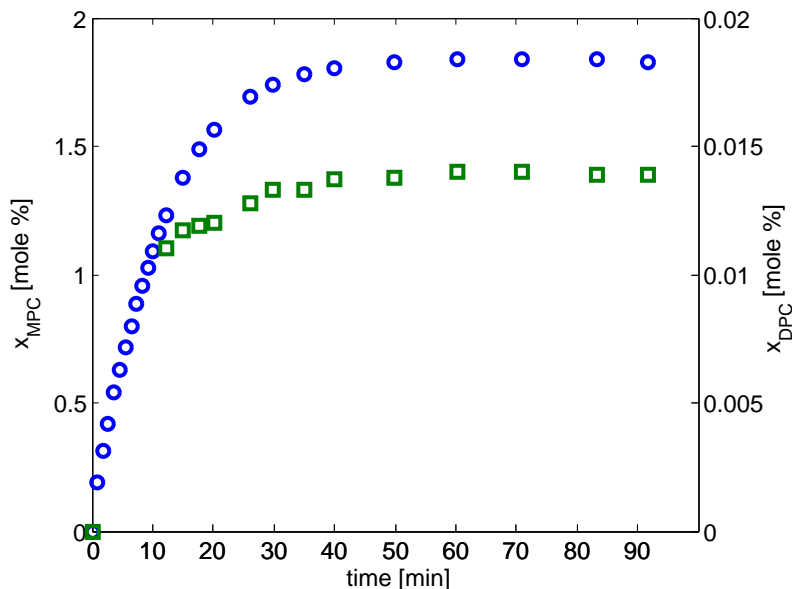


**Figure 4.8:** Typical mole fraction profiles over time for the reaction products MPC (circles) and DPC (squares) at 180°C. Note: for reaction times below 10 minutes the DPC amount is below the detection limit of the GC.

carried out in this study. Of course the time until the mole fraction profiles become flat depends on the reaction conditions (e.g. temperature and catalyst amount).

The raw data of the experiments carried out for this study are given in Table 4.4 in the appendix. Based on the experimentally determined mole fractions (Table 4.4) the equilibrium coefficient  $K_{x,1}$  (Equation 4.1) of the reaction from DMC and phenol to MPC and methanol has been calculated. In Figure 4.9 the reaction equilibrium coefficient  $K_{x,1}$  has been plotted over the initial reactant ratio DMC/phenol for temperatures of 160°C, 180°C and 200°C. At 200°C only experiments at a DMC/phenol ratio of 1 have been carried out and therefore only the  $K_{x,1}$  values at this ratio are shown in Figure 4.9. From thermodynamic considerations (see also Table 4.1) it was expected that the equilibrium coefficient will increase slightly with increasing temperature, as the transesterification reaction of DMC to MPC is endothermic. This behavior is confirmed by experimental results as shown in Figure 4.9.

As can be seen from Figure 4.9, the mole-fraction-based reaction equilib-

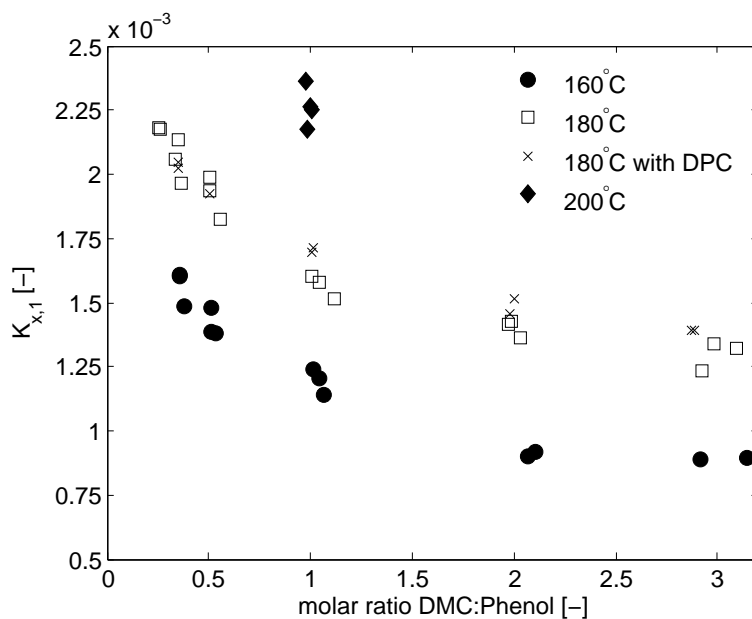


**Figure 4.9:**  $K_{x,1}$  over the initial reactant ratio at three different temperatures.

rium coefficients show the same trend regardless of the temperature. For initial DMC/phenol ratios lower than 1, the equilibrium coefficient is increasing more strongly with decreasing DMC/phenol ratio than for ratios above 1. For the lowest measured DMC/phenol ratio of 0.25, the equilibrium coefficient at 180°C is around 35% larger than the equilibrium coefficient at a DMC/phenol ratio of 1. A similar trend, although less pronounced, can be observed for the equilibrium coefficient at 160°C.

The experiments at 180°C where an initial amount of DPC far beyond the expected equilibrium mole fraction ( $\sim 10$ -50 times more than expected) is added, show that nearly the same values of the equilibrium coefficient  $K_{x,1}$  are attained as in the experiments with no DPC present initially. Moreover, the trend of  $K_{x,1}$  over the initial ratio of DMC/phenol is the same for the experiments with and without the initial presence of DPC at 180°C. The experimental results show that the GC error is probably lower for the experiments with initial DPC present as the reproducibility is generally better (the deviation is  $< 5\%$ ) than that of the DPC 'free' experiments

(where the deviation generally is < 10%).

As the experiments reported in literature as summarized in Table 4.1 have been carried out at different temperatures, the current experiments cannot easily be compared with them. However, a relative comparison is possible by using the van't Hoff equation:

$$\ln K_{x,1} = \frac{-\Delta H_r}{RT} + \frac{\Delta S}{R} \quad (4.7)$$

In Figure 4.10 a van't Hoff plot with some of the present experimental results and the literature data (see Table 4.1) is shown. The experimental  $K_{x,1}$ - and  $K_{x,2}$ - values along with those taken from literature have been fitted to the van't Hoff equation (Eq. 4.7) to determine the reaction enthalpies and entropies for reaction 4.1 and 4.2. The following averaged values of the equilibrium coefficients (at a 1:1 DMC/Phenol ratio) derived from the present experiments have been used in Figure 4.10: at 160°C  $K_{x,1} = 1.30 \cdot 10^{-3}$  and  $K_{x,2} = 3.56 \cdot 10^{-4}$ , at 180°C  $K_{x,1} = 1.70 \cdot 10^{-3}$  and  $K_{x,2} = 3.84 \cdot 10^{-4}$ , at 200°C  $K_{x,1} = 2.25 \cdot 10^{-3}$  and  $K_{x,2} = 5.65 \cdot 10^{-4}$ .

As can be seen in Figure 4.10, the data points are very well in line, with the exception of the single data point of Tundo et al. (1988). If the value taken from Tundo et al. (1988) is omitted, the reaction enthalpies  $\Delta H_i$  and the reaction entropies  $\Delta S_i$  of reaction 4.1 and 4.2 can be determined from the equations given in Figure 4.10 by rearranging them according to the van't Hoff equation (Eq. 4.7):

$$\ln K_{x,1} = \frac{-23.8 \text{ kJ mole}^{-1}}{RT} - \frac{0.346 \text{ J mole}^{-1} \text{ K}^{-1}}{R} \quad (4.8)$$

$$\ln K_{x,2} = \frac{-25.2 \text{ kJ mole}^{-1}}{RT} - \frac{9.48 \text{ J mole}^{-1} \text{ K}^{-1}}{R} \quad (4.9)$$

The two reaction enthalpies  $\Delta H_1 = 23.8 \text{ kJ mole}^{-1}$  and  $\Delta H_2 = 25.2 \text{ kJ mole}^{-1}$  (see Eq. 4.8 and 4.9) are within 1% and 10% of the corresponding Gibbs free energy



values given by Rivetti (2000), respectively. As the two reactions are only slightly endothermic - in this case the reaction entropy  $\Delta S$  is small- the inferred values of the reaction enthalpy appear to be reliable.

The values of the two reaction entropies  $\Delta S_1 = -0.346 \text{ Jmole}^{-1} \text{ K}^{-1}$  and  $\Delta S_2 = -9.48 \text{ Jmole}^{-1} \text{ K}^{-1}$  -as given in Eq. 4.8 and 4.9- should be interpreted with care as the experimental error has the same order of magnitude as the estimated  $\Delta S$  values. Thus, the  $\Delta S$  cannot be considered reliable.

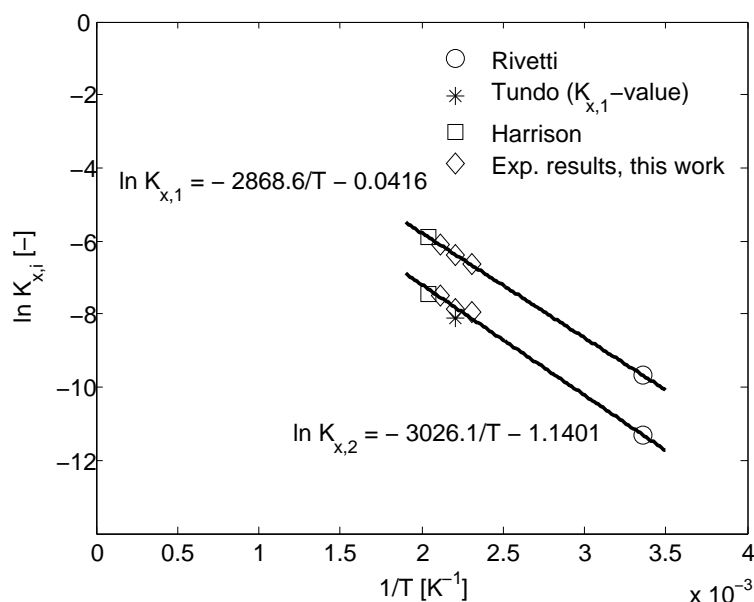


**Figure 4.10:** Van't Hoff plot for  $K_{x,1}$  with own experimental results and literature values taken from Table 4.1.

## 4.9 Equilibrium coefficient $K_{x,2}$

As already indicated, the reaction from the intermediate MPC to the desired product DPC can proceed via two different pathways. Since the equilibrium value  $K_{x,3}$  can be computed from the values of  $K_{x,2}$  and  $K_{x,1}$  (see Equation 4.3), only the results of  $K_{x,2}$  will be shown.

In Figure 4.11 the reaction equilibrium coefficient  $K_{x,2}$  has been plotted over the initial reactant ratio DMC/phenol for temperatures of 160°C, 180°C and 200°C. At 200°C only experiments at a DMC/phenol ratio of 1 have been carried out and therefore only the  $K_{x,2}$  values at this ratio are shown in Figure 4.11.

From the data in Table 4.1 it was expected that the value of the equilibrium coefficient  $K_{x,2}$  will increase slightly with temperature, something that also is observed in the present study (see in Figure 4.11).

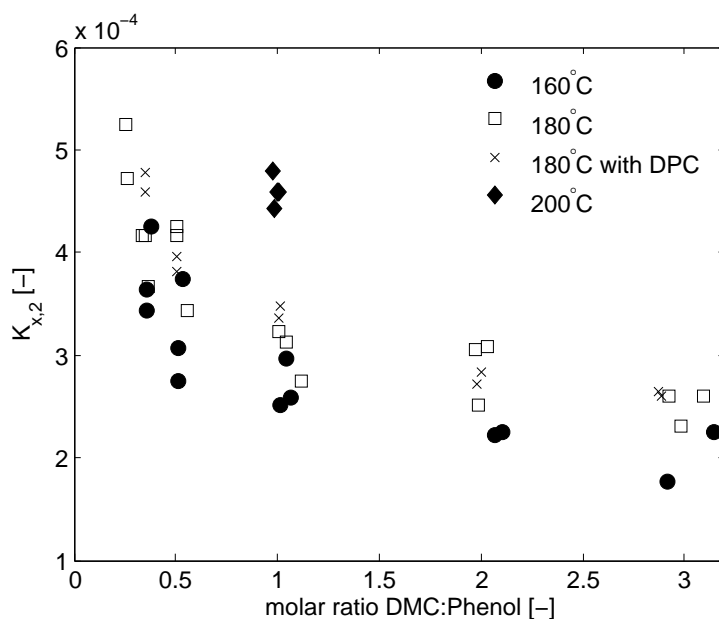


**Figure 4.11:**  $K_{x,2}$  over the initial reactant ratio at three different temperatures.

As can be seen from Figure 4.11 the equilibrium coefficient shows the same trend irrespective of temperature. The equilibrium coefficient is increasing with decreasing DMC/phenol ratio, especially for ratios below 1. For the lowest measured DMC/phenol ratio of 0.25 the equilibrium coefficient at 180°C is around 50% larger than the equilibrium coefficient at a DMC/phenol ratio of 1.

Moreover, it can be concluded that the initial presence of DPC seems to reduce the scatter of the inferred equilibrium coefficient at 180°C. In the experiments with DPC present initially, the relative error made in the GC analysis, especially for

DPC and MPC, is lower than that in the DPC 'free' experiments. This is logical as in the DPC 'free' experiments the mole fraction of DPC is in the lower part of the measuring range of the GC, resulting in a relatively large DPC analysis error ( 10-20%) for these experiments. This would also result in a larger scatter of the equilibrium coefficient  $K_{x,2}$  in the DPC 'free' experiments as compared to the scatter of the  $K_{x,1}$  equilibrium coefficients (see Figure 4.9), where DPC is no part of the equilibrium expression  $K_{x,1}$ . Comparison of Figure 4.9 and Figure 4.11 shows that the scatter of the  $K_{x,2}$  coefficients in the DPC 'free' experiments is indeed larger compared to the corresponding  $K_{x,1}$  coefficients.

## 4.10 Equilibrium coefficient $K_{a,1}$

Before presenting the results of the reaction equilibrium coefficients including activity coefficients in the equilibrium coefficient according to Equation 4.6, it is worthwhile to look at the course of the activity coefficients over the initial ratio of DMC/phenol depending on temperature. For this purpose the activity coefficients of the species involved in the reactions 4.1 to 4.3 were plotted as a function of the initial ratio of DMC/phenol for temperatures at 160°C and 180°C ( Figure 8 and Figure 4.5, respectively).

As can be seen from Figure 4.5 and Figure 4.12 UNIFAC predicts that the activity coefficients depend only slightly on temperature. The activity coefficients  $\gamma_i$  that are most seriously influenced by temperature are those of phenol and DPC, but even in those cases the influence of temperature is limited. The largest deviation can be found for DMC/Phenol ratios around 3 where the activity coefficients at 160°C differ from those at 180°C by around 10%. Looking at the considerable change of the activity coefficients over the initial DMC/phenol ratio (i.e. Methanol and DPC), a generally substantial deviation from unity can be observed for various components (i.e. Methanol, Phenol and DPC). Thus it can be expected that the equilibrium coefficient  $K_{a,1}$  based on activity coefficients (see Equation 4.6) will deviate from the equilibrium coefficient  $K_{x,1}$  based on mole fractions (see Equation 4.1) to a significant extent.

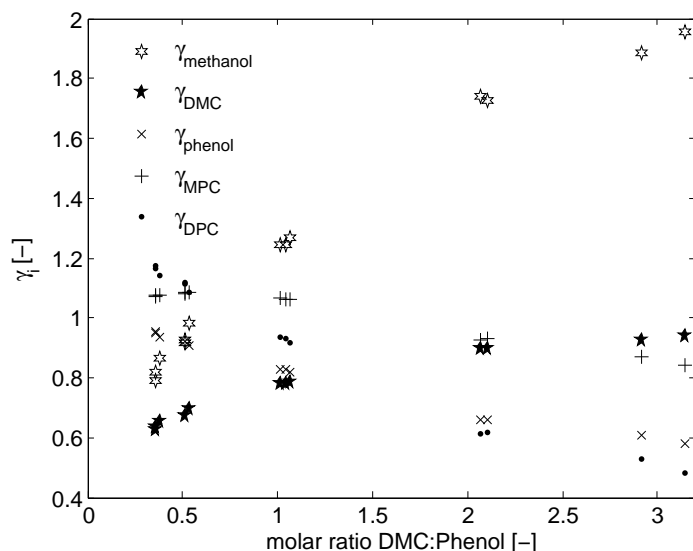


**Figure 4.12:** UNIFAC predicted  $\gamma_i$  for different initial DMC-Phenol ratios at 160°C (at chemical equilibrium); Conversions w.r.t. phenol are between 0.5 and 3%.

The equilibrium coefficient  $K_{a,1}$  based on activities at temperatures of 160°C, 180°C and 200°C is plotted versus the initial reactant ratio DMC/phenol in Figure 4.13. It can be clearly seen that the equilibrium coefficient  $K_{x,1}$  depicted in Figure 4.9 shows a completely different trend than the activity based equilibrium coefficient  $K_{a,1}$  as shown in Figure 4.13.

Of course, this difference is due to the activity coefficients introduced in the equilibrium coefficient  $K_{a,1}$ . The activity coefficients are supposed to account for the non-idealities in the system and to cause normalization. Hence, it was expected that the equilibrium coefficient  $K_{a,1}$  would be nearly independent of the initial concentration of DMC/phenol and would only be a function of temperature.

As can be seen from Figure 4.13 the relative difference between the largest value of  $K_{a,1}$  and the smallest value of  $K_{a,1}$  at 160°C is considerably lower than the relative deviation between the largest and the smallest  $K_{x,1}$  value (see Figure 4.9). This is also reflected in the average value of  $K_{a,1}$  of  $2.41 \cdot 10^{-3}$  with a 95% confidence

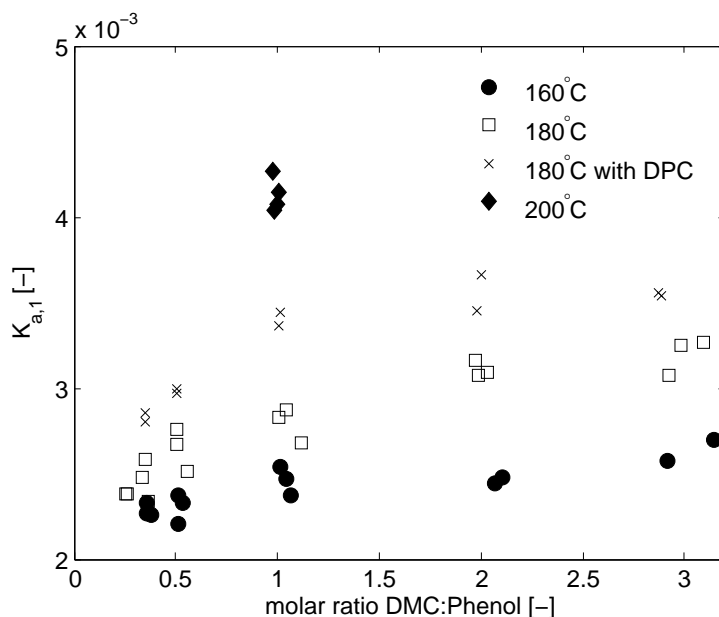


**Figure 4.13:**  $K_{a,1}$  over the initial reactant ratio at three different temperatures.

interval of  $7.6 \cdot 10^{-5}$  compared to an average value of  $K_{x,1}$  of  $1.24 \cdot 10^{-3}$  with a 95% confidence interval of  $1.49 \cdot 10^{-4}$ . However, at a temperature of 180°C the results are less convincing when using the activity based approach. The trend of the equilibrium coefficient  $K_{a,1}$  at 180°C differs from that of the equilibrium coefficient  $K_{a,1}$  at 160°C in that way that it still depends slightly on the reactant ratio of DMC/phenol. Moreover, also the results for the experiments where initially a large excess of DPC was present now deviate by a constant off-set of about 15% from the results of the "normal" experiments, where initially no DPC was present (see Figure 4.13). When no activity coefficients were used in the equilibrium expression, the results using either an initial excess of DPC or no initial DPC matched very well (see Figure 4.9). When looking further into the results, the dependence of  $K_{a,1}$  on the DMC/phenol ratio is strongest at low initial reactant ratios (DMC/Phenol=0.25) while this influence levels off at ratios of around 2. The trend of the equilibrium coefficient  $K_{a,1}$  at especially 180°C (see Figure 4.13) is almost the same as the trend of  $K_{x,1}$  at 180°C where the value of the equilibrium coefficient is steadily decreasing with increasing

DMC/phenol ratio. When comparing the deviation from the average value, it becomes clear that at 180°C, the mole fraction based approach ( $K_{x,1} = 1.68 \cdot 10^{-3}$  with a 95% confidence interval of  $1.59 \cdot 10^{-4}$ ) yields a slightly larger deviation than the activity based approach ( $K_{a,1} = 2.82 \cdot 10^{-3}$  with a 95% confidence interval of  $1.52 \cdot 10^{-4}$ ) if the experiments, where DPC is initially present, are neglected. The deviation of the  $K_{x,1}$  values of less than 10% found between the two experimental series at 180°C can mainly be attributed to an error in the GC analysis as the absolute amounts of MPC and DPC are significantly lower in the experiments without DPC present compared to those with DPC present.

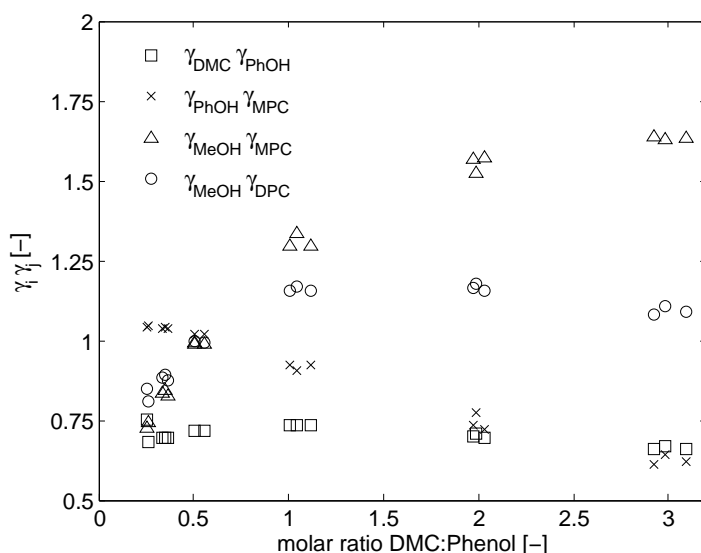


**Figure 4.14: UNIFAC predicted nominators and denominators for  $K_{\gamma,1}$  and  $K_{\gamma,2}$  180°C (experimental series where no initial DPC was present).**

The reason for both, the remaining dependency on the ratio of DMC/Phenol and the offset of the experiments with and without the initial presence of an excess of DPC, can probably be attributed to an error in the prediction of one or more activity coefficients. As mentioned previously, UNIFAC typically predicts activity coefficients within an accuracy of 15% and this is also: 1. the margin seen in the offset of the experiments at 180°C with and without initial DPC, and 2. the variation

around the average value when changing the ratio of DMC to Phenol. A margin of about 15% is not bad at all, considering the inherent (but at this point unavoidable) inaccuracy of UNIFAC.

As the results for  $K_{x,i}$  for both the experimental series with and without any initial DPC were - within experimental uncertainty - identical, the difference between the two series, when expressed as  $K_{a,i}$  (see Figure 4.13 and Figure 4.18), must originate from the UNIFAC predicted value of  $K_\gamma$ . First the denominators and nominators of  $K_\gamma$  as predicted by UNIFAC were plotted as a function of the initial DMC/Phenol ratio at a temperature of 180°C for the experiments with and without the initial presence of DPC, respectively (see Figure 4.14 as an example for the experiments without the initial presence of DPC).

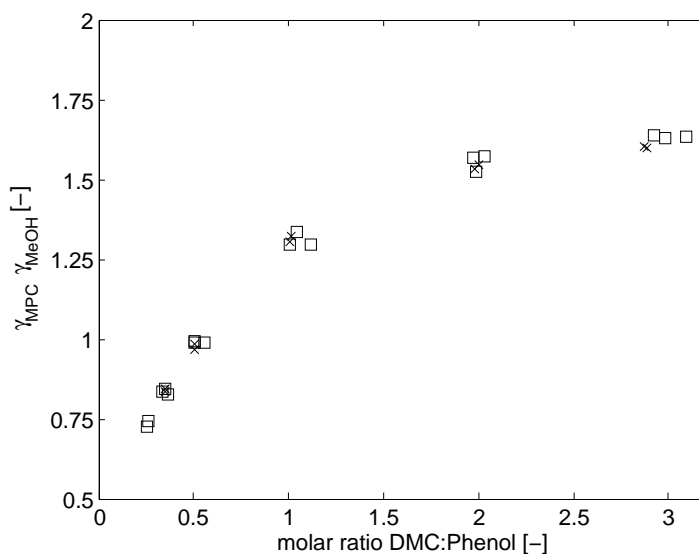


**Figure 4.15: Comparison of UNIFAC predicted  $\gamma_{MPC} \cdot \gamma_{MeOH}$  for experiments with (crosses) and without (squares) the initial presence of DPC at 180°C.**

The products of the activity coefficients for  $\gamma_{MPC} \cdot \gamma_{MeOH}$  and  $\gamma_{DMC} \cdot \gamma_{PhOH}$  are depicted in Figure 4.15 and Figure 4.16, respectively as a function of the initial reactant ratio DMC/phenol. All nominators and denominators involved in both,  $K_{\gamma,1}$  and  $K_{\gamma,2}$  were identical within the experimental accuracy (see as an example

Figure 4.15 for  $\gamma_{MPC} \cdot \gamma_{MeOH}$ ), except for the denominator  $\gamma_{DMC} \cdot \gamma_{PhOH}$  in  $K_{\gamma,1}$ . The UNIFAC predicted product of the activity coefficients for the experiments with and without the initial presence of DPC is shown in Figure 4.16, in which a more or less constant offset for the two experimental series can be seen. When the UNIFAC predicted activity coefficients of DMC and Phenol for the experiments with and without the initial presence of DPC are plotted, the results as depicted in Figure 4.17 are obtained. From this figure it is clear that the offset in the experimental series for  $K_{a,1}$  at 180°C with and without the initial presence of DPC, must be attributed to a difference in the UNIFAC predicted value for. This is not completely unexpected, as the carbonate group in DMC has a relatively large contribution to the behavior of the molecule DMC, and, therefore, also on the activity coefficient of DMC.

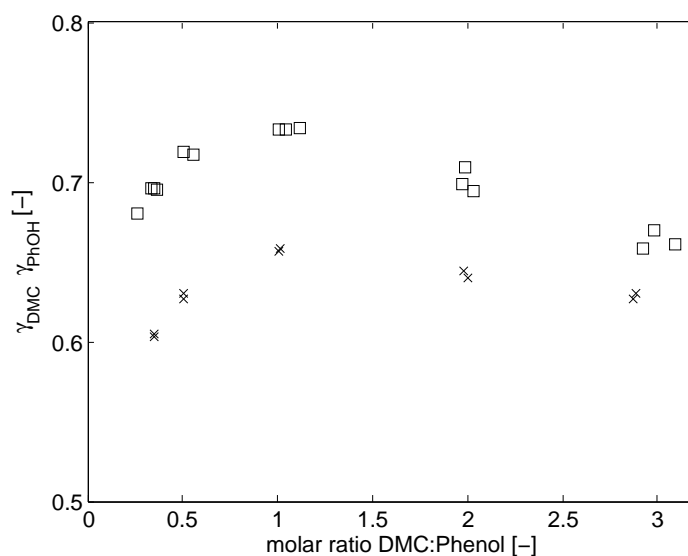


**Figure 4.16:** Comparison of UNIFAC predicted  $\gamma_{DMC} \cdot \gamma_{PhOH}$  for experiments with (crosses) and without (squares) the initial presence of DPC at 180°C.

Before the start of this work, only limited information on the carbonate group was available in the UNIFAC framework (Rodriguez et al., 2002a,b), and was specifically targeted at in another study of our group (Haubrock et al., 2007a). However, considering the limited number of available data sources, it is not unlikely that there



is still some uncertainty in the predicted value of the activity coefficient of especially DMC. Of course, the uncertainty in  $\gamma_{DMC}$  might also explain the remaining dependency of  $K_{a,1}$  on the ratio of DMC/Phenol as observed in Figure 4.13, but it should be kept in mind that also the inaccuracy in one or more of the other activity coefficients might be responsible for the still noticeable dependence of the  $K_{a,1}$  value as depicted in Figure 4.13.

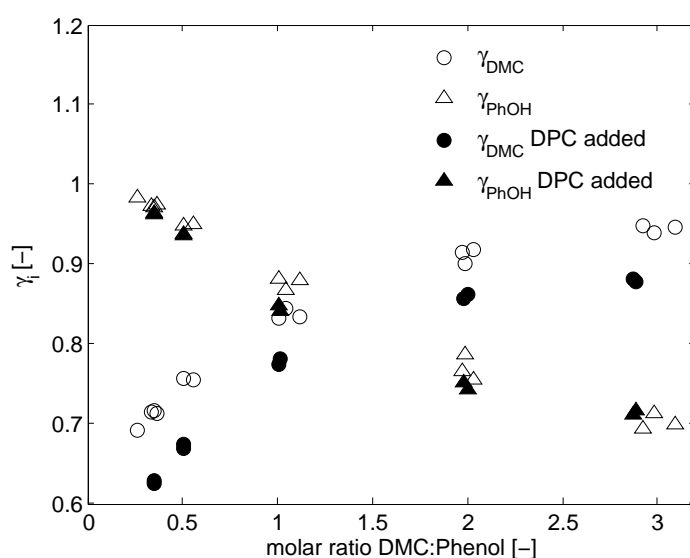


**Figure 4.17:** Comparison of UNIFAC predicted  $\gamma_{DMC}$  (circles) and  $\gamma_{PhOH}$  (triangles) for experiments with (closed symbols) and without (open symbols) the initial presence of DPC at 180°C.

## 4.11 Equilibrium coefficient $K_{a,2}$

The equilibrium coefficient  $K_{a,2}$  based on activities at temperatures of 160°C, 180°C and 200°C as a function of the initial reactant ratio DMC/phenol is depicted in Figure 4.18. It can be seen that, just like  $K_{x,1}$ , the equilibrium coefficient  $K_{a,2}$  (see Figure 4.18) shows a completely different trend than the activity based equilibrium coefficient  $K_{x,2}$  (Figure 4.11). Furthermore, it can be observed that the  $K_{a,2}$  values at

160°C, 180°C and 180°C with initial DPC present, are (for each series) located within a much smaller bandwidth than the corresponding  $K_{x,2}$  values (about a factor of 2), and do not seem to systematically depend on the initial ratio of DMC to Phenol. Finally, it can also be seen that there is no systematic offset for the results for  $K_{a,2}$  for the two experimental series at 180°C with and without the initial presence of DPC.

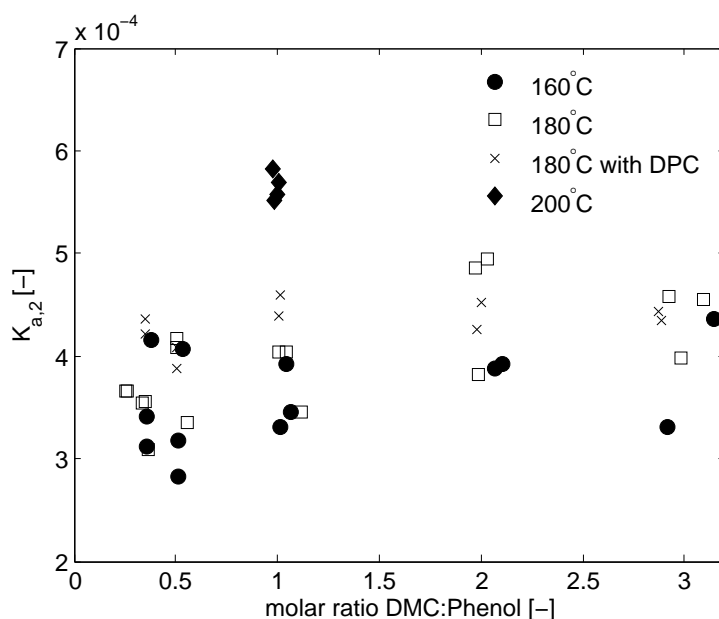


**Figure 4.18:  $K_{a,2}$  over the initial reactant ratio at three different temperatures.**

The average  $K_{a,2}$  value at 180°C of  $3.98 \cdot 10^{-4}$  with a 95% confidence interval of  $2.65 \cdot 10^{-5}$  (no initial DPC present) is close to the average  $K_{a,2}$  (initial DPC present) value at 180°C of  $4.31 \cdot 10^{-4}$  with a 95% confidence interval of  $1.30 \cdot 10^{-5}$ . The 95%-confidence intervals show quantitatively that the scatter of the  $K_{a,2}$  values at 180°C resulting from DPC 'free' experiments is nearly twice as large as that of the  $K_{a,2}$  values derived from experiments where initial DPC was present. This is partly caused by the larger error in the determination in the mole fraction of DPC for the experiments where no initial DPC is present (as already highlighted in section "Equilibrium coefficient  $K_{a,1}$ "), but, can -with respect to  $K_{a,2}$  - additionally be

influenced by a difference in accuracy of  $K_\gamma$  for both situations.

In all three cases the  $K_{a,2}$  value is reasonably constant with a relative deviation of around 10% ( $K_{a,2}$  at 180°C initial DPC) and <15% ( $K_{a,2}$  at 160°C and 180°C) in the 95% confidence interval. Hence, it seems that for  $K_{a,2}$  the influence of the reactant ratio DMC/phenol on the equilibrium coefficient as observed for  $K_{x,2}$  can be reduced by applying activity coefficients.

## 4.12 Temperature dependence of the equilibrium coefficients $K_{a,1}$ and $K_{a,2}$

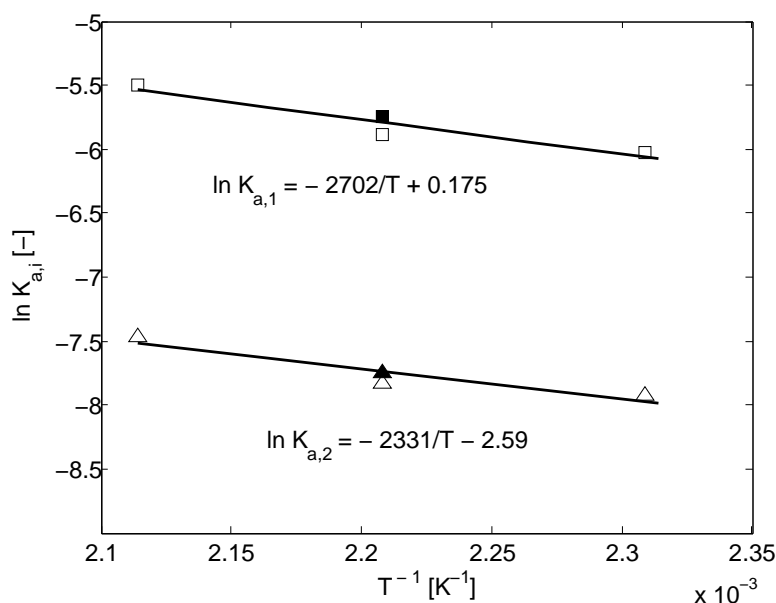


**Figure 4.19:** Van't Hoff plot for  $K_{a,1}$  and  $K_{a,2}$ . Open symbols are for experiments without the initial presence of DPC, closed symbols for the experiments with the initial presence of DPC.

The experimental results for all molar DMC/Phenol ratios at three different temperatures, namely 160°C, 180°C and 200°C (see Figure 4.13 and Figure 4.18),

were used to determine the temperature dependence of the equilibrium coefficient  $K_{a,1}$  of reaction 4.1 and the equilibrium coefficient  $K_{a,2}$  of reaction 4.2. The values for  $K_{a,1}$  and  $K_{a,2}$  as used in this analysis were the averaged values for these parameters, based on the results presented in Figure 4.13 and Figure 4.18. The van't Hoff plots for  $K_{a,1}$  and  $K_{a,2}$  in the temperature range between 160°C and 200°C are shown in Figure 4.19.

**Table 4.2:** Parameter values for the equilibrium coefficients according to equation  $\ln K_{a,i} = -\Delta H_r/(RT) + \Delta S/R$  (see Eq. 4.7)

Equilibrium coefficient	$\Delta H_r$ [kJ mol <sup>-1</sup> ]	$\Delta S$ [kJ mol <sup>-1</sup> K <sup>-1</sup> ]
$K_{a,1}$	22.5	$1.46 \cdot 10^{-3}$
$K_{a,2}$	19.4	$21.5 \cdot 10^{-3}$

As the previous sections showed there is still a dependence of the ratio of DMC/Phenol on the respective  $K_{a,i}$  values (especially  $K_{a,1}$  -most probably to a large extent caused by uncertainties in the activity coefficients predicted by UNIFAC) ,the proposed relation for  $K_{a,1}$  and  $K_{a,2}$  -and the corresponding thermodynamic parameters as reported in Table 4.2- might change when in future years more reliable data for the activity coefficients become available. To facilitate the reevaluation of the temperature dependence, the originally measured equilibrium data are reported in the Appendix of this study and can be used to update the relation for  $K_{a,1}$  and  $K_{a,2}$ .

### 4.13 Comparison between $K_{a,i}$ values derived from own experiments and literature

In the patent of Harrison et al. (1995) experimental data for a series of experiments are given. In contrast to the batch experiments in this work, Harrison et al. (1995)

used a setup that consisted primarily of a continuous stirred tank reactor in which gaseous products (i.e. methanol) as well as reactants (i.e. DMC) could leave the reactor via the vapour overhead section to enable high conversions. The experiments described in that patent were carried out using an equimolar DMC/phenol feed stream (containing a specified amount of catalyst). The feed rate (between 200 and 400 ml/h) among other parameters was varied in the experiments as well as the duration of the experiments (30 min up to 1 hour). As no reactor volume is given in the patent, it is unfortunately not possible to calculate the residence time in the continuous stirred tank reactor. The reaction temperature in the experiments taken from the patent and used for the comparison was always 218°C. Considering the amount of catalyst used in the experiments ( $\sim 30$  times larger than in the experiments reported in this study) and the high reaction temperature of 218°C, the residence time was probably enough to justify the assumption that chemical equilibrium in the liquid phase is approached quite closely (see also Section Thermodynamics). Of course this assumption can only be justified when exact information on the residence time, kinetics and the mass transfer rates of the various volatile products is available, and this should be kept in mind when comparing the results of our calculations.

As the mole fractions of all components in the liquid product stream are given in the patent, it is possible to calculate  $K_{a,i}$  values from the work of Harrison et al. (1995) and allow a comparison with predictions by the currently proposed relations (see Eq. 4.7 and Table 4.2). It should be noted that also for the experimental data of Harrison the calculation of  $K_{a,i}$  involves the use of UNIFAC, however, at a totally different liquid composition than in this work (very low methanol content, high MPC and DPC content). The results of the comparison between the  $K_{a,i}$  values derived from experimental data and the data as predicted based on the currently derived relations for  $K_{a,1}$  and  $K_{a,2}$  are given in Table 4.3.

The deviation between theoretically predicted and experimentally determined  $K_{a,i}$  values is larger for the  $K_{a,1}$  values than for the  $K_{a,2}$  values. Considering the inherent uncertainties in the activity coefficient prediction which affect especially the  $K_{a,1}$  value, this was more or less expected. The large deviation of  $K_{a,1}$  of more than 50% and of  $K_{a,2}$  of more than 25% (see Table 4.3) in case of example 4 might

be attributed to the lower catalyst amount in this experiment (see also Harrison et al. (1995) Example 4) which is only half the catalyst amount employed in the other experiments used for the comparison while otherwise maintaining the same operating conditions. Because of the lower catalyst amount it might be possible that chemical equilibrium was not completely reached during the residence time in the reactor and thus the calculated equilibrium coefficients are lower than expected.

Comparing the experimentally derived and predicted  $K_{a,2}$  values in Table 4.3 the difference of less than 12% seems to support the assumption that equilibrium is actually achieved in the Harrison experiments. Keeping in mind the rather different experimental conditions, -especially the reaction temperature of 220°C which is outside the range (160°C - 200°C) where the temperature fitting of the  $K_{a,i}$  values has been performed-, the values predicted with the  $K_{a,i}$  equations as depicted in Figure 4.19 and those derived from Harrison's patent, match quite well.

As already mentioned above it was not possible to calculate the residence time as no reactor volume was mentioned in the patent of Harrison. Thus the reaction time needed to achieve equilibrium in the experiments presented in this study cannot be compared to the reaction time of Harrison et al. (1995). However, from present -explorative- experiments with comparable amounts of catalyst (see Harrison et al. (1995) Example 1-3) it is known that chemical equilibrium in the batch experiments was achieved within 5 minutes at the maximum. Based on a reactant flow rate of 400ml/h and a residence time of 5min the corresponding required reactor volume would be 33ml. Even for laboratory scale experiments this seems a rather small volume considering reactant flow rates of 200ml/h and larger, as used by Harrison et al. (1995). Hence, it is likely that the reactor volume as used by Harrison et al. (1995) was large enough to ensure residence times of more than 5 minutes. As the temperatures were about 30°C higher than those used in this study, it seems reasonable to assume the liquid to be at equilibrium in the experiments of Harrison. Of course, both remarks only indicate and by no means prove that equilibrium was achieved in the experiments given in the patent as these were also carried out under the continuous removal of (gaseous) reactants and products.

**Table 4.3:**  $K_{a,i}$  derived from experimental data (Harrison et al. (1995), example 1-4) and predicted by equations for  $K_{a,i}$  at 218°C ( $K_{a,1} = 4.86 \cdot 10^{-3}$  and  $K_{a,2} = 6.52 \cdot 10^{-4}$ ) as shown in Figure 4.19

Example	yield								rel. error [%]	
	MPC [%]	DPC [%]	$K_{x,1}$	$K_{x,2}$	$K_{\gamma,1}$	$K_{\gamma,2}$	$K_{a,1}$	$K_{a,2}$	$\Delta K_{a,1}$	$\Delta K_{a,2}$
1	11.36	0.644	$2.18 \cdot 10^{-3}$	$5.52 \cdot 10^{-4}$	1.51	1.04	$3.29 \cdot 10^{-3}$	$5.71 \cdot 10^{-4}$	-32.3	-12.3
2	10.88	0.584	$2.37 \cdot 10^{-3}$	$5.90 \cdot 10^{-4}$	1.50	1.03	$3.57 \cdot 10^{-3}$	$6.08 \cdot 10^{-4}$	-26.6	-6.7
3	11.88	0.558	$3.07 \cdot 10^{-3}$	$5.93 \cdot 10^{-4}$	1.50	1.03	$4.60 \cdot 10^{-3}$	$6.11 \cdot 10^{-4}$	-5.3	-6.3
4	8.80	0.490	$1.54 \cdot 10^{-3}$	$4.82 \cdot 10^{-4}$	1.46	1.00	$2.26 \cdot 10^{-3}$	$4.84 \cdot 10^{-4}$	-53.6	-25.8

Based on the results in Table 4.3 and the preceding discussion above, the temperature dependent  $K_{a,i}$  relations as given in this section seem to have a strong predictive character and might find their application in the design and modelling of the process from DMC to DPC. If the herein presented equations for  $K_{a,i}$  are used for modelling purposes it should always be kept in mind for what experimental conditions the relations for  $K_{a,1}$  and  $K_{a,2}$  have been determined and validated.

## 4.14 Conclusion

In this study the experimentally determined equilibrium coefficient of the reaction of DMC with phenol yielding the intermediate MPC and the equilibrium coefficient of the consecutive transesterification reaction of MPC with phenol have been presented. The influence of temperature on these equilibrium coefficients in the temperature range between 160°C and 200°C has been measured as well as the influence of the initial reactant ratio of DMC/phenol on the equilibrium coefficient.

It is shown that the chemical equilibrium coefficients in terms of mole fractions display a pronounced dependency on the initial reactant ratio of DMC/phenol. By employing activities instead of 'only' mole fractions in the calculation of the equilibrium coefficient the influence on the reactant ratio DMC/phenol could be reduced. The  $K_{a,2}$  value of the transesterification reaction 4.2 is nearly constant over the whole range of employed initial DMC/phenol ratios, whereas the  $K_{a,1}$  value of the

first transesterification reaction still shows a dependence, especially at 180°C. The remaining dependence of the  $K_{a,1}$  value on the initial DMC/phenol ratio might on one hand be attributed to experimental (analysis) errors, in particular in the experiments without initial DPC present. Since the experimentally determined mole fractions serve as input for the activity coefficient calculations any errors in the experimental GC results will be amplified. On the other hand, there is also uncertainty in the UNIFAC parameters derived from the scarce available VLE data in literature as well as the expected increasing inaccuracy of applying the UNIFAC  $G^E$ -model to temperatures above 150°C.

The temperature dependence of the equilibrium coefficients  $K_{a,1}$  and  $K_{a,2}$  in the temperature range between 160°C and 200°C has been fitted to the well known Van't Hoff equation. The fitting procedure yielded  $\ln K_{a,1} = -22.46[kJmol^{-1}]/(RT) + 1.45 \cdot 10^{-3}[kJmol^{-1}K^{-1}]$  and  $\ln K_{a,2} = -19.38[kJmol^{-1}]/(RT) + 21.53 \cdot 10^{-3}[kJmol^{-1}K^{-1}]$ . The activity based equilibrium coefficients  $K_{a,1}$  and  $K_{a,2}$  show only a moderate temperature dependence. It might be expected that another  $G^E$ -model based on experimental VLE data for the components of interest in this study might yield significantly better results with respect to the derived  $K_{a,1}$  values, but unfortunately there is insufficient data in the literature to apply such a model. Nevertheless it is not the goal of this study to eliminate or reduce the remaining uncertainties in the applied  $G^E$ -model by fitting the interaction parameters to new experimental VLE data as this would require various complete new and extensive VLE studies and is therefore beyond the scope of this work. Despite the inherent uncertainties of the UNIFAC model, the activity based equilibrium coefficients  $K_{a,1}$  and  $K_{a,2}$  derived from experimental data presented in this work and the activity coefficients calculated with UNIFAC show a fair (in case of  $K_{a,1}$ ) to good (in case of  $K_{a,2}$ ) predictive character.

However, the derived  $K_{a,i}$  equations should be used with precautions at completely different experimental conditions as the validity of the  $K_{a,i}$  equations at severe other experimental has not been tested exhaustively. Nevertheless, it is expected that the herein presented activity based temperature dependent correlations of  $K_{a,1}$  and  $K_{a,2}$  can find its application in the modelling of equilibrium based reactive distillation



processes for the industrial relevant system presented in this work.

## Acknowledgement

The author gratefully acknowledges the financial support of Shell Global Solutions International B.V. Furthermore Henk Jan Moed is acknowledged for building the setup and Wouter Wermink for his contributions to the experimental work.

## Notation

$\Delta H_r$	Reaction enthalpy, [kJ/mol]
$\Delta S$	Reaction entropy, [kJ/mol/K]
$\gamma$	Activity coefficient, [-]
$K_{x,i}$	Mole fraction based equilibrium coefficient, [-]
$K_{\gamma,i}$	Product of activity coefficients belonging to $K_{x,i}$ , [-]
$K_{a,i}$	Activity based equilibrium coefficient, [-]
$R$	Gas constant $8.314 \cdot 10^{-3}$ , [kJ/mole/K]
$T$	Temperature, [K]
$x_j$ or $x_k$	mole fraction of component j and k, respectively [-]
j,k	component j and k, respectively [-]
i	reaction i, [-]

## 4.A Raw data

**Table 4.4:** Raw data equilibrium measurements and activity coefficients at 160°C, 180°C and 200°C. Mole fractions at equilibrium have been experimentally determined, the activity coefficients at equilibrium have been determined using UNIFAC (see Haubrock et al. (2007a)).

Ratio		$X_{DMC}$	$X_{MeOH}$	$X_{PhOH}$	$X_{DPC}$	$\gamma_{MeOH}$	$\gamma_{DMC}$	$\gamma_{MPC}$	$\gamma_{PhOH}$	$\gamma_{DPC}$	
T [°C]	$\frac{n_{DMC}}{n_{PhOH}}$	$X_{DMC}$	$X_{MeOH}$	$X_{PhOH}$	$X_{DPC}$	$\gamma_{MeOH}$	$\gamma_{DMC}$	$\gamma_{MPC}$	$\gamma_{PhOH}$	$\gamma_{DPC}$	
160°C	1.06	$1.884 \cdot 10^{-2}$	$4.872 \cdot 10^{-1}$	$4.797 \cdot 10^{-2}$	$9.324 \cdot 10^{-1}$	1.267	0.788	1.060	0.820	0.918	
	1.04	$1.909 \cdot 10^{-2}$	$4.763 \cdot 10^{-1}$	$4.898 \cdot 10^{-2}$	$1.121 \cdot 10^{-4}$	1.245	0.781	1.064	0.827	0.933	
	1.02	$2.018 \cdot 10^{-2}$	$4.760 \cdot 10^{-1}$	$4.894 \cdot 10^{-2}$	$8.684 \cdot 10^{-5}$	1.245	0.782	1.065	0.826	0.934	
	2.11	$1.705 \cdot 10^{-2}$	$6.783 \cdot 10^{-1}$	$1.071 \cdot 10^{-2}$	$4.163 \cdot 10^{-1}$	1.727	0.900	0.932	0.660	0.619	
	2.07	$1.501 \cdot 10^{-2}$	$6.816 \cdot 10^{-1}$	$1.189 \cdot 10^{-2}$	$5.129 \cdot 10^{-1}$	1.740	0.900	0.928	0.659	0.613	
	3.14	$1.453 \cdot 10^{-2}$	$7.621 \cdot 10^{-1}$	$1.004 \cdot 10^{-2}$	$3.314 \cdot 10^{-1}$	1.958	0.942	0.840	0.580	0.482	
	2.91	$1.350 \cdot 10^{-2}$	$7.342 \cdot 10^{-1}$	$1.160 \cdot 10^{-2}$	$2.406 \cdot 10^{-1}$	1.884	0.928	0.872	0.609	0.527	
	0.53	$2.031 \cdot 10^{-2}$	$3.437 \cdot 10^{-1}$	$1.451 \cdot 10^{-2}$	$6.214 \cdot 10^{-1}$	1.662 $\cdot 10^{-4}$	0.983	0.698	1.086	0.906	1.087
	0.51	$1.866 \cdot 10^{-2}$	$3.103 \cdot 10^{-1}$	$1.610 \cdot 10^{-2}$	$6.548 \cdot 10^{-1}$	$1.736 \cdot 10^{-4}$	0.925	0.676	1.081	0.923	1.113
	0.51	$2.000 \cdot 10^{-2}$	$3.081 \cdot 10^{-1}$	$1.402 \cdot 10^{-2}$	$6.577 \cdot 10^{-1}$	$1.268 \cdot 10^{-4}$	0.919	0.675	1.083	0.924	1.119
	0.38	$1.981 \cdot 10^{-2}$	$2.754 \cdot 10^{-1}$	$1.426 \cdot 10^{-2}$	$6.904 \cdot 10^{-1}$	$2.115 \cdot 10^{-4}$	0.865	0.655	1.078	0.938	1.142
	0.35	$2.072 \cdot 10^{-2}$	$2.290 \cdot 10^{-1}$	$1.310 \cdot 10^{-2}$	$7.370 \cdot 10^{-1}$	$1.601 \cdot 10^{-4}$	0.791	0.627	1.070	0.955	1.174
0.36	$2.134 \cdot 10^{-2}$	$2.467 \cdot 10^{-1}$	$1.330 \cdot 10^{-2}$	$7.185 \cdot 10^{-1}$	$1.630 \cdot 10^{-4}$	0.819	0.638	1.076	0.948	1.166	
180°C	1.04	$1.961 \cdot 10^{-2}$	$4.926 \cdot 10^{-1}$	$1.862 \cdot 10^{-2}$	$1.392 \cdot 10^{-4}$	1.280	0.844	1.042	0.868	0.912	
	1.12	$1.941 \cdot 10^{-2}$	$4.729 \cdot 10^{-1}$	$1.806 \cdot 10^{-2}$	$1.253 \cdot 10^{-4}$	1.237	0.835	1.049	0.879	0.934	
	1.01	$1.808 \cdot 10^{-2}$	$4.700 \cdot 10^{-1}$	$2.046 \cdot 10^{-2}$	$1.793 \cdot 10^{-4}$	1.235	0.832	1.048	0.881	0.935	

Table 4.4 – Continued

T [°C]	Ratio	$\frac{n_{DMC}}{n_{PhOH}}$	$X_{MeOH}$	$X_{DMC}$	$X_{MPC}$	$X_{PhOH}$	$X_{DPC}$	$\gamma_{MeOH}$	$\gamma_{DMC}$	$\gamma_{MPC}$	$\gamma_{PhOH}$	$\gamma_{DPC}$
1.99		$2.149 \cdot 10^{-2}$	$6.160 \cdot 10^{-1}$	$1.426 \cdot 10^{-2}$	$3.482 \cdot 10^{-1}$	$5.797E-05$	1.549	0.900	0.984	0.787	0.761	
2.03		$2.156 \cdot 10^{-2}$	$6.592 \cdot 10^{-1}$	$1.278 \cdot 10^{-2}$	$3.064 \cdot 10^{-1}$	$5.592E-05$	1.649	0.919	0.954	0.755	0.701	
1.97		$1.880 \cdot 10^{-2}$	$6.512 \cdot 10^{-1}$	$1.541 \cdot 10^{-2}$	$3.145 \cdot 10^{-1}$	$7.887E-05$	1.634	0.914	0.958	0.765	0.712	
3.10		$1.790 \cdot 10^{-2}$	$7.330 \cdot 10^{-1}$	$1.279 \cdot 10^{-2}$	$2.363 \cdot 10^{-1}$	$4.391E-05$	1.834	0.947	0.890	0.698	0.593	
2.92		$1.656 \cdot 10^{-2}$	$7.393 \cdot 10^{-1}$	$1.275 \cdot 10^{-2}$	$2.313 \cdot 10^{-1}$	$4.632E-05$	1.852	0.948	0.884	0.694	0.584	
2.99		$1.656 \cdot 10^{-2}$	$7.172 \cdot 10^{-1}$	$1.460 \cdot 10^{-2}$	$2.515 \cdot 10^{-1}$	$5.124E-05$	1.801	0.939	0.904	0.713	0.616	
0.56		$1.890 \cdot 10^{-2}$	$3.007 \cdot 10^{-1}$	$1.917 \cdot 10^{-2}$	$6.610 \cdot 10^{-1}$	$2.304 \cdot 10^{-4}$	0.922	0.755	1.072	0.950	1.079	
0.51		$2.091 \cdot 10^{-2}$	$3.007 \cdot 10^{-1}$	$1.888 \cdot 10^{-2}$	$6.592 \cdot 10^{-1}$	$2.526 \cdot 10^{-4}$	0.926	0.758	1.074	0.948	1.081	
0.50		$2.138 \cdot 10^{-2}$	$2.989 \cdot 10^{-1}$	$1.793 \cdot 10^{-2}$	$6.616 \cdot 10^{-1}$	$2.314 \cdot 10^{-4}$	0.922	0.757	1.075	0.949	1.083	
0.36		$1.766 \cdot 10^{-2}$	$2.084 \cdot 10^{-1}$	$1.753 \cdot 10^{-2}$	$7.562 \cdot 10^{-1}$	$2.750 \cdot 10^{-4}$	0.778	0.713	1.064	0.974	1.126	
0.34		$1.863 \cdot 10^{-2}$	$2.134 \cdot 10^{-1}$	$1.769 \cdot 10^{-2}$	$7.500 \cdot 10^{-1}$	$2.966 \cdot 10^{-4}$	0.785	0.715	1.067	0.973	1.127	
0.35		$2.137 \cdot 10^{-2}$	$2.154 \cdot 10^{-1}$	$1.608 \cdot 10^{-2}$	$7.470 \cdot 10^{-1}$	$2.343 \cdot 10^{-4}$	0.785	0.717	1.074	0.971	1.135	
0.27		$2.017 \cdot 10^{-2}$	$1.557 \cdot 10^{-1}$	$1.362 \cdot 10^{-2}$	$8.102 \cdot 10^{-1}$	$2.581 \cdot 10^{-4}$	0.701	0.692	1.062	0.983	1.155	
180°C	1.01	$1.211 \cdot 10^{-2}$	$4.555 \cdot 10^{-1}$	$3.191 \cdot 10^{-2}$	$5.000 \cdot 10^{-1}$	$4.434 \cdot 10^{-4}$	1.239	0.774	1.052	0.849	0.940	
with	1.02	$1.274 \cdot 10^{-2}$	$4.659 \cdot 10^{-1}$	$3.076 \cdot 10^{-2}$	$4.902 \cdot 10^{-1}$	$4.108 \cdot 10^{-4}$	1.259	0.782	1.050	0.842	0.929	
DPC	2.00	$1.045 \cdot 10^{-2}$	$6.291 \cdot 10^{-1}$	$3.011 \cdot 10^{-2}$	$3.300 \cdot 10^{-1}$	$2.699 \cdot 10^{-4}$	1.577	0.862	0.981	0.742	0.735	
	1.98	$1.011 \cdot 10^{-2}$	$6.236 \cdot 10^{-1}$	$3.013 \cdot 10^{-2}$	$3.359 \cdot 10^{-1}$	$2.722 \cdot 10^{-4}$	1.552	0.857	0.987	0.752	0.750	
	2.87	$8.962 \cdot 10^{-3}$	$7.058 \cdot 10^{-1}$	$2.819 \cdot 10^{-2}$	$2.569 \cdot 10^{-1}$	$2.138 \cdot 10^{-4}$	1.684	0.881	0.951	0.712	0.674	
	2.88	$8.571 \cdot 10^{-3}$	$6.997 \cdot 10^{-1}$	$2.978 \cdot 10^{-2}$	$2.617 \cdot 10^{-1}$	$2.370 \cdot 10^{-4}$	1.674	0.879	0.954	0.717	0.682	

Table 4.4 – Continued

T [°C]	Ratio $\frac{\eta_{DMC}}{\eta_{PhOH}}$	$X_{MeOH}$	$X_{DMC}$	$X_{MPC}$	$X_{PhOH}$	$X_{DPC}$	$\gamma_{MeOH}$	$\gamma_{DMC}$	$\gamma_{MPC}$	$\gamma_{PhOH}$	$\gamma_{DPC}$
	0.51	$1.200 \cdot 10^{-2}$	$2.908 \cdot 10^{-1}$	$3.100 \cdot 10^{-2}$	$6.655 \cdot 10^{-2}$	$6.815 \cdot 10^{-1}$	0.932	0.674	1.056	0.935	1.091
	0.50	$1.201 \cdot 10^{-2}$	$2.840 \cdot 10^{-1}$	$3.056 \cdot 10^{-2}$	$6.728 \cdot 10^{-2}$	$6.523 \cdot 10^{-1}$	0.919	0.669	1.055	0.938	1.097
	0.35	$1.082 \cdot 10^{-2}$	$2.135 \cdot 10^{-1}$	$2.972 \cdot 10^{-2}$	$7.449 \cdot 10^{-2}$	$9.770 \cdot 10^{-1}$	0.805	0.625	1.036	0.963	1.132
	0.35	$1.138 \cdot 10^{-2}$	$2.188 \cdot 10^{-1}$	$2.909 \cdot 10^{-2}$	$7.399 \cdot 10^{-2}$	$8.668 \cdot 10^{-1}$	0.813	0.629	1.038	0.962	1.131
200°C	0.98	$2.459 \cdot 10^{-2}$	$4.585 \cdot 10^{-1}$	$2.181 \cdot 10^{-2}$	$4.949 \cdot 10^{-2}$	$2.103 \cdot 10^{-1}$	1.142	0.757	1.054	0.881	0.990
	0.99	$2.266 \cdot 10^{-2}$	$4.702 \cdot 10^{-1}$	$2.192 \cdot 10^{-2}$	$4.850 \cdot 10^{-2}$	$2.076 \cdot 10^{-1}$	1.174	0.767	1.053	0.870	0.972
	1.00	$2.392 \cdot 10^{-2}$	$4.722 \cdot 10^{-1}$	$2.155 \cdot 10^{-2}$	$4.821 \cdot 10^{-2}$	$1.996 \cdot 10^{-1}$	1.141	0.756	1.052	0.882	0.988

## Chapter 5

# The conversion of Dimethyl carbonate (DMC) to Diphenyl carbonate (DPC): Experimental measurements and reaction rate modelling

### Abstract

The kinetics of the reaction of Dimethyl Carbonate (DMC) and Phenol to Methyl Phenyl Carbonate (MPC) and the subsequent disproportion and transesterification reaction of Methyl Phenyl Carbonate (MPC) to Diphenyl Carbonate (DPC) have been studied. Experiments were carried out in a closed batch reactor in the temperature range from 160° C to 200° C for initial reactant ratios of DMC/phenol from 0.25 to 3 and varying catalyst (Titanium-(n-butoxide)) concentrations. The concept of a closed ideally stirred, isothermal batch reactor incorporating an activity based reaction rate model, has been used to fit kinetic parameters to the experimental data taking into account the catalyst concentration, the initial reactant ratio DMC/phenol and the temperature.

## 5.1 Introduction

Diphenyl carbonate is a precursor in the production of Polycarbonate (PC) which is widely employed as an engineering plastic in various applications basic to the modern lifestyle: electronic appliances, office equipment and in automobiles, for example. About 2.7 million tons of PC are produced annually, a figure that is expected to increase by 5-7% yearly up to at least 2010 (Westervelt, 2006).

Traditionally PC is produced using phosgene as an intermediate. This process suffers from a number of drawbacks: 4 tons of phosgene is needed for the production of 10 tons of PC; phosgene is very toxic and when it is used, the formation of undesired salts cannot be avoided; and the process uses 10 times as much solvent (on a weight base) as PC produced. The solvent, methylene chloride, is suspected to be carcinogenic and it is soluble in water. This results in a large amount of waste water that has to be treated prior to discharge (Ono, 1997).

Many attempts have been made to overcome the disadvantages of the phosgene based process (Kim et al., 2004). The main focus has been a route that produces Diphenyl carbonate (DPC) via Dimethyl carbonate (DMC), which then reacts further with Bisphenol-A to form PC. The critical step in this route is the synthesis of DPC from DMC that takes place via a transesterification reaction to methyl phenyl carbonate (MPC), usually followed by a disproportionation and/or transesterification step to DPC. However, in a batch reactor with an equimolar feed, an equilibrium conversion to MPC of only about 3% can be expected. Therefore, creative process engineering is required to successfully carry out the reaction of DMC to DPC on a commercial scale.

To make viable the process from DMC to DPC the conversion of DMC to the intermediate MPC has to be substantially increased. As one of the reaction products, methanol in this case, is the most volatile component in the mixture, it might be attractive to use reactive distillation to remove methanol directly from the reaction zone to enhance the conversion of DMC towards MPC. A reactive distillation process to produce DPC would need to be operated as close to chemical equilibrium as possible in order to achieve the highest possible conversion of the

reactants towards DPC. This, in turn, requires the reactions to proceed sufficiently fast. To assess whether reactive distillation is an attractive process alternative to improve the conversion of DMC towards MPC, it is essential to know how fast chemical equilibrium can be achieved, as this determines the required residence time in the reaction zone and, hence, also the dimensions of the equipment.

In this section reaction rate data for the conversion of DMC to DPC at different initial molar ratios of DMC/phenol in the temperature range between 160° C to 200° C is presented. In addition, an activity based reaction rate model is employed to model the experimental data, with the reaction rate constants being the actual fit parameters. The required activity coefficients as applied in the reaction rate model are estimated with the UNIFAC group contribution method (Fredenslund et al., 1975).

## 5.2 Reactions

The synthesis of diphenyl carbonate (DPC) from dimethyl carbonate (DMC) and phenol takes place through the formation of methyl phenyl carbonate (MPC) and can be catalyzed either by homogeneous or heterogeneous catalysts. The reaction of DMC to DPC is a two-step reaction. The first step is the transesterification of DMC with phenol to the intermediate MPC and methanol (Ono, 1997; Fu and Ono, 1997):

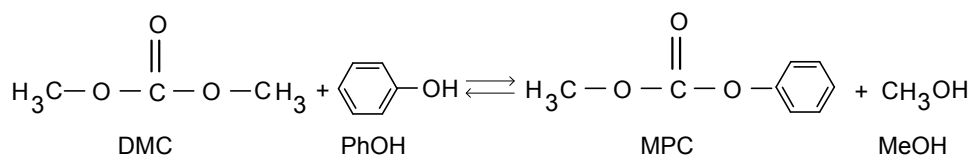


Figure 5.1: Transesterification 1

For the second step two possible routes exist: The transesterification of MPC with phenol and the disproportionation of two molecules of MPC yielding DPC and

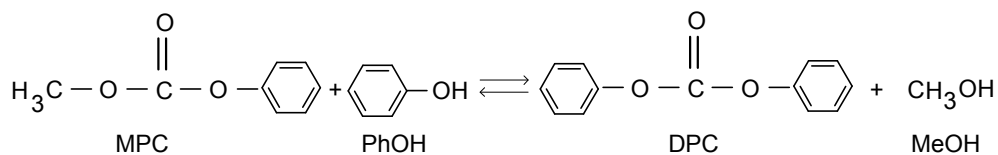


Figure 5.2: Transesterification 2

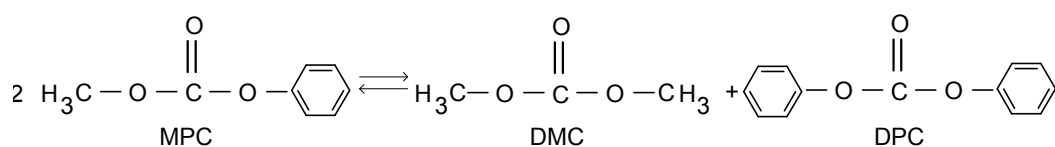


Figure 5.3: Disproportionation

DMC (Reaction 5.3).

According to Ono (1997) side reactions also may occur. For this kind of reaction system anisole is the main by-product, which can be formed from DMC and phenol through methylation

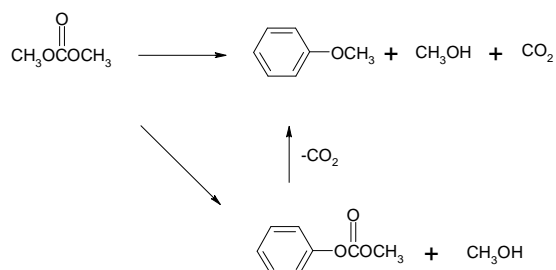


Figure 5.4: Side reaction forming anisole, methanol and carbon dioxide



### 5.3 Catalysts

Numerous catalysts are known to promote common transesterification reactions. Nevertheless, many of these catalysts are not suitable for the transesterification of DMC to DPC as they also catalyze the decarboxylation to anisole (Ono, 1997). First it has to be decided whether a heterogeneous or homogenous catalyst is preferred.

In industrial use, heterogeneous catalysts usually are considered to be more desirable than homogeneous catalysts because of the ease of separation and regeneration of the catalyst (Kim and Lee, 1999). Most of these catalysts are supported metal oxides, such as  $\text{MoO}_3$  on silica. Ono (1997) investigated different types of heterogeneous catalysts and showed that the selectivity of these catalysts for the reaction towards anisole is much higher than that of homogeneous catalysts where only traces of anisole were detected. As anisole formation should be avoided if at all possible, it was decided to adopt a homogeneous catalyst in this study.

Advantages of the use of homogenous catalysts when doing kinetic experiments are as follows:

- 1) Experimental results may be used directly to derive the kinetics. Mass transfer issues (e.g. diffusion limitations to/or inside the catalyst particles) might cloud the interpretation of experiments with heterogeneous catalysts.

- 2) For the chemical system in this study, homogenous catalysts are commercially available and hence no tailor-made manufacture of a supported heterogeneous catalyst is necessary.

- 3) The reproducibility of the kinetic experiments is better when utilizing a homogenous, commercially available catalyst, as the grade of this kind of catalyst will change only marginally compared to tailor-made heterogeneous catalysts.

Shaikh and Sivaram (1992) studied the performance of various homogeneous catalysts for the reaction of DMC and phenol and the subsequent disproportionation of the intermediate MPC. The reaction was carried out under continuous removal of the methanol/DMC azeotrope, while the temperature of the reaction vessel was increased gradually from 120 to 180° C. For the three tin-based catalysts, the authors

reported yields of 41% and 44% for DPC and yields of MPC between 3 and 12% achieved in 24 hours reaction time. The two titanium-based catalysts exhibited yields between 27% and 33 % for DPC and yields of 6% for MPC also achieved in 24 hours reaction time.

In another study Fuming et al. (2002) presented a newly developed catalyst, namely Samarium-trifluoromethanesulfonate (STFMS) that was compared to a tin-based, a titanium-based, an aluminum-based and a zinc-based catalyst, respectively. The selectivity of the new STFMS catalyst towards DPC was between 2% (w.r.t. the tin based catalysts) and 12% (w.r.t. the zinc based catalyst) higher, respectively. The conversion that was achieved in 12 hours with the new STFMS catalyst was 35%, which is close to the conversion that can be obtained with the zinc based catalyst (37%) and the titanium based catalyst (31%). The aluminum and zinc based catalysts exhibited conversions of DMC of less than 20% within 12 hours of reaction time. It is worthwhile to mention that while employing the samarium-, the aluminum- and the zinc-based catalyst there was always a small amount of anisole formed which corresponded to roughly 1% of the converted DMC (Fuming et al., 2002). Furthermore, it was reported that the DPC obtained when using the tin-based catalyst showed a grayish color due to the contamination with tin; this is undesirable if DPC is used as a precursor for polycarbonate production. All catalysts except the STFMS and the tin-based catalyst tend to hydrolyze in aqueous media. Thus, these catalysts cannot be utilized in aqueous environments and contact with air also should be avoided.

For this study, Titanium(*n*-butoxide) was used as catalyst. The selection for this catalyst is based on different considerations. A tin-based catalyst ( $n\text{-Bu}_2\text{SnO}$ ) has been disregarded as the DPC made with this catalyst exhibits a grayish color (Fuming et al., 2002), so that this catalyst does not seem suitable for the manufacture of Polycarbonate without additional processing steps.  $\text{AlCl}_3$  and  $\text{ZnCl}_2$  have been disregarded as these catalysts are both susceptible towards water and thus tend to hydrolyze in the presence of aqueous media (Fuming et al., 2002).

To avoid the lab synthesis of a new catalyst and to eliminate the undesired formation of anisole, also the use of the Samarium-trifluoromethanesulfonate (STFMS)



reaction temperature and to prevent cold spots and possible condensation of phenol. Valve 8 separates the two vessels (see Figure 5.5) and was opened to start the reaction; this is also the moment when the recording of data was started. The two reactants were heated separately to prevent reaction prior to their introduction into the reactor. The catalyst was located in the reactor with the reactant phenol. Both vessels were connected to a nitrogen source, which allowed the reaction to proceed under a complete nitrogen atmosphere to suppress possible oxidation reactions. The temperature of both vessels was monitored. The reactor itself was also provided with a pressure transducer for recording the pressure during the experiment. During the reaction, samples of 1 ml were taken from the liquid phase in the reactor by means of a syringe sampling system.

After the sampling procedure, the filled vials were cooled down in an ice-bath to stop the reaction. The time from the start of the experiment ( $t=0$ ) to the moment the vials were put in the ice-bath was taken as the reaction time. All vials were analyzed with a GC within 24 hours after the experiment concluded. The gas chromatograph used in this study was a Varian 3900 equipped with a FID detector. The column in the GC was a 50-meter long fused silica column (Varian CP 7685). The gas chromatograph applied a temperature ramp for the analysis: the column temperature was kept at 50° C for 2 minutes, then the temperature was raised 20° C per minute until a temperature of 300° C was reached. This temperature was maintained for three minutes before the column oven was cooled down to 50° C for the next analysis run.

Two internal standards were used in the GC analysis of the samples; toluene and n-tetradecane. Toluene was used as internal standard for methanol and DMC, whereas n-tetradecane was applied for the quantification of phenol, MPC and DPC.

To determine the reaction rate constants  $k_1$  to  $k_3$  from the experimental measurements, the question arises which key components should be used as indicator of the progress of the reaction. As the equilibrium conversion of the reactants phenol and DMC is less than 3%, it was decided not to use the concentration of either to determine the reaction rate parameters as the relative error would be large. Instead, the concentrations of the products, methanol, MPC and DPC, respectively

were initially chosen as the key components. Eventually the use of methanol as key component also has been omitted as GC analysis of the reactant DMC showed that it contained always a small amount ( $<1$  weight %) of methanol. Apart from that, methanol is also the most volatile component and a small part of it might evaporate to the gas phase (5% of the overall amount at V-L equilibrium), which would require an additional correction of the GC results of the liquid samples. For these reasons also methanol was disregarded as a key component and only MPC and DPC have been taken as the key components for the determination of the reaction rate parameters. Nevertheless, the initial amount of methanol introduced with the reactant DMC has been taken into account in the analysis of the experimental data.

Experiments were carried out at temperatures of 160° C, 180° C and 200° C at different catalyst concentrations and DMC/phenol reactant ratios. The catalyst mole fractions  $x_{cat}$  added in the experiments varied between  $1.0 \cdot 10^{-4}$  and  $4.5 \cdot 10^{-4}$ . The time to achieve equilibrium typically varied between 60 minutes for the lowest catalyst amount and 15 minutes for the highest catalyst amount (chemical equilibrium was judged to be reached when a plot of the concentration profile as a function of time leveled off). Additional experiments with mole fractions  $x_{cat}$  of around  $1.5 \cdot 10^{-3}$  have been carried out, which demonstrated that chemical equilibrium could be achieved in less than 5 minutes. This already indicates that the reaction can be quite fast, using reasonable amounts of catalyst. Some prior studies have reported reaction times of up to 20 hours (see, e.g. (Shaikh and Sivaram, 1996), (Niu et al., 2006)), but from our present perspective such long times do not seem to be required.

To ascertain that the initial level of mixing did not influence the measurements, experiments with two different stirrer speeds (800 and 1600 rpm) have been carried out, while otherwise maintaining the same experimental conditions. At both stirrer speeds the measured conversion rates were identical within experimental uncertainty. We conclude that it is safe to assume that mixing is sufficient to justify adopting an ideally mixed reactor in order to model this process (see below).

The catalyst, Titanium-n-butoxide, tends to hydrolyze in the presence of water. To study the occurrence of any unwanted hydrolysis of the catalyst, several experiments with varying amounts of catalyst were carried out, while maintaining

the same conditions ( $180^\circ\text{C}$ , reactant ratio phenol/DMC=1, nitrogen atmosphere). No detectable traces of degradation products in the GC diagram were found, which seems to indicate that catalyst degradation does not occur or, if it does, only to a negligible extent.

All chemicals employed in the experiments were used as received from the supplier. Dimethyl carbonate (purity: 99+%) was purchased from Aldrich, Phenol (99+%) and Tetra-(n-butyl orthotitanate) (98+%) were acquired from Merck. The catalyst was stored over molecular sieves (Type 4a) to prevent degradation due to moisture from air.

## 5.5 Effect of catalyst concentration

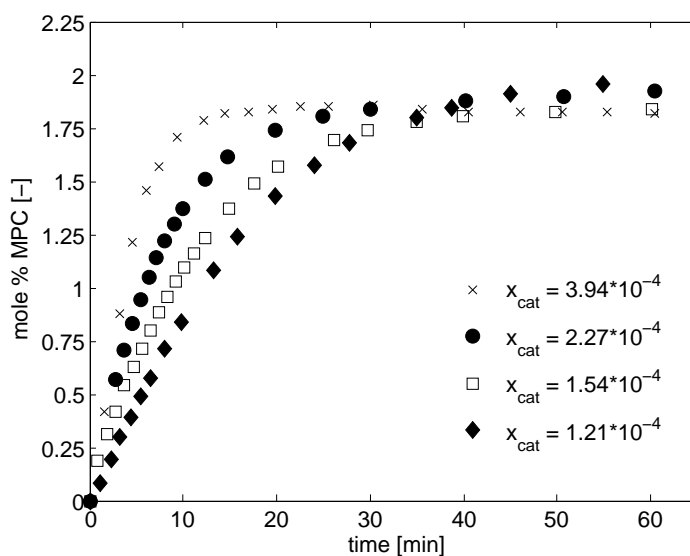


**Figure 5.6:** Dependence of the catalyst concentration on the temporal evolution of the MPC concentration ( $T=180^\circ\text{C}$ , molar ratio DMC/Phenol = 1)

To investigate the extent to which the catalyst concentration influences the reaction rate a series of experiments with relatively low catalyst mole fractions ( $1.0 \cdot 10^{-4}$  and  $2.5 \cdot 10^{-4}$ ) were carried out at identical initial concentrations of DMC

and phenol and at the same temperature (180° C). The results of these experiments are shown in Figure 5.6, which suggest that the equilibrium concentration is reached in times that vary from around 15 minutes at the higher concentrations of catalyst to something just over an hour at the lower concentrations. It has also been confirmed by additional experiments at 180° C that in the absence of catalyst the MPC mole fraction reaches only 6 % of the equilibrium mole fraction after 2 hours.

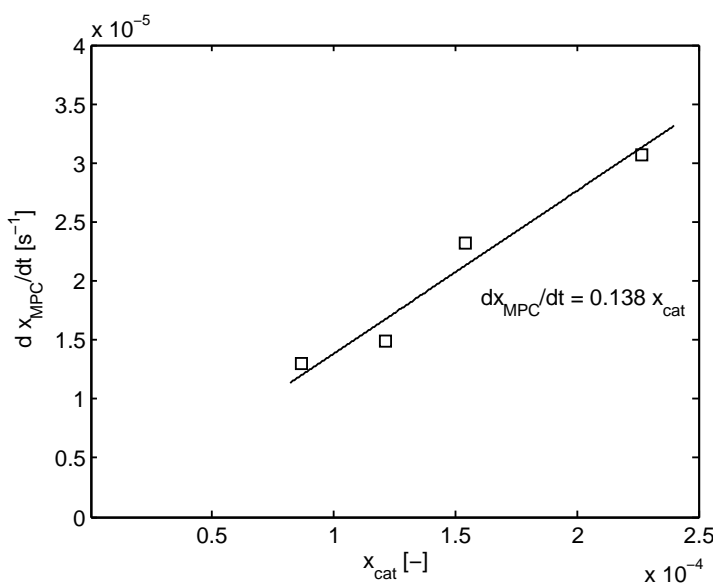


**Figure 5.7:** Dependence of the initial reaction rate of MPC on the catalyst mole fraction at 180° C and a DMC/Phenol ratio of 1 (markers = initial slope of concentration vs. time for MPC taken at low MPC yields; solid line = linear fit)

The initial forward rate of reaction 5.1 can be obtained by differentiation of the data in Figure 5.6 and is shown as a function of catalyst concentration in Figure 5.7, which suggests that the initial rate of reaction is directly proportional to the amount of catalyst and that the initial reaction rate can be expressed in the form:  $\frac{dx_{MPC}}{dt} \Big|_{t=0} = x_{cat} k x_{DMC}^{initial} x_{Phenol}^{initial}$ . This kinetic expression is equivalent to assuming that an elementary irreversible reaction (Reaction 5.1) is taking place. At low yields of MPC (<1%) - the equilibrium yield of MPC is only around 2% - it can be assumed that the backward reaction rate of MPC with methanol is much lower than

the forward reaction rate of DMC with phenol.

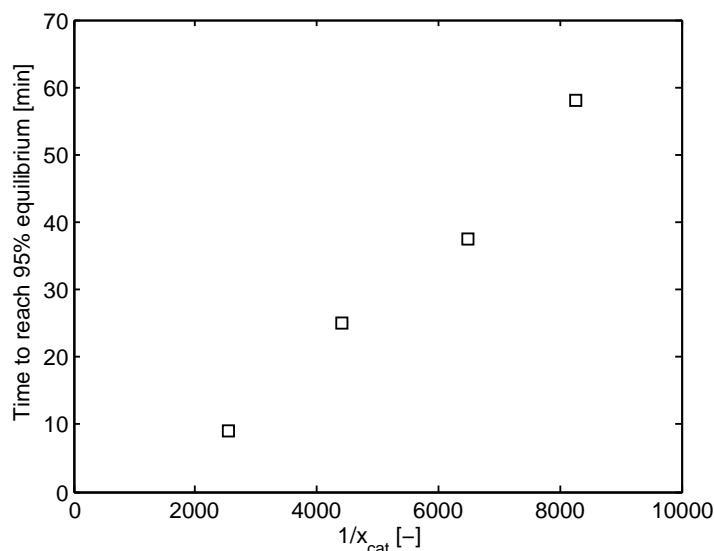


**Figure 5.8: Time to reach 95% equilibrium versus the reciprocal catalyst mole fraction**

Figure 5.8 shows the time required to reach 95% of equilibrium as a function of the reciprocal amount of catalyst. At the highest catalyst mole fraction employed in the experiments ( $3.94 \cdot 10^{-4}$ ) the MPC mole fraction reached 95% of the mole fraction at chemical equilibrium after just 10 minutes (see Figure 5.8). This time increases to about 60 minutes for the lowest catalyst mole fraction ( $1.21 \cdot 10^{-4}$ ). This lends additional support to the notion that we can model this system with a linear dependence of the reaction rate on the catalyst mole fraction, not only for the initial phase of the conversion but over the entire time of these experiments where the backward reaction also becomes important.

## 5.6 Does the disproportionation reaction occur?

To investigate whether or not the disproportionation reaction proceeds sufficiently fast experiments were carried out with no reactive component other than MPC



present. Solvents DMC and phenol were replaced by inert n-heptane. In the absence of phenol, MPC can only react to DPC via the disproportionation reaction and not at all via the transesterification reaction. Thus, if DPC is found within the usual time frame of an experiment, this should mean that the disproportionation reaction is able to proceed at an appreciable rate and must be considered in the analysis of the data. To determine the influence of n-heptane an experiment with an equimolar ratio of DMC/PhOH, catalyst and 50 mole% n-heptane was carried out. This experiment yielded the same results in terms of the chemical equilibrium constant and - corrected for the mole fractions of DMC and phenol - the same reaction rate as in the experiments without added solvent. We infer that it is likely that n-heptane does not influence the reaction rate in these experiments.

The results of the experiments with MPC dissolved in n-heptane indicate that DPC and DMC are formed at nearly the same rate (deviation <10%). Furthermore, the amounts of DPC and DMC created are identical within experimental accuracy which supports the presumption that DPC and DMC are formed from MPC in equimolar amounts via the disproportionation reaction. Methanol is present only in trace amounts. This suggests that the formation of DPC is - under the present experimental conditions - not taking place via the transesterification of MPC and phenol.

## 5.7 Reaction kinetics and modelling

For a simple well-mixed batch reactor the material balances for the five components in the liquid phase can be written as follows:

$$\frac{dx_{MeOH}}{dt} = R_1 + R_2 \quad (5.1)$$

$$\frac{dx_{DMC}}{dt} = R_3 - R_1 \quad (5.2)$$

$$\frac{dx_{PhOH}}{dt} = -R_1 - R_2 \quad (5.3)$$

$$\frac{dx_{MPC}}{dt} = R_1 - R_2 - R_3 \quad (5.4)$$

$$\frac{dx_{DPC}}{dt} = R_2 + R_3 \quad (5.5)$$

We propose that the rates of the three reactions can be expressed in the following form:

$$R_1 = k_1 x_{cat} (\gamma_{PhOH} x_{PhOH} \gamma_{DMC} x_{DMC} - \frac{1}{K_{a,1}} \gamma_{MPC} x_{MPC} \gamma_{MeOH} x_{MeOH}) \quad (5.6)$$

$$R_2 = k_2 x_{cat} (\gamma_{PhOH} x_{PhOH} \gamma_{MPC} x_{MPC} - \frac{1}{K_{a,2}} \gamma_{DPC} x_{DPC} \gamma_{MeOH} x_{MeOH}) \quad (5.7)$$

$$R_3 = k_3 x_{cat} (\gamma_{MPC}^2 x_{MPC}^2 - \frac{1}{K_{a,3}} \gamma_{DMC} x_{DMC} \gamma_{DPC} x_{DPC}) \quad (5.8)$$

In equations 5.6 to 5.8  $x_{cat}$  denotes the molar amount of catalyst,  $k_i$  the forward reaction rate constant of reaction  $i$ ,  $x_j$  the mole fraction of species  $j$ ,  $\gamma_j$  the activity coefficient of species  $j$  and  $K_{a,i}$  the corresponding activity based chemical equilibrium constant. A nearly identical approach has been applied by Steyer and Sundmacher (2007) to describe the reaction rate of the esterification of cyclohexene with formic acid and subsequent splitting of the ester yielding cyclohexanol. As shown in Figure 5.6 the time taken to achieve chemical equilibrium depends strongly on the catalyst

mole fraction used in the individual experiments, it seems therefore justified and necessary to account for the catalyst amount by the introduction of the catalyst mole fraction in the reaction rate equation. One should note that the results in Figure 5.6 do not imply that the catalyst activity coefficient can also be considered constant for all experiments (e.g. for different DMC/Phenol ratios).

The activity based equilibrium constants of the reactions 5.1-5.3 are given in Equations 5.9-5.11, with the overall chemical equilibrium coefficient defined by Eq.5.12:

$$K_{a,1} = \frac{a_{MPC} a_{MeOH}}{a_{DMC} a_{PhOH}} \quad (5.9)$$

$$K_{a,2} = \frac{a_{DPC} a_{MeOH}}{a_{MPC} a_{PhOH}} \quad (5.10)$$

$$K_{a,3} = \frac{a_{DPC} a_{DMC}}{a_{MPC}^2} = \frac{K_{a,2}}{K_{a,1}} \quad (5.11)$$

$$K_{a,ov} = \frac{a_{DPC} a_{MeOH}^2}{a_{DMC} a_{PhOH}^2} = K_{a,1} K_{a,2} = (K_{a,1})^2 K_{a,3} \quad (5.12)$$

In the formulation of the reaction equilibrium equations it has been assumed that reactions 5.1-5.3 represent elementary reaction steps. To justify this assumption detailed knowledge of the reaction mechanism is required that is not available in the open literature. Based on the satisfactory description of the chemical equilibrium found by Haubrock et al. (2007b) by assuming elementary reactions, it seems reasonable to make the same assumption here. The relations for the activity based equilibrium values  $K_{a,i}$  valid in the temperature range from 160-200° C determined by Haubrock et al. (2007b) are reproduced in Table 5.1.

In order to use  $K_{a,i}$  values to predict the equilibrium composition we need to know the activity coefficients, for which Haubrock et al. (2007b) used the UNIFAC

**Table 5.1:** Activity based equilibrium constants of reactions 5.1-5.3 (Haubrock et al., 2007b)

Reaction	Activity based equilibrium value $K_{a,i}$
(5.1)	$\ln K_{a,1} = -2702/T[K] + 0.175$
(5.2)	$\ln K_{a,2} = -2331/T[K] - 2.59$
((5.3))	$\ln K_{a,3} = \ln(K_{a,2}/K_{a,1})$

method. It proved to be necessary to introduce a new UNIFAC group, the carbonate group O-CO-O, which was not then part of the published UNIFAC database. The interaction parameters of this new OCOO-group with other UNIFAC groups, which are of importance for the system presented here, were fitted to VLE data for phenol-DMC, methanol-DMC, methanol-Diethyl carbonate (DEC), alkanes-DMC/DEC, alcohols-DMC/DEC and toluene-DMC (see Haubrock et al. (2007a) for complete details).

The temperature dependence of the reaction rate constants  $k_1$ ,  $k_2$  and  $k_3$  is accounted for by using the Arrhenius equation (Eq. 5.13):

$$k_i = k_{0,i} \exp(-E_{A,i}/(R_{gas}T)) \quad (5.13)$$

There are, therefore, 6 parameters that need to be fitted to experimental data using Equations 5.1 to 5.13: the three pre-exponential factors  $k_{0,i}$  and the three activation energies  $E_{A,i}$ . Our approach was to fit  $k_1$ ,  $k_2$  and  $k_3$  for each temperature. An Arrhenius plot may then be employed to determine  $k_{0,i}$  and  $E_{A,i}$ . The similarity of the reactions forming MPC and DPC by transesterification suggests that  $k_1$  and  $k_2$  will be in the same order of magnitude.

The influence of the catalyst amount on the reaction rate is accounted for via the catalyst mole fraction  $x_{cat}$  as a linear factor implemented in the reaction rate equations (Eq.5.6 -5.8). However, this might not be sufficient as it is likely that

not only the activity coefficients of the reactants and products change at different process conditions but also the activity coefficient of the catalyst ( $\gamma_{cat}$ ). In Equations 5.6 -5.8 it is implicitly assumed that the activity coefficient of the catalyst  $\gamma_{cat}$  is constant and, therefore, independent of the liquid phase composition. If this assumption is not justified, the rate constants ( $k_1$ ,  $k_2$  and  $k_3$ ) will probably vary with composition as the influence of the "non-constant" catalyst activity coefficient is in this case lumped into the optimized rate constants. Hence, in the interpretation of the experiments,  $k_1$ ,  $k_2$  and  $k_3$  will be optimized for each experiment conducted at a specific DMC/phenol reactant ratio. The optimized values of  $k_1$ ,  $k_2$  and  $k_3$  will subsequently be compared to the optimized results of experiments at other DMC/phenol reactant ratios.

The batch reactor model neglects mass transfer from the liquid phase (where the reaction takes place) to the gas phase; even for the most volatile component methanol, exploratory VLE calculations have indicated that at gas-liquid equilibrium about 95% of the amount of methanol formed will remain in the liquid phase (volume ratio liquid/gas phase = 3:1). For the less volatile components, this percentage is near 100%. It should be noted that in case of an open system, as for example in a reactive distillation column, especially methanol would steadily evaporate from the liquid phase and mass transfer to the gas phase should be taken into account.

## 5.8 Estimation of rate constants

Physically meaningful estimates as well as the likely range of values of the reaction rate constant  $k_1$  were estimated from the initial slopes of the mole fraction-time curve of MPC applying the following equation  $\left. \frac{dx_{MPC}}{dt} \right|_{t=0} = x_{cat} k x_{DMC}^{initial} x_{Phenol}^{initial}$ . As already discussed, at low conversions (yield MPC  $\sim 1\%$ ) the reverse reaction is not important and the estimation of  $k_1$  is straightforward. The MPC mole fractions used for the estimation of  $k_1$  were not corrected by the amount of DPC formed from MPC as the amount of MPC which reacts further to DPC is less than 2 mole % under the conditions investigated here.

The initial estimates for  $k_1$  obtained this way are given in Table 5.2 for various DMC/Phenol ratios at different temperatures.

**Table 5.2:** Estimated values for  $k_1$  based on the initial slopes of the MPC mole fraction vs. time profiles (used as starting values in the optimization).

DMC/phenol ratio	T [° C]	Slope dx/dt [s <sup>-1</sup> ]	$x_{cat}$ [-]	Estimated $k_1$ [s <sup>-1</sup> ]
3:1	160	$8.50 \cdot 10^{-6}$	$1.32 \cdot 10^{-4}$	0.343
1:1	160	$9.44 \cdot 10^{-6}$	$1.77 \cdot 10^{-4}$	0.213
1:3	160	$5.61 \cdot 10^{-6}$	$2.02 \cdot 10^{-4}$	0.148
3:1	180	$1.34 \cdot 10^{-5}$	$9.64 \cdot 10^{-5}$	0.740
1:1	180	$1.53 \cdot 10^{-5}$	$1.21 \cdot 10^{-4}$	0.505
1:3	180	$1.08 \cdot 10^{-5}$	$1.48 \cdot 10^{-4}$	0.387

The reaction rate constants of the first and second transesterification reaction  $k_1$  and  $k_2$  as well as the reaction rate constant of the disproportionation reaction  $k_3$  have been optimized by fitting the theoretically predicted temporal evolution of the mole fractions of MPC and DPC (Eq.5.4 and Eq.5.5). The actual fitting of the rate coefficients was carried out using the simulation environment gProms. The objective function minimized by gProms was:

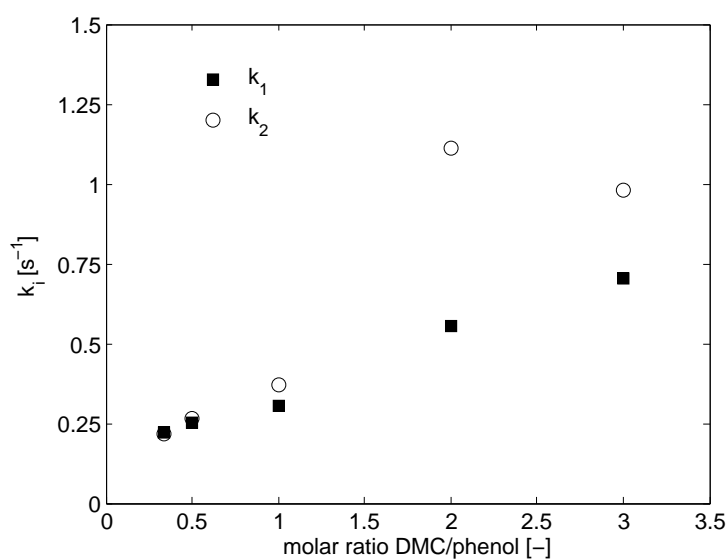
$$\Phi = \frac{N}{2} \ln(2\pi) + \frac{1}{2} \min \left\{ \sum_{k=1}^{NE} \sum_{j=1}^{NV_k} \sum_{m=1}^{NM_{kj}} \left[ \ln(\sigma_{kjm}^2) + \frac{(\tilde{x}_{kjm} - x_{kjm})^2}{\sigma_{kjm}^2} \right] \right\} \quad (5.14)$$

## 5.9 Effect of the reactant ratio DMC/phenol

The results of the optimization are summarized for  $k_1$  and  $k_2$  in Figure 5.9 (160° C) and Figure 5.10 (180° C) and for  $k_3$  in Figure 5.11 (160 and 180° C). The average deviations between the experimental and predicted values of the mole fractions were less than 10% for MPC and less than 15% for DPC in the 95% confidence interval,

respectively. In case of very low experimental MPC and DPC mole fractions, usually observed at DMC/phenol reactant ratios larger than two, the deviation between a single experimental and predicted mole fraction can amount at most up to 15% for MPC and 30% for DPC, respectively.

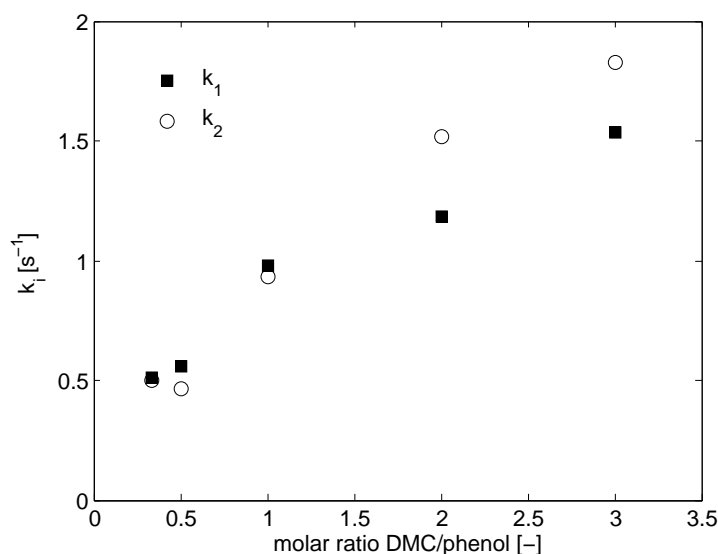
This clearly shows that the experimental set of data can be used reliably to determine  $k_1$  whereas the  $k_2$  and  $k_3$  values determined with the same experiments exhibit a somewhat larger deviation between the experimental and model predicted values of the mole fractions. However, the description of the experimental mole fractions of DPC is still good (see Figure 5.13) and the larger uncertainty in  $k_2$  and  $k_3$  does not yield a very large scatter when the individually determined values of  $k_2$  and  $k_3$  are plotted against the DMC/Phenol ratio (see Figures 5.9-5.11). The larger uncertainty in  $k_2$  and  $k_3$  is probably due to the very low amounts of DPC formed in our experiments.



**Figure 5.9: Reaction rate constants  $k_i$  as a function of the initial reactant ratio DMC/phenol ( $T = 160^\circ \text{C}$ )**

To obtain even more accurate data for  $k_2$  and  $k_3$ , it would be necessary to carry out experiments under continuous removal of methanol. Exploratory experiments

with MPC as starting component have shown that significantly larger amounts of DPC can be achieved; the absence of methanol means that the backward reaction of DPC with methanol to MPC is suppressed. The setup used in this study (Figure 5.5) does not allow for a "reactive-distillation-like" mode where methanol is evaporated at a specified pressure or temperature, respectively. Moreover, a mass transfer model would be needed, to interpret this kind of experiments and that would require physical property data (e.g.  $k_L$ -values, diffusion coefficients etc.) that are not known. For these reasons experiments under continuous removal of methanol were not included within the scope of this study. The values of  $k_2$  and  $k_3$  determined in this study should, therefore, be handled with some care, if used for completely different conditions.



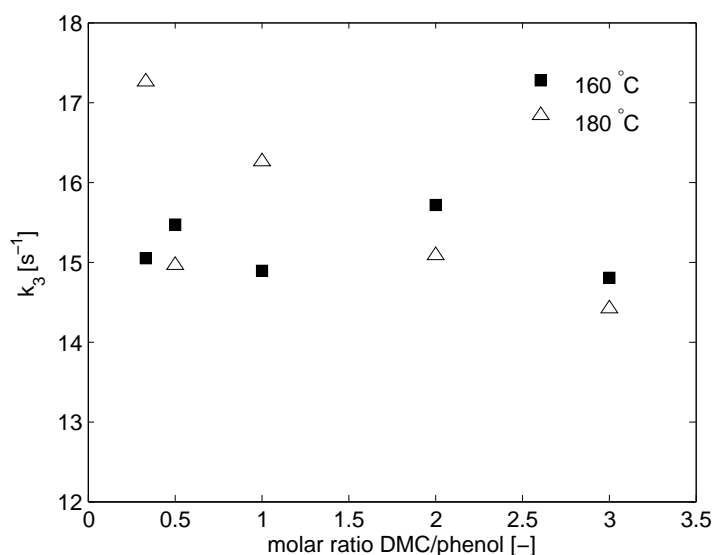
**Figure 5.10:** Reaction rate constants  $k_i$  as a function of the initial reactant ratio DMC/phenol ( $T= 180^\circ \text{ C}$ )

Figure 5.9 and 5.10 suggest that a linear relationship between the initial reactant ratio DMC/phenol and the reaction rate coefficients  $k_1$  and  $k_2$ , respectively can be deduced. The reaction rate constant  $k_3$  of the disproportionation reaction is not influenced by the DMC/Phenol ratio (Figure 5.11), and this might be attributed



to different reaction mechanisms of the disproportionation reaction and the transesterification reactions. The scatter of the  $k_3$  values is around  $\pm 10\%$  (see Figure 5.11), which corresponds to the experimental uncertainty of the DPC mole fractions used for the fitting of the reaction constant  $k_3$ .

Figure 5.10 shows that the fitted reaction rate constants  $k_1$  and  $k_2$  ( $180^\circ\text{C}$ ) have nearly the same value (within  $\pm 15\%$  on average). The deviation between the  $k_1$  and  $k_2$  ( $160^\circ\text{C}$ ) values shown in Figure 5.9 is larger -on average  $\pm 35\%$ - which is mainly due to the comparatively large  $k_2$ -value at a DMC/phenol ratio of 2. From Figure 5.9 and 5.10 it can be concluded that the values of the kinetic constants  $k_1$  and  $k_2$  are similar and - for DMC/phenol ratios  $< 1$  - nearly identical. Considering the very similar reactions it could have been expected that also the reaction mechanism is identical and the kinetic rate similar which is supported by the nearly identical reaction rate constants.



**Figure 5.11: Reaction rate constants  $k_3$  as a function of the initial reactant ratio DMC/phenol.**

In view of the fact that activity coefficients of all reactants and products were included in the model, we would hope that "nearly" constant values of the reaction

rate constants might have been expected on purely fundamental grounds. This is obviously not the case for  $k_1$  and  $k_2$  (see Figure 5.9 and 5.10). There seem to be two possible reasons: it might be that either one or more of the activity coefficients are inaccurate or that the catalyst activity changes with the DMC/Phenol ratio. A previous study on the equilibria of the reactions 5.1 to 5.3 has shown that the activity coefficient of DMC, important in the proper determination of  $k_1$ , might be prone to error because the equilibrium value of the first transesterification reaction showed some variation ( $\pm 20\%$ ) with the DMC/Phenol ratio. As depicted in Figure 5.9 and 5.10,  $k_1$  changes by approximately a factor of three and it does not seem likely that an inaccuracy in the activity coefficient can be held responsible for the shifting value of  $k_1$ .

Accordingly, the linear increase of  $k_1$  most probably has to be attributed to a change in the activity of the catalyst. In which case, it is also likely that  $k_2$  will be affected in the same way as  $k_1$ ; the two transesterification reactions are similar and we would expect that both reactions should be affected to a comparable extent by a change in the catalyst activity. Although the linear relationship of  $k_2$  on the DMC/Phenol ratio seems to suggest this fact, it cannot be concluded beyond a reasonable doubt because of the larger uncertainty in the individual  $k_2$  values.

Nevertheless, a possible change of the catalyst activity with a change of the DMC/Phenol ratio is not unlikely, considering the interaction of the in-situ formed Ti-catalyst with the reactant phenol. Assuming that one or more of the four butoxide ligands of the Titanium(*n*-butoxide) catalyst have been substituted by phenol (Sibum et al., 2000), the in-situ formed Titanium(phenoxide) catalyst is likely to show a substantial interaction with phenol. As the activity coefficient of phenol changes with a change of the DMC/Phenol ratio, the activity of the catalyst is likely to change accordingly. There is no detailed information in the literature on the activity of the Titanium(phenoxide) catalyst as a function of the composition of the mixture, and the present experiments also do not provide enough information to unambiguously establish any such dependence; thus, the influence of the reactant ratio of DMC/phenol on the catalyst activity can only be hypothesized. In order to establish the activity of the catalyst as a function of composition, an extensive

study including various vapour-liquid-equilibrium (VLE) experiments with changing DMC/phenol ratios and catalyst concentrations would have to be carried out to determine the interactions between the catalyst and the various species in the system. Moreover, the interpretation of this kind of experiments is complicated by the fact that the species in the system are chemically reacting.

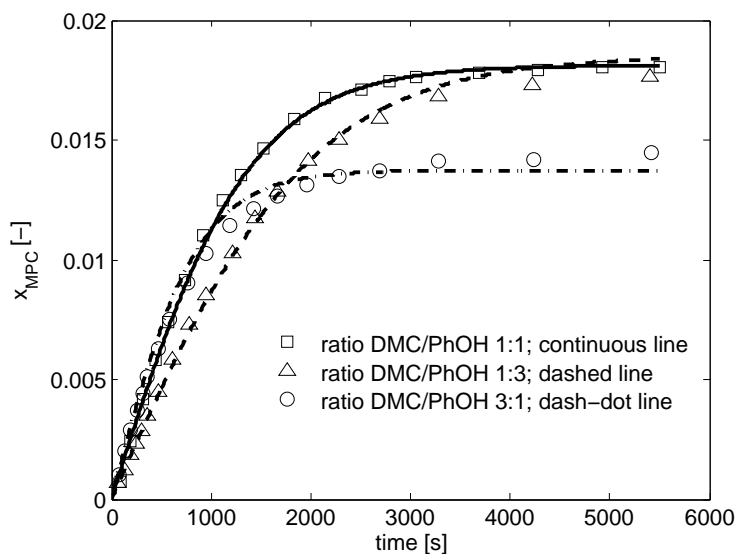


**Figure 5.12:** MPC mole fraction as function of time for different initial DMC/phenol reactant ratios ( $T=180^{\circ}\text{C}$ ). Markers - experimental data; continuous line - model.

Looking again at Figure 5.9-5.11 and comparing the values of  $k_3$  to those of  $k_1$  and  $k_2$ , it can be seen that the reaction rate constant  $k_3$  is one order of magnitude larger than the values for  $k_1$  and  $k_2$ . This indicates that the disproportionation reaction is intrinsically faster than the two transesterification reactions; this is in agreement with the literature (Buysch, 2000). Since there is normally an excess of phenol in these experiments, the formation rates of DPC by the second transesterification and the disproportionation reaction respectively, are of the same order of magnitude. However, in industrial processes and at high reactant conversions, the concentration of phenol might be much lower and MPC much higher than in

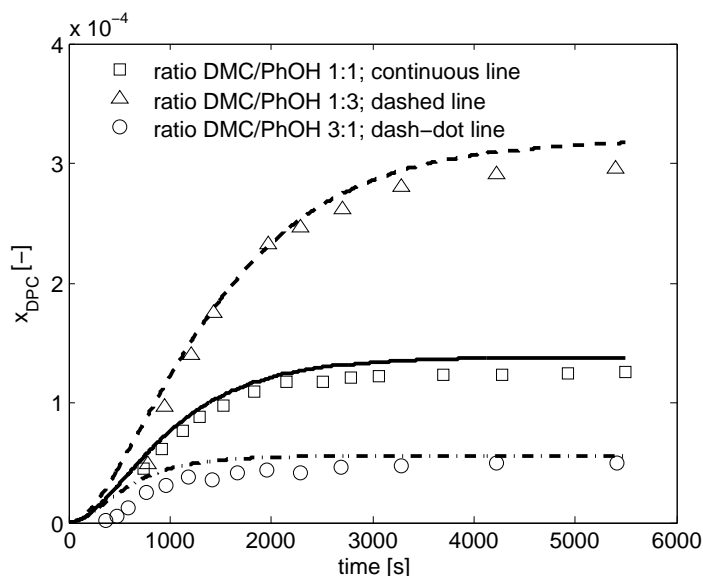


**Figure 5.13:** DPC mole fraction as function of time for different initial DMC/phenol reactant ratios ( $T=180^{\circ}\text{C}$ ). Markers - experimental data; continuous line - model.

this study, so that the disproportionation reaction may be the main route of MPC to DPC; this should be kept in mind when scaling up the process.

Typical results of some experimental results at different reactant ratios together with the accompanying theoretical predictions are given in Figure 5.12 and Figure 5.13 using the individual fitted reaction rate constants  $k_1, k_2$  and  $k_3$  (Figures 5.9-5.11) and activity based equilibrium constants  $K_{a,i}$  at nearly identical catalyst amounts ( $8.4 \cdot 10^{-5} < x_{cat} < 1.7 \cdot 10^{-5}$ ). It can be seen that the experimental MPC and DPC mole fractions are well in line with the model predictions when using the individual fitted reaction rate constants  $k_1, k_2$  and  $k_3$  for the appropriate reactant ratio DMC/phenol. This suggests that the proposed reaction rate model is well suited to reproduce the experimental results.

Since the experiments as depicted in Figures 5.12-5.13 were carried out at slightly varying catalyst mole fractions ( $8.4 \cdot 10^{-5} < x_{cat} < 1.7 \cdot 10^{-5}$ ) the reaction rates determined from the individual experiments cannot directly be compared to

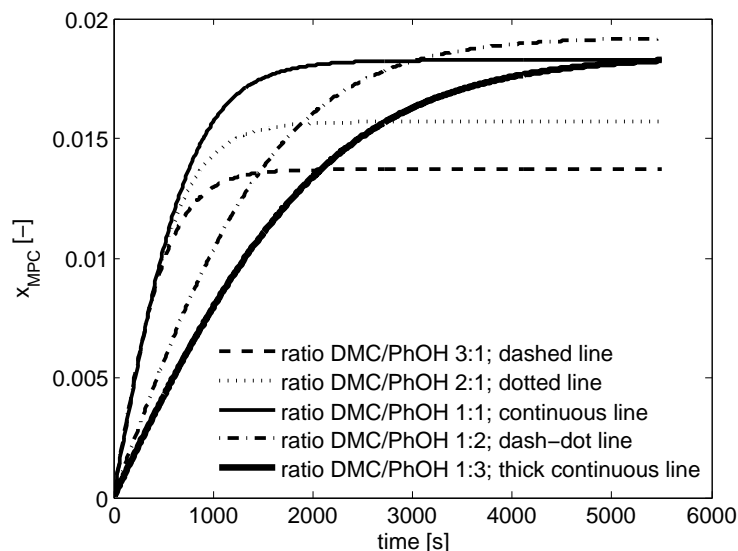


**Figure 5.14: Model prediction: MPC mole fraction as a function of time for different initial reactant ratios of DMC/phenol at 180° C ( $x_{cat} = 1.50 \cdot 10^{-4}$ ).**

each other. However, the individually fitted  $k_1$ ,  $k_2$  and  $k_3$  values as given in Figure 5.9-5.11 can be used with the batch reactor model to simulate the concentration-time profiles scaled to the same catalyst mole fraction (Eq.5.4 -Eq.5.5) thereby excluding the effect of the catalyst amount on the reaction rate and making it possible to investigate the corresponding reaction rates at various DMC/phenol ratios. In Figure 5.14 the course of the MPC mole fraction versus time for different DMC/phenol ratios using a catalyst amount of  $x_{cat} = 1.50 \cdot 10^{-4}$  is shown and it can be seen that DMC rich reactant mixtures (DMC/phenol ratio  $> 1$ ) have only a slight influence on the formation rate of MPC, whereas in phenol rich reactant mixtures (DMC/phenol ratios  $< 1$ ) the reaction rate of MPC slows down considerably. The time to reach equilibrium roughly doubles for phenol rich reactant mixtures.

As the same amount of catalyst is used in the simulations shown in Figure 5.14, the different reaction rates can either be attributed to changing activity coefficients of the involved species or to a varying catalyst activity. The product of the activity coefficients of DMC and phenol,  $\gamma_{DMC}\gamma_{PhOH}$ , changes only about 10% over the entire

range of employed DMC/phenol ratios and can, therefore, not be held responsible for the slower reaction rates observed for reactant ratios less than 1. This supports the hypothesis that a varying catalyst activity is indeed responsible for the change in the reaction rate.

## 5.10 Effect of temperature

An Arrhenius plot (Figures 5.15 and 5.16) may be used to determine the pre-exponential factor  $k_{0,i}$  and the activation energy  $E_{A,i}$  of the three reactions (see Eq.5.13) from linear regression. The results of such a calculation are summarized in Table 5.3.

**Table 5.3:** Values of the pre-exponential factor  $k_{0,i}$  and the activation energy  $E_{A,i}$  (derived from regression lines in Figure 5.15 and Figure 5.16, respectively).

Reaction	$k_{0,i}$ [ $s^{-1}$ ]	$E_{A,i}$ [ $kJ\ mole^{-1}$ ]
Trans 1 (i=1)	$2.42 \cdot 10^{+8}$	73.5
Trans 2 (i=2)	$6.61 \cdot 10^{+6}$	59.9
Disprop (i=3)	14.88	-

In Figure 5.15 the Arrhenius plots of  $k_1$  and  $k_2$  and the corresponding fitted  $k_i$ -values in the temperature range between 160° C and 200° C are shown. As already mentioned earlier the two transesterification reactions seem to have the same reaction mechanism and the numerical values of the reaction rate constants derived from the experiments are similar. Hence it could be expected that the temperature dependence of the two reaction rate constants  $k_1$  and  $k_2$  (Figure 5.15) would yield similar activation energies. The Arrhenius plot of  $k_3$  and the corresponding fitted  $k_3$ -values in the temperature range between 160° C and 200° C are depicted in Figure 5.16. The disproportion reaction exhibits no significant temperature dependence - the scatter shown in Figure 5.16 is within the experimental error margin.

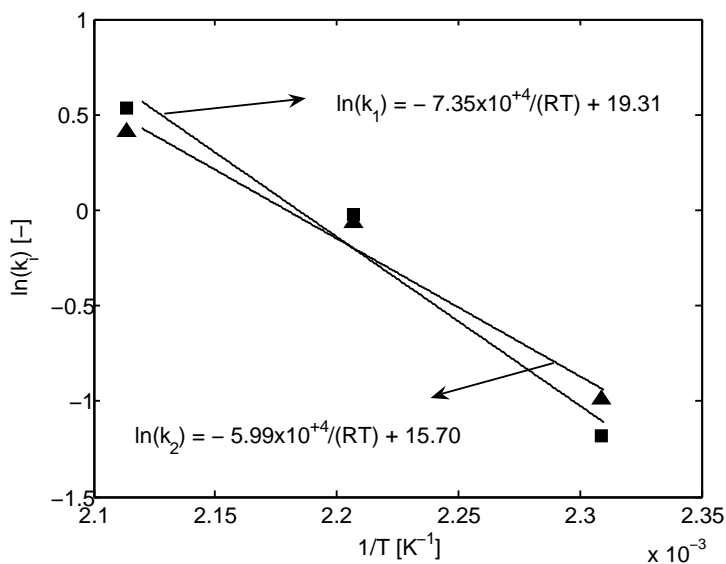


Figure 5.15: Arrhenius plot: markers indicate fitted  $k_i$ -values derived from kinetic experiments ( $T=160-200^\circ$  C; 1:1 DMC/phenol ratio). Transesterification 1 (squares) and Transesterification 2 (triangles).

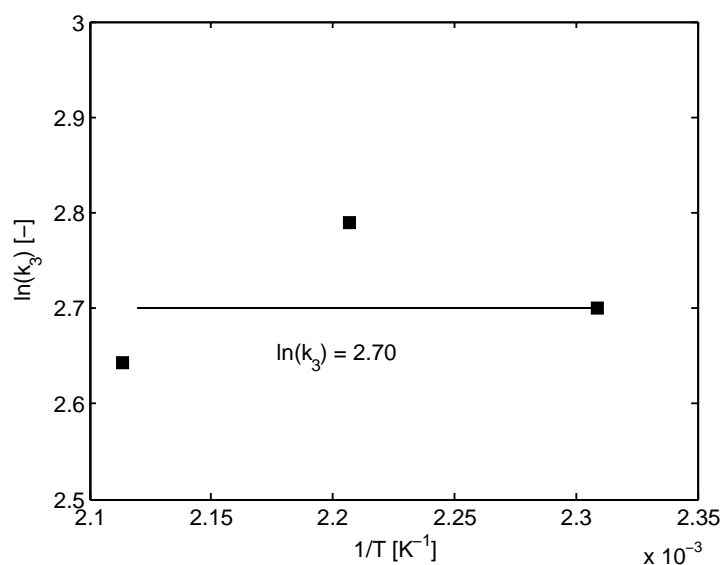


Figure 5.16: Arrhenius plot: markers indicate fitted  $k_3$ -values from kinetic experiments ( $T=160-200^\circ$  C; 1:1 DMC/phenol ratio)

## 5.11 Conclusion

In this study the reaction rate constants of the transesterification reaction of DMC with phenol yielding the intermediate MPC, the reaction rate constants of the consecutive transesterification reaction of MPC with phenol and the reaction rate constants of the disproportionation of MPC have been experimentally determined in a batch reactor.

The influence of the catalyst concentration (Titanium(*n*-butoxide)) and the temperature on the reaction rate constants in the temperature range between 160° C and 200° C has been investigated as well as the influence of the initial reactant ratio of DMC/phenol. The concept of a closed, ideally stirred, isothermal batch reactor incorporating an activity based reaction rate model, has been used to fit the values of the three reaction rate constants  $k_1$ ,  $k_2$  and  $k_3$  to the experimental data.

The numerical values of the fitted reaction rate constants  $k_1$  and  $k_2$  are found to be similar whereas the numerical value of  $k_3$ , belonging to the disproportionation reaction, is about one order of magnitude larger. Moreover, it was shown that the reaction rate constants of the two transesterification reactions ( $k_1$  and  $k_2$ ) are strongly influenced by the initial reactant ratio of DMC/phenol which was attributed to inaccuracies in the activity coefficients and to a changing catalyst activity. Nevertheless, the change of the reaction rate constants over the initial reactant ratio of DMC/phenol by a factor of 3 is too large to be caused only by flawed activity coefficients. Therefore, it is likely that the activity coefficient of the catalyst changes over the initial reactant ratio of DMC/phenol. However, at the moment this can only be regarded as a hypothesis as no detailed information of the catalyst activity is available. Additional VLE experiments should be carried out to determine the interactions between the catalyst and the other involved species yielding the activity coefficient of the catalyst to confirm the aforementioned hypothesis.

Experiments have shown that it seems necessary to remove methanol from the reaction mixture for two reasons: Firstly, the removal of methanol increases the conversion of DMC and phenol thereby promoting the formation of the intermediate MPC via transesterification 1. Secondly, in the absence of methanol the disproportionation of MPC will contribute to the overall conversion of MPC to DPC as



the backward reactions of transesterification 1 and 2, respectively are suppressed. Therefore, the removal of methanol is important to achieve a selectivity towards DPC that is viable for industrial processes.

Reactive distillation might be used on an industrial scale not only to allow for higher conversions of the reactants but also for a higher selectivity towards the desired product DPC. It is expected that the correlations presented in this section could be used in the modelling of reactive distillation processes for the industrial relevant system presented in this work.

## Acknowledgement

The author gratefully acknowledges the financial support of Shell Global Solutions International B.V. We would like to thank H.J. Moed for the construction of the equipment and M. Raspe for her contributions to the experimental work.

## Notation

$a_j$	Activity of component j	[-]
$E_{A,i}$	Activation energy of reaction i	[kJ mol <sup>-1</sup> ]
$k_{0,i}$	Pre-exponential factor of reaction i	[s <sup>-1</sup> ]
$K_{a,i}$	Activity based equilibrium coefficient of reaction i	[-]
$k_i$	Reaction rate constant of reaction i	[s <sup>-1</sup> ]
N	Total number of measurements taken during all experiments	[-]
NE	Number of experiments performed	[-]
$NM_{k,j}$	Number of measurements in the j <sup>th</sup> mole fraction in the k <sup>th</sup> experiment	[-]
$NV_k$	Number of variables measured in the k <sup>th</sup> experiment	[-]
$R_{Gas}$	Ideal gas constant	[kJ mol <sup>-1</sup> K <sup>-1</sup> ]

$R_i$	Reaction rate of reaction i	$[\text{s}^{-1}]$
T	temperature	[K]
t	time	[min] or [s]
$x_j$	Mole fraction of component j	[-]
$\tilde{x}_{k,j,m}$	mth measured value of mole fraction j in experiment k	[-]
$x_{k,j,m}$	mth predicted value of mole fraction j in experiment k	[-]
$\gamma_j$	Activity coefficient of component j	
$\sigma_{k,j,m}^2$	Variance of the mth measurement of mole fraction j in experiment k	[-]
<b>Indices</b>		[-]
cat	catalyst	[-]
i	Reaction i	[-]
j	Component j	[-]
k	Experiment k	[-]
m	Measurement m	[-]

## Chapter 6

# Preliminary process design for the production of Diphenyl carbonate from Dimethyl carbonate: Parameter studies and process configuration

### Abstract

In this chapter the process from dimethyl carbonate (DMC) to diphenyl carbonate (DPC) via the intermediate methyl phenyl carbonate (MPC) carried out in a reactive distillation column has been modelled with the commercial software package ChemSep. The influence of various parameters on the yields of MPC and DPC has been studied to find suitable optimization parameters. Activity based chemical equilibrium expressions and activity based reaction kinetics of the three involved reactions as well as relevant vapour-liquid equilibria of the studied system have been taken into account in the simulations. The influence of the feed location of phenol, the number of stages, the molar feed ratio DMC/phenol on the yield of MPC and

DPC have been investigated for two different tray residence times. For the investigated range of the parameters above it has been found that the MPC and DPC yield, respectively can be maximized by placing the phenol feed location on the top of the column, using 15 stages and a molar DMC/phenol feed ratio of 1. Furthermore it has been shown that the residence time should be large enough to get close to chemical equilibrium. When operating close to chemical equilibrium a decreased reflux ratio leads to higher MPC and DPC yields whereas an increased bottom flow rate leads to increasing MPC yields but an almost constant DPC yield.

Based on the modelling results of the "first" column - with DMC, phenol and catalyst as feed- it seems necessary to use a "second" column in which MPC is converted to DPC and moreover excess phenol is separated from the product DPC. As feed condition for the "second" column the bottom product specification and composition of the "first" column has been taken. The influence of the reflux ratio, bottom flow rate and the number of stages on the DPC yield in the bottom of the "second" column has been studied. The impact of the reflux ratio on the DPC yield is negligible in the investigated range and a decrease of the bottom flow rate as well as an increase of the number of stages leads to a marginally larger DPC yield (<10% increase).

This chapter concludes with a comparison of the calculated composition profiles taken from Tung and Yu (2007) and those calculated in this work for a column producing DPC from phenol and DMC. The comparison between the simulation results from this work and those from literature has shown that there is a large quantitative as well as a qualitative difference between the two simulated composition profiles over the column. It is likely that the different physical properties which, in case of Tung and Yu (2007) are completely hypothetical, cause the very different simulation results. As there are neither experimental liquid composition profiles of a column available nor experimentally measured liquid composition of at least one stage, it cannot be safely said which simulation results are closer to reality.

## 6.1 Introduction

Diphenyl carbonate is a precursor in the production of Polycarbonate (PC). Polycarbonate is widely employed as an engineering plastic, important to the modern lifestyle and used in, for example, the manufacture of electronic appliances, office equipment and automobiles. About 3.4 million tons of PC was produced worldwide in 2006. Production is expected to increase by approximately 6% per year until 2010 with the fastest regional growth anticipated in East Asia, averaging 8.7% per year through 2009 (Westervelt, 2006).

Traditionally, PC is produced using phosgene as an intermediate. The phosgene process entails a number of drawbacks. Firstly, 4 tons of phosgene is needed to produce 10 tons of PC. Phosgene is very toxic and when it is used in the production of PC the formation of undesired hazardous salts as by-products cannot be avoided. Furthermore, the phosgene-based process consumes 10 times as much solvent (on a weight basis) compared to the amount of PC is produced. The solvent, methylene chloride, is suspected carcinogen and is soluble in water. This means that large quantities of waste water have to be treated prior to their discharge (Ono, 1997).

Many attempts have been made to overcome the disadvantages of the phosgene based process (Kim et al., 2004). The main point of focus has been a route through dimethyl carbonate (DMC) to diphenyl carbonate (DPC), which then reacts further with Bisphenol-A to produce PC. The most critical step in this route is the synthesis of DPC from DMC via the transesterification of DMC to methyl phenyl carbonate (MPC), followed by a disproportionation and/or transesterification step of MPC to DPC. The equilibrium conversions of the reactions to MPC and DPC are highly unfavorable: in a batch reactor with an equimolar feed, an equilibrium conversion of DMC of only  $\sim 3\%$  can be expected. Therefore, good process engineering is required in the design of a process to successfully carry out the reaction of DMC to DPC in a commercial attractive manner. The reaction appears to be a candidate for being carried out in a reactive distillation column to realize high conversions (Rivetti, 2000) as methanol, an intermediate reaction product, can be separated simultaneously from the other components by distillation and hence the conversion

of DMC and phenol in the transesterification step can be increased. For a general introduction to the concept of *Reactive Distillation* the reader is referred to e.g. Taylor and Krishna (2000) and Sundmacher and Kienle (2003).

In this work the process from DMC to DPC in a reactive tray column will be modelled to study the influence of various process parameters on the yields of the intermediate MPC and the end product DPC. This study will give increased insight in the process and furthermore identify appropriate optimization opportunities for the reactive distillation process.

## 6.2 The Equilibrium Stage model

The starting point for this work was an existing computer program for performing multicomponent, multi-stage steady state separation process calculations included in the software package ChemSep (Taylor and Kooijman, 2000). The form of this process model used in the study is outlined below.

The equations that describe the various stages in the column are termed the MESH equations where MESH is an abbreviation of the different types of equations that form the mathematical model. A schematic drawing of a stage is shown in Figure 6.1. Vapour from the stage below and liquid from a stage above are brought into contact on stage  $j$  together with any fresh or recycle feeds. The vapour and liquid streams leaving the stage are assumed to be at vapour-liquid equilibrium (Taylor and Kooijman, 2000).

The MESH equations at *steady state* consist of the following relations: The M equations are the Material balance equations, of which there are two types: The Total Material Balance

$$M_j \equiv V_{j+1} + L_{j-1} + F_j - (1 + r_j^V)V_j - (1 + r_j^L)L_j + \varepsilon_j \sum_{m=1}^r \sum_{i=1}^c \nu_{i,m} R_{m,j} = 0 \quad (6.1)$$

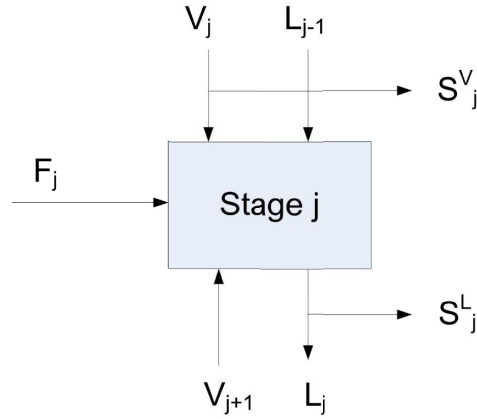


**Figure 6.1: Schematic diagram of an equilibrium stage.**

and the Component Material Balances

$$\begin{aligned}
 M_{ij} &\equiv V_{j+1} y_{i,j+1} + L_{j-1} x_{i,j-1} + F_j z_{i,j} - (1 + r_j^V) V_j y_{i,j} - (1 + r_j^L) L_j x_{i,j} \\
 \varepsilon_j \sum_{m=1}^r \nu_{i,m} R_{m,j} &= 0
 \end{aligned} \tag{6.2}$$

In equations 6.1 and 6.2  $r_j$  represents the ratio of the side-stream flows to interstage flow:

$$r_j^V = S_j^V / V_j; \quad r_j^L = S_j^L / L_j \tag{6.3}$$

The E equations are the Vapour-Liquid Equilibrium relations

$$E_{i,j} \equiv y_{i,j} - K_{i,j} x_{i,j} = 0 \tag{6.4}$$

The S equations are the Summation equations

$$S_j^L \equiv \sum_{i=1}^c x_{i,j} - 1 = 0; \quad S_j^V \equiv \sum_{i=1}^c y_{i,j} - 1 = 0 \tag{6.5}$$

And the H equations are the Heat Balance equations

$$H_j \equiv V_{j+1} H_{j+1}^V + L_{j-1} H_{j-1}^L + F_j H_j^F - (1 + r_j^V) V_j H_j^V - (1 + r_j^L) L_j H_j^L - Q_j = 0 \tag{6.6}$$

where the  $H$ 's are the enthalpies of the appropriate phases and streams.

In total there are  $2c+4$  equations per stage. It must be noted however, that only  $2c+3$  of these equations are independent. In ChemSep both, the total and component material balances are used, respectively and the two summation equations are combined to give

$$S_j \equiv \sum_{i=1}^c y_{i,j} - \sum_{i=1}^c x_{i,j} - 1 = 0 \quad (6.7)$$

The  $2c + 3$  unknown variables determined by the equations are the  $c$  vapour mole fractions,  $y_{i,j}$ , the  $c$  liquid mole fractions,  $x_{i,j}$ ; the stage temperature,  $T_j$ , and the vapour and liquid flow rates:  $V_j$  and  $L_j$ .

### 6.3 Phase equilibrium, thermodynamics and reaction kinetics

In this study the vapour-liquid equilibria are described with a simplified version of the so called "gamma-phi" model (Sandler, 1999). For the conditions  $(T,p)$  and the species used in this study the following simplifications apply to the gamma-phi model (Sandler, 1999): the vapour and liquid phase fugacity coefficient as well as the Poynting correction factor can be set equal to unity. The resulting model is referred to as the DECHEMA-K-model (Taylor and Kooijman, 2000) (see Eq. 6.8):

$$y_i p = x_i \gamma_i p_i^{vap} \Leftrightarrow K_i = \frac{y_i}{x_i} = \frac{\gamma_i p_i^{vap}}{p} \quad (6.8)$$

In Equation 6.8  $y_i$  denotes the vapour phase mole fractions of species  $i$ ,  $p$  the overall pressure in the gas phase,  $x_i$  the mole fractions of species  $i$  in the liquid phase,  $\gamma_i$  the liquid phase activity coefficient of species  $i$  and  $p_i^{vap}$  the vapour pressure of species  $i$ , respectively.  $K_i$  is the distribution ratio of component  $i$ , often referred as the  $K$ -value (Taylor and Kooijman, 2000). The  $K_i$  value is generally changing



with composition in a non-linear way; a constant value of  $K_i$  is only observed when Raoult's law applies as in an ideal system. The pure vapour pressures of all species are calculated with the Antoine equation and the activity coefficients, as needed in Eq. 6.8, are computed with the UNIFAC model (Fredenslund et al., 1975).

## 6.4 Reactions

The synthesis of diphenyl carbonate (DPC) from dimethyl carbonate (DMC) and phenol takes place through the formation of methyl phenyl carbonate (MPC) catalyzed either by homogeneous or by heterogeneous catalysts. The reaction of DMC to DPC is a two-step reaction. The first step is the transesterification of DMC with phenol (PhOH) to the intermediate MPC and methanol (MeOH) (Eq. 6.2) (Ono, 1997; Fu and Ono, 1997):

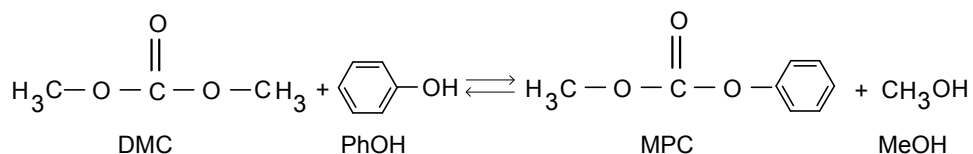


**Figure 6.2: Transesterification 1**

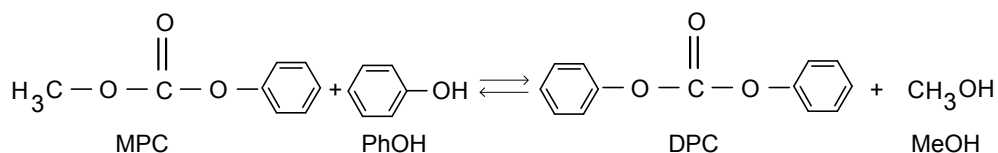


**Figure 6.3: Transesterification 2**

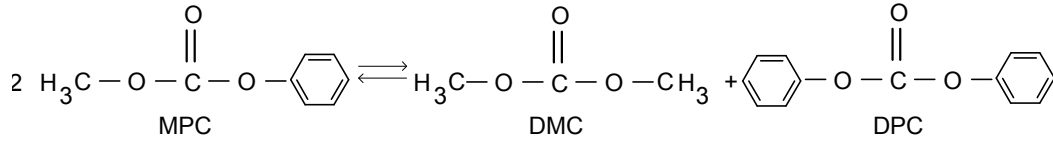


**Figure 6.4: Disproportionation**

For the second step two possible routes exist: the transesterification of MPC with phenol (Reaction 6.3) and the disproportionation of two molecules MPC yielding DPC and DMC (Reaction 6.4).

## 6.5 Thermodynamics

The activity based equilibrium constants of the reactions 6.2 - 6.4 as also employed in the reaction rate equations (15)-(17) are given in Equations 6.9 to 6.11:

$$K_{a,1} = \frac{a_{MPC} \ a_{MeOH}}{a_{DMC} \ a_{PhOH}} \quad (6.9)$$

$$K_{a,2} = \frac{a_{DPC} \ a_{MeOH}}{a_{MPC} \ a_{PhOH}} \quad (6.10)$$

$$K_{a,3} = \frac{a_{DPC} \ a_{DMC}}{a_{MPC}^2} = \frac{K_{a,2}}{K_{a,1}} \quad (6.11)$$

In the formulation of the reaction equilibrium equations it has been assumed that reactions 6.2 - 6.4 represent elementary reaction steps. The relations for the activity based equilibrium values  $K_{a,i}$  are given in Table 6.1 and have been experimentally determined in the temperature range from 160-200 °C (Haubrock et al., 2007b).

**Table 6.1:** Activity based equilibrium constants of reactions 6.2-6.4 (Haubrock et al., 2007b)

Reaction	Activity based equilibrium value $K_{a,i}$
(6.2)	$\ln K_{a,1} = -2702/T[K] + 0.175$
(6.3)	$\ln K_{a,2} = -2331/T[K] - 2.59$
(6.4)	$\ln K_{a,3} = \ln(K_{a,2}/K_{a,1})$

## 6.6 Reaction rate equations

The three reaction rate equations of reactions 6.2-6.4, under the assumption of elementary molecular reactions, can be expressed in the following form:

$$R_1 = k_1 x_{cat} (\gamma_{PhOH} x_{PhOH} \gamma_{DMC} x_{DMC} - \frac{1}{K_{a,1}} \gamma_{MPC} x_{MPC} \gamma_{MeOH} x_{MeOH}) \quad (6.12)$$

$$R_2 = k_2 x_{cat} (\gamma_{PhOH} x_{PhOH} \gamma_{MPC} x_{MPC} - \frac{1}{K_{a,2}} \gamma_{DPC} x_{DPC} \gamma_{MeOH} x_{MeOH}) \quad (6.13)$$

$$R_3 = k_3 x_{cat} (\gamma_{MPC}^2 x_{MPC}^2 - \frac{1}{K_{a,3}} \gamma_{DMC} x_{DMC} \gamma_{DPC} x_{DPC}) \quad (6.14)$$

In equations 6.12 to 6.14  $x_{cat}$  denotes the molar amount of the homogeneous catalyst Titanium n-butanoate,  $k_i$  the forward reaction rate constant of reaction  $i$ ,  $x_j$  the mole fraction of species  $j$ ,  $\gamma_j$  the activity coefficient of species  $j$  and  $K_{a,i}$  the corresponding activity based chemical equilibrium constant. The reaction rate constants  $k_i$  used in reaction rate equations 6.12 to 6.14 have been taken from Haubrock et al. (2007c) who has determined the rates of these reactions in the temperature range of 160-200 °C experimentally:

$$\ln k_1 = \frac{-7.35 \cdot 10^4}{RT} + 19.31 \quad (6.15)$$

$$\ln k_2 = \frac{-5.99 \cdot 10^4}{RT} + 15.70 \quad (6.16)$$

$$\ln k_3 = 2.70 \quad (6.17)$$

In the temperature range between 160-200 °C the reaction rate constants  $k_1$  and  $k_2$  exhibit a distinct temperature dependence whereas for the reaction rate constant  $k_3$  no temperature influence could be observed. For more information on the experimental determination of the reaction rate constants 6.15-6.17 the reader is referred to Haubrock et al. (2007c).

For a reliable description of the process it is necessary to have activity coefficients for the system in this study. These activity coefficients are required for the description of the chemical equilibria, the reaction kinetics and for the phase equilibrium calculations. Haubrock et al. (2007a) used the UNIFAC method to estimate the activity coefficients for the system in the present study. It turned out necessary to introduce a new UNIFAC group, the carbonate group O-CO-O, which was not part of the published UNIFAC database. The interaction parameters of this new O-CO-O-group with other UNIFAC groups, which are of importance for the system presented here, were fitted to VLE data for phenol-DMC, methanol-DMC, methanol-Diethyl carbonate (DEC), alkanes-DMC/DEC, alcohols-DMC/DEC, and ketones-DEC (Haubrock et al., 2007a).

## 6.7 Process description and assumptions

There is only very little information in literature dealing with the (conceptual) design of the process from DMC to DPC. From the patents (Fukuoka and Tojo, 1993;

Schon et al., 1994) and the work of Fukuoka et al. (2003) it can be concluded that two coupled reactive distillation units are required to obtain the desired end product DPC in industrial feasible yields. In this two-column configuration DMC, phenol and catalyst are fed to the first column reacting predominantly to the intermediate MPC and methanol. The top product of the first contactor consists mainly of DMC and methanol whereas the bottom product contains essentially phenol, the intermediate MPC and some DPC. The bottom product is fed to the second contactor where the intermediate MPC reacts further to the end-product DPC.

The transesterification reaction (Fig. 6.2) of DMC and phenol yielding MPC and methanol possesses a very unfavorable equilibrium conversion - the mole fraction based value  $K_{x,1}$  is  $1.7 \times 10^{-3}$  and the activity based value  $K_{a,1}$  is  $2.8 \times 10^{-3}$ , respectively at 180 °C (Haubrock et al., 2007b)- and the reaction rate constant  $k_1$  is also one order of magnitude lower than reaction rate constant  $k_3$  of the disproportionation reaction to DPC. Therefore the reaction to the intermediate MPC must be regarded as the most critical step in the process from DMC to DPC. Of course, if the intermediate MPC is only present in low amounts also the reaction of MPC to DPC via either transesterification reaction 2 (Fig. 6.3) or the disproportionation reaction (Fig. 6.4) is severely affected and the net formation rate of DPC will be rather low.

First, a single reactive distillation unit with the reactants DMC and phenol and a homogeneous catalyst as feed will be investigated. The physical properties and the UNIFAC-interaction parameters used for the modelling in this chapter can be found in Tables 3.7, 3.10 and 3.12 of this thesis. The heat balance (Eq. 6.6) will not be taken into account in these simulations as on one hand there is a lack of required physical data ( $c_p$  values and  $H_{vap}$ ) for some components and on the other hand it is not the main goal of this work to optimize the energy consumption and hence the operating costs of the DMC to DPC process.

The impact of various process parameters will be studied for this one-column setup to identify the critical parameters and to quantify the impact of them on the attainable yields of MPC and DPC. The different parameters will be successively varied while keeping the remaining parameters constant. The simulation results will be as-

essed by comparing the calculated yields of MPC and DPC to those accomplished in a base case configuration.

The results of the case studies investigating the influence of different parameters on the yields of MPC and DPC are employed to find an "optimized" single reactive distillation column to achieve the maximum yields of MPC and DPC. The composition of the product flow from the bottom of the optimized "first column" will then be used as a feed for the "second" column where the intermediate MPC reacts further to the end product DPC. For the second column also a parameter study will be performed to quantify the impact of the various parameters on the yields of DPC.

The base case of the "first" column represents a technically feasible, not optimized column design which has been based on the information given in the patent by Schon et al. (1994) and Buysch et al. (1993). The ranges of parameters reported in the patent of Schon et al. (1994) are summarized in Table 6.2 as well as the actual chosen parameters for the simulations in ChemSep.

The liquid composition profile of the base case using a tray volume of  $0.5 \text{ m}^3$  (Regime 1) is shown in Figure 6.5. As it can be seen the mole fractions of MPC and DPC are both around 10% in the bottom of the column (Stage 10). Although seemingly quite low, the achievable MPC mole fractions are 4 times larger and the DPC mole fractions are 600 times larger than those obtained in batch reactor experiments, respectively (Haubrock et al., 2007b). This can likely be attributed to the instantaneous removal of excess methanol from the reaction zone thereby preventing the backward reaction of MPC (Fig. 6.2) and DPC (Fig. 6.3) with methanol, respectively. Moreover, a substantial increase of DPC from 1 mole % to 10 mole % can be observed from stage 9 to 10. The increase of DPC is probably due to the very low amount of methanol on stage 10 (around 20 times smaller than on stage 9) which prevents the backward reaction of DPC to MPC (Fig. 6.3).

For elucidating the effect of the different adjustable parameters in a distillation column case studies have been performed by changing the following parameters:

- feed location of phenol
- number of stages

**Table 6.2:** Parameters specifying the base case of the "first" column. The discrimination between Regime 1 and 2 is made via different tray volumes.

Parameter	Range or Specification taken from patent (Schon et al., 1994)	Parameter value Base case
Trays	5-15	10
Liquid holdup	10-50% of column internal	-
Feed stage Phenol	Top Tray	2
State Phenol Feed	Liquid form	Liquid
T of Phenol feed	Same T as on Top tray	
Feed stage DMC	Tray above stripping section	9
State DMC Feed	Vapour Form	Vapour
Feed stage catalyst	Same as phenol	2
Molar DMC/phenol feed ratio	0.5-2.0	1
T range in column	140-230 °C	160-180 °C
Catalyst mole fraction on reactive trays	-	$1.5 \times 10^{-3}$
Tray Volume (Regime 1/Regime 2)	-	$0.5\text{m}^3 / 0.1\text{m}^3$
Pressure p	0.5-10 bar	1.013 bar
Molar Feed Flows (each)	Not specified	6 mol/s

- molar feed ratio DMC/phenol

These parameters will be altered for two different residence times on the reactive trays of the column. These residence times are:

1. The residence time where the conversion is mainly influenced by the concentration of the to be separated component methanol in the liquid phase.

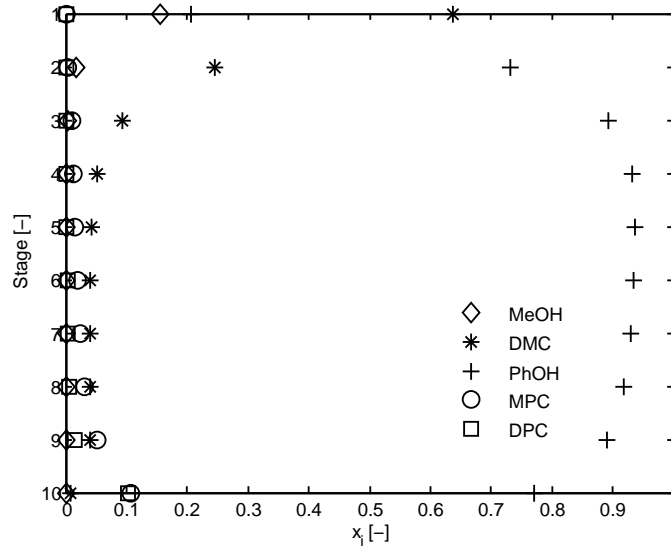


**Figure 6.5:** Liquid phase composition profile for the base case of the "first" column ("Regime 1":  $V_{tray}=0.5 \text{ m}^3$ ) (see Table 6.2).

For this regime the residence time on the trays was chosen such as to realize a conversion level close to chemical equilibrium ( 35-60 %; ratio between the "equilibrium constant" calculated with the prevailing mole fractions on a stage and the real theoretical  $K_{x,1}$  value at the corresponding temperature as calculated by the relations in Table 6.1 ) of transesterification reaction 1 (Fig. 6.2) and 2 (Fig. 6.3). This regime will further be referred to as "Regime 1".

2. The residence time for which the conversion is mainly influenced by the kinetic limitations of transesterification reaction 1 and 2, demanding low conversions per tray. This regime is sometimes referred to as the "Controlled by kinetics regime" (Schoenmakers and Bessling, 2003). In this study and for this regime the residence time on each reactive tray was chosen such that transesterification reaction 1 (Fig. 6.2) could proceed to only an extent of 1-4 % of chemical equilibrium on each reactive tray. This regime will further be referred to as "Regime 2".

Of course it would have been more desirable if "Regime 1" represented a sit-



uation in which chemical equilibrium of transesterification reaction 1 and 2 (Fig. 6.2 and 6.3) is completely attained. Unfortunately this is not possible due to convergence problems with the used simulation tool ChemSep which -in this specific case- did not allow simulations where 100% of chemical equilibrium on the trays was achieved. Therefore, the residence time on the tray was enlarged until convergence problems occurred resulting in an attainment of 35-60% of equilibrium (Regime 1). It should be noted that due to the lower temperature at the top of the column- and resulting slower reaction rate- the composition is further from equilibrium than indicated.

Still, the two regimes as specified above will show to what extent the yields of the intermediate MPC and the end product DPC are influenced by the residence time and on approach of equilibrium.

The base case, as defined in Table 6.2, reflects these two regimes by a difference in the tray volume: for "Regime 1" a tray volume of 0.5 m<sup>3</sup> turned out to be appropriate while for the "Regime 2" a tray volume of 0.1 m<sup>3</sup> sufficed. The calculated volume per tray for the two different residence times was based on the reaction kinetics taken from Haubrock et al. (2007c) in which the catalyst mole fraction was taken at the value from the base case in Table 6.2 (see Eq. 6.12). For both regimes the feed flows of DMC and phenol (Table 6.2) were taken identical and a fixed molar flow of catalyst was fed to the column on the phenol feed tray.

Figure 6.6 shows the calculated yields of MPC and DPC depending on the phenol feed stage location for the "first" column (Table 6.2). From Figure 6.6 it can be deduced that the residence time as specified for "Regime 2" is indeed far from sufficient to get close to chemical equilibrium and this is reflected in the MPC and DPC yields which are around a factor of 3 lower with respect to MPC and between a factor of 4 -7 lower for DPC as for "Regime 1". The yields of MPC and DPC in the two regimes rise with an increasing length of the reaction zone which indicates that the reaction zone must guarantee a certain residence time and number of separation stages to make it kinetically and thermodynamically possible to get higher conversions of the reactants DMC and phenol therewith permitting feasible yields of MPC and DPC.

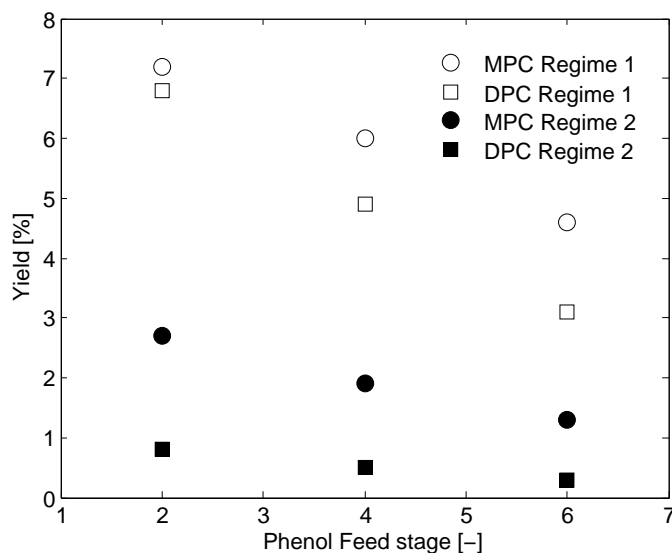


**Figure 6.6:** Influence of the phenol feed stage on the yield [%] of MPC and DPC (Stage 1 = condenser, Stage 10 = reboiler).

Figure 6.7 shows the calculated yields of MPC and DPC as a function of the total number of stages for a one-column configuration (specification see Table 6.2). Here, a nearly linear increase of the MPC and DPC yield with an increasing length of the reaction zone is observed. The increasing yield of DPC is more pronounced in "Regime 1" than in "Regime 2". This could be expected as in "Regime 1" at each reactive tray at least 35% of chemical equilibrium of transesterification 1 is achieved leading to larger amounts of formed MPC on each tray which allows an increasing conversion of MPC to DPC. In "Regime 2" the yield of MPC is to a very large extent determined by the reaction rate of transesterification 1 and barely by an equilibrium limitation due to a formed product (methanol). As the reactions, especially transesterification 1, are still substantially away from chemical equilibrium for "Regime 2" the dependency of the yield of MPC and DPC, respectively, on the number of stages is less pronounced compared to "Regime 1".

Figure 6.8 shows the calculated "modified yields" of MPC and DPC depending on the molar DMC/phenol feed ratio for the "first" column (Table 6.2). A "modified

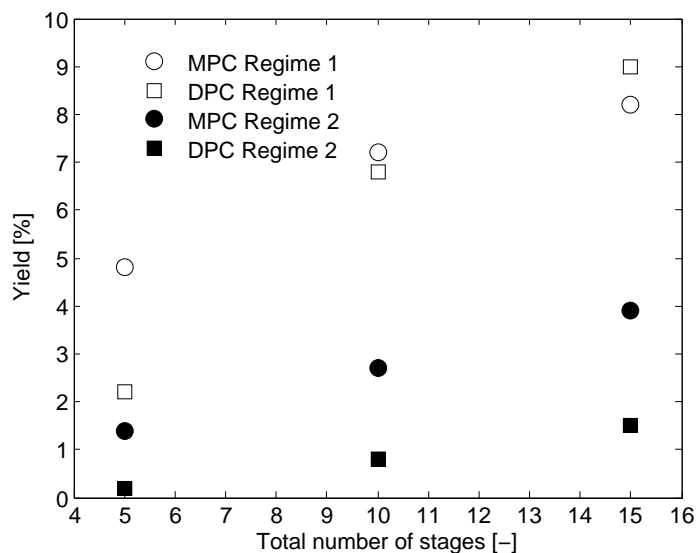


**Figure 6.7: Influence of the total number of stages on the yield [%] of MPC and DPC.**

yield” has been introduced as changing the molar reactant ratio will also affect the calculated yields that are usually related to just one reactant, DMC or phenol in this case. The ”modified yield” is defined as the ratio between the moles of formed MPC and DPC, respectively to the overall feed of phenol and DMC which is constant and equal to 12 moles/s for all three DMC/phenol ratios.

In ”Regime 1” the ”modified yields” of MPC and DPC increase moderately for DMC/phenol ratios from 0.5 to 1, respectively. When this ratio is further increased to 2, a step decrease of the modified DPC yield and a moderate decrease of the modified MPC yield can be observed. In ”Regime 1” the course of the ”modified yields” with maxima at a DMC/phenol ratio of 1 can most likely be attributed to a change in the vapour liquid equilibria (VLE) and corresponding tray temperatures caused by the different DMC/phenol reactant ratios. In ”Regime 2” the modified yields of MPC and DPC are much less dependent on the different DMC/phenol ratios. The moderate differences observed for the ”modified yield” in ”Regime 2” can probably be attributed to varying column temperature profiles for the three

different DMC/phenol ratios (see Figure 6.9).

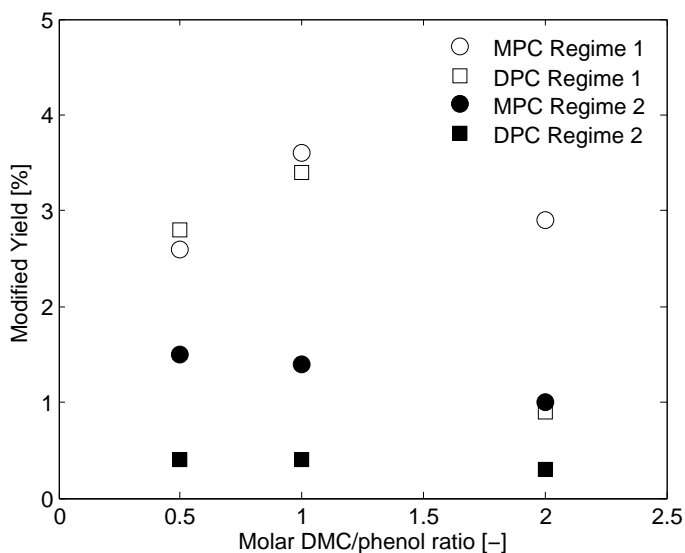


**Figure 6.8:** Influence of the reactant ratio DMC/phenol on the "modified yield" [%] of MPC and DPC. (DMC feed stage = 9, Phenol feed stage = 2.)

The lower "modified yields" of MPC and DPC at a molar ratio of DMC/phenol of 2 for especially "Regime 2" are due to a larger mole fraction of DMC in the liquid phase resulting in a higher vapour pressure of the mixture and therewith lower boiling point on each tray. The temperature profiles in "Regime 1" for the three different molar DMC/phenol ratios are shown in Figure 6.9. The lower temperature on the trays in case of a molar DMC/phenol ratio of 2 causes slower reaction rates resulting in lower yields of MPC and DPC, respectively compared to the yields calculated for molar DMC/phenol ratios of 0.5 and 1.0, respectively. As the reaction rate slows down considerably at lower temperatures, a considerable conversion of the reactants phenol and DMC (chemical equilibrium >35%) in case of a DMC/phenol ratio of 2 is therefore only safely achieved on the last two trays (e.g. the required residence time to achieve near 100% chemical equilibrium of reaction 1 at a temperature of 95 °C and a catalyst mole fraction of  $1.5 \times 10^{-3}$  is around a factor of 40 larger compared to a temperature of  $\sim 180$  °C). Apart from that, it is also question-

able if the correlations used to describe the reaction kinetics (Eq. 6.15-6.17) and chemical equilibria (Eq. 6.9-6.11) are valid at temperatures far away from the range (160-200 °C) where they have been determined for. For the latter reason the results calculated at a DMC/phenol ratio of 2 should be handled with care.

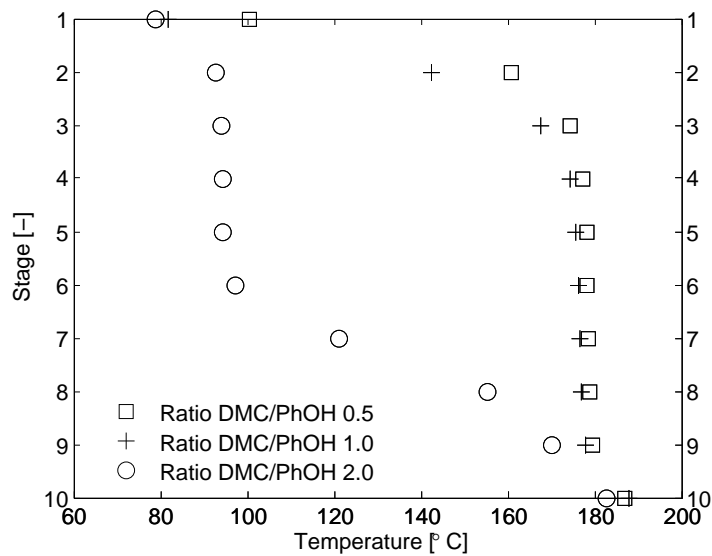


**Figure 6.9:** Temperature profile for the three different molar DMC/phenol ratios corresponding to the yields of MPC and DPC in "Regime 1" shown in Figure 6.8.

The parameter studies investigating the influence of the phenol feed location, the number of stages and feed ratio of DMC/phenol have shown that it is indeed advantageous or even inevitable to perform the reactive distillation process as close as possible to chemical equilibrium to achieve feasible yields of MPC and DPC. The influence of the operating parameters "reflux ratio" and "bottom flow rate" will therefore only be investigated in "Regime 1".

In Figure 6.10 the influence of the reflux ratio on the MPC and DPC yields in the bottom product of the column for "Regime 1" is shown. Increasing the reflux ratio from 3 to 5.5 decreases the residence time per tray compared to the base case in "Regime 1" by  $\pm 20\%$  (which corresponds to an equilibrium conversion of 50%).

For decreasing reflux ratios a linear increase of the MPC and DPC yield is observed. This could also be expected as at a lower reflux ratio the low boilers -methanol and DMC- are removed from the column to a larger extent and therefore chemical equilibrium, especially for the transesterification reactions, is shifted to the product side due to the low concentrations of the product methanol in the liquid phase.

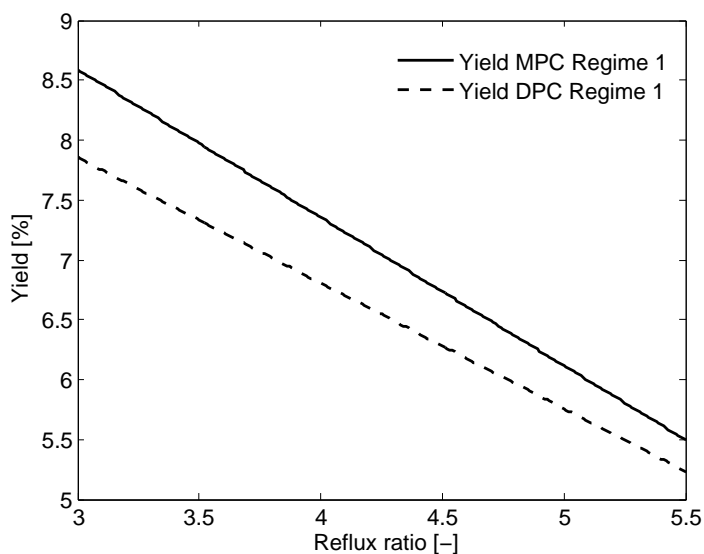


**Figure 6.10: Influence of the Reflux Ratio on the yield [%] of MPC and DPC in the bottom product of the column in "Regime 1". Smoothed curves are shown.**

In Figure 6.11 the influence of the bottom flow rate on the yield of MPC and DPC in the bottom product of the column for "Regime 1" is shown. The DPC yield is barely influenced by the bottom flow rate in the investigated range whereas the MPC yield increases linearly with an increasing bottom flow rate. This behavior can be explained with the different volatilities of MPC and DPC. The pure vapour pressure of MPC is considerably higher ( $\Delta T_{\text{boilingpoint}} \sim 60 \text{ }^\circ\text{C}$ ) than the vapour pressure of DPC and therefore at the same temperature MPC goes "easier" to the gas phase than DPC. When the bottom flow rate is low (3 mol/s) more MPC is

forced into the gas phase compared to higher bottom flow rates (

>

3mol/s). This means that MPC either leaves the column via the top or condenses again at stages close to the column top where it can react back with methanol to DMC and phenol. The temperature in the bottom, and also on the stages above, increases only marginally ( $\sim 4$  °C) with decreasing bottom flow rate in the investigated range.

The amount of MPC "lost" is thus decreased with an increasing bottom flow rate. The amount of DPC going to the gas phase is small compared to that of MPC. The weight based ratio between MPC leaving the column via the bottom and the top changes from a value of 47 for a bottom flow rate of 3 mol/s to a value of 136 for a bottom flow rate of 4.5 mol/s. The corresponding ratios for DPC are a factor of 500 larger supporting the presumption that DPC is almost completely present in the liquid phase.

Based on the results of the performed parameter studies an "optimized" column setup aiming at the highest yield of MPC and DPC, respectively, can be defined. The "optimized" design parameters for the "first" column giving the highest yield of MPC and DPC for the investigated parameters are given in Table 6.3 and the properties as well as the composition of the corresponding bottom product stream of this column are given in Table 6.4.

As the software package ChemSep does only allow the simulation of one single, stand alone reactive distillation column it is at the moment not possible to model the process from DMC to DPC with two interconnected units (and possible recycles) as e.g. suggested in the patent of Schon et al. (1994). Nevertheless, it is possible to use the specifications of the bottom product stream of the "first" column (Table 6.4) as feed stream (6.6 moles/s) for a "second" column. The "second" column then especially serves to convert MPC to DPC and moreover to separate excess phenol from the product DPC.

The parameters of the base case design for the "second" column -taking into account the parameters/specifications of the "second" column as given in the patent of Schon

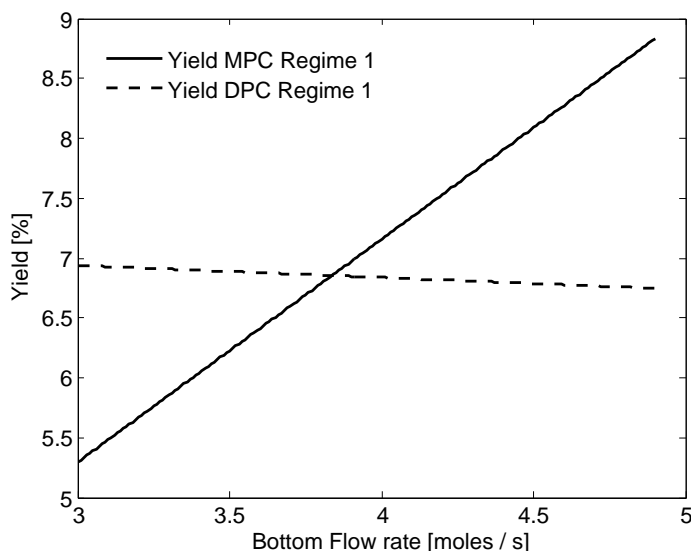


**Figure 6.11: Influence of the Bottom Flow rate [mole/s] on the yield [%] of MPC and DPC in the bottom product of the column in "Regime 1". Smoothed curves are shown.**

et al. (1994)- are given in Table 6.5. It seems necessary to operate the "second" column also close to chemical equilibrium (Regime 1) to guarantee a large conversion of MPC towards DPC and therefore the parameter study will solely be performed in "Regime 1". The base case serves as benchmark for the studies investigating the following parameters:

- Reflux ratio
- Bottom flow rate
- Number of stages

The composition profile for the base case defined in Table 6.5 is shown in Figure 6.12. The increase of DPC from tray 9 to the bottom tray 10 is remarkably large (from 10 to 50 mole %) and can probably be attributed to the decreasing amount of DMC (from  $1.2 \times 10^{-4}$  to  $1.2 \times 10^{-5}$  mole %) which - close to equilibrium-



**Table 6.3:** Optimized column parameters for the "first" column (Regime 1).

Parameter	Range studied	Parameter value "optimized"
Trays	5-15	15
Feed stage Phenol	4-6	2
State Phenol Feed	Liquid	Liquid
T of Phenol feed	182 °C	182 °C
Feed stage DMC	14	14
State DMC Feed	Vapour	Vapour
Feed stage catalyst	2	2
Molar DMC/phenol ratio feed	0.5-2.0	1
T range in column	75-190 °C	167-188 °C
Catalyst mole fraction on reactive trays	$1.5 \times 10^{-3}$	$1.5 \times 10^{-3}$
Tray Volume	0.1 m <sup>3</sup> / 0.5 m <sup>3</sup>	0.5 m <sup>3</sup>
Pressure p	1 bar	1 bar
Molar Feed Flows	4-8 mole /s	Each 8 mole /s (DMC and phenol)
Reflux ratio	3-5.5	3.5
Bottom product flow rate	3-5 mole /s	5 mole /s

enables a substantial increase of the mole fraction of DPC (see Eq. 6.11) when the MPC mole fraction changes only marginally (<20% in this case). This indicates that under the conditions in the "second" column the disproportionation reaction contributes significantly to the DPC formation. It can be seen that a fairly large amount of DPC ( 50 mole %) is present in the bottom of the second column with the remainders mostly being phenol. Nevertheless, it should be possible to further decrease the amount of phenol in the bottom of the column to less than 35 mole %

**Table 6.4:** Properties and composition of the bottom product of the "first column".

Pressure [bar]	1.01325
Temperature [K]	461
Mole fractions (-)	
Methanol	$2.12 \times 10^{-5}$
Dimethyl carbonate	$8.74 \times 10^{-3}$
Phenol	$7.58 \times 10^{-1}$
Methyl phenyl carbonate	$1.25 \times 10^{-1}$
Diphenyl carbonate	$1.06 \times 10^{-1}$
Catalyst	$1.54 \times 10^{-3}$

(Figure 6.12).

It is also the intention of the case studies to show which parameters have a significant influence on the yield of DPC - the yield is defined as the ratio of the molar flow of DPC in the bottom product of the "second" column to the molar feed flow of DMC introduced in the "first" column - and on the amount of excess phenol in the bottom. According to Schon et al. (1994) the excess phenol can be discharged at the bottom of the column together with the DPC or - preferably- together with the low-boiling products at the top of the column. These exploratory simulations are expected to give an indication which parameters have to be altered to achieve a low amount of phenol in the bottom to prevent additional separation steps of the bottom stream to get the pure product DPC.

The reflux ratio has been altered between 3.6 and 6.0 and no significant influence on the DPC yields has been observed in this reflux ratio range (results are not shown). It is likely that the reflux ratio has no significance here as the low boilers (methanol, DMC and phenol) are easily separated from the mixture. In Figure 6.13 the DPC yield as a function of the number of stages is shown. An increase of the number of stages from 5 to 10 increases the DPC yield from around 11.2% to

**Table 6.5:** Parameters specifying the base case of the "second" column.

Parameter	Range or Specification taken from patent (Schon et al., 1994)	Parameter value Base case
Trays	2-15	10
Feed stage	Top Tray	8
State Feed	Liquid	Liquid
T range in column	150-250 °C	180-240 °C
Catalyst mole fraction on reactive trays	-	$1.5 \times 10^{-3}$
Tray Volume	-	0.5 m <sup>3</sup>
Pressure p	0.2-2 bar	1.013 bar
Molar Feed Flow	Not specified	6.6 mol/s
Reflux ratio	Not specified	5
Bottom product flow rate	Not specified	2 mol/s

11.8% whereas a further increase from 10 to 15 stages yields to only a slightly higher DPC yield of 12.0%. Chemical equilibrium of transesterification 2 and the disproportionation reaction (Fig. 6.3 & 6.4), respectively is almost completely achieved (>98%). It seems therefore that 5 stages are not providing sufficient separation efficiency which limits the DPC yield somewhat whereas this influence levels off for 10 and 15 stages, respectively which means that a further increase of stages is not likely to enhance the DPC yields.

In Figure 6.14 the DPC yield depending on the bottom flow rate is depicted. A decreasing bottom flow rate leads to a slightly increasing DPC yield. This can be explained with an increasing temperature (475-510 °C) at the bottom of the column with a decreasing bottom flow rate. The higher temperature leads on the one hand

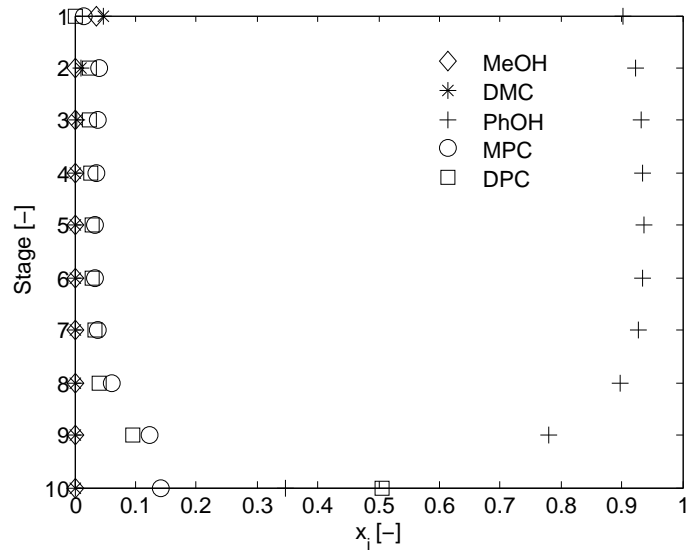


**Figure 6.12:** Liquid phase composition profile for the base case of the "second" column (see Table 6.5).

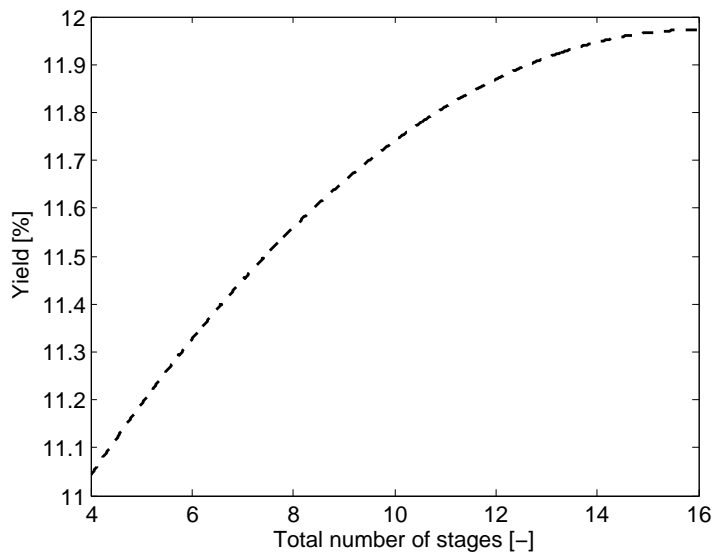


**Figure 6.13:** Influence of the total number of stages on the yield [%] of DPC in the bottom product stream of the "second" column.

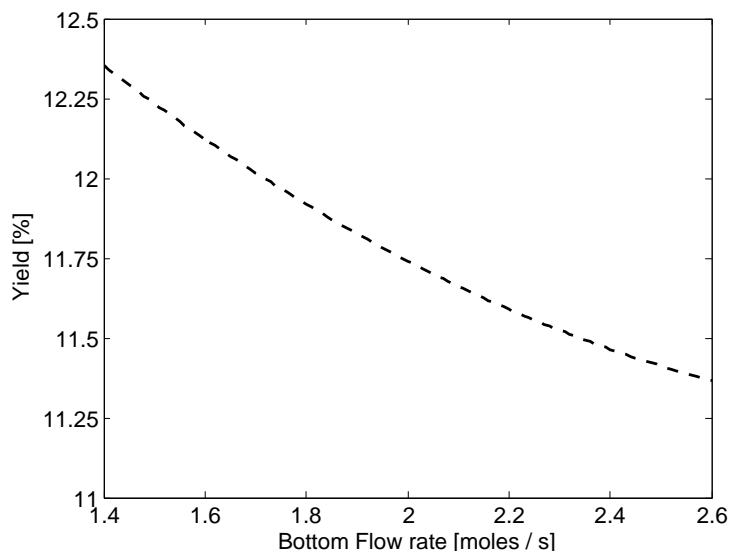


**Figure 6.14: Influence of the Bottom Flow rate [mol/s] on the yield of DPC [%] in the bottom product of the "second" column.**

to an increased chemical equilibrium value for the reactions to DPC (Eq. 6.10 & 6.11) and hence a larger DPC equilibrium concentration and on the other hand a decreasing mole fraction (from 0.5-0.15 mole %) of the more volatile phenol in the liquid phase of the bottom product.

After investigating the influence of the reflux ratio, the number of stages and the bottom flow rate on the DPC yield obtainable in the "second" column it can be stated that the reflux ratio does affect the DPC yield only negligibly and that also the other two parameters, the number of stages and the bottom flow rate, do only influence the DPC yield marginally in the investigated ranges.

## 6.8 Comparison between the simulation results of Tung and Yu (2007) and this work

Finally a comparison between the results of a simulation study recently published by Tung and Yu (2007) and those derived in this work will be carried out. The

simulation results in this study have been calculated for the herein investigated system on the basis of proper chemical equilibrium data and reaction kinetics for all three reactions (Fig. 6.2-6.4) as well as a proper description of the VLE based on the UNIFAC method (see section "Phase equilibrium, Reactions, thermodynamics and reaction kinetics"). Tung and Yu (2007) use a hypothetical chemical equilibrium value ( $K_{x,ov}=2$ ) and hypothetical reaction kinetics ( $k_f=8\times 10^{-3} \text{ s}^{-1}$  and  $k_b=4\times 10^{-3} \text{ s}^{-1}$ ) for the overall reaction from DMC to DPC ( $\text{DMC} + 2 \text{ PhOH} = \text{DPC} + 2 \text{ MeOH}$ ) thereby not taking into account that actually three reactions are taking place. Apart from that, their overall equilibrium constant is remarkably high: the chemical equilibrium value of the overall reaction from DMC to DPC calculated with the relations given by Haubrock et al. (2007b) equals  $K_{x,ov}=6\times 10^{-7}$  which is several orders of magnitude lower than the mole fraction based  $K_{x,ov}=2$  value used by Tung and Yu. The rate limiting steps in the investigated system are the forward reaction rates of reaction 6.2 and 6.3. The  $k_1$  and  $k_2$  values (Eq. 6.15-6.16) taken from Haubrock et al. (2007c) as used in the simulations are both around  $1.4\times 10^{-3} \text{ s}^{-1}$  at a catalyst mole fraction of  $1.5\times 10^{-3}$  and a temperature of  $180 \text{ }^\circ\text{C}$ . This means that the forward reaction rate constant employed by Tung and Yu is more than a factor of 5 larger, which means that chemical equilibrium is achieved substantially faster and therefore also the required tray volume is considerably smaller. Moreover, Tung and Yu only employ hypothetical vapour pressures in their simulations which have been ranked according to the volatility of the four components DMC, phenol, DPC and methanol (so not taking into account non-idealities by means of activity coefficients).

The column specifications used by Tung and Yu are briefly summarized in Table 6.6. The same conditions will be also used in the Chemsep calculations -implementing the physical/chemical data as given in this study- to compare both component profiles.

Tung and Yu (2007) assumed to have a heterogeneous catalyst located on each of the reactive trays (5-20). This makes it possible to have non-reactive trays at the bottom not containing catalyst (tray 21-24), which are only used for the separation of the mixture. This configuration is of course physically not possible for a system with a homogenous catalyst as this catalyst will be present on each tray below the

**Table 6.6:** Specification of the reactive distillation column for making DPC from DMC according to (Tung and Yu, 2007).

Parameter	Parameter value Base case
Trays overall	24
Reactive Trays	16
Separation Trays (Bottom + Top)	4+4
Feed stage phenol	16
Feed stage DMC	11
State Feed DMC	Vapour
State Feed phenol	Liquid
Molar Feed Flows (each)	12.6 moles /s
Reflux ratio	2.1
Bottom product flow rate	12.6 moles /s

feed tray of the (non-volatile) catalyst. Therefore it can already be stated at this point that the composition profiles at trays 21-24 cannot properly be compared. With the specified reflux ratio of 2.1 (see Table 6.6) it was not possible to get convergence within Chemsep. Therefore the reflux ratio has been adapted to 21.7 which is the lowest possible reflux ratio to achieve convergence within Chemsep with the specified bottom flow rate of 12.6 mole/s (see Table 6.6). The composition profile calculated in Chemsep is depicted in Figure 6.15 which shows that the conversion of the reactants DMC and phenol is very low ( $\sim 3\%$ ) and therefore only mole fractions of around 2.2% for both, DPC and MPC, can be achieved. The low conversions of DMC and phenol might partly be attributed to the relatively high reflux ratio (21.7) which has been employed in the simulations to circumvent numerical (convergence) problems in the simulation. The composition profile calculated by Tung and Yu

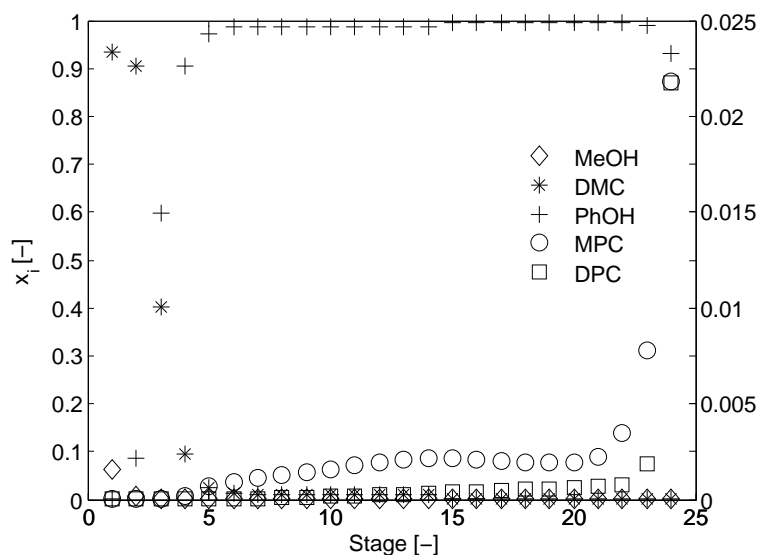


**Figure 6.15: Composition profile for the process from DMC to DPC calculated in this work (Reflux ratio=21.7, Bottom flow rate=12.6 mol/s). Right axis: Mole fractions of MPC and DPC.**

(2007) is shown in Figure 6.16. A considerable conversion of DMC and phenol can be observed in the reaction zone thereby forming methanol and DPC in large amounts (mole fractions of methanol and DPC both around 95%).

The two composition profiles (Figure 6.15 + 6.16) are by far not identical; quite the contrary not even the trends are similar. Most probably the difference in chemical equilibriums constants and the reaction rate constants as used in this work and the work of Tung and Yu are responsible for the different composition profiles. In case realistic physical/chemical input parameters are used considerably lower yields of the end product DPC are achieved (shown in Figure 6.15) as compared to the results given by Tung and Yu (Figure 6.16).

To increase the conversion using the current physical/chemical data the reflux ratio and the bottom flow rate had to be decreased simultaneously to 7 and 7 mole/s, respectively to achieve higher conversions. A change of the reflux ratio and the bottom flow rate results in larger conversions ( $\sim 25\%$ ) of DMC and phenol and thus



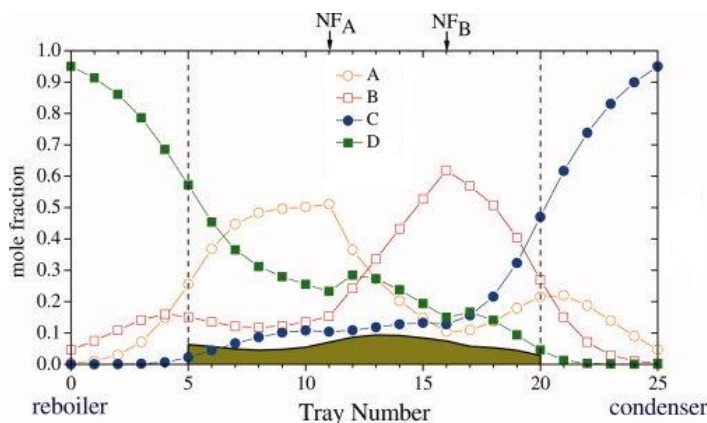


**Figure 6.16: Composition profile for the process from DMC to DPC taken from (Tung and Yu, 2007) ( A=DMC, B=phenol, C=methanol, D=DPC).**

also a larger mole fraction of DPC ( $\sim 20\%$ ) in the bottom of the column (see Figure 6.17). It might very well be that also the difference in column configuration - reactive trays (this study) and non-reactive trays (stage 1-5; Tung and Yu) in the bottom of the column- is partly responsible for the different composition profiles especially in the bottom section (stage 1-5) of the column.

Nevertheless it seems not likely that the different configuration can be held entirely responsible for the observed extreme differences between this study and the study of Tung and Yu (Figure 6.16 & 6.17).

This clearly shows the importance of using proper input data e.g. chemical equilibrium data, reaction kinetics and phase equilibrium data as not doing so leads to different -in this case most probably less reliable results- for this process. As there is no suitable experimental data available which could be used to assess the simulated column profiles it is unfortunately not possible to judge which of the simulated column profiles is closer to reality. Nevertheless an economic evaluation of the DMC-to-DPC process based on the results presented by Tung and Yu (2007)

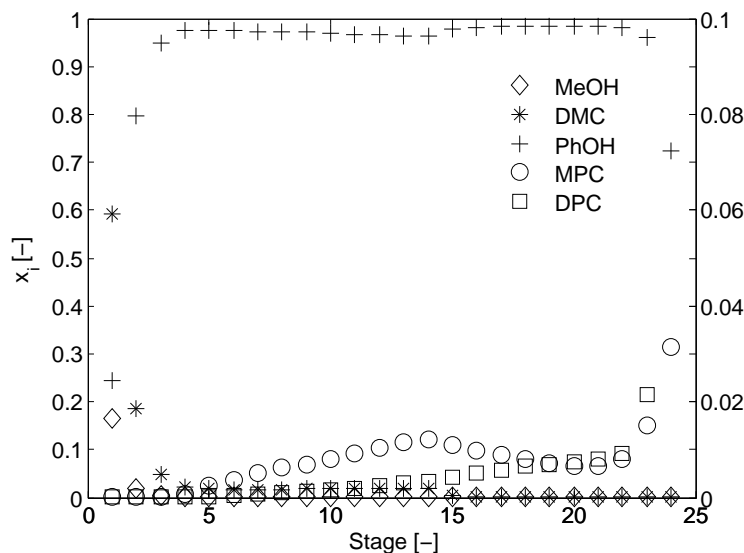


**Figure 6.17: Composition profile for the process from DMC to DPC calculated in this work (Reflux ratio=7, Bottom flow rate=7 moles/s). Right axis: Mole fractions of MPC and DPC.**

might very well lead to erroneous conclusions with respect to the estimated total costs for this process.

## 6.9 Conclusion

In this chapter the process from DMC to DPC via the intermediate MPC carried out in a reactive distillation column has been modelled with the commercial software package ChemSep. The influence of various parameters on the yields of MPC and DPC has been studied to find suitable optimization parameters. Activity based chemical equilibrium values and activity based reaction kinetics of the three involved reactions as well as relevant vapour-liquid equilibria of the studied system have been taken into account in the simulations. The influence of the feed location of phenol, the number of stages and the molar feed ratio DMC/phenol on the yield of MPC and DPC have been investigated for two different tray residence times. On the one hand

a residence time that allows only an equilibrium conversion of around 1-4% referring to reaction 6.2- has been specified. In this case reactions 6.2 and also reaction 6.3 are kinetically limited whereas reaction 6.4 is already at chemical equilibrium. On the other hand a residence time has been used which allows an equilibrium conversion of around 35-60% for reaction 6.2 and therefore also for reaction 6.3; under these conditions reaction 6.4 can be assumed to be at chemical equilibrium. In the latter case the reactions 6.2 and 6.3 are close to and in case of reaction 6.4 at chemical equilibrium and the yields of MPC and DPC are mainly influenced by the chemical equilibria and vapour liquid equilibria in the system.

The yields of MPC and DPC in the kinetically controlled regime ("Regime 2") tend to be lower than those for "Regime 1" by at least a factor of 2 up to a factor of 8 at the most, depending on the parameter investigated. It seems therefore necessary to allow for residence times in the column large enough to get close to chemical equilibrium of reaction 6.2 and therewith also reaction 6.3 and 6.4. The yields of MPC and DPC respectively can be maximized by choosing a feed tray location at the top tray of the column, a number of stages of 15 or more and a molar DMC/phenol feed ratio of 1 or smaller. The reflux ratio should be as small as possible as this leads to an increase of the MPC and DPC yields in the bottom product of the column.

As the bottom product of the "first column" contains a mole fraction of around 12% MPC and 10% DPC, respectively (with corresponding yields of around 9% and 7%, respectively), it seems necessary to use a "second" column in which the MPC is converted to DPC and moreover excess phenol is separated from the product DPC. As feed condition for the "second" column the bottom product specification and composition of the "first" column has been taken. The influence of the reflux ratio, bottom flow rate and the number of stages on the DPC yield in the bottom of the "second" column has been studied. This showed that a change of the reflux ratio has no influence on the DPC yield whereas a decreasing bottom flow rate as well as an increasing number of stages result both in larger DPC yields, which can reach an overall value of 12%.

A comparison of the calculated composition profiles taken from Tung and Yu (2007) and those calculated in this work for a column producing DPC from phenol and DMC

shows that the profiles of the different mole fractions over the column length exhibit a totally different behaviour. As Tung and Yu used hypothetical chemical equilibrium data, reaction kinetics and physical properties this discrepancy could have been expected. It is likely that simulation studies with proper input parameters -as used in the simulations of this study- yield more reliable information about the DMC to DPC process and therewith can serve as a basis for a sound economic evaluation of different configurations of the investigated process. Eventually the comparison of the simulation results to experimentally derived column profiles (even if the "column" is just a one tray column) will show the quality and the applicability of the model presented in this work.

## Acknowledgement

The authors gratefully acknowledges the financial support of Shell Global Solutions International B.V.

## Notation

$a_i$	Activity of species i	[-]
$c$	Number of components	[-]
$\varepsilon_j$	Moles reaction mixture on stage j	[mol]
$\gamma_i$	Activity coefficient of species i	[-]
$H^v$	Molar Enthalpy of the corresponding phase and stream	[J mol <sup>-1</sup> ]
$k_k$	Reaction rate constant of reaction k	[s <sup>-1</sup> ]
$K_i$	Separation Factor	[-]
$K_{a,k}$	Activity based equilibrium coefficient of reaction k	[-]
$K_{x,k}$	Molefraction based equilibrium coefficient of reaction k	[-]
$L_j$	Liquid flow from tray j	[mol s <sup>-1</sup> ]
$\nu_{i,m}$	Stoichiometric coefficient	[-]
$p$	Pressure	[Pa]
$p_i^{vap}$	Saturated vapour pressure of molecule i	[Pa]
$Q$	Heat duty	[J s <sup>-1</sup> ]
$R$	Ideal gas constant	[J mol <sup>-1</sup> K <sup>-1</sup> ]
$R_{m,j}$	Reaction rate	[s <sup>-1</sup> ]
$r_j$	Side stream flow to interstage flow	[-]

$r$	Number of reactions	[-]
$T$	Temperature	[K or C]
$V_j$	Vapour flow from tray $j$	[mol s <sup>-1</sup> ]
$x_i$	Liquid phase mole fraction of species $i$	[-]
$x_{cat}$	catalyst mole fraction	[-]
$y_i$	Vapour phase mole fraction of species $i$	[-]
<b>Indices</b>		[-]
$i,j,k,m$	Indices	[-]



# Bibliography

- M. Baerns, H. Hofmann, and A. Renken. *Chemische Reaktionstechnik*. Thieme, Stuttgart, 3 Edition, 1992.
- D. Beutier and H. Renon. Representation of  $\text{NH}_3\text{-H}_2\text{S-H}_2\text{O}$ ,  $\text{NH}_3\text{-CO}_2\text{-H}_2\text{O}$  and  $\text{NH}_3\text{-SO}_2\text{-H}_2\text{O}$  vapour-liquid equilibria. *Ind. Eng. Chem. Process Des. Dev.*, 17 (3):220–230, 1978.
- R.B. Bird, W.E. Stewart, and E.N. Lightfoot. *Transport Phenomena*. Wiley/VCH, Weinheim, 1 Edition, 1960.
- A. Bondi. van der waals volumes and radii. *The Journal of Physical Chemistry*, 68 (3):441–451, 1964.
- S.W. Brelvi and J.P. O’Connell. Corresponding states correlations for liquid compressibility and partial molar volumes of gases at infinite dilution. *AIChE J.*, 18: 1239–1243, 1972.
- H.J. Buysch. Ullmann’s encyclopedia of industrial chemistry - carbonic esters, 2000.
- H.J. Buysch, A. Klausener, R. Langer, and F.J. Mais. Process for the continuous preparation of dialkyl carbonates (US 5231212), July 27, 1993.
- Fabio Comelli and Romolo Francesconi. Isothermal vapor-liquid equilibria, densities, refractive indices, excess molar volumes, and excess molar enthalpies of dimethyl carbonate + 1,2-dichloroethane and + 1,1,1-trichloroethane. *J. Chem. Eng. Data*, 39(3):560–564, 1994.

- L. Constantinou and R. Gani. New group-contribution method for estimating properties of pure compounds. *AIChE Journal*, 40(10):1697–1710, 1994.
- P. V. Danckwerts. *Gas-Liquid reactions*. McGraw-Hill Book Company, London, 1970.
- T.L. Deng, H.A. Yin, and M.L. Tang. Experimental and predictive phase equilibrium of the  $\text{Li}^+$ ,  $\text{Na}^+$ ,  $\text{Cl}^-$ ,  $\text{CO}_3^{2-}$  -  $\text{H}_2\text{O}$  system at 298.15 K. *J. Chem. Eng. Data*, 47(1):26–29, 2002.
- P.W.J. Derks, T. Kleingeld, C. van Aken, J.A. Hogendoorn, and G.F. Versteeg. Kinetics of absorption of carbon dioxide in aqueous piperazine solutions. *Chem. Eng. Sci.*, 61(20):6837–6854, 2006.
- J.H. Dymond and E.B. Smith, editors. *The virial coefficients of pure gases and mixtures*. Oxford University Press, Oxford U.K., 1980.
- T.J Edwards, G. Maurer, J. Newman, and J.M. Prausnitz. Vapour-liquid equilibria in multicomponent aqueous solutions of weak electrolytes. *AIChE J.*, 24(6):966–976, 1978.
- D.C. Engel. *Palladium catalysed hydrogenation of aqueous bicarbonate salts in formic acid production*. PhD thesis, University of Twente, 1994.
- A. Fredenslund, R. L. Jones, and J. M. Prausnitz. Group-contribution estimation of activity-coefficients in non-ideal liquid-mixtures. *AIChE Journal*, 21(6):1086–1099, 1975.
- Z. Fu and Y. Ono. Two-step synthesis of diphenyl carbonate from dimethyl carbonate and phenol using  $\text{MoO}_3/\text{SiO}_2$  catalysts. *Journal of Molecular Catalysis A: Chemical*, 118:293–299, 1997.
- S. Fukuoka and M. Tojo. Process for continuously producing an aromatic carbonate (US 5210268), May 11, 1993.



- S. Fukuoka, M. Kawamura, K. Komiya, M. Tojo, H. Hachiya, M. Aminaka, H. Okamoto, I. Fukawa, and S. Konno. A novel non-phosgene polycarbonate production process using by-product CO<sub>2</sub> as starting material. *Green Chemistry*, 5:497–507, 2003.
- S. Fukuoka, M. Tojo, H. Hachiya, M. Aminaka, and K. Hasegawa. Green and sustainable chemistry in practice: Development and industrialization of a novel process for polycarbonate production from CO<sub>2</sub> without using phosgene. *Polymer Journal*, 39(2):91–114, 2007. 0032-3896.
- M. Fuming, L. Guangxing, N. Jin, and X. Huibi. A novel catalyst for transesterification of dimethyl carbonate with phenol to diphenyl carbonate – samarium trifluoromethanesulfonate. *J. Mol. Catal. Chem.*, 184:465–468, 2002.
- J. Gmehling, U. Onken, W. Arlt, P. Grenzhauer, U. Weidlich, B. Kolbe, and J. Rarey. *Vapor-Liquid Equilibrium Data Collection: Aqueous-Organic Systems*, volume 1 of *Chemistry Data Series*. DECHEMA, Frankfurt, 1991.
- G.E. Harrison, A.J. Dennis, and M. Sharif. Continuous production process of diarylcarbonates (US 5426207), 1995.
- J. Haubrock, J. A. Hogendoorn, and G. F. Versteeg. The applicability of activities in kinetic expressions: a more fundamental approach to represent the kinetics of the system CO<sub>2</sub>–OH<sup>−</sup> in terms of activities. *IJCRE*, 3:A40, 2005.
- J. Haubrock, J. A. Hogendoorn, H. A. Kooijman, R. Taylor, and G. F. Versteeg. A new UNIFAC group: the -OCOO-group of carbonates. *to be submitted*, 2007a.
- J. Haubrock, J. A. Hogendoorn, M. Raspe, G. F. Versteeg, H. A. Kooijman, and R. Taylor. Experimental determination of the chemical equilibria involved in the reaction from dimethyl carbonate to diphenyl carbonate. *Industrial and Engineering Chemistry Research*, Submitted 08-15-2007, 2007b.
- J. Haubrock, W. Wermink, J. A. Hogendoorn, M. van Sint Annaland, G. F. Versteeg, H. A. Kooijman, and R. Taylor. Kinetics of the reactions from DMC via MPC

- to DPC. *Industrial and Engineering Chemistry Research*, Submitted 08-29-2007, 2007c.
- J.G. Hayden and J.P. O'Connell. A generalized method for predicting second virial coefficients. *Ind. Eng. Chem. Process Des. Dev.*, 14:209–216, 1975.
- H. Hikita and S. Asai. Gas absorption with a two step chemical reaction. *Chem. Eng. J.*, 11:123–129, 1976.
- A.L. Horvath. *Handbook of aqueous electrolyte solutions: physical properties, estimation and correlation methods*. Ellis Horwood series in Physical Chemistry. Ellis Horwood, Chichester, U.K., 1985.
- Wang-Ming Hu, Lv-Ming Shen, and Lu-Jun Zhao. Measurement of vapor-liquid equilibrium for binary mixtures of phenol-dimethyl carbonate and phenol-methanol at 101.3 kPa. *Fluid Phase Equilibria*, 219(2):265, 2004.
- K. Kawazuishi and J.M Prausnitz. Correlation of vapour-liquid equilibria for the system ammonia-carbon dioxide-water. *Ind. Eng. Chem. Res.*, 26(7):1482–1485, 1987.
- W. Kim and J. Lee. A new process for the synthesis of diphenyl carbonate from dimethyl carbonate and phenol over heterogeneous catalysts. *Catalysis Letters*, 59:83–88, 1999.
- W.B. Kim, U.A. Joshi, and J.S. Lee. Making polycarbonates without employing phosgene: An overview on catalytic chemistry of intermediate and precursor synthesis. *Ind. Eng. Chem. Res.*, 43:1897–1914, 2004.
- H. A. Kooijman and R. Taylor. Chemsep lite pure component data library (ChemSep version 6.05), 2007.
- L. Kucka, E. Kenig, and A. Gorak. Kinetics of the gas-liquid reaction between carbon dioxide and hydroxide ions. *Ind. Eng. Chem. Res.*, 41:5952–5957, 2002.

- P. S. Kumar, J. A. Hogendoorn, G. F. Versteeg, and P. H. M. Feron. Kinetics of the reaction of carbon dioxide with aqueous potassium salt of taurine and glycine. *AiChE J.*, 49(1):203–213, 2003.
- S. S. Laddha, J. M. Diaz, and P. V. Danckwerts. The N<sub>2</sub>O analogy: The solubilities of CO<sub>2</sub> and N<sub>2</sub>O in aqueous solutions of organic compounds. *Chem. Eng. Sci.*, 36(1):228–229, 1981.
- D. R. Lide. *CRC Handbook of Chemistry and Physics 2004-2005*. Taylor and Francis, Boca Raton/Florida, 85 Edition, 2004.
- J. Lohmann and J. Gmehling. Modified UNIFAC (Dortmund): Reliable model for the development of thermal separation processes. *Journal of Chemical Engineering of Japan*, 34(1):43–54, 2001.
- Hu-Ping Luo, Wen-De Xiao, and Kai-Hong Zhu. Isobaric vapor-liquid equilibria of alkyl carbonates with alcohols. *Fluid Phase Equilibria*, 175(1-2):91, 2000.
- R. A. T. O. Nijssing, R. H. Hendriks, and H. Kramers. Absorption of carbon dioxide in jets and falling films of electrolyte solutions, with and without chemical reaction. *Chem. Eng. Sci.*, 10:88–104, 1959.
- Hongying Niu, Haiming Guo, Jie Yao, Yue Wang, and Gongying Wang. Transesterification of dimethyl carbonate and phenol to diphenyl carbonate catalyzed by samarium diiodide. *Journal of Molecular Catalysis A: Chemical*, 259(1-2):292, 2006.
- J. H. Oh, K. J. Han, and S. J. Park. Excess molar volumes at 298.15 K and isothermal vapor-liquid equilibria at 333.15 K for the binary mixtures of dimethyl carbonate with benzene, toluene, n-heptane and isooctane. *J. Chem. Eng. Data*, 51(5):1868–1872, 2006.
- Y. Ono. Catalysis in the production and reactions of dimethyl carbonate, an environmentally friendly building block. *Applied Catalysis A*, 155:133–166, 1997.

- E.M. Pawlikowski, J. Newman, and J.M Prausnitz. Phase equilibria for aqueous solutions of ammonia and carbon dioxide. *Ind. Eng. Chem. Process Des. Dev.*, 21(4):764–770, 1982.
- A. B. Pereiro, A. Rodriguez, J. Canosa, and J. Tojo. Vapor-liquid equilibria for systems of diethyl carbonate and ketones and determination of group interaction parameters for the UNIFAC and ASOG methods. *Fluid Phase Equilibria*, 235(1):83, 2005.
- K.S. Pitzer. Thermodynamics of electrolytes. 1. Theoretical basis and general equations. *J. Phys. Chem.*, 77:268, 1973.
- K.S. Pitzer. *Activity coefficients in electrolyte solutions*. CRC Press, Boca Raton, 2 Edition, 1991.
- K.S. Pitzer and J.C. Peiper. Thermodynamics of aqueous carbonate solutions including mixtures of sodium carbonate, bicarbonate and chloride. *J. Chem. Therm.*, 14:613–638, 1982.
- R. Pohorecki and W. Moniuk. Kinetics of reaction between carbon dioxide and hydroxyl ions in aqueous electrolyte solutions. *Chem. Eng. Sci.*, 43(7):1677–1684, 1988.
- J. M. Prausnitz and F. W. Tavares. Thermodynamics of fluid-phase equilibria for standard chemical engineering operations. *AIChE Journal*, 50(4):739–761, 2004.
- R.C. Reid, J.M. Prausnitz, and B.M. Poling. *The properties of gases and liquids*. McGraw-Hill, New York, 4th Edition, 1988.
- H. Renon and J.M. Prausnitz. Local compositions in thermodynamic excess functions for liquid mixtures. *AIChE Journal*, 14(1):135, 1968.
- F. Rivetti. The role of dimethylcarbonate in the replacement of hazardous chemicals. *Comptes Rendus de l'Academie des Sciences - Series IIC: Chemistry*, 3:497–503, 2000.

- A. Rodriguez, J. Canosa, A. Dominguez, and J. Tojo. Isobaric vapour-liquid equilibria of dimethyl carbonate with alkanes and cyclohexane at 101.3 kPa. *Fluid Phase Equilibria*, 198(1):95, 2002a.
- A. Rodriguez, J. Canosa, A. Dominguez, and J. Tojo. Vapour-liquid equilibria of dimethyl carbonate with linear alcohols and estimation of interaction parameters for the UNIFAC and ASOG method. *Fluid Phase Equilibria*, 201(1):187, 2002b.
- A. Rodriguez, J. Canosa, A. Dominguez, and J. Tojo. Isobaric vapor-liquid equilibria of diethyl carbonate with four alkanes at 101.3 kPa. *J. Chem. Eng. Data*, 47(5):1098–1102, 2002c.
- A. Rodriguez, J. Canosa, A. Dominguez, and J. Tojo. Isobaric phase equilibria of diethyl carbonate with five alcohols at 101.3 kPa. *J. Chem. Eng. Data*, 48(1):86–91, 2003.
- R.N. Roy, J.J. Gibbons, R.W. Williams, L. Godwin, G. Baker, J.M. Simonson, and K.S. Pitzer. The thermodynamics of aqueous carbonate solutions II. Mixtures of potassium carbonate, bicarbonate and chloride. *J. Chem. Therm.*, 16:303–315, 1984.
- R.N. Roy, J.M. Simonson, and J.J. Gibbons. Thermodynamics of aqueous mixed potassium carbonate, bicarbonate and chloride solutions to 368 K. *J. Chem. Eng. Data*, 32:41–45, 1987.
- B. Rumpf and G. Maurer. An experimental and theoretical investigation on the solubility of carbon dioxide in aqueous electrolyte solutions. *Berichte der Bunsen-Gesellschaft fuer Physikalische Chemie*, 97:85, 1993.
- B. Rumpf, J. Xia, and G. Maurer. Solubility of carbon dioxide in aqueous solutions containing acetic acid or sodium hydroxide in the temperature range from 313 to 433 K and total pressures up to 10 MPa. *Ind. Eng. Chem. Res.*, 37:2012–2019, 1998.
- S.I. Sandler. *Chemical and Engineering Thermodynamics*. John Wiley and Sons, New York, 3 Edition, 1999.

- A. Saul and W. Wagner. International equations for the saturation properties of ordinary water substance. *J. Phys. Chem. Ref. Data*, 16:893–901, 1987.
- H.G. Schoenmakers and B. Bessling. Reactive and catalytic distillation from an industrial perspective. *Chem. Eng. Process.*, 42:145–155, 2003.
- N. Schon, R. Langer, H.J. Buysch, and P. Wagner. Process for the continuous preparation of diaryl carbonates from dialkyl carbonates (US 5334742), 1994.
- A. Schumpe. The estimation of gas solubilities in salt solutions. *Chem. Eng. Sci.*, 48(1):153–158, 1993.
- V. Serini. Ullmann’s encyclopedia of industrial chemistry - Polycarbonates, 2000.
- A. G. Shaikh and S. Sivaram. Dialkyl and diaryl carbonates by carbonate interchange reaction with dimethyl carbonate. *Ind. Eng. Chem. Res.*, 31:1167–1170, 1992.
- A. G. Shaikh and S. Sivaram. Organic carbonates. *Chemical Reviews*, 96:951–976, 1996.
- H. Sibum, V. Gaether, O. Roidl, F. Habashi, and H.U. Wolf. Ullmann’s encyclopedia of industrial chemistry - titanium, titanium alloys, and titanium compounds, 2000.
- P. Sipos, A. Stanley, S. Bevis, G. Hefter, and P. M. May. Viscosities and densities of concentrated aqueous NaOH/NaAl(OH)<sub>4</sub> mixtures at 25 C. *J. Chem. Eng. Data*, 46(3):657–661, 2001.
- F. Steyer and K. Sundmacher. Cyclohexanol production via esterification of cyclohexene with formic acid and subsequent hydration of the ester-reaction kinetics. *Industrial and Engineering Chemistry Research*, 46(4):1099–1104, 2007.
- K. Sundmacher and A. (Eds.) Kienle. *Reactive Distillation – Status and Future Directions*. WILEY-VCH, Weinheim, 1 Edition, 2003.
- R. Taylor and H. A. Kooijman. *The ChemSep book*, volume 1. Books on Demand, 2000.

- R. Taylor and R. Krishna. Modelling reactive distillation. *Chem. Eng. Sci.*, 55 (5183-5229), 2000.
- P. Tundo, F. Trotta, G. Moraglio, and F. Ligorati. Continuous-flow processes under gas liquid phase transfer catalysis (GL-PTC) conditions: The reaction of dialkyl carbonates with phenols, alcohols and mercaptans. *Ind. Eng. Chem. Res.*, 27: 1565–1571, 1988.
- S. T. Tung and C. C. Yu. Effects of relative volatility ranking to the design of reactive distillation. *AIChE Journal*, 53(5):1278–1297, 2007.
- J.H.G. van der Stegen, H. Weerdenburg, A.J. van der Veen, J.A. Hogendoorn, and G.F. Versteeg. Application of the Pitzer model for the estimation of activity coefficients of electrolytes in ion selective membranes. *Fluid Phase Equil.*, 157(2): 181–196, 1999.
- W.P.M. van Swaaij and G.F. Versteeg. Mass transfer accompanied with complex reversible reactions in gas-liquid systems: An overview. *Chem. Eng. Sci.*, 47: 3181–3195, 1992.
- G. F. Versteeg and W. P. M. Vanswaaij. Solubility and diffusivity of acid gases (CO<sub>2</sub>, N<sub>2</sub>O) in aqueous alkanolamine solutions. *J. Chem. Eng. Data*, 33(1):29–34, 1988.
- R. Westervelt. Polycarbonate. *Chemical Week*, 168(7):27, 2006.
- S. Xu, Z. Qing, Z. Zhen, C. Zhang, and J.J. Carrol. Vapor pressure measurements of aqueous n-methyldiethanolamine solutions. *Fluid Phase Equilibria*, 67:197–201, 1991.
- J.F. Zemaitis, D.M. Clark, M. Rafal, and N.C. Scrivner. *Handbook of aqueous electrolyte thermodynamics: theory and application*. DIPPR, New York, 1 Edition, 1986.





# List of Publications

J. Haubrock, J.A. Hogendoorn and G.F. Versteeg and G.F. Versteeg (2005). The applicability of activities in kinetic expressions: a more fundamental approach to represent the kinetics of the system  $\text{CO}_2\text{-OH}^-$  in terms of activities, *IJCRE*, vol. 3, A40

J. Haubrock, J.A. Hogendoorn and G.F. Versteeg (2007). The applicability of activities in kinetic expressions: A more fundamental approach to represent the kinetics of the system  $\text{CO}_2 - \text{OH}^-$  -salt in terms of activities, *Chemical Engineering Science*, vol. 62(21), pp. 5753-5769

J. Haubrock, J.A. Hogendoorn, M. Raspe, G.F. Versteeg, H.A. Kooijman and R. Taylor (2007). Experimental determination of the chemical equilibria involved in the reaction from Dimethyl carbonate to Diphenyl carbonate, *Industrial and Engineering Chemistry Research*, submitted 08-15-2007

J. Haubrock, W. Wermink, J.A. Hogendoorn, M. van Sint Annaland, G.F. Versteeg, H.A. Kooijman and R. Taylor (2007). Kinetics of the reactions from DMC via MPC to DPC, *Industrial and Engineering Chemistry Research*, submitted 08-29-2007

J. Haubrock, J.A. Hogendoorn, H.A. Kooijman, R. Taylor and G.F. Versteeg (2007). A new UNIFAC group: the -OCOO-group of carbonates, to be submitted

J. Haubrock, J.A. Hogendoorn, H.A. Kooijman, R. Taylor and G.F. Versteeg (2008). Process design for the production of Diphenyl carbonate from Dimethyl carbonate: Parameter studies and process configuration, to be submitted

## Presentations

J. Haubrock, J.A. Hogendoorn and G.F. Versteeg (2006). The applicability of activities in kinetic expressions: A more fundamental approach to represent the kinetics of the system  $\text{CO}_2$  -  $\text{OH}^-$  -salt in terms of activities, In *Proceedings of the 17th International Congress of Chemical Engineering (CHISA 2006)*, Prague, Czech Republic, 27 - 31 August 2006

# Curriculum Vitae

Jens Haubrock was born on April 13<sup>th</sup>, 1977 in Herford/Germany. He grew up in *Elverdissen*, one of Herford's rural districts, where he also attended elementary school. From 1987 until 1996 he attended the *Friedrichs-Gymnasium* in Herford where he got his university entrance diploma in June 1996.

After finishing school Jens did his alternative civilian service in Herford from 1996-1997.

In October 1997 he started to study Chemical Engineering at the University of Dortmund. During the course of his studies Jens spent one semester abroad at the Lehigh University in Pennsylvania/USA in 2000 and did a 12-week internship at Degussa Hanau/Germany in 2002. In June 2003 Jens completed his studies with a diploma thesis entitled "Assessment of a CO<sub>2</sub> adsorption/absorption process with liquid and immobilized amines by means of computer simulations" under supervision of Prof. dr. D.W. Agar.

In September 2003 he began with his PhD studies in the group "Development and Design of Industrial Processes" of Prof. dr. ir. G.F. Versteeg. In his research project Jens investigated the process from DiMethyl-Carbonate to DiPhenyl-Carbonate. The results of this research can be found in this PhD thesis.

Since October 2007 Jens is working as a process engineer at Evonik Industries in Marl/Germany in the Chemical Reactor Technology Department.



# Acknowledgements

Finally I have reached the last part of my PhD thesis; at the same time probably also the most read part of this thesis. Of course such a PhD thesis can only be realized with the help of many people, which I would like to thank here.

First of all I am indebted to my assistant promoter and mentor Kees Hogendoorn. His scientific input, ideas and suggestions during my research, but also his critical view on the achieved results have helped to improve the quality of this thesis considerably. Moreover, Kees was also helping me to get through the problems that I was facing during the reorganization. Apart from that a friendship has grown throughout our collaboration in the last four years which I really appreciate. Kees bedankt!

I also would like to thank my promoter Geert Versteeg who gave me the opportunity to do a PhD project in his group. With your experience in the field of process design and reactor technology you contributed a lot to my research project. Furthermore I was impressed by your clear and structured way to reduce complicated things to the essentials, which helped me to follow the red line in my research project.

Furthermore I would like to thank Hans Kuipers and Martin van Sint Annaland who accommodated me in the FCRE group after I was literally dropped there as a consequence of the reorganization. I also appreciate it very much that Hans is now acting as my promoter and Martin as my assistant promoter.

I am also indebted to Harry Kooijman and Ross Taylor who supported me with the modelling issues in this PhD project. Moreover, during the discussions with both of you about thermodynamics and distillation modelling I learned a bunch of new things, and that way some pitfalls have surely been avoided.

A large part of this thesis is based on experimental data, which are presented and discussed in the various chapters of this thesis. The experimental data would not have been obtained without the help of several people. First of all I would like to thank Henk-Jan Moed who built and debugged all my setups. Moreover, I would like to thank Benno Knaken, Wim Leppink and Gerrit Schorfhaar who always helped to fix the small problems with the setups during operation.

There was also a number of students who worked with my setups. I would like to thank you for the efforts each of you put into his work. Jiri van Straelen, Marloes Raspe, Wouter Wermink and Bas ten Donkelaar heel erg bedankt.

Furthermore I would like to thank Nicole Haitjema who managed all the clerical stuff in a close to perfect manner. I am also indebted to all the service units within the CT/TNW faculty who provided all the materials necessary to conduct my research. To those people whom I have missed to mention here explicitly: Thank you all for your endeavors.

The last four years were, of course, not only filled with work. I met a lot of interesting and diverse people during my PhD studies and have to admit that I really enjoyed my four years in the Netherlands. It is of course not possible to mention everybody individually as this would surely double the number of pages of this thesis. Nevertheless I would like to highlight a few people.

First of all I have to mention Peter, who helped me initially with getting around the UT and introduced me to the very Dutch habit of having a borrel. Over

the years a friendship has grown which I don't want to miss. Furthermore there is my friend and roommate Espen with whom it was always a pleasure to share a room even if work sometimes slightly suffered. I also enjoyed the morning coffee with you guys, usually mixed with a lot of fun. I should not forget to mention Jacco who was often joking with us; I am sure he would like to be present today.

My thanks go also to my parents, my (little) brother and grandmother who always supported and encouraged me during my PhD studies. Finally I want to thank Ruth who has helped me to get through all the ups and downs that go along with pursuing a PhD.

Jens, December 14<sup>th</sup> 2007